



Universiteit
Leiden
The Netherlands

Modelling the lung in vitro

Riet, S. van

Citation

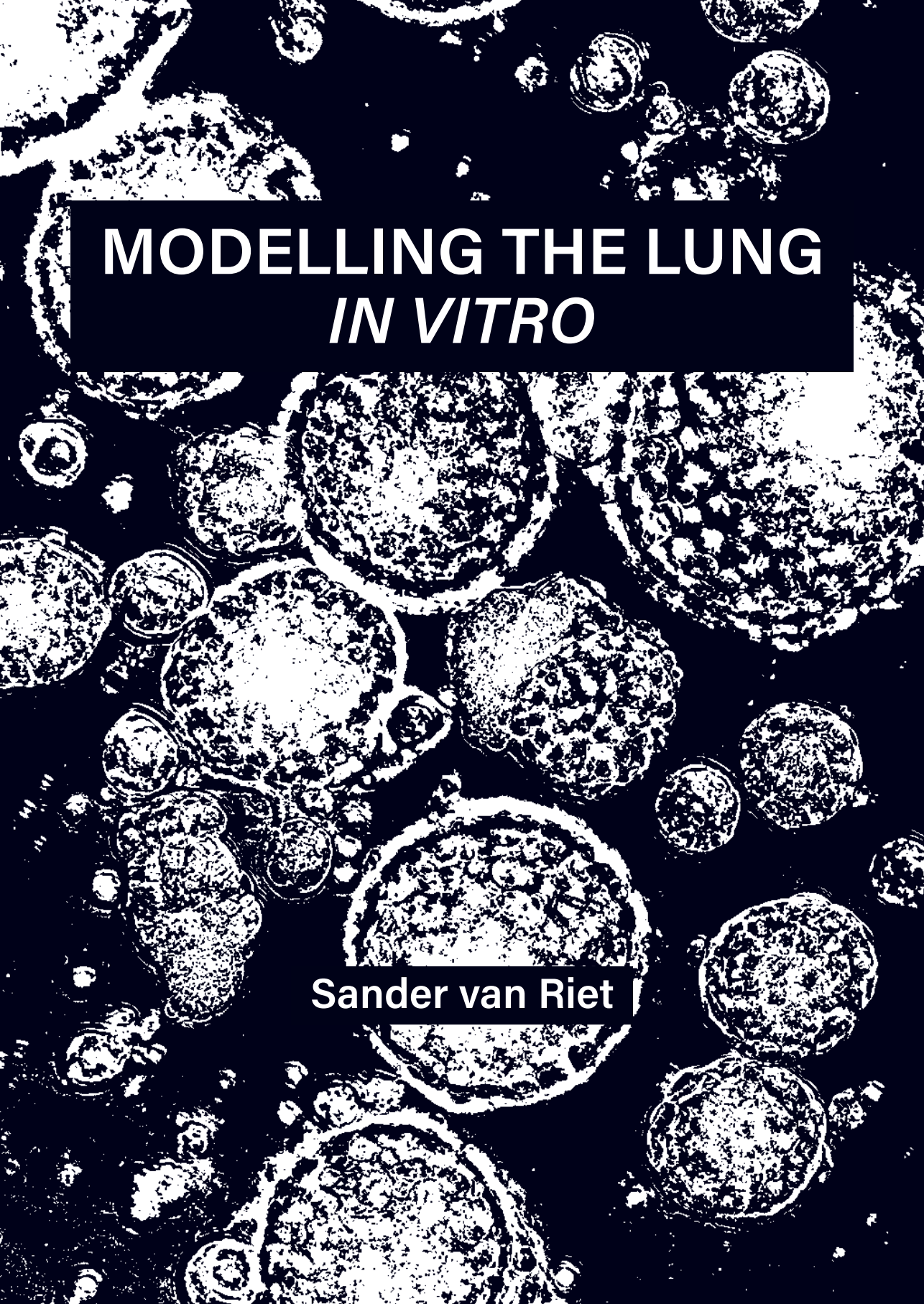
Riet, S. van. (2021, September 23). *Modelling the lung in vitro*. Retrieved from <https://hdl.handle.net/1887/3213533>

Version: Publisher's Version

License: [Licence agreement concerning inclusion of doctoral thesis in the Institutional Repository of the University of Leiden](#)

Downloaded from: <https://hdl.handle.net/1887/3213533>

Note: To cite this publication please use the final published version (if applicable).

A high-contrast, black and white microscopic image of lung tissue, showing numerous alveoli and capillaries. A solid black rectangular box is superimposed over the upper portion of the image, containing the title text in white.

MODELLING THE LUNG
IN VITRO

Sander van Riet

Modelling the lung *in vitro*

Sander van Riet

Colophon

Modelling the lung *in vitro*

Sander van Riet

Thesis Leiden University Medical Center

The research presented in this thesis was financially supported by the Lung Foundation Netherlands (project code: 6.1.14.010) and The Netherlands Organization for Health Research and Development (ZonMw; project code: 114021508)

ISBN: 978-94-6416-739-9

Printing: Ridderprint, Alblasterdam

© 2021 S. van Riet, All rights reserved. No part of this thesis may be reproduced, stored, or transmitted in any form or by means, without prior written permission of the author.

Modelling the lung *in vitro*

Proefschrift

ter verkrijging van
de graad van doctor aan de Universiteit Leiden
op gezag van rector magnificus prof.dr.ir. H. Bijl,
volgens besluit van het college voor promoties
te verdedigen op donderdag 23 september 2021
klokke 16.15

door

Sander van Riet

geboren te Goes in 1989

Promotor: Prof. dr. P.S. Hiemstra

Copromotor: Dr. R.J. Rottier

Leden promotiecommissie: Prof. dr. M.J.T.H. Goumans
Dr. H.H. Smits
Prof.dr. R. Gosens
Rijksuniversiteit Groningen, Groningen
Dr. A. van der Meer
Universiteit Twente, Enschede
Prof.dr. R.W. Hendriks
Erasmus MC, Rotterdam

Table of contents

CHAPTER 1	7
Introduction	
Scope of this thesis	
CHAPTER 2	29
<i>In vitro</i> modelling of alveolar repair at the air-liquid interface using alveolar epithelial cells derived from human induced pluripotent stem cells <i>Scientific Reports 2020 Mar 26;10(1):5499</i>	
CHAPTER 3	59
Alveolus Lung-Chip cultures of patient-derived primary alveolar type-2 cells <i>In revision at the American Journal of Physiology-Lung Cellular and Molecular Physiology</i>	
CHAPTER 4	83
Disease modelling following organoid-based expansion of airway epithelial cells <i>American Journal of Physiology-Lung Cellular and Molecular Physiology; Accpeted July 2021, In Press</i>	
CHAPTER 5	115
Modulation of airway epithelial innate immunity and wound repair by M(GM-CSF) and M(M-CSF) macrophages <i>Journal of Innate Immunity 2020 Apr 14:1-12</i>	
CHAPTER 6	143
Flexible poly(trimethylene carbonate) membranes for use in <i>in vitro</i> modelling of the airway epithelium <i>Work in progress</i>	
CHAPTER 7	165
Summary and General discussion	
ADDENDUM	183
Nederlandse samenvatting	
Curriculum Vitae	
List of publications	
Dankwoord / Acknowledgements	

CHAPTER 1

Introduction

Scope of this thesis

The lungs are a complex organ that can be sub-divided in regional sections that are defined by their function, structure and cellular composition. The respiratory compartment consists of the trachea, bronchi, bronchioles or small airways, alveoli or air sacs, and the supporting mesenchymal compartment of connective tissue, blood vessels and lymphoid tissue. The lungs consists of as many as 40 different resident cells types and more cell types are being discovered or redefined with the current advances in single cell RNA sequencing technology (Montoro et al. 2018; Plasschaert et al. 2018; Schiller et al. 2019). The function of the lungs is to facilitate the exchange of oxygen and carbon dioxide between the oxygen carriers in the blood and the air that we breathe. For the lungs to achieve this, the different compartments need to work together seamlessly. The conducting lower airways are composed of the trachea that divides into bronchi and bronchioles. The bronchioles lead to the alveoli that constitute most of the lung surface area and enable gas exchange with the circulating blood. The conducting airways are lined with highly specialized pseudostratified epithelial cells including ciliated cells, mucus-producing goblet cells and club cells, while the underlying basal cells act as progenitors (Crystal et al. 2008). The distal part of the lungs contain an average of 450 million pulmonary alveoli lined by thin, flat, non-dividing alveolar epithelial type 1 cells (AEC1) that form a semi-permeable barrier that selectively exchanges O_2 and CO_2 . The AEC1 are accompanied by cuboidal alveolar epithelial type 2 cells (AEC2) that produce pulmonary surfactant proteins that reduce surface tension, and function as a progenitor for the alveolar epithelium (Barkauskas et al. 2013). The lung epithelium has the capacity to provide defence against pathogens and the toxins and pollutants in the inhaled air from the outside world (Hiemstra, McCray, and Bals 2015). They are supported in their role in host defence by numerous resident - and circulating immune cells (Byrne et al. 2015). Among all immune cells present, the alveolar macrophages are of special note as they reside permanently in the alveolar compartment to both protect the alveolar epithelium from external threats as well as controlling the inflammatory response to mitigate collateral damage (Guilliams et al. 2013; Garbi and Lambrecht 2017). These defences are vital as the lungs are continuously challenged by inhaled pathogens, noxious particles, and toxic gases present in inhaled air. These inhaled substances pose a health threat as both acute and repeated exposure can cause and/or contribute to a range of acute and chronic lung conditions that constitute a global health burden. All respiratory diseases combined, of which the most frequent are chronic

obstructive pulmonary disease (COPD), respiratory infections and lung cancer, are directly responsible for one in six deaths worldwide (World Health Organization 2018). Furthermore, chronic respiratory conditions affect more than one billion people worldwide (World Health Organization 2017).

The study of lung biology and pathology is therefore vital but also complicated when considering the high diversity in cell types, numbers, function and tissue morphology among the different lung regions and disease states. Animal models have been widely used to study the lungs, but ethical considerations, poor translatability of results obtained from animal experiments to human physiology and substantial differences in lung structure and function between humans and e.g. mice, have led to an increased demand for alternative human *in vitro* methods to study both lung biology and pathology. However, the aforementioned complexity and diversity in lung cell populations are important elements to consider when designing an *in vitro* model of the human lungs. This also indicates that at this point in time a single *in vitro* model to study the lung in its entirety is not feasible. Instead, the appropriate model will depend on the experimental questions one wishes to answer, with the goal of recapitulating the key morphological and functional features of (part of) the organ.

Modelling of the human lung

The study of lung disease pathogenesis and drug development, as well as inhalation toxicology, requires physiologically relevant models of human lung tissue. For many years, animal models have been central in many forms of research and still play a role in disease modelling and the study of lung development, as well as the development and testing of new drugs. However, it is becoming more clear that animal models are not always suitable to study human processes (Leist and Hartung 2013). While animals have provided seminal insight into lung physiology and pathophysiology, they are limited in recapitulating the development, structure, disease symptoms, and responses of the human respiratory system. Notably, cellular composition differs between mouse and human lungs. In the mouse airways, mucus-producing goblet cells are rare and secretory club cells are abundant, whereas the opposite applies to human airways (Rock, Randell, and Hogan 2010). Although animal models provide access to native tissues and are indeed used for modelling human diseases and assessing efficacy of therapeutics in

a number of tissues and organs, they are often poor predictors of clinical success due to species-species differences in mechanisms of action or toxicities of drugs (Uhl and Warner 2015). Lung specific studies equally suffer from these limitations, and over-reliance on animals alone to model complex human respiratory diseases such as asthma has contributed to the lack of new efficacious treatment despite huge research efforts, as animal models have a long record of failing to predict clinical efficacy of novel therapies in human (Mullane 2011). Furthermore, gene mutations can induce different, if any, phenotypes in mice compared to humans (Liao and Zhang 2008). Taken together, this summary of limitations demonstrates that animals alone cannot be relied upon and are often an imperfect model to provide answers for increasingly specialized questions regarding a range of human lung diseases and their drug treatment, necessitating the need for human-specific preclinical or patient specific *in vitro* models of the lung.

2D cultures and cell sources

The initial difficulty in modelling the lung or features of any organ *in vitro* lies in the challenge to identify and recapitulate the essential structural and functional elements of the human organ that govern both healthy and pathological responses. In the lung, as in various other organs, the epithelial cells lining the organ surfaces facilitate many functions of the lung. Since epithelial function and dysfunction is frequently associated with organ disease, epithelial cells are a topic of intense research. In trying to mimic the lung epithelial layer *in vitro*, scientists have predominantly relied on simpler surrogate models to gain insight into human physiology and pathophysiology. 2D monolayer cultures of cancer or immortalized cell lines still represents the “standard” and most common culture model and alternative to animal models. Frequently used examples are the cell line A549 that is derived from a lung carcinoma from a patient in 1972 and has an alveolar background which enables it to mimic some alveolar features (Lieber et al. 1976). Another frequently used cell line is the BEAS-2B cell line, which is derived from the bronchial epithelium obtained during autopsy of an individual without cancer and immortalized using replication-defective SV40/adenovirus transfection (Reddel et al. 1988). These cell lines are relatively cheap to maintain, remain stable in culture and can be expanded reliably, making them relatively easy to use in (high-throughput) experiments. However, these advantages are offset by their limited physiological relevance and clinical predictivity. Due to the derivation from tumours, or the immortalization by oncogenic

transformation, these cells do not recapitulate the differentiated cell types of the adult airway, resulting in an improper replication of tissue specific function, and also their barrier formation is limited. It often remains unclear to what extent the cell lines truly recapitulate the physiological situation, which restricts their experimental use. This limited physiological relevance results in improper prediction of *in vivo* tissue function and clinical predictivity of drug efficiency.

A function that is lacking in most cell line cultures and which is central to lung function is the exposure to air. The next level of complexity from 2D cultures and a more advanced representation of the epithelial compartment of the lung can be obtained by air-liquid interface cultures. Although this can be done with some cell lines, notably Calu-3 (Banga et al. 2012), these types of cultures are frequently established with primary cells. Primary cells are usually freshly isolated from tissue and used directly or after limited expansion. Notable drawbacks of the use of these cells are their limited lifespan, proliferative capacity and specific culture requirements. The primary tracheal and bronchial epithelial cells can be obtained from various sources. For instance, from macroscopically normal, tumour-free resected lung tissue from patients that are diagnosed with lung cancer, collected during lung volume reduction surgery for late stage COPD, derived from tissue that has become available in the context of lung transplantation, or from bronchial biopsies or brushings/scrapings that are obtained during bronchoscopy. The obtained epithelial cells can be expanded as basal cells and frozen until required (Amatngalim et al. 2016). Upon thawing and expansion, the basal cells can be seeded on Transwell inserts, with a porous membrane, that facilitate both air exposure and nutrient absorption from the bottom compartment. The exposure to air initiates differentiation of the basal cells and over the course of 2-3 weeks these will develop in a pseudostratified epithelial culture resembling the composition of the lining of the airways. These cultures have a similar gene expression signature as the human airway epithelium *in vivo* (Dvorak et al. 2011; Ross et al. 2007), recapitulate several key functional hallmarks of human airway epithelium, and have been successfully used in studying numerous biological processes in lung repair, function, host defence and pathophysiology (Gray et al. 1996; Crystal et al. 2008; Livraghi and Randell 2007; Malavia et al. 2009; Amatngalim et al. 2018). As mentioned above, the epithelial cells are often isolated from tissue derived from patients that had to undergo surgery

because of a disease, mostly lung cancer or COPD. The influence of these known and unknown lung diseases or other pathologies on the epithelial cell function *in vitro* is often unknown and can further increase the already existing donor variability. Alternative ways in which primary nasal, tracheal or bronchial epithelial cells can be obtained is via biopsies or brushes (Banerjee et al. 2009; Brewington et al. 2018). These methods do not rely on surgical resection and allow sampling of otherwise healthy individuals, although especially bronchoscopy required for collection of tracheal and bronchial epithelial cells is still invasive. The cells obtained through these methods are limited in number and require expansion for use in further experiments. This can be problematic as primary cells have a limited proliferative capacity and there is thus a risk of cellular senescence. Interestingly, another culture technique has shown that this exhaustion could potentially be overcome. The inhibition of TGF- β /BMP/SMAD signalling pathways was recently found to enable the long-term expansion of primary TP63⁺ airway basal cells by inhibiting terminal differentiation and promoting self-renewal (Mou et al. 2016). However, it is at present insufficiently clear whether the cells pushed beyond their “normal” limits behave in a similar manner compared to the freshly obtained cells. Nevertheless, this technique could prove very useful in expanding limited cell populations for use in further experiments.

Human induced pluripotent stem cells

When human embryonic stem (ES) cells were first isolated (Thomson et al. 1998) there was a strong interest in using these cells in therapy. These cells could be obtained from the inner cell mass of a blastocyst and remained karyotypically stable in culture and could differentiate to different cell types of all three germ layers (Xu et al. 2002). Protocols were developed to direct this differentiation but the ethical considerations remained pressing. Then in 2006, Yamanaka and colleagues offered new opportunities when they first described a method for generating mouse induced pluripotent stem cells (Takahashi and Yamanaka 2006). The following year they reported successful generation of human induced pluripotent stem cells (hiPSC) (Takahashi et al. 2007). By forcefully expressing 4 specific transcription factors, now known as the Yamanaka factors, adult human somatic cells can be reprogrammed to a pluripotent state. From this pluripotent state, the cells can be directed through the embryonic development to the organ or tissue of interest. In addition, these cells can proliferate virtually indefinitely while maintaining genetic integrity. hiPSC retain the genomic makeup of the

donor and therefore hold great potential to build advanced patient specific *in vitro* models of human tissue and to further our understanding of lung physiology and disease. Although the genetic sequence is unaltered during reprogramming to hiPSC, the remaining epigenetic memory could influence cell behaviour (Takahashi and Yamanaka 2006; Papp and Plath 2011; Brix, Zhou, and Luo 2015; Nishizawa et al. 2016). Retaining epigenetic memory from the source cell could be interesting for studying patient specific features but can also interfere with reprogramming as it can lead to insufficient silencing of tissue specific modification (Vaskova et al. 2013; Horvath 2013). Nevertheless, these cells give interesting prospects for their use in regenerative medicine. As they retain the genetic makeup of the donor, upon transplantation there is no risk of graft versus host disease, and their use allows for the intriguing possibility to become one's own donor. As of yet it is not possible to generate a complete functioning organ, but transplantation of organ specific cells or progenitor cells is an enticing possibility. This approach has in fact been implemented in various case studies, notably in Japan. Initial data of implantation of retinal cells in an individual suffering from age-related macular degeneration has shown positive results (reviewed in (Cuevas, Parmar, and Sowden 2019; Oswald and Baranov 2018)). The retinal progenitor cells were grafted in the eye and were able to slow or completely stop disease progression. As of yet no side effects have been reported, although the long-term effects remain unclear.

Initial studies first reported efficient induction into mesodermal and ectodermal lineages; however, maturation into the third endodermal germ layer remained limited (Kadzik and Morrisey 2012). The induction of posterior endoderm cell derivatives that give rise to organs such as the liver, intestine, and pancreas became possible in the early 2000s (Spence et al. 2011; D'Amour et al. 2006; Cai et al. 2007). In 2011, a key study elucidated a mechanism permitting stem cell differentiation into lung-specific endoderm precursor (Green et al. 2011).

Generation of endodermal cells from hiPSC *in vitro* is accomplished through directed differentiation, a process in which *in vivo* developmental stages are mimicked *in vitro* using controlled sequences of endogenous signalling factors (Murry and Keller 2008). hiPSC are first directed into definitive endoderm through activin A stimulation, followed by anterior foregut endoderm (AFE) induction through dual inhibition of the SMAD pathway by inhibiting the bone morphogenic protein (BMP) and transforming growth factor (TGF- β)

signalling pathways (Green et al. 2011). Following AFE establishment, a ventral patterning step is needed mirroring the morphogenesis of the endoderm where the trachea and lung buds eventually emerge ventrally (Morrisey and Hogan 2010). AFE ventralization is largely achieved through WNT, BMP, retinoic acid and fibroblast growth factor (FGF) signalling (Lee et al. 2014; Green et al. 2011) yielding cells expressing transcription factor NKX2-1, the earliest marker for lung epithelial lineages (Kimura et al. 1996; Xu et al. 2016). From this overall lung progenitor cell, the differentiation can be directed to either a proximal or distal fate, to obtain airway and alveolar epithelial cells, respectively (Fig. 1).

hiPSC-derived airway epithelial cells

Progression in the differentiation of NKX2-1⁺ lung progenitor cells towards proximal airway epithelial cells advanced in the past few years. Differentiation of hiPSC into airway epithelial cells was achieved in spheroid cultures using FGF10, KGF, WNT agonist and Notch inhibition (Konishi et al. 2016). More recently, it was shown that activating WNT signalling during differentiation efficiently induced a distal fate, whereas suppressing WNT signalling following ventralization directed cells towards a proximal fate, and resulted in epithelial cells expressing the classic markers SCGB1A1/CC10 for club cells, MUC5AC (goblet cells), and p63 and Keratin 5 (basal cells) (McCauley et al. 2017). Although the timing, concentration and method of WNT activation likely plays an important role, since in another study it was shown that promoting WNT by inhibiting GSK-3 β resulted in a mixed population (de Carvalho et al. 2019). To promote cilia development of the airway derived hiPSC, Notch inhibition was needed to produce motile multiciliated cells characterized by acetylated alpha-tubulin (α -Tub) staining (McCauley et al. 2017; Wong et al. 2012; Firth et al. 2014). Another protocol used 2D air-liquid interface cultures with FGF18 stimulation to generate a mature and polarized epithelial layer, in which motile cilia and mucus could be observed at the apical surface (Wong et al. 2015). It was shown that the scaffold and micro-environment of hiPSC-derived lung progenitors is a major determinant for achieving a mature airway epithelial phenotype, as shown using human hiPSC-derived lung organoids (Dye et al. 2015; Dye et al. 2016).

hiPSC-derived alveolar epithelial cells

Over the past years, notable progress has been made using NKX2-1⁺ lung progenitors to generate human alveolar epithelial cells by establishing protocols to direct these progenitors towards a distal fate. The combination of glucocorticoids, growth factors, and cAMP effectors (dexamethasone, 8-br-cAMP, IBMX, and KGF/FGF7; collectively known as DCIK) (Gonzales et al. 2002; Wade et al. 2006) has been shown to induce alveolar maturation through activation of PKA and CDP-choline pathways which upregulate lamellar body surfactant production in AEC2 (Andreeva, Kutuzov, and Voyno-Yasenetskaya 2007) (Fig. 1). Recognized markers of the distal alveolar epithelium include Surfactant Protein C (SFTPC), Surfactant Protein B (SFTPB), HTII-280, ABCA3, and LAMP3/DC-LAMP for AEC2, while Podoplanin (PDPN), Caveolin (CAV1), and Aquaporin 5 (AQP5) primarily define AEC1 cells. Stimulation of 2D cultures of NKX2-1⁺ differentiated distal progenitors with DCIK, FGF10 and WNT activators leads to expression of AEC1 and AEC2 markers, mature phenotypic characteristics of lamellar bodies, and functional surfactant uptake capability (Huang et al. 2015). AEC2 markers were found to be abundant in this protocol while AEC1 markers were minimally expressed (Chen et al. 2017).

Taken together, the advances in hiPSC differentiation protocols have made these approaches very interesting for the study of lung biology. The major drawback however is the lengthy and labour-intensive maintenance and

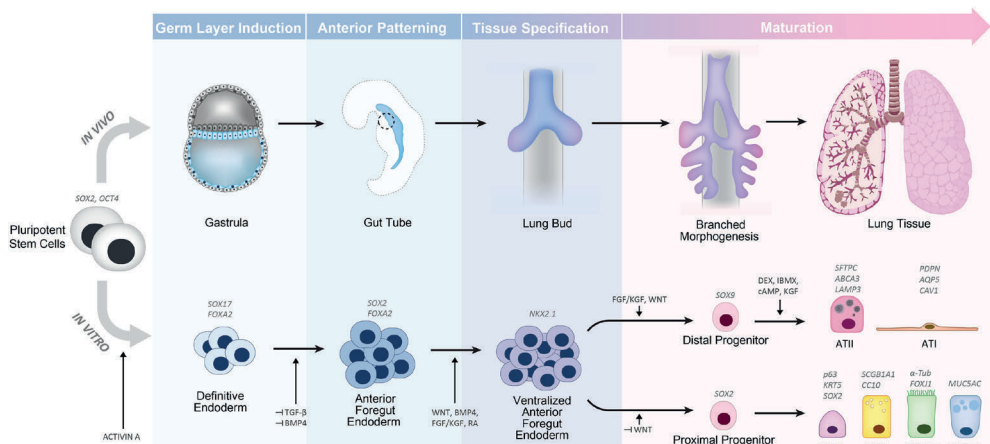


Fig. 1. Overview of the major stages of lung development in humans corresponding to the directed differentiation pathways of pluripotent stem cells towards a lung epithelial fate. The various intermediate steps of development with key signalling factors and common markers are indicated. Reproduced from Nawroth et al. (Nawroth et al. 2019).

differentiation timelines resulting in limited efficiency. Despite substantial advances in differentiation of lung stem cells, full maturation is still a challenge. For example, demonstrating SFTPC and SFTPB gene expression was initially sufficient to claim AEC2 cell differentiation. Furthermore, achieving an optimal balance between AEC1 and ACE2 is complicated. However, with the accelerated progress in lung PSC protocols, more strict metrics are now being considered to reach the ultimate goal of generating a supply of cells that recapitulates the same molecular, biochemical, phenotypical, and functional features found in the adult lung (Beers and Moodley 2017). Nevertheless, the capability of generating patient specific cell lines that can be directed to any cell types will be crucial in eventually developing a truly patient specific model.

The 3D culture of lung organoids

Whereas hiPSC have gained importance next to primary lung cells to obtain airway and alveolar cells, there have also been important developments in culture models. One culture model that has risen in prominence during the past couple of years is the culture of spheroids or organoids. An organoid can be described as a “miniature organ” suspended in a hydrogel which overcomes the 2D constraints and relies on the self-organisation of the cells to form 3D structures. Such a structure need consists of different organ specific cells and rely on self-organization and self-renewal. As this culture technique focusses on the progenitor/stem cells of the organ and because the culture conditions facilitate the selection of these cells, organoids can be passaged and propagated longer when compared to their 2D equivalents.

Airway organoids

The first airway organoids were described as early as 1993 (Benali et al. 1993). Since then, lung organoids derived from human lung tissues or derived from hiPSC have been successfully used to study lung development and disease (Barkauskas et al. 2013; Tata et al. 2013; Chen et al. 2017). These methods previously required supporting feeder cells to grow, but more recently the long-term mesenchymal cell-free expansion of airway organoids was demonstrated (Sachs et al. 2019). This allows for the reliable clonal expansion of airway cells and has opened new avenues of research.

Alveolar organoids

Growing organoids from alveolar tissue has proven to be more challenging, however the reward could potentially be much greater as the proliferating AEC2, that serves as a progenitor for the non-proliferating AEC1, rapidly loses its phenotype when plated on conventional culture plastic (Mao et al. 2015). However, when seeded in a 3D hydrogel the phenotype appears to be maintained for longer periods of time and the cells could be expanded and used for experiments (Glisinski et al. 2020; Barkauskas et al. 2017). To date, unfortunately, limited work has been done on primary human alveolar epithelial organoids and various studies describe the need for supporting mesenchymal cells. The ability to expand the AEC2 reliably under feeder-free conditions while maintaining phenotype could have major implications for the field. The 3D culture also has major implications in the hiPSC field, both in differentiation and in propagation. hiPSC-derived organoid cultures showed cell maturation of the alveolar epithelium (Jacob et al. 2017; Dye et al. 2015). Interestingly, 3D co-culture with human fetal lung fibroblasts and stimulation with DCIK resulted in expression of AEC2 specific markers and lamellar bodies formation, although functional maturity was not confirmed (Gotoh et al. 2014). Long-term expansion of hiPSC-derived alveolar epithelial cells, a challenge with conventional 2D distal lung cell cultures, was recently achieved using an organoid approach and a refined differentiation sequence after AFE induction (Yamamoto et al. 2017). This sequence differs from previous protocols by more closely mimicking the distal tip cell microenvironment through a preconditioning step of WNT activation, Notch inhibition, and FGF10 plus KGF supplementation. These cells were then matured using DCIK in organoids co-cultured with fibroblasts. Interestingly, co-cultures with fetal lung fibroblasts lines resulted in SFTPC-expressing cells (with substantial variability ranging from 2% to 51% SFTPC⁺ cells), whereas incorporating a dermal fibroblast line showed no SFTPC induction. Upon passaging, the proportion of AEC2 cells in the culture increased to approximately 70%, and AEC1-like cells were also present.

Nevertheless, there are also limitations as reviewed by Fatehullah et al. (Fatehullah, Tan, and Barker 2016). Lung organoids consist solely of epithelial cells (with or without supporting feeder fibroblasts) and thus lack the native organ microenvironment and appropriate architecture that is facilitated by structural cells and is often essential in disease development, tissue growth and repair. A further drawback of organoid culture is that they are fluid-filled

with an inward turned lumen, making the apical side of the epithelial cells inaccessible. Analysis or stimulation via the physiological relevant side (e.g. using airborne substances) is impossible or at least impractical. Measuring transmembrane transporter activity via indirect methods in gut organoids have been optimized in the context of cystic fibrosis research (Dekkers et al. 2016). Evaluating the transport and metabolism of drugs across the cell layer, or quantifying the release of inflammatory mediators or newly formed virions, is often precluded by the difficulty of accessing and sampling luminal contents. Furthermore, as the organoids are suspended in a hydrogel matrix, it is unclear if all stimuli concentrations are equally distributed as their distribution may be hampered by slow diffusion through the matrix. In addition, as the organoids consist of only epithelial cells, they lack tissue-tissue interfaces, such as the interface between vascular endothelium and surrounding stroma and the accompanying immune cells, which are essential for the morphology and function of virtually all organs.

All the above discussed culture methods or techniques are frequently used in pulmonary research and have provided seminal insight in lung biology. However, all these methods lack basic biomechanical forces. The lung is a flexible dynamic organ that is in continuous motion. The next step in modelling the human lung is incorporating physiological fluidic and biomechanical cues, including flow of air or liquid, in an effort to mimic what cells experience *in vivo*.

Organ-on-Chip technology

Organ-on-Chip or Lung-on-Chip are another culture model that has rapidly evolved in the past decade. These platforms are micro-engineered culture systems that allow continuous perfusion of microchannels on which the cells can be exposed to the biomechanical forces discussed in the previous section. The “chip” can be constructed to focus on key aspects of the organ of interest. For lung physiology, air and liquid flow are important as well as cyclic stretch which represents breathing (Benam et al. 2016; Huh, Hamilton, and Ingber 2011; Huh et al. 2010). The lung-on-chip would provide more complexity than can be achieved using static air-liquid interface culture. This is important as the influence of the biomechanical forces on the lung and alveolar biology is incompletely understood and the lung-on-chip could play a critical role in elucidating these interactions (Waters, Roan, and Navajas 2012). The Lung-on-Chip has the potential to play a role in large scale screening of compounds

and therapeutics, although further development in both our understanding of the biology of cell behaviour in chips as well as a wider distribution and acceptance is needed to achieve this. This is however important, since for instance the mechanical forces, like stretch, of the chip on the cells influence cell function and can alter drug and compound responses (Hassell et al. 2017), and therefore testing on a Lung-on-Chip may better predict the *in vivo* situation. Another interesting possibility would be to mimic the mechanical consequences of disease progression like the remodelling of the epithelium that occurs in COPD or asthma (Grainge et al. 2011). A further consideration is the material used in the chip as the properties of the material influence different aspects. The materials need to be selected to provide structural support to the cells, but also needs to tolerate the mechanical forces, and support instrumentation for tissue maintenance and experimental readouts. Optimally, the material of the chip needs to be non-toxic, optically clear, affordable, non-degrading under cell culture conditions, flexible to allow stretching, and not altering the chemistry of the fluid environment. Furthermore, the properties of the substrate the cells are grown on, such as the stiffness, flexibility, curvature or adsorption, among others can influence different cellular differentiation and function (Riaz et al. 2016; Discher, Janmey, and Wang 2005). These parameters can influence migration (Zaman et al. 2006), proliferation (Ulrich, de Juan Pardo, and Kumar 2009), metabolism (Park et al. 2020) or differentiation (Engler et al. 2004) and likely much more cellular properties, that we are only just starting to uncover. The integration all these factors and considerations into a chip allows for many new lines of research which have previously been impossible.

At present the organ-on-chip technology is in its infancy despite major developments in the last decade. Further development is essential and requires research performed by multidisciplinary teams, including biologists and engineers. The fact that the technique is both novel and expensive, explains why only few studies have been performed using this technology, making it difficult to validate and assess the applications.

Scope of this thesis

The study of airway repair, homeostasis and function requires suitable models. Human *in vitro* culture models could provide a way to reduce the use of animal models and generate data that can be better translated to patients. In the studies described in this thesis, an effort is made to explore various improvements of different current human *in vitro* models. In **chapter 2**, the use of human induced pluripotent stem cells as a source for obtaining alveolar cells is described. The use of these cells as a cell source could provide a patient-specific model for *in vitro* screenings. The generation of alveolar type 2 (AEC2)-like cells using our protocol is discussed and these cells were subsequently cultured at the air-liquid interface (ALI) to create a model of alveolar wound healing at the ALI. In **chapter 3**, we describe a method to utilize organoids to expand human alveolar cells to obtain sufficient numbers to reliably establish alveolar epithelial cell cultures. We isolated AEC2 from resected lung tissue using HTII-280 coated magnetic beads, and expanded these using organoid culture. Once sufficient cells were obtained, we seeded the cells on a lung-on-chip system to study the effect of flow and mechanical stretch on the alveolar cells. In **chapter 4** we continue on the use of organoids as a method of expanding cell populations. The technique is applied to obtain airway epithelial from clinical samples with low epithelial cell numbers. broncho-alveolar lavage (BAL) fluid from adults and tracheal aspirates (TA) from preterm new-borns was used to expand airway epithelial cells in organoid culture, followed by establishment of ALI cultures to allow exposure to airborne substances which is not possible using organoid models. In these studies, expansion using organoid or conventional submerged 2D culture (from respectively BAL and TA, or bronchial tissue) was compared using the properties of ALI cultures as read-out. The proposed culture method could provide a tool to study the early factors involved in the development of lung diseases, including those occurring early in life such as bronchopulmonary dysplasia (BPD). In **chapter 5**, we increased the cellular complexity of our models by including the cross-talk between polarized macrophages and airway epithelial cells. In lung tissue, every process relies on the interplay between various cell types, which is often not reflected in *in vitro* models. We therefore developed a co-culture model to study the effect of macrophage-epithelial interactions on airway epithelial wound repair. In **chapter 6**, we focussed on the substrates on which lung epithelial cells can be grown. To this end, we evaluated the use of a bio-compatible polymer of poly(trimethylene carbonate) (PTMC) for generation of culture membranes. PTMC has the

theoretical advantage over competitors used in organ-chips, that it is not rigid, more flexible (and thus allows stretching) and may be less susceptible to non-specific adsorption. We thus aimed evaluated the use of PTMC membranes in our primary human airway epithelial culture model. Finally, in **chapter 7** the findings of the studies presented in this thesis are summarized and discussed in a wider context of the field together with possible future perspectives.

References

- Amatngalim, G. D., W. Broekman, N. M. Daniel, L. E. van der Vlugt, A. van Schadewijk, C. Taube, and P. S. Hiemstra. 2016. 'Cigarette Smoke Modulates Repair and Innate Immunity following Injury to Airway Epithelial Cells', *PLoS One*, 11: e0166255.
- Amatngalim, G. D., J. A. Schrupf, F. Dishchekenian, T. C. J. Mertens, D. K. Ninaber, A. C. van der Linden, C. Pilette, C. Taube, P. S. Hiemstra, and A. M. van der Does. 2018. 'Aberrant epithelial differentiation by cigarette smoke dysregulates respiratory host defence', *Eur Respir J*, 51.
- Andreeva, A. V., M. A. Kutuzov, and T. A. Voyno-Yasenetskaya. 2007. 'Regulation of surfactant secretion in alveolar type II cells', *Am J Physiol Lung Cell Mol Physiol*, 293: L259-71.
- Banerjee, B., A. Kicic, M. Musk, E. N. Soutanto, S. M. Stick, and D. C. Chambers. 2009. 'Successful establishment of primary small airway cell cultures in human lung transplantation', *Respir Res*, 10: 99.
- Banga, A., F. A. Witzmann, H. I. Petrache, and B. L. Blazer-Yost. 2012. 'Functional effects of nanoparticle exposure on Calu-3 airway epithelial cells', *Cell Physiol Biochem*, 29: 197-212.
- Barkauskas, C. E., M. I. Chung, B. Fioret, X. Gao, H. Katsura, and B. L. Hogan. 2017. 'Lung organoids: current uses and future promise', *Development*, 144: 986-97.
- Barkauskas, C. E., M. J. Crouce, C. R. Rackley, E. J. Bowie, D. R. Keene, B. R. Stripp, S. H. Randell, P. W. Noble, and B. L. Hogan. 2013. 'Type 2 alveolar cells are stem cells in adult lung', *J Clin Invest*, 123: 3025-36.
- Beers, M. F., and Y. Moodley. 2017. 'When Is an Alveolar Type 2 Cell an Alveolar Type 2 Cell? A Conundrum for Lung Stem Cell Biology and Regenerative Medicine', *Am J Respir Cell Mol Biol*, 57: 18-27.
- Benali, R., J. M. Tournier, M. Chevillard, J. M. Zahm, J. M. Klossek, J. Hinnrasky, D. Gaillard, F. X. Maquart, and E. Puchelle. 1993. 'Tubule formation by human surface respiratory epithelial cells cultured in a three-dimensional collagen lattice', *Am J Physiol*, 264: L183-92.
- Benam, K. H., R. Villenave, C. Lucchesi, A. Varone, C. Hubeau, H. H. Lee, S. E. Alves, M. Salmon, T. C. Ferrante, J. C. Weaver, A. Bahinski, G. A. Hamilton, and D. E. Ingber. 2016. 'Small airway-on-a-chip enables analysis of human lung inflammation and drug responses *in vitro*', *Nat Methods*, 13: 151-7.
- Brewington, J. J., E. T. Filbrandt, F. J. LaRosa, 3rd, J. D. Moncivais, A. J. Ostmann, L. M. Strecker, and J. P. Clancy. 2018. 'Brushed nasal epithelial cells are a surrogate for bronchial epithelial CFTR studies', *JCI Insight*, 3.
- Brix, J., Y. Zhou, and Y. Luo. 2015. 'The Epigenetic Reprogramming Roadmap in Generation of iPSCs from Somatic Cells', *J Genet Genomics*, 42: 661-70.
- Byrne, A. J., S. A. Mathie, L. G. Gregory, and C. M. Lloyd. 2015. 'Pulmonary macrophages: key players in the innate defence of the airways', *Thorax*, 70: 1189-96.
- Cai, J., Y. Zhao, Y. Liu, F. Ye, Z. Song, H. Qin, S. Meng, Y. Chen, R. Zhou, X. Song, Y. Guo, M. Ding, and H. Deng. 2007. 'Directed differentiation of human embryonic stem cells into functional hepatic cells', *Hepatology*, 45: 1229-39.
- Chen, Y. W., S. X. Huang, Alrt de Carvalho, S. H. Ho, M. N. Islam, S. Volpi, L. D. Notarangelo, M. Ciancanelli, J. L. Casanova, J. Bhattacharya, A. F. Liang, L. M. Palermo, M. Porotto, A. Moscona, and H. W. Snoeck. 2017. 'A three-dimensional model of human lung development and disease from pluripotent stem cells', *Nat Cell Biol*, 19: 542-49.
- Crystal, R. G., S. H. Randell, J. F. Engelhardt, J. Voynow, and M. E. Sunday. 2008. 'Airway epithelial cells: current concepts and challenges', *Proc Am Thorac Soc*, 5: 772-7.
- Cuevas, E., P. Parmar, and J. C. Sowden. 2019. 'Restoring Vision Using Stem Cells and Transplantation', *Adv Exp Med Biol*, 1185: 563-67.
- D'Amour, K. A., A. G. Bang, S. Eliazzer, O. G. Kelly, A. D. Agulnick, N. G. Smart, M. A. Moorman, E. Kroon, M. K. Carpenter, and E. E. Baetge. 2006. 'Production of pancreatic hormone-expressing endocrine cells from human embryonic stem cells', *Nat Biotechnol*, 24: 1392-401.
- de Carvalho, Alrt, A. Strikoudis, H. Y. Liu, Y. W. Chen, T. J. Dantas, R. B. Vallee, J. Correia-Pinto, and H. W. Snoeck. 2019. 'Glycogen synthase kinase 3 induces multilineage maturation of human pluripotent stem cell-derived lung progenitors in 3D culture', *Development*, 146.
- Dekkers, J. F., G. Berkers, E. Kruijselbrink, A. Vonk, H. R. de Jonge, H. M. Janssens, I. Bronsveld, E. A. van de Graaf, E. E. Nieuwenhuis, R. H. Houwen, F. P. Vleggaar, J. C. Escher, Y. B. de Rijke, C. J. Majoor, H. G. Heijerman, K. M.

- de Winter-de Groot, H. Clevers, C. K. van der Ent, and J. M. Beekman. 2016. 'Characterizing responses to CFTR-modulating drugs using rectal organoids derived from subjects with cystic fibrosis', *Sci Transl Med*, 8: 344ra84.
- Discher, D. E., P. Janmey, and Y. L. Wang. 2005. 'Tissue cells feel and respond to the stiffness of their substrate', *Science*, 310: 1139-43.
- Dvorak, A., A. E. Tilley, R. Shaykhiev, R. Wang, and R. G. Crystal. 2011. 'Do airway epithelium air-liquid cultures represent the *in vivo* airway epithelium transcriptome?', *Am J Respir Cell Mol Biol*, 44: 465-73.
- Dye, B. R., P. H. Dedhia, A. J. Miller, M. S. Nagy, E. S. White, L. D. Shea, and J. R. Spence. 2016. 'A bioengineered niche promotes *in vivo* engraftment and maturation of pluripotent stem cell derived human lung organoids', *Elife*, 5.
- Dye, B. R., D. R. Hill, M. A. Ferguson, Y. H. Tsai, M. S. Nagy, R. Dyal, J. M. Wells, C. N. Mayhew, R. Nattiv, O. D. Klein, E. S. White, G. H. Deutsch, and J. R. Spence. 2015. '*In vitro* generation of human pluripotent stem cell derived lung organoids', *Elife*, 4.
- Engler, A. J., M. A. Griffin, S. Sen, C. G. Bonnemant, H. L. Sweeney, and D. E. Discher. 2004. 'Myotubes differentiate optimally on substrates with tissue-like stiffness: pathological implications for soft or stiff microenvironments', *J Cell Biol*, 166: 877-87.
- Fatehullah, A., S. H. Tan, and N. Barker. 2016. 'Organoids as an *in vitro* model of human development and disease', *Nat Cell Biol*, 18: 246-54.
- Firth, A. L., C. T. Dargitz, S. J. Qualls, T. Menon, R. Wright, O. Singer, F. H. Gage, A. Khanna, and I. M. Verma. 2014. 'Generation of multiciliated cells in functional airway epithelia from human induced pluripotent stem cells', *Proc Natl Acad Sci U S A*, 111: E1723-30.
- Garbi, N., and B. N. Lambrecht. 2017. 'Location, function, and ontogeny of pulmonary macrophages during the steady state', *Pflugers Arch*, 469: 561-72.
- Glisinski, K. M., A. J. Schlobohm, S. V. Paramore, A. Birukova, M. A. Moseley, M. W. Foster, and C. E. Barkauskas. 2020. 'Interleukin-13 disrupts type 2 pneumocyte stem cell activity', *JCI Insight*, 5.
- Gonzales, L. W., S. H. Guttentag, K. C. Wade, A. D. Postle, and P. L. Ballard. 2002. 'Differentiation of human pulmonary type II cells *in vitro* by glucocorticoid plus cAMP', *Am J Physiol Lung Cell Mol Physiol*, 283: L940-51.
- Gotoh, S., I. Ito, T. Nagasaki, Y. Yamamoto, S. Konishi, Y. Korogi, H. Matsumoto, S. Muro, T. Hirai, M. Funato, S. Mae, T. Toyoda, A. Sato-Otsubo, S. Ogawa, K. Osafune, and M. Mishima. 2014. 'Generation of alveolar epithelial spheroids via isolated progenitor cells from human pluripotent stem cells', *Stem Cell Reports*, 3: 394-403.
- Grainge, C. L., L. C. Lau, J. A. Ward, V. Dulay, G. Lahiff, S. Wilson, S. Holgate, D. E. Davies, and P. H. Howarth. 2011. 'Effect of bronchoconstriction on airway remodeling in asthma', *N Engl J Med*, 364: 2006-15.
- Gray, T. E., K. Guzman, C. W. Davis, L. H. Abdullah, and P. Nettesheim. 1996. 'Mucociliary differentiation of serially passaged normal human tracheobronchial epithelial cells', *Am J Respir Cell Mol Biol*, 14: 104-12.
- Green, M. D., A. Chen, M. C. Nostro, S. L. d'Souza, C. Schaniel, I. R. Lemischka, V. Gouon-Evans, G. Keller, and H. W. Snoeck. 2011. 'Generation of anterior foregut endoderm from human embryonic and induced pluripotent stem cells', *Nat Biotechnol*, 29: 267-72.
- Guilliams, M., I. De Kleer, S. Henri, S. Post, L. Vanhoutte, S. De Prijck, K. Deswarte, B. Malissen, H. Hammad, and B. N. Lambrecht. 2013. 'Alveolar macrophages develop from fetal monocytes that differentiate into long-lived cells in the first week of life via GM-CSF', *J Exp Med*, 210: 1977-92.
- Hassell, B. A., G. Goyal, E. Lee, A. Sontheimer Phelps, O. Levy, C. S. Chen, and D. E. Ingber. 2017. 'Human Organ Chip Models Recapitulate Orthotopic Lung Cancer Growth, Therapeutic Responses, and Tumor Dormancy *In Vitro*', *Cell Rep*, 21: 508-16.
- Hiemstra, P. S., P. B. McCray, Jr., and R. Bals. 2015. 'The innate immune function of airway epithelial cells in inflammatory lung disease', *Eur Respir J*, 45: 1150-62.
- Horvath, S. 2013. 'DNA methylation age of human tissues and cell types', *Genome Biol*, 14: R115.
- Huang, S. X., M. D. Green, A. T. de Carvalho, M. Mumau, Y. W. Chen, S. L. D'Souza, and H. W. Snoeck. 2015. 'The *in vitro* generation of lung and airway progenitor cells from human pluripotent stem cells', *Nat Protoc*, 10: 413-25.
- Huh, D., G. A. Hamilton, and D. E. Ingber. 2011. 'From 3D cell culture to organs-on-chips', *Trends Cell Biol*, 21: 745-54.

- Huh, D., B. D. Matthews, A. Mammoto, M. Montoya-Zavala, H. Y. Hsin, and D. E. Ingber. 2010. 'Reconstituting organ-level lung functions on a chip', *Science*, 328: 1662-8.
- Jacob, A., M. Morley, F. Hawkins, K. B. McCauley, J. C. Jean, H. Heins, C. L. Na, T. E. Weaver, M. Vedaie, K. Hurley, A. Hinds, S. J. Russo, S. Kook, W. Zacharias, M. Ochs, K. Traber, L. J. Quinton, A. Crane, B. R. Davis, F. V. White, J. Wambach, J. A. Whitsett, F. S. Cole, E. E. Morrissey, S. H. Guttentag, M. F. Beers, and D. N. Kotton. 2017. 'Differentiation of Human Pluripotent Stem Cells into Functional Lung Alveolar Epithelial Cells', *Cell Stem Cell*, 21: 472-88 e10.
- Kadzik, R. S., and E. E. Morrissey. 2012. 'Directing lung endoderm differentiation in pluripotent stem cells', *Cell Stem Cell*, 10: 355-61.
- Kimura, S., Y. Hara, T. Pineau, P. Fernandez Salguero, C. H. Fox, J. M. Ward, and F. J. Gonzalez. 1996. 'The T/ebp null mouse: thyroid-specific enhancer-binding protein is essential for the organogenesis of the thyroid, lung, ventral forebrain, and pituitary', *Genes Dev*, 10: 60-9.
- Konishi, S., S. Gotoh, K. Tateishi, Y. Yamamoto, Y. Korogi, T. Nagasaki, H. Matsumoto, S. Muro, T. Hirai, I. Ito, S. Tsukita, and M. Mishima. 2016. 'Directed Induction of Functional Multi-ciliated Cells in Proximal Airway Epithelial Spheroids from Human Pluripotent Stem Cells', *Stem Cell Reports*, 6: 18-25.
- Lee, J. H., D. H. Bhang, A. Beede, T. L. Huang, B. R. Stripp, K. D. Bloch, A. J. Wagers, Y. H. Tseng, S. Ryeom, and C. F. Kim. 2014. 'Lung stem cell differentiation in mice directed by endothelial cells via a BMP4-NFATc1-thrombospondin-1 axis', *Cell*, 156: 440-55.
- Leist, M., and T. Hartung. 2013. 'Inflammatory findings on species extrapolations: humans are definitely no 70-kg mice', *Arch Toxicol*, 87: 563-7.
- Liao, B. Y., and J. Zhang. 2008. 'Null mutations in human and mouse orthologs frequently result in different phenotypes', *Proc Natl Acad Sci U S A*, 105: 6987-92.
- Lieber, M., B. Smith, A. Szakal, W. Nelson-Rees, and G. Todaro. 1976. 'A continuous tumor-cell line from a human lung carcinoma with properties of type II alveolar epithelial cells', *Int J Cancer*, 17: 62-70.
- Livraghi, A., and S. H. Randell. 2007. 'Cystic fibrosis and other respiratory diseases of impaired mucus clearance', *Toxicol Pathol*, 35: 116-29.
- Malavia, N. K., C. B. Raub, S. B. Mahon, M. Brenner, R. A. Panettieri, Jr., and S. C. George. 2009. 'Airway epithelium stimulates smooth muscle proliferation', *Am J Respir Cell Mol Biol*, 41: 297-304.
- Mao, P., S. Wu, J. Li, W. Fu, W. He, X. Liu, A. S. Slutsky, H. Zhang, and Y. Li. 2015. 'Human alveolar epithelial type II cells in primary culture', *Physiol Rep*, 3.
- McCauley, K. B., F. Hawkins, M. Serra, D. C. Thomas, A. Jacob, and D. N. Kotton. 2017. 'Efficient Derivation of Functional Human Airway Epithelium from Pluripotent Stem Cells via Temporal Regulation of Wnt Signaling', *Cell Stem Cell*, 20: 844-57 e6.
- Montoro, D. T., A. L. Haber, M. Biton, V. Vinarsky, B. Lin, S. E. Birket, F. Yuan, S. Chen, H. M. Leung, J. Villoria, N. Rogel, G. Burgin, A. M. Tsankov, A. Waghray, M. Slyper, J. Waldman, L. Nguyen, D. Dionne, O. Rozenblatt-Rosen, P. R. Tata, H. Mou, M. Shivaraju, H. Bihler, M. Mense, G. J. Tearney, S. M. Rowe, J. F. Engelhardt, A. Regev, and J. Rajagopal. 2018. 'A revised airway epithelial hierarchy includes CFTR-expressing ionocytes', *Nature*, 560: 319-24.
- Morrissey, E. E., and B. L. Hogan. 2010. 'Preparing for the first breath: genetic and cellular mechanisms in lung development', *Dev Cell*, 18: 8-23.
- Mou, H., V. Vinarsky, P. R. Tata, K. Brazauskas, S. H. Choi, A. K. Croke, B. Zhang, G. M. Solomon, B. Turner, H. Bihler, J. Harrington, A. Lapey, C. Channick, C. Keyes, A. Freund, S. Artandi, M. Mense, S. Rowe, J. F. Engelhardt, Y. C. Hsu, and J. Rajagopal. 2016. 'Dual SMAD Signaling Inhibition Enables Long-Term Expansion of Diverse Epithelial Basal Cells', *Cell Stem Cell*, 19: 217-31.
- Mullane, K. 2011. 'The increasing challenge of discovering asthma drugs', *Biochem Pharmacol*, 82: 586-99.
- Murry, C. E., and G. Keller. 2008. 'Differentiation of embryonic stem cells to clinically relevant populations: lessons from embryonic development', *Cell*, 132: 661-80.
- Nawroth, J. C., R. Barrile, D. Conegliano, S. van Riet, P. S. Hiemstra, and R. Villenave. 2019. 'Stem cell-based Lung-on-Chips: The best of both worlds?', *Adv Drug Deliv Rev*, 140: 12-32.
- Nishizawa, M., K. Chonabayashi, M. Nomura, A. Tanaka, M. Nakamura, A. Inagaki, M. Nishikawa, I. Takei, A. Oishi, K. Tanabe, M. Ohnuki, H. Yokota, M. Koyanagi-Aoi, K. Okita, A. Watanabe,

- A. Takaori-Kondo, S. Yamanaka, and Y. Yoshida. 2016. 'Epigenetic Variation between Human Induced Pluripotent Stem Cell Lines Is an Indicator of Differentiation Capacity', *Cell Stem Cell*, 19: 341-54.
- Oswald, J., and P. Baranov. 2018. 'Regenerative medicine in the retina: from stem cells to cell replacement therapy', *Ther Adv Ophthalmol*, 10: 2515841418774433.
- Papp, B., and K. Plath. 2011. 'Reprogramming to pluripotency: stepwise resetting of the epigenetic landscape', *Cell Res*, 21: 486-501.
- Park, J. S., C. J. Burckhardt, R. Lazcano, L. M. Solis, T. Isogai, L. Li, C. S. Chen, B. Gao, J. D. Minna, R. Bachoo, R. J. DeBerardinis, and G. Danuser. 2020. 'Mechanical regulation of glycolysis via cytoskeleton architecture', *Nature*, 578: 621-26.
- Plasschaert, L. W., R. Zilionis, R. Choo-Wing, V. Savova, J. Knehr, G. Roma, A. M. Klein, and A. B. Jaffe. 2018. 'A single-cell atlas of the airway epithelium reveals the CFTR-rich pulmonary ionocyte', *Nature*, 560: 377-81.
- Reddel, R. R., Y. Ke, B. I. Gerwin, M. G. McMenamin, J. F. Lechner, R. T. Su, D. E. Brash, J. B. Park, J. S. Rhim, and C. C. Harris. 1988. 'Transformation of human bronchial epithelial cells by infection with SV40 or adenovirus-12 SV40 hybrid virus, or transfection via strontium phosphate coprecipitation with a plasmid containing SV40 early region genes', *Cancer Res*, 48: 1904-9.
- Riaz, M., M. Versaevel, D. Mohammed, K. Glinel, and S. Gabriele. 2016. 'Persistence of fan-shaped keratocytes is a matrix-rigidity-dependent mechanism that requires alpha5beta1 integrin engagement', *Sci Rep*, 6: 34141.
- Rock, J. R., S. H. Randell, and B. L. Hogan. 2010. 'Airway basal stem cells: a perspective on their roles in epithelial homeostasis and remodeling', *Dis Model Mech*, 3: 545-56.
- Ross, A. J., L. A. Dailey, L. E. Brighton, and R. B. Devlin. 2007. 'Transcriptional profiling of mucociliary differentiation in human airway epithelial cells', *Am J Respir Cell Mol Biol*, 37: 169-85.
- Sachs, N., A. Paspaspyropoulos, D. D. Zomer-van Ommen, I. Heo, L. Bottinger, D. Klay, F. Weeber, G. Huelsz-Prince, N. Iakobachvili, G. D. Amatngalim, J. de Ligt, A. van Hoeck, N. Proost, M. C. Viveen, A. Lyubimova, L. Teeven, S. Derakhshan, J. Korving, H. Begthel, J. F. Dekkers, K. Kumawat, E. Ramos, M. F. van Oosterhout, G. J. Offerhaus, D. J. Wiener, E. P. Olimpio, K. K. Dijkstra, E. F. Smit, M. van der Linden, S. Jaksani, M. van de Ven, J. Jonkers, A. C. Rios, E. E. Voest, C. H. van Moorsel, C. K. van der Ent, E. Cuppen, A. van Oudenaarden, F. E. Coenjaerts, L. Meyaard, L. J. Bont, P. J. Peters, S. J. Tans, J. S. van Zon, S. F. Boj, R. G. Vries, J. M. Beekman, and H. Clevers. 2019. 'Long-term expanding human airway organoids for disease modeling', *EMBO J*, 38.
- Schiller, H. B., D. T. Montoro, L. M. Simon, E. L. Rawlins, K. B. Meyer, M. Strunz, F. A. Vieira Braga, W. Timens, G. H. Koppelman, G. R. S. Budinger, J. K. Burgess, A. Waghray, M. van den Berge, F. J. Theis, A. Regev, N. Kaminski, J. Rajagopal, S. A. Teichmann, A. V. Misharin, and M. C. Nawijn. 2019. 'The Human Lung Cell Atlas: A High-Resolution Reference Map of the Human Lung in Health and Disease', *Am J Respir Cell Mol Biol*, 61: 31-41.
- Spence, J. R., C. N. Mayhew, S. A. Rankin, M. F. Kuhar, J. E. Vallance, K. Tolle, E. E. Hoskins, V. V. Kalinichenko, S. I. Wells, A. M. Zorn, N. F. Shroyer, and J. M. Wells. 2011. 'Directed differentiation of human pluripotent stem cells into intestinal tissue *in vitro*', *Nature*, 470: 105-9.
- Takahashi, K., K. Tanabe, M. Ohnuki, M. Narita, T. Ichisaka, K. Tomoda, and S. Yamanaka. 2007. 'Induction of pluripotent stem cells from adult human fibroblasts by defined factors', *Cell*, 131: 861-72.
- Takahashi, K., and S. Yamanaka. 2006. 'Induction of pluripotent stem cells from mouse embryonic and adult fibroblast cultures by defined factors', *Cell*, 126: 663-76.
- Tata, P. R., H. Mou, A. Pardo-Saganta, R. Zhao, M. Prabhu, B. M. Law, V. Vinarsky, J. L. Cho, S. Breton, A. Sahay, B. D. Medoff, and J. Rajagopal. 2013. 'Dedifferentiation of committed epithelial cells into stem cells *in vivo*', *Nature*, 503: 218-23.
- Thomson, J. A., J. Itskovitz-Eldor, S. S. Shapiro, M. A. Waknitz, J. J. Swiergiel, V. S. Marshall, and J. M. Jones. 1998. 'Embryonic stem cell lines derived from human blastocysts', *Science*, 282: 1145-7.
- Uhl, E. W., and N. J. Warner. 2015. 'Mouse Models as Predictors of Human Responses: Evolutionary Medicine', *Curr Pathobiol Rep*, 3: 219-23.
- Ulrich, T. A., E. M. de Juan Pardo, and S. Kumar. 2009. 'The mechanical rigidity of the extracellular matrix regulates the structure, motility, and proliferation of glioma cells', *Cancer Res*, 69: 4167-74.

- Vaskova, E. A., A. E. Stekleneva, S. P. Medvedev, and S. M. Zakian. 2013. "Epigenetic memory" phenomenon in induced pluripotent stem cells', *Acta Naturae*, 5: 15-21.
- Wade, K. C., S. H. Guttentag, L. W. Gonzales, K. L. Maschhoff, J. Gonzales, V. Kolla, S. Singhal, and P. L. Ballard. 2006. 'Gene induction during differentiation of human pulmonary type II cells *in vitro*', *Am J Respir Cell Mol Biol*, 34: 727-37.
- Waters, C. M., E. Roan, and D. Navajas. 2012. 'Mechanobiology in lung epithelial cells: measurements, perturbations, and responses', *Compr Physiol*, 2: 1-29.
- Wong, A. P., C. E. Bear, S. Chin, P. Pasceri, T. O. Thompson, L. J. Huan, F. Ratjen, J. Ellis, and J. Rossant. 2012. 'Directed differentiation of human pluripotent stem cells into mature airway epithelia expressing functional CFTR protein', *Nat Biotechnol*, 30: 876-82.
- Wong, A. P., S. Chin, S. Xia, J. Garner, C. E. Bear, and J. Rossant. 2015. 'Efficient generation of functional CFTR-expressing airway epithelial cells from human pluripotent stem cells', *Nat Protoc*, 10: 363-81.
- World Health Organization. 2017. 'The Global Impact of Respiratory Disease'. https://www.who.int/gard/publications/The_Global_Impact_of_Respiratory_Disease.pdf
- World Health Organization. 2018. 'The top 1 causes of death'. <http://www.who.int/mediacentre/factsheets/fs310/en/>
- Xu, R. H., X. Chen, D. S. Li, R. Li, G. C. Addicks, C. Glennon, T. P. Zwaka, and J. A. Thomson. 2002. 'BMP4 initiates human embryonic stem cell differentiation to trophoblast', *Nat Biotechnol*, 20: 1261-4.
- Xu, Y., T. Mizuno, A. Sridharan, Y. Du, M. Guo, J. Tang, K. A. Wikenheiser-Brokamp, A. T. Perl, V. A. Funari, J. J. Gokey, B. R. Stripp, and J. A. Whitsett. 2016. 'Single-cell RNA sequencing identifies diverse roles of epithelial cells in idiopathic pulmonary fibrosis', *JCI Insight*, 1: e90558.
- Yamamoto, Y., S. Gotoh, Y. Korogi, M. Seki, S. Konishi, S. Ikeo, N. Sone, T. Nagasaki, H. Matsumoto, S. Muro, I. Ito, T. Hirai, T. Kohno, Y. Suzuki, and M. Mishima. 2017. 'Long-term expansion of alveolar stem cells derived from human iPS cells in organoids', *Nat Methods*, 14: 1097-106.
- Zaman, M. H., L. M. Trapani, A. L. Sieminski, D. Mackellar, H. Gong, R. D. Kamm, A. Wells, D. A. Lauffenburger, and P. Matsudaira. 2006. 'Migration of tumor cells in 3D matrices is governed by matrix stiffness along with cell-matrix adhesion and proteolysis', *Proc Natl Acad Sci U S A*, 103: 10889-94.

CHAPTER 2

In vitro modelling of alveolar repair at the air-liquid interface using alveolar epithelial cells derived from human induced pluripotent stem cells

Sander van Riet¹, Dennis K. Ninaber¹, Harald M. M. Mikkers^{2,3}, Teresa D. Tetley⁵, Carolina R. Jost², Aat A. Mulder², Thijs Pasman⁶, Danielle Baptista⁷, André A. Poot⁶, Roman Truckenmüller⁷, Christine L. Mummery⁴, Christian Freund^{3,4}, Robbert J. Rottier⁸, Pieter S. Hiemstra¹

¹Department of Pulmonology, ²Department of Cell and Chemical Biology, ³LUMC hiPSC core facility, ⁴Department of Anatomy and Embryology, Leiden University Medical Center, Leiden, The Netherlands; ⁵National Heart & Lung Institute, Imperial College London, London, United Kingdom; ⁶Department of Biomaterials Science and Technology, Technical Medical (TechMed) Centre, Faculty of Science and Technology, University of Twente, Enschede, The Netherlands; ⁷Department of Instructive Biomaterials Engineering, MERLN Institute for Technology-Inspired Regenerative Medicine, Maastricht University, Maastricht, The Netherlands; ⁸Department of Pediatric Surgery, Erasmus MC-Sophia Children's Hospital, Rotterdam, The Netherlands

Scientific Reports 2020 Mar 26;10(1):5499.

Abstract

Research on acute and chronic lung diseases would greatly benefit from reproducible availability of alveolar epithelial cells (AEC). Primary alveolar epithelial cells can be derived from human lung tissue but the quality of these cells is highly donor dependent. Here, we demonstrated that culture of EpCAM⁺ cells derived from human induced pluripotent stem cells (hiPSC) at the physiological air-liquid interface (ALI) resulted in type 2 AEC-like cells (iAEC2) with alveolar characteristics. iAEC2 cells expressed native AEC2 markers (surfactant proteins and LPCAT-1) and contained lamellar bodies. ALI-iAEC2 were used to study alveolar repair over a period of 2 weeks following mechanical wounding of the cultures and the responses were compared with those obtained using primary AEC2 (pAEC2) isolated from resected lung tissue. Addition of the Wnt/ β -catenin activator CHIR99021 reduced wound closure in the iAEC2 cultures but not pAEC2 cultures. This was accompanied by decreased surfactant protein expression and accumulation of podoplanin-positive cells at the wound edge. These results demonstrated the feasibility of studying alveolar repair using hiPSC-AEC2 cultured at the ALI and indicated that this model can be used in the future to study modulation of alveolar repair by (pharmaceutical) compounds.

Introduction

Alveolar injury resulting in decreased lung function is a hallmark of various acute and chronic lung diseases. These include acute respiratory distress syndrome (ARDS), emphysema in chronic obstructive pulmonary disease (COPD) and idiopathic pulmonary fibrosis (Guillot et al. 2013; Whitsett and Weaver 2015). The alveolar epithelium consists of flattened type 1 alveolar epithelial cells (AEC1) that allow gas exchange and the cuboidal type 2 alveolar epithelial cells (AEC2) that produce surfactant, mediate host defence and act as local progenitors for the AEC1 (Herriges and Morrissey 2014; Whitsett and Weaver 2015). These AEC are a primary target for inhaled substances; injury to these cells is considered a major initiating event for many lung diseases, including those above. Endogenous repair has been shown to contribute to recovery following injury, but in chronic lung diseases these repair processes are either insufficient or impaired (Hogan et al. 2014; Chambers and Mercer 2015; Rock and Konigshoff 2012; Kneidinger et al. 2011; Skronska-Wasek et al. 2017). This results in cumulative damage to the alveolar compartment and subsequently reduced diffusion capacity and lung function. Treatments aimed at alveolar repair and improving the alveolar barrier integrity are urgently needed but none are yet available. Targeting signalling pathways that have been shown to be involved in lung repair, including bone morphogenetic protein (BMP)/transforming growth factor- β (TGF- β), Hedgehog, fibroblast growth factor (FGF), Notch and Wnt signalling (Rock and Konigshoff 2012; Schilders et al. 2016), might be attractive therapeutic options. Notably among these, Wnt/ β -catenin signalling is impaired in AEC in COPD as well as in experimental emphysema in mice (Baarsma et al. 2017; Kneidinger et al. 2011; Skronska-Wasek et al. 2017).

For the development of therapies that target AEC, a human (preferable patient-specific) *in vitro* alveolar repair model would be of great benefit. Tumour cell lines (A549), immortalized AEC1 and primary AEC are currently most widely used for *in vitro* studies (van den Bogaard et al. 2009; Mao et al. 2015). However, immortal cell lines do not fully capture the complexity of the alveolar epithelium. Primary human AEC2 (pAEC2) can be isolated from resected lung tissue but nearly all patients undergoing lung surgery have an underlying disease that affects the yield and function of the isolated cells, making them less than ideal for large-scale screening or direct extrapolation of outcomes to other conditions (Witherden and Tetley 2001). The availability of normal lung tissue, e.g. from non-diseased human lungs otherwise discarded

as unsuitable for lung transplantation, is limited. Furthermore, fetal lungs, which could also be a source of AEC, may not be ideal to study repair of adult lung tissue. Importantly, the use of pAEC2 is further complicated by their inability to undergo passage in culture and tendency to differentiate spontaneously to terminally differentiated AEC1 confounding their use in lung repair studies (Logan and Desai 2015).

Since their initial description in 2007, human induced pluripotent stem cells (hiPSC) have been intensely used to study development and disease *in vitro*, and more recently for toxicity screening and drug discovery (Takahashi et al. 2007). hiPSC lines can be generated from any healthy individual or patient and thus potentially represent an unlimited source of tissue-specific cells, which can be used as *in vitro* models for screening effectiveness or toxicity of candidate therapeutic agents. Human AEC cultures have been successfully derived from human embryonic stem cells (Roszell et al. 2009; Rippon et al. 2008) and from hiPSC previously (Dye et al. 2015; Ghaedi et al. 2013; Ghaedi et al. 2014; Huang et al. 2014; Gotoh et al. 2014; Jacob et al. 2017; McCauley et al. 2017; Yamamoto et al. 2017; Tamo et al. 2018). These latter studies relied on directed differentiation of hiPSC into the endodermal lineage using Activin A, followed by differentiation of this definitive endoderm into foregut endoderm through inhibition of TGF- β and BMP signalling. An essential next step was the development of NKX2-1⁺ lung progenitors using a mixture of growth factors, that can be directed to an alveolar fate by continued culture on tissue culture plastic or embedding in an extracellular matrix as organoids (McCauley et al. 2017; Gotoh et al. 2014; Dye et al. 2015). Although, hiPSC-derived lung epithelial cells have been used for disease modelling (Crane et al. 2015), they have not yet been used to study alveolar repair. The aim of the present study was to investigate the feasibility of using hiPSC-derived AEC2 (iAEC2) cultured at the air-liquid interface (ALI) as an *in vitro* model to study alveolar repair and to compare this model with that using pAEC2 isolated from lung tissue.

Materials and methods

hiPSC maintenance and differentiation into alveolar epithelial cells

The hiPSC lines LUMC0044iCTRL44.9 and LUMC0065iCTRL08 were generated and characterized at the LUMC hiPSC core facility from female skin fibroblasts (Chen et al. 2017) or from erythroblasts derived from a healthy male donor using lentiviral (Warlich et al. 2011) or episomal vectors (Okita et al. 2011), respectively. The cells were maintained under fully defined serum-free conditions on vitronectin- (StemCell Technologies, Vancouver, Canada) coated 6-well tissue culture dishes (Corning, Corning, NY) in mTeSR1 medium (StemCell Technologies). The cells were passaged weekly (1:15 split ratio) using “Gentle Cell Dissociation Reagent” (StemCell Technologies).

iAEC2s were generated from hiPSCs by stepwise recapitulation of fetal lung development as shown schematically in Fig. 1, and outlined in the Results. A detailed description of the culture method and key reagents is listed in the online Supplement.

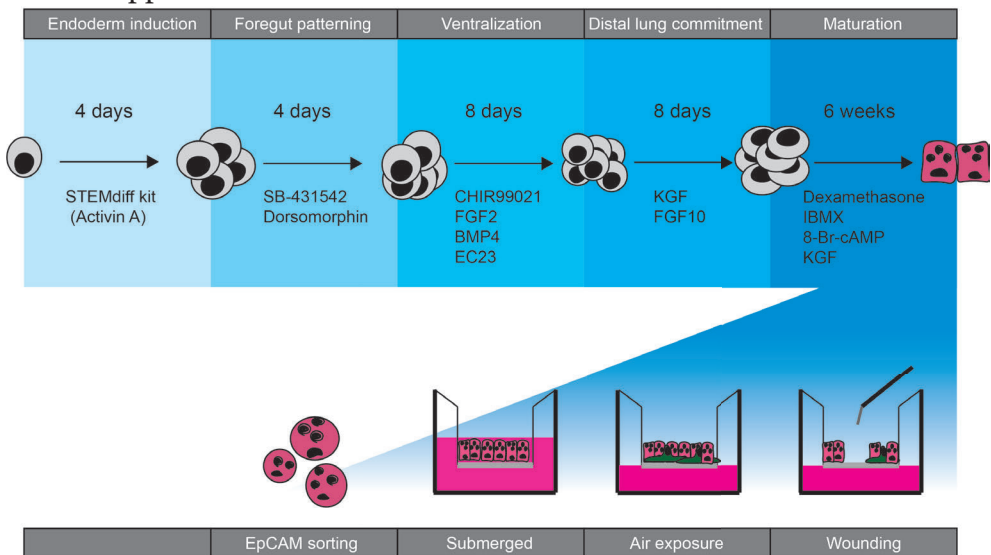


Figure 1. Overview of human induced pluripotent stem cell (hiPSC) differentiation into alveolar-like cells and culture at the air-liquid interface. The various steps followed to achieve differentiation of hiPSC towards an alveolar fate is schematized. Following 4 weeks of maturation, the cells are sorted based on EpCAM expression and seeded on the Transwell insert for further maturation and culture at the air-liquid interface. See supplement for details.

Isolation and culture of primary alveolar epithelial cells

pAEC2 were isolated from tumour-free lung tissue of patients undergoing lung resection at the Leiden University Medical Center (LUMC, The Netherlands). The use of surplus lung tissue for research following surgery was within the framework of patient care and in line with the “Human Tissue and Medical

Research: Code of conduct for responsible use” (2011) (www.federa.org) and followed advice of the LUMC Medical Ethical Committee. Tissue donation was based on a no-objection system for coded anonymous use of waste tissue, left-over from diagnostic or therapeutic procedures. “No-objection” negates the need for individual informed consent and was approved by the IRB. All methods were carried out in accordance with relevant guidelines and regulations. pAEC2 were isolated and cultured essentially as described (Witherden and Tetley 2001). Briefly, resected lung tissue was cut into pieces of approximately 5 cm³ and incubated with 10 ml trypsin (0.25% w/v in Hanks’ Balanced Salt Solution) for 15 min; this was repeated multiple times for a total incubation time of 45 min. Trypsin was then blocked using newborn calf serum (NBCS) (Sigma-Aldrich, St. Louis, MO). The tissue was cut into smaller pieces in the presence of NBCS and DNase (Sigma-Aldrich), and passed through strainers of different sizes to obtain single cells in suspension. These were plated in uncoated T75 flasks for 2 hours at 37 °C with serum-free DCCM-1 (Biological Industries, Kibbutz Beit-Haemek, Israel) medium to allow attachment of most non-AEC2. Following 2 hours of attachment, non-attached (pAEC2) cells were collected and seeded on 1% Purecol- (Advanced Biomatrix, Carlsbad, CA) coated Transwell inserts with 0.4 µm diameter pores (Corning). The pAEC2 were maintained in DCCM-1 with 10% (v/v) NBCS.

Quantitative real-time PCR

RNA isolation was performed using Maxwell tissue RNA extraction kit (Promega, Leiden, The Netherlands) according to the manufacturer’s protocol. RNA concentrations were determined using the NanoDrop

Gene	Forward (5’ to 3’)	Reverse (3’ to 5’)
<i>SOX2</i>	TGGACAGTTACGCGCACAT	CGAGTAGGACATGCTGTAGGT
<i>FOXA2</i>	ACTACCCCGGCTACGGTTC	AGGCCCGTTTTGTTCGTGA
<i>CPM</i>	GCGCTGGATTTCAACTACCAC	TCCCGCCAACAGTCTCAT
<i>NKX2-1</i>	AGCACACGACTCCGTTCTC	GCCCACTTTCTGTAGCTTTCC
<i>SOX17</i>	GTGGACCGCACGGAATTTG	GGAGATTCACACCGGAGTCA
<i>SOX9</i>	AGCGAACGCACATCAAGAC	CTGTAGGCGATCTGTTGGGG
<i>SFTPB</i>	CTTCCAGAACCAGACTGACTCA	GCTCGGAGAGATCCTGTGTG
<i>SFTPC</i>	CTCTCTGCAGGCCAAGCCCG	TTCCACTGACCCGGAGGCGT
<i>SFTPD</i>	CCTTACAGGGACAAGTACAGCA	CTGTGCCTCCGTAAATGGTTT
<i>OAZ1</i>	GGATCCTCAATAGCCACTGC	TACAGCAGTGGAGGGAGACC
<i>ATP5B</i>	TCACCCAGGCTGGTTCAGA	AGTGCCAGGGTAGGCTGAT
<i>PDPN</i>	AACCAGCGAAGACCGCTATAA	CGAATGCCTGTTACTACTGTTGA

Table 1. Primer sequences.

ND-1000 Spectrophotometer (NanoDrop Technologies, Wilmington, DE) and cDNA was synthesized by reversed transcription of 1 µg of RNA, using oligo-dT primers (Qiagen), dNTP (Promega), and M-MLV Polymerase (Promega) in the presence of RNasin (Promega). Quantitative real-time PCR (qPCR) was conducted using IQ SYBR green supermix (Bio-Rad, Hercules, CA) and a CFX-384 real-time PCR detection system (Bio-Rad). qPCR reactions were performed using the primers shown in Table 1. Reference genes *OAZ1* and *ATP5B* were selected using the NormFinder method (Andersen, Jensen, and Orntoft 2004). Bio-Rad CFX manager 3.1 software (Bio-Rad) was used to calculate the arbitrary gene expression using the Livak method.

Immunofluorescence

Cells were fixed in 4% paraformaldehyde for 1 hour at 4 °C, 100% methanol was added for permeabilization for 10 min at 4 °C, and non-specific binding sites were blocked in blocking solution consisting of 5% (w/v) BSA and 0.3% (v/v) Triton X100 in PBS. Between each step, cells were washed 3 times with PBS. Subsequently the cells were incubated overnight at 4 °C with primary antibody (Table 2) diluted in blocking solution. Next, filters were washed 3 times in PBS and stained with secondary antibody, and DAPI as nuclear staining. Secondary antibodies (Table 2) and DAPI were also diluted in blocking solution and incubated in the dark for 1 hour at room temperature. Afterwards, filters were washed 3 times with PBS and mounted on microscope slides using ProLong gold antifade (Thermo Fisher). Images were made using a Leica TCS SP8 confocal inverted microscope (Leica Microsystems, Wetzlar, Germany) and processed using the Leica Application Suite Advanced Fluorescence software (LAS AF, Leica Microsystems).

Protein	Company	Cat#	Dilution
<i>Primary antibodies</i>			
NKX2-1	Novus biological	NBP2-29434	1:100
Pro-SFTPC	R&D	H00006440-Do1P	1:200
LPCAT1	Atlas antibodies	HPA012501	1:100
Podoplanin	Abcam	ab10288	1:100
<i>Secondary antibodies</i>			
Alexa 568 donkey-anti-mouse	Invitrogen	A10037	1:200
Alexa 488 goat-anti-rabbit	Invitrogen	A11008	1:200
Alexa 568 donkey-anti-rabbit	Invitrogen	A10047	1:200

Table 2. Antibodies used for immunofluorescence.

Transepithelial electrical resistance

The epithelial barrier function of epithelial monolayer cultures was determined

by measuring the transepithelial electrical resistance (TEER) using the MilliCell-ERS (Millipore, Bedford, MA). TEER was expressed as $\Omega \cdot \text{cm}^2$.

Electron microscopy

Cells cultured on filter were fixed by adding double concentrated fixative 1 on 1 to the culture medium (3% GA / 0.2 M cacodylate, final concentration 1.5% GA / 0.1 M cacodylate buffer). After an 1 hour fixation cells were rinsed with 0.1 M cacodylate buffer and postfixed with 1% OsO₄ / 1.5% ferricyanide / 0.1 M cacodylate buffer. After rinsing with cacodylate buffer a second postfixation with 0.5% RuO₄ / MQ was performed. After rinsing with cacodylate buffer the filter with the fixed cells was carefully cut out from the Transwell, cut in small pieces of about 1 x 2 mm and dehydrated up to ethanol 70%, followed by mixtures of EPON LX-112 and ethanol 70%. The filter pieces were positioned in a mold, allowing cross sections of the filter. After polymerization of the EPON, 80 nm ultrathin sections were made, and after staining with uranyl acetate and lead citrate, the sections were examined with an electron microscope (FEI Tecnai T12 Twin, 120 kV). Overlapping images were collected and stitched together into separate images as previously described (Faas et al. 2012).

Wound healing assay

A circular wound assay was performed as described in (Amatngalim et al. 2016). Briefly, 500 μl PBS was added to the apical surface of the ALI-cultured AEC2 to facilitate mechanical wounding. The wound was applied by using a sterile Pasteur pipette with a soft tip to scrape the cell layer, creating a wound with a diameter of 3 mm. After wounding, the apical surface of the cultures was washed with 200 μl PBS to remove cellular debris. Wound healing was assessed by light microscopy, and images were taken at different time points. Images were analysed using NIH-ImageJ software (v1.50i).

Data analysis

Statistical analysis was performed in GraphPad PRISM 6.0 (GraphPad Software Inc., La Jolla, CA). Data was analysed using one-way ANOVA with Tukey correction, or for wound closure with two-way ANOVA multiple comparison test. Error bars depict SEM. Differences were considered significant at $p < 0.05$.

Results

Generation of induced type 2 alveolar epithelial cells (iAEC2s) from hiPSC

Selection of reference genes for monitoring differentiation. Gene expression is commonly used to monitor hiPSC differentiation since the cells undergo extensive phenotypic changes which can be monitored accurately using cell-type specific reference genes.

To identify the most suitable reference genes, we performed NormFinder analysis at the first step of differentiation (Andersen, Jensen, and Orntoft 2004). The variation of expression stability of 13 candidate reference genes in hiPSC and definitive endoderm (DE) cells was analysed. Fig. 2 shows the distribution of Cq values of 13 reference genes (Supplemental Table 1) in our hiPSC lines and their corresponding differentiated DE derivatives. Table 3 shows the stability values of all candidate reference genes as well as the inter-group variation. The three genes with the highest stability were *ATP5B* (0.243), *GNB2L* (0.278) and *OAZ1* (0.281), of which the former and latter were chosen for further studies. Notably, other frequently used reference genes

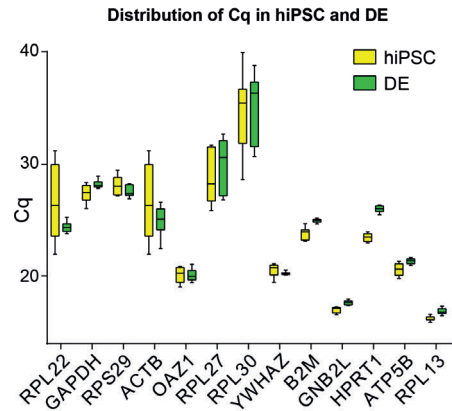


Figure 2. Identification of suitable reference genes using NormFinder. Expression value of commonly used reference genes showing the threshold values obtained by qPCR. Expression in LUMCoo44iCTRL44.9 and LUMCoo65iCTRL08 and derived definitive endoderm. (n=8 independent experiments)

Gene name	Stability value	Intergroup variation	hiPSC	DE
<i>ATP5B</i>	0.243	<i>ATP5B</i>	0.061	0.161
<i>GNB2L</i>	0.278	<i>GNB2L</i>	0.205	0.252
<i>OAZ1</i>	0.281	<i>OAZ1</i>	0.118	0.029
<i>RPL13</i>	0.305	<i>RPL13</i>	0.246	0.323
<i>GAPDH</i>	0.355	<i>GAPDH</i>	0.795	0.061
<i>B2M</i>	0.372	<i>B2M</i>	0.089	0.117
<i>YWHAZ</i>	0.393	<i>YWHAZ</i>	0.063	0.158
<i>RPS29</i>	0.556	<i>RPS29</i>	0.966	0.268
<i>RPL27</i>	0.625	<i>RPL27</i>	1.248	1.934
<i>RPL30</i>	0.786	<i>RPL30</i>	4.020	3.831
<i>HPRT1</i>	0.804	<i>HPRT1</i>	0.120	0.033
<i>ACTB</i>	0.845	<i>ACTB</i>	3.498	0.402

Table 3. Evaluation of reference gene stability using NormFinder in hiPSC and DE.

like *GAPDH*, *B2M* and *ACTB* showed either poor stability values or high Cq, making them less suitable for monitoring differentiation.

Development of differentiation protocol. An overview of the final differentiation protocol based on optimized procedures is shown in Fig. 1 and described in detail in the online supplement. Differentiation was monitored using markers described as being associated with different stages of differentiation as shown in Fig. 3 and SFig. 1. hiPSC were first plated in 6-well plates and directed towards DE. 4 days later, DE cells were present as evidenced by decreased expression of pluripotency genes and increased expression of the endodermal markers *SOX17* and *FOXA2* (Fig. 3A). DE cells were exposed to the SMAD2/3 inhibitor SB-431542 and the BMP inhibitor dorsomorphin to induce anterior foregut endoderm (AFE). Dorsomorphin resulted in a stronger increase in expression of AFE markers compared to treatment with the recombinant BMP inhibitor Noggin (SFig. 1). Successful generation of AFE was confirmed after 4 days of differentiation based on the decreased expression of the endodermal marker *SOX17*, maintenance of *FOXA2* expression, and increased *SOX2* expression (Fig. 3A) (Green et al. 2011). Following AFE induction, formation of ventral anterior foregut endoderm (VAFE) was induced using FGF2, BMP4, CHIR99021 (canonical Wnt-activator) and EC23 (retinoic acid pathway agonist). Following 8 days of differentiation directed towards VAFE, increased expression of *NKX2-1* and *CPM* was observed (Fig. 3A), which have been described as the earliest markers of lung development expressed in the VAFE (Gotoh et al. 2014; Huang et al. 2015). Expression of *NKX2-1* at this stage of differentiation was markedly enhanced by the presence of FGF2, and this was confirmed at the protein level by immunofluorescent staining of *NKX2-1* (Fig. 3B, C). Expression was observed in a subset of cells, indicating a heterogeneous population. Subsequently, the cells were directed to a lung progenitor phenotype expressing *SOX9* and *ID2* by 8 days of exposure to KGF and FGF10 (SFig. 3). Following progenitor differentiation, the cells were exposed to dexamethasone, KGF, IBMX and 8-Br-cAMP for 6 weeks to direct cells to an AEC2 phenotype. The development of AEC2-like cells was verified by immunofluorescent staining (Fig 3D, E) and mRNA expression of surfactant proteins (Fig. 3J).

In order to obtain a more enriched cell population, after 4 weeks of alveolarization EpCAM⁺ cells were isolated by MACS-based sorting, and the cells were next seeded on a Transwell insert and cultured for 2 weeks at the air-

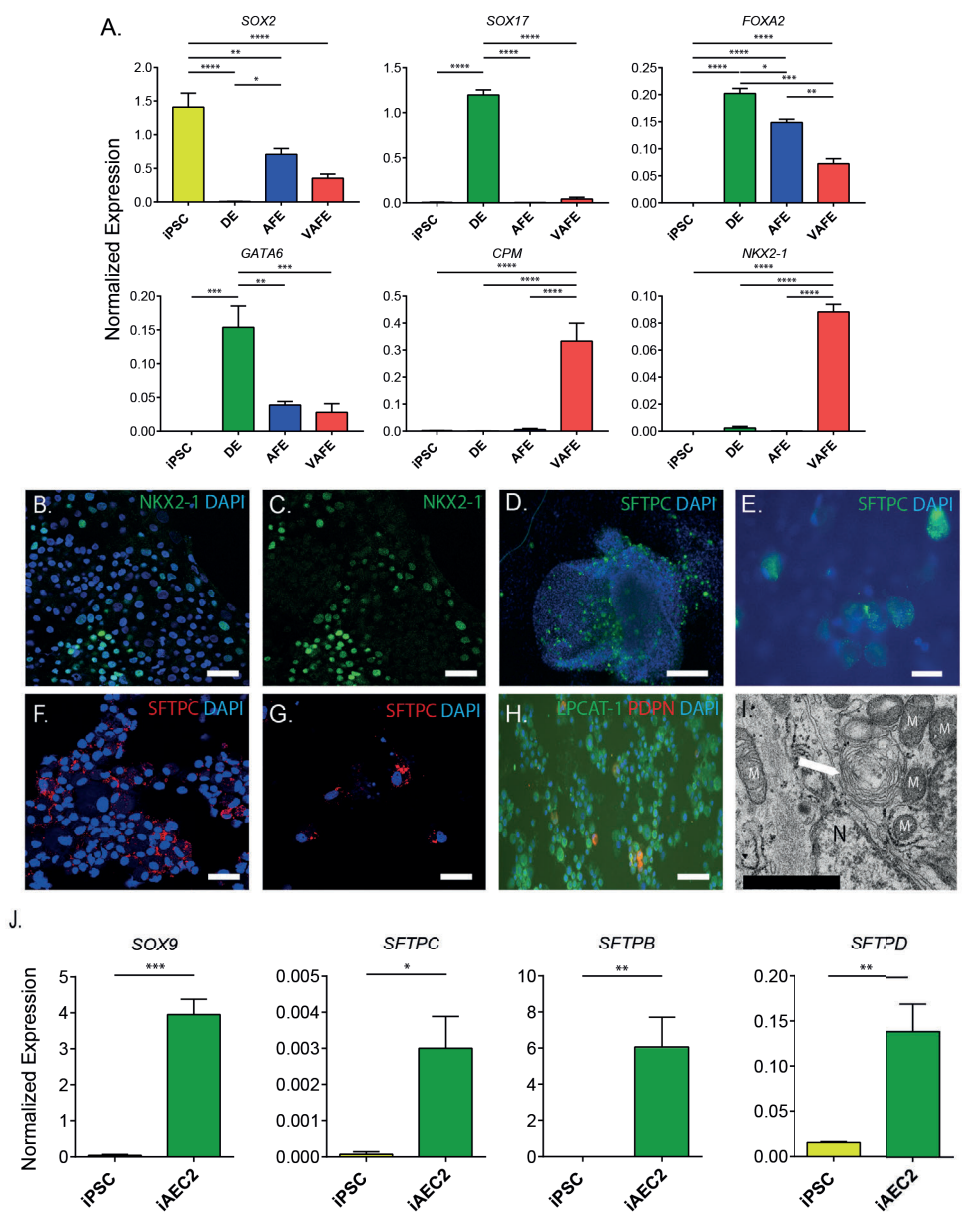


Figure 3. Differentiation of human induced pluripotent stem cells towards an alveolar fate. Expression of differentiation-associated genes in undifferentiated hiPSC, DE, AFE and VAFE (n=6 separate experiments from 2 cell lines). (B-I) Representative images of cells at various differentiation stages stained for (B-C) NKX2-1 scale bar=50 μ m, (D, E) Pro-surfactant protein C expression pre-EpCAM sorting, scale bar=50 μ m and 20 μ m respectively (F, G) Pro-surfactant protein C expression post-EpCAM sorting, scale bar=50 μ m (H) LPCAT-1 (green) Podoplanin (Red), scale bar=50 μ m Nuclei (blue) stained with DAPI. (I) Electron microscopical image of lamellar body in iAEC2 cells following 2 weeks of ALI culture (n=1) N=Nucleus, M=mitochondria, Arrow=lamellar body, scale bar=1 μ m. (J) Normalized gene expression of genes associated with a distal lung and alveolar fate (n=3 independent experiments). Data shown as mean; error bars represent SEM, * p < 0.05, ** p < 0.01, *** p < 0.001, **** p < 0.0001

liquid interface (ALI). Expression of pro-surfactant protein C (pro-SFTPC) was assessed using fluorescent staining (Fig. 3F, G). Following selection and 2-week ALI culture of EpCAM⁺ cells, the majority of the cells stained weakly positive for the lamellar body-associated enzyme Lysophosphatidylcholine acyltransferase 1 (LPCAT-1) (Fig. 3H). Remarkably, after 2 weeks of culture the expression of surfactant protein C was maintained and expression of podoplanin (PDPN) was detected in some cells. PDPN was not detected directly following EpCAM isolation, suggesting a loss of type 2 phenotype and an increased expression of protein classically associated with type 1 phenotype during ALI culture. Staining of EpCAM-isolated cells showed 64.7% (n=3, SEM=2.53) positive for NKX2-1 (SFig. 2). To explore contamination with other lineages, we analysed expression of genes associated with other endodermal and non-endodermal lineages during the differentiation process (SFig. 3). We found that none of the markers analysed were expressed at higher levels than in pAEC2. Furthermore, staining for various airway epithelial cell-associated cellular markers (TP63, FOXJ1, SCGB1A1) indicated these were not present in our cultures (data not shown). We further validated the final differentiation protocol for generation of iAEC2 by using electron microscopy to confirm the presence of lamellar bodies (Fig. 3I).

Comparison of primary and induced AEC2 cultured at the air-liquid interface

We next compared characteristics of cultured iAEC2 and pAEC2. To this end, EpCAM-sorted iAEC2 and pAEC2 were seeded on Transwell inserts to allow culture at the ALI. The cells grew to confluence in approximately 2 weeks. They then formed a functional barrier that prevented leakage of medium from the basal compartment upon removal of the medium from the apical compartment. Establishment of this barrier was confirmed by assessing TEER. This showed that pAEC2 increased their barrier over the 2-week culture period to 200 $\Omega \cdot \text{cm}^2$ (Fig. 4A). In contrast, TEER values of iAEC2 reached a plateau of 80 $\Omega \cdot \text{cm}^2$ after 1 week of culture. AEC2 were cultured for 2 weeks at the ALI and expression of the AEC2-associated markers surfactant protein B, C and D (*SFTPB*, *SFTPC* and *SFTPD*), aquaporin 5 (*AQP5*) and *PDPN*, markers associated with an AEC1 phenotype, were analysed at the mRNA level (Fig. 4B). Whereas iAEC2 cells showed overall lower levels of expression of AEC2 markers compared to pAEC2 cells, their expression was detected at the protein level using fluorescent staining. In order to determine if the epithelial cell maintenance could be improved by

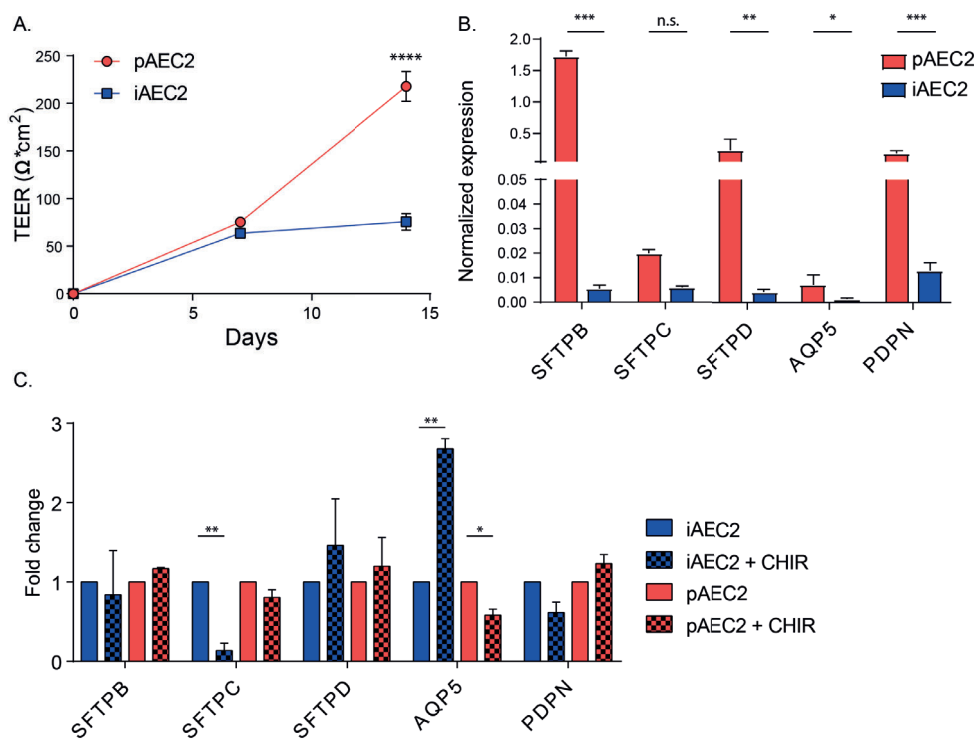


Figure 4. Comparison of hiPSC-derived and isolated AEC2 cells. (A) Change of TEER over 2 weeks of culture at the air-liquid interface (n=3 independent experiments from 2 cell lines). (B) Normalized expression of markers associated with AEC2 and AEC1 phenotype following 2 week culture at the air-liquid interface (n=7). (C) Normalized expression alveolar associated markers following 2 weeks of culture at the air-liquid interface and following stimulation with CHIR99021 (n=3). SFTPB/C/D = Surfactant protein B/C/D, AQP5 = Aquaporin 5, PDPN = Podoplanin. Data shown as mean; error bars represent SEM, * p < 0.05, ** p < 0.01, *** p < 0.001, **** p < 0.0001

canonical Wnt activation, we stimulated the ALI cultured cells for 1 week with the Wnt-activator CHIR99021. Culture of iAEC2 cells with CHIR99021 caused a significant decrease in expression of *SFTPC* and an increase of *AQP5*, suggesting bias towards an AEC1 phenotype (Fig. 4). In contrast, in the pAEC2, no significant effect of CHIR99021 on expression of AEC markers was noted.

Circular wound closure assay

To study repair in the alveolar epithelial ALI model, a circular mechanical wound was created by scraping pAEC2 layers cultured at the ALI. In this assay, epithelial wound closure was monitored over time showing that under control conditions full wound closure was achieved between 72 and 84 hours. Exposure to the Wnt-activator CHIR99021 following wounding caused a non-significant decrease in wound closure rate, whereas exposure

to the TGF- β signalling inhibitor SB-431542 significantly increased the rate of wound closure (Fig. 5A). Microscopic analysis suggested that in the early phases of wound repair, cells migrated into the wound area and displayed an elongated morphology. These observations suggested that wound closure is achieved by a mix of proliferation and migration. Notably, in cultures exposed to CHIR99021, more elongated cells were observed at the wound edge, which appeared to delay wound closure (Fig. 5D).

Similar wound closure assays were then performed on iAEC2. Closure was slower compared to that observed with pAEC2 and full wound closure was only achieved at day 17. This is in line with our observation that the growth rate of iAEC2 was markedly lower than of pAEC2. Also in line with the observations with pAEC2, exposure of iAEC2 to CHIR99021 following injury reduced wound closure compared to control, and for iAEC2 this effect was statistically significant. Interestingly, in contrast to pAEC2, SB-431542 did not affect iAEC2 wound closure compared to control.

In line with our findings in pAEC2, CHIR99021 also caused accumulation of elongated cells at the wound edge in iAEC2 cultures (Fig. 5B). These cells were further characterized by staining for pro-SFTPC and PDPN. The results showed that CHIR99021 treatment increased the number of PDPN⁺ cells while decreasing the number of pro-SFTPC⁺ cells at the wound edge, indicating a change in the number of cells retaining AEC2-like phenotype (Fig. 5D). Whether this phenotypical change contributes to the decrease in wound closure, requires further investigation.

Discussion

In this study, we demonstrated that selection of EpCAM⁺ cells from differentiating hiPSC and followed by ALI culture generates hiPSC-derived AEC2-like cells (iAEC2) suitable for studying alveolar wound repair. The introduction of an EpCAM-based sorting step during the maturation phase resulted in a more homogeneous population of pro-SFTPC⁺ cells that contained lamellar bodies evident by electron microscopy. When analysing wound closure at the ALI, we found that the Wnt-activator CHIR99021 delayed wound closure in both pAEC2 and iAEC2 cultures, with this effect being more pronounced and significant in iAEC2. In iAEC2 cultures, and not in pAEC2 cultures, this treatment was accompanied by an increase in cells positive for PDPN, a marker associated with an AEC1 phenotype, with a concomitant decrease in pro-SFTPC positive cells at the wound edge.

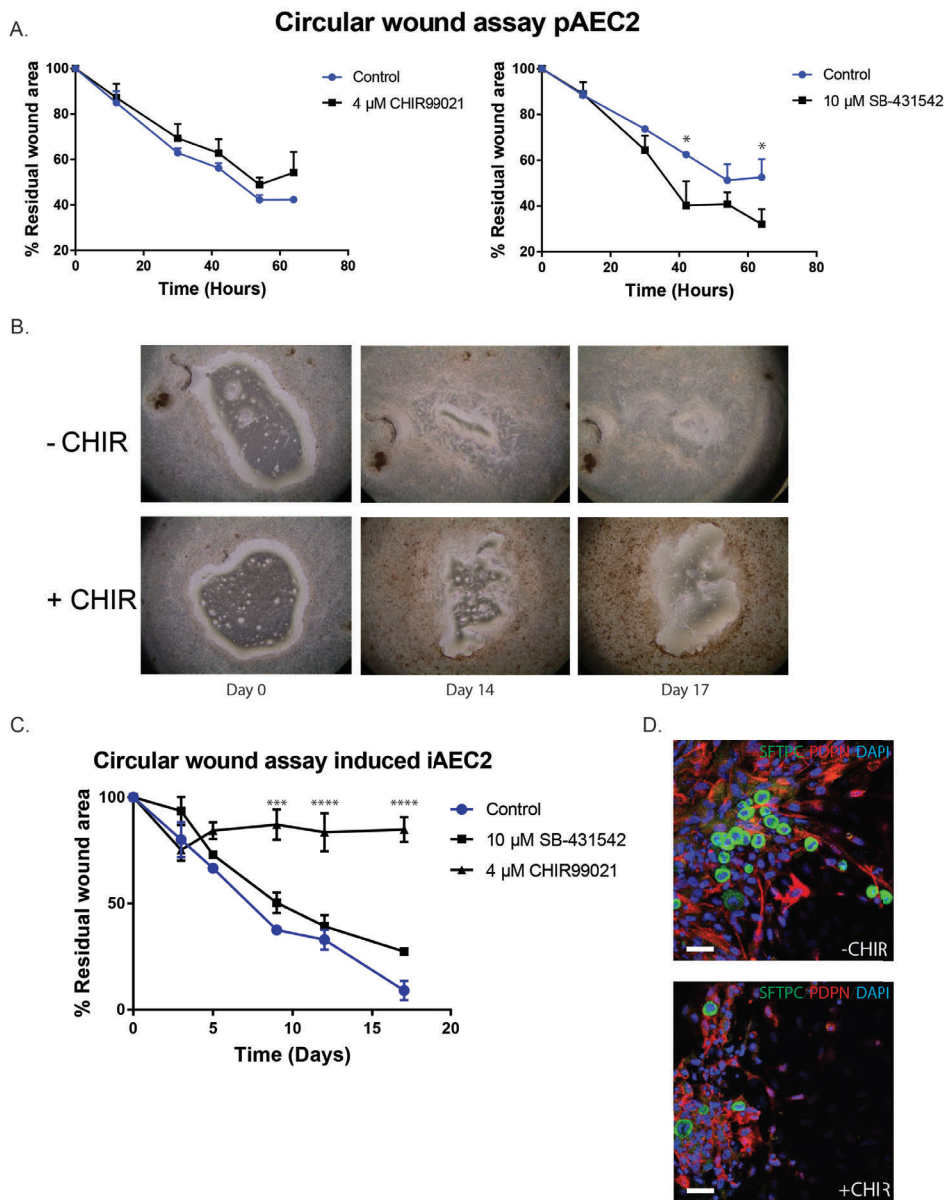


Figure 5. Wound closure assay at the air-liquid interface. (A) Quantification of wound closure of isolated pAEC2 cells stimulated with SB-431542 or CHIR99021 (n=3). (B) Representative images of wound closure of iAEC2 at the air liquid interface. (C) Quantification of wound closure of iAEC2 stimulated with SB-431542 or CHIR99021 (n=3). (D) Wound edge of iAEC2 during wound closure. SFTPC (Green), Podoplanin (Red). Data shown as mean; error bars represent SEM, * $p < 0.05$, *** $p < 0.001$, **** $p < 0.0001$

Before our study, other groups had reported the generation of AEC2 from embryonic- (Roszell et al. 2009; Rippon et al. 2008) and induced pluripotent stem cells (Gotoh et al. 2014; Dye et al. 2015; Ghaedi et al. 2013; Ghaedi et al. 2014; McCauley et al. 2017; Huang et al. 2014; Jacob et al. 2017;

Yamamoto et al. 2017; Tamo et al. 2018). Our protocol was largely based on these published protocols, with some modifications that improved purity and maturity in our hiPSC cell lines. Notably, our differentiation protocol required FGF2 for a robust induction of NKX2-1 expression during the ventralization step. Another difference with published protocols is that we isolated EpCAM⁺ cells after 4 weeks of maturation of distal progenitor cells in the dexamethasone mixture. EpCAM⁺-sorted cells were further matured for 2 weeks before assessing AEC2-associated marker expression. However, based on NKX2-1 staining, the isolated EpCAM⁺ population appeared heterogeneous which may be partly because EpCAM is not an alveolar-specific marker. Other studies included sorting at earlier stages of differentiation on the basis of carboxypeptidase M (CPM) surface expression or using NKX2-1 or pro-SFPTC reporter constructs, to enhance the efficiency and homogeneity of AEC2 population (Gotoh et al. 2014; Jacob et al. 2017). We reasoned that, compared to these approaches, EpCAM has the advantage of being an easily accessible cell surface protein expressed at the last stage of differentiation. Furthermore, using surface EpCAM as a marker does not require introduction of reporter constructs in hiPSC lines, facilitating wider application when using multiple hiPSC lines. Until recently, many studies have relied on the expression of pro-SFTPC at the mRNA or protein level to determine AEC2 identity but immature AEC2 may also express pro-SFTPC, whereas lamellar bodies as examined here by electron microscopy are a characteristic of mature AEC2 (Crapo et al. 1983). In addition, we obtained indirect evidence for the presence of these lamellar bodies by staining for the lamellar body-associated protein LPCAT-1. An important and acknowledged drawback in the use of hiPSC-derived cells is their heterogeneity with respect to maturation, even when using optimized protocols (Schwartzentruber et al. 2018; Wu et al. 2018). In our cultures, we have also assessed markers of airway epithelial cells and non-lung epithelial cells in view of the fact that it is known that NKX2-1 cells are plastic and may differentiate to other lung and non-lung phenotypes (Hurley et al. 2020). Expression of these markers was absent or not higher compared to primary alveolar cells. Although our iAEC2 cells displayed markers and functions typical of pAEC2, it was unclear whether additional cues are required for these cells to fully mature and become identical to AEC2 *in situ* in lung tissue. Single cell RNAseq analysis, epigenetic and other –omics based analyses of the iAEC2 might provide more information on the maturation state of subgroups of cells in the population. This was clearly demonstrated in a recent report by Hurley et al. (Hurley et

al. 2020), showing how the use of single cell transcriptomics, computational modelling and lineage tracing using DNA barcoding can be applied to further improve differentiation of hiPSC-derived lung progenitors towards alveolar epithelial cells.

In an effort to mimic the structural orientation of the alveoli more closely, we cultured the cells on Transwell inserts to allow air exposure. Our culture setup demonstrated the feasibility of culturing and maintaining both the pAEC2 and iAEC2 at the ALI. This setup is not only more physiological than using submerged cultures as it mimics the luminal air exposure in the alveolus, but importantly it also allows exposure to airborne substances such as inhaled toxicants and micro-organisms through a more anatomically accurate route. Furthermore, the effect of change in conditions as following birth when submerged cells are suddenly air-exposed or in ARDS when air-exposed cells are suddenly submerged in fluid as a result of vascular leakage, could be studied in this setup.

Interestingly, it was reported that in hiPSC-derived AEC2 cultures only few cells that express proteins associated with an AEC1 phenotype are detected (Huang et al. 2015), which is in marked contrast to cultures of pAEC2 from adult lung tissue that rapidly lose surfactant and other AEC2-associated markers *in vitro* (Logan and Desai 2015). This may suggest that the pathway driving spontaneous transdifferentiation in adult pAEC2 is not (yet) as active in iAEC2. Interestingly, we observed that treatment of iAEC2 cultures at the ALI with the Wnt-activator CHIR99021 decreased the number of cells with AEC2 characteristics while increasing AEC1-associated markers. Whether our findings are related to the use of ALI culture, is unclear at present. Furthermore, we cannot firmly conclude that we have obtained AEC1-like cells based on the loss of AEC2 markers and the upregulation of PDPN or AQP5. In our alveolar wounding model, we noted that this appearance of iAEC1-like cells was most pronounced at the wound edge. These findings on the effect of CHIR99021 are in apparent contrast to a recent mouse study, which suggested that Wnt signalling is required to maintain stemness of AEC2 cells, and that Wnt signalling prevents transdifferentiation of AEC2 (Nabhan et al. 2018; Zacharias et al. 2018). In addition, Xu et al. previously showed that the canonical Wnt ligand Wnt3a blocked transdifferentiation of AEC2 to AEC1 (Xu et al. 2015). To add to the complexity of Wnt signalling during generation of hiPSC-derived AEC2, it was demonstrated that temporary withdrawal of CHIR99021 is associated with iAEC2 maturation (Hurley et

al. 2020; Jacob et al. 2017), whereas maintenance of proliferation requires adding back CHIR99021 (Hurley et al. 2020). A note of caution is needed, since CHIR99021 activates Wnt signalling through GSK3beta inhibition, and its mode of action is therefore not specific. Tamo et al. (Tamo et al. 2018) recently reported that the Wnt-signalling inhibitor IWT increased transdifferentiation of iAEC2 to iAEC1 under submerged conditions, further pointing to a possible role of experimental design and agents used to study AEC transdifferentiation. Another mechanism that has been implicated in transdifferentiation of AEC2 to AEC1 is the autocrine action of TGF- β (Bhaskaran et al. 2007), which may be antagonized by BMP signalling (Zhao, Yee, and O'Reilly 2013). Using the TGF- β inhibitor SB-431542, we noted that the wound closure in iAEC2 cultures was unchanged compared to control, suggesting that TGF- β induced transdifferentiation does not play a dominant role in wound closure of iACE2 at the ALI.

The marker profile of iAEC2 was largely similar to that of pAEC2 but there were differences. First, expression levels of AEC2-specific markers were lower in iAEC2. Second, in our wound model, closure of iAEC2 wounds was notably slower than that of pAEC2, which might partly be explained by differences in culture media. Whereas pAEC2 are maintained in a rich, newborn calf serum supplemented medium, iAEC2 are grown in a fully defined medium which is suitable for maintenance, but possibly suboptimal for expansion. Another important difference between iAEC2 and pAEC2 is that the latter were derived *in situ* in the presence of supporting cells, whereas similar cells were absent during differentiation of iACE2 from hiPSC. Our pAEC2 isolation protocol yielded a highly enriched population, but we cannot exclude minor contamination with mesenchymal cells. Various studies have shown the ability of mesenchymal cells (Gotoh et al. 2014; Yamamoto et al. 2017) as well as endothelial cells (Lee et al. 2014) to support alveolar epithelial cell development. Miller recently reported on the generation of a bud tip progenitor-like population of cells by culturing hiPSC-derived NKX2-1⁺ ventral foregut spheroids in presence of FGF7, CHIR99021 and retinoic acid (Miller et al. 2018). These cells maintained their multi-lineage potential and upon engraftment into murine airways developed into cells with characteristics of alveolar and airway cells. We did not use supporting cells during the generation of alveolar epithelial cells from hiPSC. Furthermore, in our current model of wound repair, we studied closure of alveolar epithelial wounds in the absence of other cell types that might influence closure rates. *In vivo* AEC are in close proximity to the surrounding endothelial cells

allowing efficient gas transfer. Therefore, a limitation of our model is that endothelial cells, as well as other alveolar structural cells and for example intraluminal macrophages are absent. Furthermore, whereas AEC2 in lung tissue are exposed to the mechanical forces of breathing, these forces are absent in our model. It has been described that stretching of alveolar cells can contribute to maturation and surfactant secretion (Nakamura et al. 2000). *In vivo* mechanical cues play a crucial role in organ formation and development. The differentiation pressure that could be provided by stretch in a lung-on-chip model could provide a more realistic alveolar environment and possibly more homogenous populations.

A major advantage of using hiPSC lines for the development of disease-relevant models, is that it allows the possibility of generating various differentiated cell types from the same cellular and genetic source, for example, cells with endothelial functions expressing endothelial markers (CD31, CD144, VWF) (Orlova et al. 2014; Nakamura et al. 2000). We are currently exploring which media combinations are suitable for long-term co-culture of AEC2 and endothelial cells, either derived from resected lung tissue or hiPSC. The cell types that can be generated from hiPSC are not limited to AEC2 or endothelial cells, and with the continuous development of differentiation protocols, the generation of other cells present in the lung parenchyma becomes reality.

In summary, our study provides support for the use of hiPSC in generating relatively mature populations of AEC2 and both confirms and extends previous studies in this area (Ghaedi et al. 2014; Gotoh et al. 2014; Huang et al. 2015; Jacob et al. 2017; Dye et al. 2015; Tamo et al. 2018; Hurley et al. 2020). In addition, the study shows that iAEC2 can be used to study epithelial repair processes. This is relevant for future studies to evaluate drugs or cells that may enhance alveolar repair, an unmet medical need in regenerative medicine.

Acknowledgements

This study was supported by a grant of the Lung Foundation Netherlands (grant # 6.1.14.010). The authors thank Winifred Broekman (LUMC) for help in setting up the primary AEC2 cultures, and Matthew Hind (Imperial College, London) for hosting Winifred Broekman during her ERS Short-term Research Fellowship (STRTF 383-2011).

Author contributions

SR designed, performed and analysed the experiments, interpreted the data, prepared the figures and drafted the manuscript; DN provided technical support in cell culture; HM, CF and CM provided expertise and training in working with hiPSC; TT provided expertise for isolation and culture of primary AEC2; CJ and AM performed the EM analysis; TP, DB, AP, RT contributed to project discussions as members of the Lung Foundation Netherlands consortium (grant # 6.1.14.010) and contributed to manuscript preparation; CM provided critical input during manuscript preparation; RR and PH designed the study, and supervised experiments and manuscript writing. All authors have read and approved the final version of this manuscript.

Competing interests

The authors declare no competing interests.

Data availability

The datasets of the current study are available from the corresponding author upon reasonable request.

References

- Amatngalim, G. D., W. Broekman, N. M. Daniel, L. E. van der Vlugt, A. van Schadewijk, C. Taube, and P. S. Hiemstra. 2016. 'Cigarette Smoke Modulates Repair and Innate Immunity following Injury to Airway Epithelial Cells', *PLoS One*, 11: e0166255.
- Andersen, C. L., J. L. Jensen, and T. F. Orntoft. 2004. 'Normalization of real-time quantitative reverse transcription-PCR data: a model-based variance estimation approach to identify genes suited for normalization, applied to bladder and colon cancer data sets', *Cancer Res*, 64: 5245-50.
- Baarsma, H. A., W. Skronska-Wasek, K. Mutze, F. Ciolek, D. E. Wagner, G. John-Schuster, K. Heinzlmann, A. Gunther, K. R. Bracke, M. Dagouassat, J. Boczkowski, G. G. Brusselle, R. Smits, O. Eickelberg, A. O. Yildirim, and M. Konigshoff. 2017. 'Noncanonical WNT-5A signaling impairs endogenous lung repair in COPD', *J Exp Med*, 214: 143-63.
- Bhaskaran, M., N. Kolliputi, Y. Wang, D. Gou, N. R. Chintagari, and L. Liu. 2007. 'Trans-differentiation of alveolar epithelial type II cells to type I cells involves autocrine signaling by transforming growth factor beta 1 through the Smad pathway', *J Biol Chem*, 282: 3968-76.
- Chambers, R. C., and P. F. Mercer. 2015. 'Mechanisms of alveolar epithelial injury, repair, and fibrosis', *Ann Am Thorac Soc*, 12 Suppl 1: S16-20.
- Chen, X., J. M. Janssen, J. Liu, I. Maggio, A. E. J. t Jong, H. M. M. Mikkers, and Mafv Goncalves. 2017. 'In trans paired nicking triggers seamless genome editing without double-stranded DNA cutting', *Nat Commun*, 8: 657.
- Crane, A. M., P. Kramer, J. H. Bui, W. J. Chung, X. S. Li, M. L. Gonzalez-Garay, F. Hawkins, W. Liao, D. Mora, S. Choi, J. Wang, H. C. Sun, D. E. Paschon, D. Y. Guschin, P. D. Gregory, D. N. Kotton, M. C. Holmes, E. J. Sorscher, and B. R. Davis. 2015. 'Targeted correction and restored function of the CFTR gene in cystic fibrosis induced pluripotent stem cells', *Stem Cell Reports*, 4: 569-77.
- Crapo, J. D., S. L. Young, E. K. Fram, K. E. Pinkerton, B. E. Barry, and R. O. Crapo. 1983. 'Morphometric characteristics of cells in the alveolar region of mammalian lungs', *Am Rev Respir Dis*, 128: S42-6.
- Dye, B. R., D. R. Hill, M. A. Ferguson, Y. H. Tsai, M. S. Nagy, R. Dyal, J. M. Wells, C. N. Mayhew, R. Nattiv, O. D. Klein, E. S. White, G. H. Deutsch, and J. R. Spence. 2015. 'In vitro generation of human pluripotent stem cell derived lung organoids', *Elife*, 4.
- Faas, F. G., M. C. Avramut, B. M. van den Berg, A. M. Mommaas, A. J. Koster, and R. B. Ravelli. 2012. 'Virtual nanoscopy: generation of ultra-large high resolution electron microscopy maps', *J Cell Biol*, 198: 457-69.
- Ghaedi, M., E. A. Calle, J. J. Mendez, A. L. Gard, J. Balestrini, A. Booth, P. F. Bove, L. Gui, E. S. White, and L. E. Niklason. 2013. 'Human iPS cell-derived alveolar epithelium repopulates lung extracellular matrix', *J Clin Invest*, 123: 4950-62.
- Ghaedi, M., J. J. Mendez, P. F. Bove, A. Sivarapatna, M. S. Raredon, and L. E. Niklason. 2014. 'Alveolar epithelial differentiation of human induced pluripotent stem cells in a rotating bioreactor', *Biomaterials*, 35: 699-710.
- Gotoh, S., I. Ito, T. Nagasaki, Y. Yamamoto, S. Konishi, Y. Korogi, H. Matsumoto, S. Muro, T. Hirai, M. Funato, S. Mae, T. Toyoda, A. Sato-Otsubo, S. Ogawa, K. Osafune, and M. Mishima. 2014. 'Generation of alveolar epithelial spheroids via isolated progenitor cells from human pluripotent stem cells', *Stem Cell Reports*, 3: 394-403.
- Green, M. D., A. Chen, M. C. Nostro, S. L. d'Souza, C. Schaniel, I. R. Lemischka, V. Gouon-Evans, G. Keller, and H. W. Snoeck. 2011. 'Generation of anterior foregut endoderm from human embryonic and induced pluripotent stem cells', *Nat Biotechnol*, 29: 267-72.
- Guillot, L., N. Nathan, O. Tabary, G. Thouvenin, P. Le Rouzic, H. Corvol, S. Amselem, and A. Clement. 2013. 'Alveolar epithelial cells: master regulators of lung homeostasis', *Int J Biochem Cell Biol*, 45: 2568-73.
- Herriges, M., and E. E. Morrisey. 2014. 'Lung development: orchestrating the generation and regeneration of a complex organ', *Development*, 141: 502-13.
- Hogan, B. L., C. E. Barkauskas, H. A. Chapman, J. A. Epstein, R. Jain, C. C. Hsia, L. Niklason, E. Calle, A. Le, S. H. Randell, J. Rock, M. Snitow, M. Krummel, B. R. Stripp, T. Vu, E. S. White, J. A. Whitsett, and E. E. Morrisey. 2014. 'Repair and regeneration of the respiratory system: complexity, plasticity, and mechanisms of lung stem cell function', *Cell Stem Cell*, 15: 123-38.
- Huang, S. X., M. D. Green, A. T. de Carvalho, M. Mumau, Y. W. Chen, S. L. D'Souza, and H. W.

- Snoeck. 2015. 'The *in vitro* generation of lung and airway progenitor cells from human pluripotent stem cells', *Nat Protoc*, 10: 413-25.
- Huang, S. X., M. N. Islam, J. O'Neill, Z. Hu, Y. G. Yang, Y. W. Chen, M. Mumau, M. D. Green, G. Vunjak-Novakovic, J. Bhattacharya, and H. W. Snoeck. 2014. 'Efficient generation of lung and airway epithelial cells from human pluripotent stem cells', *Nat Biotechnol*, 32: 84-91.
- Hurley, K., J. Ding, C. Villacorta-Martin, M. J. Herriges, A. Jacob, M. Vedaie, K. D. Alysandratos, Y. L. Sun, C. Lin, R. B. Werder, J. Huang, A. A. Wilson, A. Mithal, G. Mostoslavsky, I. Oglesby, I. S. Caballero, S. H. Guttentag, F. Ahangari, N. Kaminski, A. Rodriguez-Fraticelli, F. Camargo, Z. Bar-Joseph, and D. N. Kotton. 2020. 'Reconstructed Single-Cell Fate Trajectories Define Lineage Plasticity Windows during Differentiation of Human PSC-Derived Distal Lung Progenitors', *Cell Stem Cell*.
- Jacob, A., M. Morley, F. Hawkins, K. B. McCauley, J. C. Jean, H. Heins, C. L. Na, T. E. Weaver, M. Vedaie, K. Hurley, A. Hinds, S. J. Russo, S. Kook, W. Zacharias, M. Ochs, K. Traber, L. J. Quinton, A. Crane, B. R. Davis, F. V. White, J. Wambach, J. A. Whitsett, F. S. Cole, E. E. Morrissey, S. H. Guttentag, M. F. Beers, and D. N. Kotton. 2017. 'Differentiation of Human Pluripotent Stem Cells into Functional Lung Alveolar Epithelial Cells', *Cell Stem Cell*, 21: 472-88 e10.
- Kneidinger, N., A. O. Yildirim, J. Callegari, S. Takenaka, M. M. Stein, R. Dumitrescu, A. Bohla, K. R. Bracke, R. E. Morty, G. G. Brusselle, R. T. Schermuly, O. Eickelberg, and M. Konigshoff. 2011. 'Activation of the WNT/beta-catenin pathway attenuates experimental emphysema', *Am J Respir Crit Care Med*, 183: 723-33.
- Lee, J. H., D. H. Bhang, A. Beede, T. L. Huang, B. R. Stripp, K. D. Bloch, A. J. Wagers, Y. H. Tseng, S. Ryeom, and C. F. Kim. 2014. 'Lung stem cell differentiation in mice directed by endothelial cells via a BMP4-NFATc1-thrombospondin-1 axis', *Cell*, 156: 440-55.
- Logan, C. Y., and T. J. Desai. 2015. 'Keeping it together: Pulmonary alveoli are maintained by a hierarchy of cellular programs', *Bioessays*, 37: 1028-37.
- Mao, P., S. Wu, J. Li, W. Fu, W. He, X. Liu, A. S. Slutsky, H. Zhang, and Y. Li. 2015. 'Human alveolar epithelial type II cells in primary culture', *Physiol Rep*, 3.
- McCauley, K. B., F. Hawkins, M. Serra, D. C. Thomas, A. Jacob, and D. N. Kotton. 2017. 'Efficient Derivation of Functional Human Airway Epithelium from Pluripotent Stem Cells via Temporal Regulation of Wnt Signaling', *Cell Stem Cell*, 20: 844-57 e6.
- Miller, A. J., D. R. Hill, M. S. Nagy, Y. Aoki, B. R. Dye, A. M. Chin, S. Huang, F. Zhu, E. S. White, V. Lama, and J. R. Spence. 2018. '*In Vitro* Induction and *In Vivo* Engraftment of Lung Bud Tip Progenitor Cells Derived from Human Pluripotent Stem Cells', *Stem Cell Reports*, 10: 101-19.
- Nabhan, A. N., D. G. Brownfield, P. B. Harbury, M. A. Krasnow, and T. J. Desai. 2018. 'Single-cell Wnt signaling niches maintain stemness of alveolar type 2 cells', *Science*, 359: 1118-23.
- Nakamura, T., M. Liu, E. Mourgeon, A. Slutsky, and M. Post. 2000. 'Mechanical strain and dexamethasone selectively increase surfactant protein C and tropoelastin gene expression', *Am J Physiol Lung Cell Mol Physiol*, 278: L974-80.
- Okita, K., Y. Matsumura, Y. Sato, A. Okada, A. Morizane, S. Okamoto, H. Hong, M. Nakagawa, K. Tanabe, K. Tezuka, T. Shibata, T. Kunisada, M. Takahashi, J. Takahashi, H. Saji, and S. Yamanaka. 2011. 'A more efficient method to generate integration-free human iPS cells', *Nat Methods*, 8: 409-12.
- Orlova, V. V., F. E. van den Hil, S. Petrus-Reurer, Y. Drabsch, P. Ten Dijke, and C. L. Mummery. 2014. 'Generation, expansion and functional analysis of endothelial cells and pericytes derived from human pluripotent stem cells', *Nat Protoc*, 9: 1514-31.
- Rippon, H. J., S. Lane, M. Qin, N. S. Ismail, M. R. Wilson, M. Takata, and A. E. Bishop. 2008. 'Embryonic stem cells as a source of pulmonary epithelium *in vitro* and *in vivo*', *Proc Am Thorac Soc*, 5: 717-22.
- Rock, J., and M. Konigshoff. 2012. 'Endogenous lung regeneration: potential and limitations', *Am J Respir Crit Care Med*, 186: 1213-9.
- Roszell, B., M. J. Mondrinos, A. Seaton, D. M. Simons, S. H. Koutzaki, G. H. Fong, P. I. Lelkes, and C. M. Finck. 2009. 'Efficient derivation of alveolar type II cells from embryonic stem cells for *in vivo* application', *Tissue Eng Part A*, 15: 3351-65.
- Schilders, K. A., E. Eenjes, S. van Riet, A. A. Poot, D. Stamatiadis, R. Truckenmuller, P. S. Hiemstra, and R. J. Rottier. 2016. 'Regeneration of the lung: Lung stem cells and the development of lung mimicking devices', *Respir Res*, 17: 44.

- Schwartzentruber, J., S. Foskolou, H. Kilpinen, J. Rodrigues, K. Alasoo, A. J. Knights, M. Patel, A. Goncalves, R. Ferreira, C. L. Benn, A. Wilbrey, M. Bictash, E. Impey, L. Cao, S. Lainez, A. J. Loucif, P. J. Whiting, Hipsi Consortium, A. Gutteridge, and D. J. Gaffney. 2018. 'Molecular and functional variation in iPSC-derived sensory neurons', *Nat Genet*, 50: 54-61.
- Skronska-Wasek, W., K. Mutze, H. A. Baarsma, K. R. Bracke, H. N. Alsafadi, M. Lehmann, R. Costa, M. Stornaiuolo, E. Novellino, G. G. Brusselle, D. E. Wagner, A. O. Yildirim, and M. Konigshoff. 2017. 'Reduced Frizzled Receptor 4 Expression Prevents WNT/beta-Catenin-driven Alveolar Lung Repair in Chronic Obstructive Pulmonary Disease', *Am J Respir Crit Care Med*, 196: 172-85.
- Takahashi, K., K. Tanabe, M. Ohnuki, M. Narita, T. Ichisaka, K. Tomoda, and S. Yamanaka. 2007. 'Induction of pluripotent stem cells from adult human fibroblasts by defined factors', *Cell*, 131: 861-72.
- Tamo, L., Y. Hibaoui, S. Kallol, M. P. Alves, C. Albrecht, K. E. Hostettler, A. Feki, J. S. Rougier, H. Abriel, L. Knudsen, A. Gazdhar, and T. Geiser. 2018. 'Generation of an alveolar epithelial type II cell line from induced pluripotent stem cells', *Am J Physiol Lung Cell Mol Physiol*.
- van den Bogaard, E. H., L. A. Dailey, A. J. Thorley, T. D. Tetley, and B. Forbes. 2009. 'Inflammatory response and barrier properties of a new alveolar type 1-like cell line (TT1)', *Pharm Res*, 26: 1172-80.
- Warlich, E., J. Kuehle, T. Cantz, M. H. Brugman, T. Maetzig, M. Galla, A. A. Filipczyk, S. Halle, H. Klump, H. R. Scholer, C. Baum, T. Schroeder, and A. Schambach. 2011. 'Lentiviral vector design and imaging approaches to visualize the early stages of cellular reprogramming', *Mol Ther*, 19: 782-9.
- Whitsett, J. A., and T. E. Weaver. 2015. 'Alveolar development and disease', *Am J Respir Cell Mol Biol*, 53: 1-7.
- Witherden, I. R., and T. D. Tetley. 2001. 'Isolation and Culture of Human Alveolar Type II Pneumocytes', *Methods Mol Med*, 56: 137-46.
- Wu, H., K. Uchimura, E. L. Donnelly, Y. Kirita, S. A. Morris, and B. D. Humphreys. 2018. 'Comparative Analysis and Refinement of Human PSC-Derived Kidney Organoid Differentiation with Single-Cell Transcriptomics', *Cell Stem Cell*, 23: 869-81 e8.
- Xu, W., Y. Zhao, B. Zhang, B. Xu, Y. Yang, Y. Wang, and C. Liu. 2015. 'Wnt3a Mediates the Inhibitory Effect of Hyperoxia on the Transdifferentiation of AECIIs to AECIs', *J Histochem Cytochem*, 63: 879-91.
- Yamamoto, Y., S. Gotoh, Y. Korogi, M. Seki, S. Konishi, S. Ikeo, N. Sone, T. Nagasaki, H. Matsumoto, S. Muro, I. Ito, T. Hirai, T. Kohno, Y. Suzuki, and M. Mishima. 2017. 'Long-term expansion of alveolar stem cells derived from human iPSC cells in organoids', *Nat Methods*, 14: 1097-106.
- Zacharias, W. J., D. B. Frank, J. A. Zepp, M. P. Morley, F. A. Alkhaleel, J. Kong, S. Zhou, E. Cantu, and E. E. Morrissey. 2018. 'Regeneration of the lung alveolus by an evolutionarily conserved epithelial progenitor', *Nature*, 555: 251-55.
- Zhao, L., M. Yee, and M. A. O'Reilly. 2013. 'Transdifferentiation of alveolar epithelial type II to type I cells is controlled by opposing TGF-beta and BMP signaling', *Am J Physiol Lung Cell Mol Physiol*, 305: L409-18.

Supplementary methods

Generation of induced iAEC2 from hiPSC

Directed differentiation of hiPSC into AEC2-like cells was achieved by guiding the cells through sequential embryonic developmental stages. hiPSC colonies were grown and maintained on vitronectin (StemCell Technologies, Vancouver, Canada) coated (10 $\mu\text{g}/\text{ml}$) 6 well plates (Corning, Corning, NY) and cultured in mTESR1 media (StemCell Technologies). The cells were passaged weekly 1:15 using Gentle Cell Dissociation reagent (StemCell Technologies). Differentiation into definitive endoderm was achieved using the STEMdiff definitive endoderm kit (StemCell Technologies) according to the manufacturer's instructions. Single cell suspensions were obtained by using Gentle Cell Dissociation reagent at room temperature. After cell counting, 2×10^6 cells were seeded in vitronectin-coated 6 well plates. During the first 24 hours, 10 μM Y-27632 (Cayman Chemicals, Ann Arbor, MI) was added. The following day the medium was changed to endoderm medium, supplemented with compound A and B (StemCell Technologies), and for the next 3 days with addition of only supplements B. Following endoderm induction, cells were dissociated using TrypLE select (ThermoFisher, Waltham, MA) at room temperature and split in a 1:4 ratio for culture in 6-well plates pre-coated with vitronectin. The cells were maintained in serum-free basal differentiation medium, consisting of IMDM (ThermoFisher), Ham's F12 (ThermoFisher) containing B27 (Invitrogen, Carlsbad, CA), N2 (Invitrogen), 0.1% (w/v) bovine serum albumin Fraction V (Invitrogen), Glutamax (ThermoFisher), and primocin (Invivogen, San Diego, USA). To next achieve anterior foregut endoderm (AFE) induction, the medium was supplemented with 10 μM SB-431542 (Sigma-Aldrich, St. Louis, MO) and 2 μM dorsomorphin (Sigma). During the first day of AFE formation, medium was supplemented with 10 μM Y-27632. Using our cell lines, we found that use of dorsomorphin resulted in a more robust induction of SOX2 compared to use of the recombinant protein noggin (SFig. 1). After 4 days of anteriorization, the cells were washed and medium switched to ventralization medium for 8 days for induction of ventral anterior foregut endoderm (VAFE). Ventralization medium is basal medium supplemented with 2 μM CHIR99021 (Sigma-Aldrich), 30 ng/ml recombinant human BMP4 (Life Technologies), 100 ng/ml recombinant human FGF2 (Miltenyi Biotech, Bergisch Gladbach, Germany) and 50 nM EC23 (Bio-Techne, Minneapolis, MN). During the first day, 10 μM Y-27632 was added. Importantly, we found that FGF2 was required in our protocol

to achieve a robust expression of NKX2-1. This was observed both when using AFE obtained using noggin (Supplementary Figure 1, middle) as well as that obtained using dorsomorphin (Supplementary Figure 1, lower part). Following 8 days of ventralization the cells were washed and dissociated using TrypLE select at room temperature and split in a 1:2 to 1:4 ratio. The cells were maintained in basal differentiation medium supplemented with 50 ng/ml recombinant human FGF7 (Tebu-Bio, Heerhugowaard, The Netherlands) and 100 ng/ml recombinant human FGF10 (Miltenyi Biotech) for 8 days with 10 μ M Y-27632 present during the first 24 hours. After 8 days, the cells were washed and medium replaced with alveolarization medium, consisting of basal differentiation medium supplemented with 50 ng/ml recombinant human FGF7, 50 nM dexamethasone (Sigma-Aldrich), 100 μ M 3-Isobutyl-1-methylxanthine (IBMX; Sigma-Aldrich) and 100 μ M 8-Bromoadenosine 3',5'-cyclic monophosphate (Sigma-Aldrich). After 4 weeks of “alveolarization” the cells were sorting using MACS beads coated with anti-EpCAM (Miltenyi Biotech) according to the manufacturer’s instructions. The isolated cells are cultured on semipermeable Transwell membranes with 0.4- μ m pore size (Corning Costar, Cambridge, MA). Transwells were coated with a mixture of 30 μ g/ml PureCol (Advanced BioMatrix, San Diego, CA), 10 μ g/ml BSA (invitrogen) and 10 μ g/ml fibronectin (Alfa Aeser, Karlsruhe, Germany) in PBS, at 37 °C, 5% CO₂. Once confluent, the apical medium was removed and the cells were exposed to air. On the insert and at ALI the cells were maintained in the “alveolarization” medium.

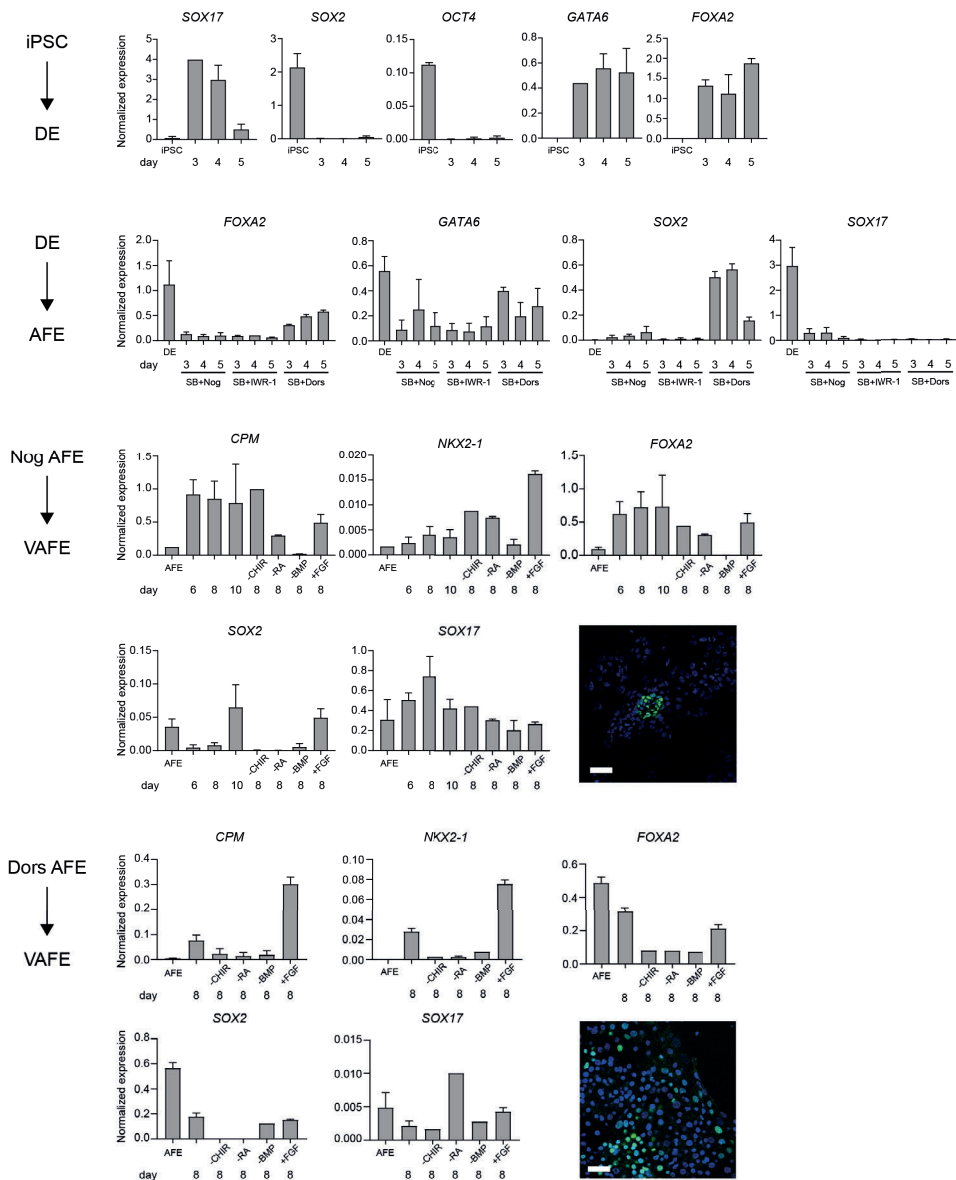
Compound	Concentration	Company	Cat#
Y-27632	10 μ M	Cayman Chemical	10005583-10
SB-431542	10 μ M	Sigma	S4317
Dorsomorphin	2 μ M	Sigma	P5499-5MG
CHIR99021	2 μ M	Sigma	SML1046-5MG
FGF2	100 ng/ml	Miltenyi Biotech	130-104-925
BMP4	30 ng/ml	Life technologies	PHC9534
EC23	50 nM	Bio-Techne	4011
FGF7	50 ng/ml	Tebu-Bio	100-19 B
FGF10	100 ng/ml	Miltenyi Biotech	130-093-850
Dexamethasone	50 nM	Sigma	D4902-25MG
IBMX	100 μ M	Sigma	I5879
8-Br-cAMP	100 μ M	Sigma	B5386-5MG

Table S1. Key reagents used for generation of iAEC2.

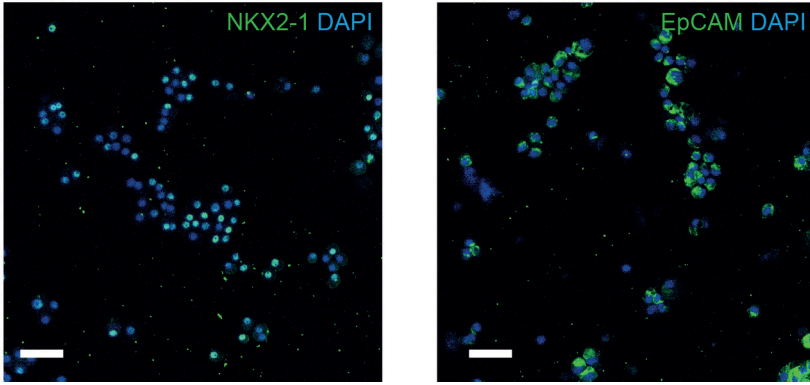
Gene	Forward (5' to 3')	Reverse (3' to 5')
<i>RPL22</i>	TCGCTCACCTCCCTTTCTAA	TCACGGTGATCTTGCTCTTG
<i>GAPDH</i>	TTCCAGGAGCGAGATCCCT	CACCCATGACGAACATGGG
<i>RPS29</i>	GCACTGCTGAGAGCAAGATG	ATAGGCAGTGCCAAGGAAGA
<i>ACTB</i>	TGCGTGACATTAAGGAGAAG	TGAAGGTAGTTTTCGTGGATG
<i>OAZ1</i>	GGATCCTCAATAGCCACTGC	TACAGCAGTGGAGGGAGACC
<i>RPL27</i>	ATCGCCAAGAGATCAAAGATAA	TCTGAAGACATCCTTATTGACG
<i>RPL30</i>	ACAGCATGCGGAAAATACTAC	AAAGGAAAATTTTGCAGGTTT
<i>YWHAZ</i>	ACTTTTGGTACATTGTGGCTTCAA	CCGCCAGGACAAACCAGTAT
<i>B2M</i>	GACCACTTACGTTCAATGACTCC	CAGGGTTTCATCATAACAGCCAT
<i>GNB2L</i>	GAGTGTGGCCTTCTCCTCTG	GCTTGCAGTTAGCCAGGTTT
<i>HPRT1</i>	AACCCTGTTGTCAATGCCTC	AACACTTCGTGGGGTCCTTTTC
<i>ATP5B</i>	TCACCCAGGCTGGTTCAGA	AGTGGCCAGGGTAGGCTGAT
<i>RPL13A</i>	AAGGTGGTGGTCGTACGCTGTG	CGGGAAGGGTTGGTGTTCATCC

Table S2. Primer sequences candidate reference genes.

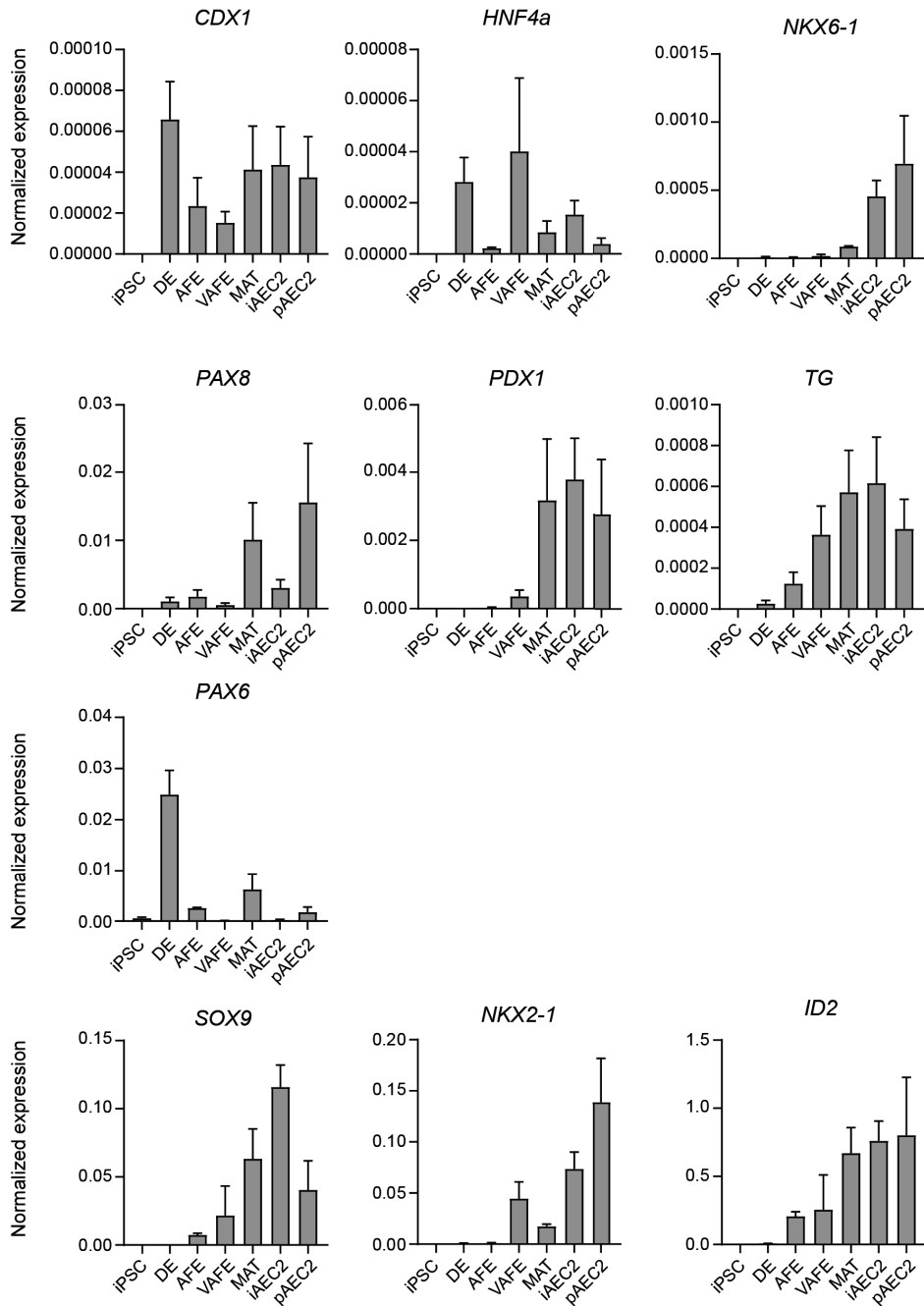
Supplementary figures



Supplemental figure 1. Overview of early optimization. Results show expression of various markers at the different stages of differentiation, including a comparison of the effect of three compounds mixes (SB [SB 431542] combined with Nog [Noggin]; the Wnt inhibitor IWR-1, or Dors [dorsomorphin]) on AFE generation (second line of figures). The lower four lines of figures show a comparison of VAFE obtained using AFE generated using the best two of these three mixes. RA, retinoic acid analogue EC23; +FGF, +FGF2, CHIR, RA and BMP4. See text for details.



Supplemental figure 2. Staining of NKX2-1 and EpCAM. Images depicting staining of NKX2-1 and EpCAM on cytopins of EpCAM-isolated iAEC2 cells.



Supplemental figure 3. Gene expression levels of other endodermal or non-endodermal lineages at the various stages of the differentiation process compared to primary AEC2 cells. iAEC2: cells cultured for 2 weeks at ALI following EpCAM isolation. The following markers were assessed: CDX1, HNF4a, NKX6-1, PAX8, PDX1, Thyroglobulin (TG), PAX6, NKX2-1, ID2 and SOX9.

CHAPTER 3

Alveolus Lung-Chip cultures of patient-derived primary alveolar type-2 cells

Sander van Riet¹, Annemarie van Schadewijk¹, P. Padmini S.J. Khedoe¹, Jan J. Stolk¹, Pieter S. Hiemstra^{1*}, Anne M. van der Does^{1*}

¹Dept. of Pulmonology, Leiden University Medical Center, Leiden, the Netherlands

*Shared senior authorship

In revision at the American Journal of Physiology - Lung cell and molecular physiology

Abstract

Development of effective treatment strategies for lung tissue destruction as seen for example in emphysema would greatly benefit from representative human *in vitro* models of the alveolar compartment. Studying how (altered) biomechanical cues in emphysema affect alveolar epithelial repair function could provide new insight for tissue repair strategies. Preclinical models of the alveolus ideally combine human primary patient-derived alveolar type-2 cells (AEC2) with advanced cell culture applications such as breathing-related stretch, to more reliably represent the alveolar microenvironment. To test the feasibility of such a model, we isolated primary alveolar type-2 cells (AEC2) from patient-derived lung tissues including from severe emphysema, using magnetic bead-based selection of cells expressing the AEC2 marker HTII-280. We obtained pure alveolar feeder-free organoid cultures with use of a minimally modified commercial medium which also allowed for further expansion of these organoids. Following expansion, cells were seeded on Transwell PET inserts and on the Chip-S1 that has a flexible PDMS membrane enabling the application of dynamic stretch to cell cultures. AEC2 cultured for seven days on Transwells or the Alveolus Lung-Chip maintained expression of HTII-280, surfactant protein C (SP-C) and zonula occludens-1. When cultures were exposed to dynamic cyclic stretch for 5 days, cells remained viable, expressed HTII-280 and SP-C and displayed a slightly elongated organization. The combination of a straightforward culture method of patient-derived AEC2 and their application in Organs-on-Chips, enabling study of biomechanical cues in AEC2 functioning, provides a next step in the development of representative human preclinical models of the alveolar compartment.

Introduction

Chronic obstructive pulmonary disease (COPD) is one of the leading causes of death worldwide (World Health Organization 2018). Due to a lack of available curative treatments, combined with persistent and long-term effects of smoking, the alarming levels of air pollution as well as ageing of the population, this is not expected to improve in the near future (Khakban et al. 2017). Chronic airway inflammation and progressive destruction of the alveolar compartment of the lungs (emphysema) are principal hallmarks of this disease (Hogg and Timens 2009; Agusti and Hogg 2019). Alveolar tissue destruction reduces the gas exchange capacity and elastic recoil of the lungs, thereby progressively affecting quality of life of these patients. Smoking is one of the main risk factors for development of COPD. In addition to smoking cessation and pulmonary rehabilitation, pharmacological treatment for COPD is largely limited to the use of long-acting β 2-agonists (LABA), long-acting muscarinic antagonists (LAMA) and inhaled corticosteroids, which do not modify the course of the disease (Miravittles et al. 2016; Celli and Wedzicha 2019). Lung volume reduction surgery (LVRS) can give alleviation for patients as it improves breathing by resection of the most damaged part of the lungs. Otherwise, lung transplantation is the remaining treatment strategy when the decrease in lung function capacity becomes life threatening, but this is limited by the availability of matching donor lungs and rejection of transplanted lungs.

Development of new treatments that could halt or reverse the destruction of the alveolar compartment or potentially induce regeneration of lung tissue, are reliant on human preclinical models of the alveolar compartment, and available alternatives such as (tumour-derived) cell lines or animal models, unfortunately provide limited translation to *in vivo* human biology (Uhl and Warner 2015). Human induced pluripotent stem cells (hiPSC) offer an alternative source, however generation of AEC2 from hiPSC is currently still time consuming, costly and the derived alveolar cells generally display an immature phenotype (Jacob et al. 2017).

Isolation protocols of human AEC2 were until recently complex procedures that were generally time consuming, required specialized equipment and/or complex cell culture media (Witherden and Tetley 2001; Hiemstra, Tetley, and Janes 2019) and carried a risk of contamination with mesenchymal cells. Furthermore, when AEC2 are propagated in conventional *in vitro* cell culture they tend to differentiate over time to alveolar epithelial type-1 cells (AEC1)

(Mao et al. 2015). Finally, since culture-based expansion of AEC2, and therefore the yield of AEC2 is limited, the number of isolated cells restricts the experimental set-up. Recently, new methods have been published that overcome many of these limitations, demonstrating the isolation of murine or human AEC2 from lung tissue and subsequent expansion in organoid culture (Glisinski et al. 2020; Salahudeen et al. 2020; Katsura et al. 2020). These much needed improvements have already shown to be a great step forward, and a logical next step is to apply primary AEC2, preferably patient-derived, in preclinical models of the alveolar compartment that include additional aspects of the alveolar environment, such as capillary blood flow and strain caused by breathing motions, as these mechanical forces are highly relevant in the alveolus environment but currently understudied (Evans and Lee 2020). The development of Organs-on-Chips that recapitulate the tissue architecture more closely and allow integration of the dynamic biomechanical changes and cellular interactions within tissues is highly needed (Benam et al. 2016; Zamprogno et al. 2021).

To provide proof-of-principle for a cell culture model that more reliably mimics the alveolus microenvironment, we used a straightforward two-step protocol for AEC2 isolation from resected human lung tissue derived from non-smokers, ex-smokers, smokers and emphysematous tissue from lung volume reduction surgery (LVRS) surgery. Dissociation of the lung tissue was followed by an HTII-280-based enrichment step of AEC2 using magnetic beads, recently also developed by Katsura and colleagues (Katsura et al. 2020). This isolation procedure was combined with a feeder-free organoid-based culture method that allows expansion and propagation of AEC2 for weeks up to several months, whilst maintaining AEC2 characteristics and preventing contamination by other cells using a minimally modified commercial medium. Once sufficiently expanded, cells were used for successful culture on conventional Transwells and innovative Organs-on-Chips, in which we demonstrated feasibility of using the organoid-expanded AEC2 to study the effect of cyclic stretch on AEC2 phenotype.

Methods

Isolation, maintenance and expansion of primary alveolar type-2 cells

Tissue processing: Alveolar type-2 cells (AEC2) were isolated from tumour-free tissue from patients undergoing lung resection surgery for lung cancer (smokers, ex-smokers and non-smokers) or from emphysematous tissue from patients undergoing LVRS at the Leiden University Medical Center (LUMC, The Netherlands) for emphysema. Patient characteristics are summarized in Table 1. The use of surplus lung tissue for research following surgery was within the framework of patient care and in line with the “Human Tissue and Medical Research: Code of conduct for responsible use” (2011) (www.federa.org) and followed advice of the LUMC Medical Ethical Committee. Tissue donation was based on a no-objection system for coded anonymous use of waste tissue, left-over from diagnostic or therapeutic procedures. “No-objection” negates the need for individual informed consent. All methods were carried out in accordance with relevant guidelines and regulations.

	Lobectomy	LVRS
Number of donors	17	14
Male/Female	12/5	4/10
Age (years) mean [SD]	62.3 [11.3]	57.1 [2.3]
BMI mean [SD]	27.1 [6.3]	23.3 [2.1]
Smoking Status (non-/ex-/smokers)	3/5/6*	0/14/0
Pack years (ex-/smokers) [SD]	22.8 [15.8]/42.40 [9.56] **	18.4 [3.4]/-
FEV1 % pred [SD]	89.40 [19.43]###	30.1 [7.7]
DLCO % pred [SD]	79.50 [24.58]#	38.1 [11.4]

Table 1. Patient characteristics of resected lung tissue from lobectomy surgery or lung volume reduction surgery (LVRS). Abbreviations: SD (standard deviation); BMI (body mass index); FEV1 (forced expired volume in 1 sec); DLCO (diffusion capacity of the lungs for carbon monoxide)

#Data available from 14 lobectomy patients

** Smokers data available from 5/6 lobectomy patients

Data available from 15 lobectomy patients

The lung tissue homogenate preparation procedure was adapted from Witherden et al. (Witherden and Tetley 2001). Resected lung tissue was cut into pieces of approximately 5 cm³ and injected with 7.5 mL trypsin (Gibco 1:250) (0.25% w/v) in Hanks’ Balanced Salt Solution (HBSS) (ThermoFisher, Waltham, MA) and incubated for 15 min at 37°C; this was repeated for a total incubation time of 45 min. Trypsin activity was inhibited by

injecting the tissue with 7.5 mL soybean trypsin inhibitor (SBTI; 0.1% w/v in HBSS; St. Louis, Sigma-Aldrich, MO). Next, tissue was manually cut to as small as possible pieces during max 10 min. at room temperature (RT). The processed tissue was collected in gentleMACS C tubes (Miltenyi, Leiden, Netherlands) and ran twice on the gentleMACS tissue dissociator program M_lung_02.01 (Miltenyi) for further processing. This solution was then passed through a metal sieve to remove the biggest remaining pieces of tissue and next through a strainer with a mesh size of 100 μm (VWR international, Amsterdam, Netherlands) to obtain a single cell suspension. The cells were centrifuged for 5 min at $265 \times g$ and supernatant was removed. If necessary (donor dependent), a red blood cell lysis (Miltenyi) was performed. To this end, the cell pellet was resuspended in 1 mL magnetic-activated cell sorting (MACS) buffer consisting of PBS, 0.1% (w/v) BSA (Sigma-Aldrich) and 2 mM EDTA (ThermoFisher) to continue with HTII-280⁺ selection.

HTII-280⁺ selection: HTII-280⁺ AEC2 were isolated using a HTII-280 monoclonal mouse IgM antibody (Terrace Biotech, San Francisco, CA). Total tissue homogenate in 1 mL of MACS buffer was incubated with 25 μL of undiluted HTII-280 antibody for 15 min at 4°C. Following 5 min. centrifugation at $265 \times g$, cells were incubated with magnetic bead-labelled anti-mouse IgM (Miltenyi) for 15 min at 4°C and subsequently MACS selection was performed according to manufacturer's instruction (Miltenyi).

Culture of alveolar type-2 cells in organoids: HTII-280⁺ cells were collected by centrifugation at $265 \times g$ for 5 min AEC2 were counted in trypan blue and resuspended in cold Basement Membrane Extract 2 (BME2, Cultrex, Gaithersburg, MD). Alveolar cells (1×10^5 viable cells/30 μL droplet/well) were seeded in a 48 well plate, after which droplets were allowed to solidify at 37°C. After 10 min, 500 μL complete alveolar organoid medium was added to the well. Alveolar cell culture medium consists of alveolar medium (Sciencell, Carlsbad, CA) with all supplements from the media kit except the antibiotics, which were replaced by the addition of Primocin (Invivogen, San Diego, CA). Alveolar cell culture medium supplemented with 4 μM CHIR99021 (CHIR; Sigma-Aldrich) is further referred to as "complete alveolar organoid medium". At the start of culture or directly upon passaging (until next medium refreshment), the complete alveolar organoid medium was supplemented with 10 μM Y-27632 (Cayman Chemical, Ann Arbor, MI) for 48 h. Medium was refreshed twice a week and cells were passaged approximately every 2 weeks adapting the passing time to the specific donor growth-rate.

For passaging, medium was aspirated, and cold PBS was added to the well to dissolve the BME2. The organoid suspension was collected and incubated for max 10 min using 1 mL 0.03% w/v trypsin (1:250; Gibco, ThermoFisher), 0.01% (w/v) EDTA (BDH, Poole, England), 0.1% glucose (BDH) in PBS per droplet at 37°C. Two mL SoyBean Trypsin Inhibitor (SBTI; Sigma) solution per droplet was added to stop the trypsin activity and organoids were further dissociated into fragments by resuspension. The disrupted organoids were centrifuged, resuspended in BME2 and re-plated. Organoids were subsequently grown under standard cell culture conditions (37°C and 5% CO₂).

Cytospin preparations: To validate the success of HTII-280⁺ isolation using magnetic beads, cytospin preparations were obtained from the lung tissue homogenate single cell suspension before selection (unsorted) and after HTII-280⁺ selection, also including the negative fraction (flow through). Cytospin preparations were fixed using 4% formaldehyde (Sigma Aldrich) in PBS for subsequent immunofluorescence staining.

Transwell cultures: Transwells were coated with a mixture of 30 µg/mL bovine collagen I (PureCol; Advanced BioMatrix, San Diego, CA), 10 µg/mL BSA (ThermoFisher), and 10 µg/mL fibronectin (Promocell, PromoKine, Bio-connect, Huissen, The Netherlands) in PBS and seeded with either the HTII-280⁺ lung cells directly isolated from tissue (Po) or with the dissociated alveolar cells from the organoids at various passages. Alveolar medium was added to the basal and apical compartment of the Transwells and refreshed twice a week. After 7 days in culture, the Transwells were fixed for immunofluorescence staining using 4% formaldehyde in PBS.

Alveolus Lung-Chip cultures: Both channels of the commercial Chip-S1 (Emulate Inc, Boston, MA) were activated using the provided reagents ER-1 and ER-2. In short, ER-1 was resuspended in 5 mL ER-2 buffer and directly pipetted into both channels of the chip. Next, the chips were placed under UV-light for 10 min followed by two washes of both channels with ER-2, followed by another round of ER-1, UV and ER-2 washes. After the second ER-2 wash, the channels were washed with PBS. Next, both channels were filled with 300 µg/mL human collagen IV (Sigma-Aldrich) solution in PBS, and incubated overnight at 37°C and 5% CO₂, to allow deposition of the collagen on the membrane in the Chip-S1.

Next, both channels were washed with complete alveolar organoid medium before cells were seeded in the top channel. To seed sufficient AEC2, 9 x 30 µl

organoid-containing drops of alveolar cells were collected per chip, and organoids were dissociated as described when passaging the organoids. The cell pellet was resuspended in complete alveolar organoid medium and 30 μ L of this cell suspension was used to seed the top channel of one chip. Cells were left to adhere for approximately 6 h in the incubator in presence of 10 μ M Y-27632. Next, top and bottom channels were infused with pre-warmed complete alveolar organoid medium containing 10 μ M Y-27632, and Chips were connected to pre-warmed media-filled fluidic manifolds, named Pods (Emulate Inc.). After obtaining liquid-liquid interface connection between Chips and Pods, these units were placed in the micro perfusion instrument, named “Zoë” (Emulate Inc.). After finishing the initial regulate cycle program (which pressurizes the medium to increase gas solubility and removes nucleating air bubbles while the system calibrates), the Alveolus Lung-Chips were continuously perfused at a flow rate of 30 μ L/h in both the top and bottom channel. Approximately 24 h after this first regulate cycle program, a so-called via-wash was performed, dislodging any bubbles in the Pod’s reservoirs fluid vials, followed by a second regulate cycle. Alveolar medium in the Pods was refreshed after 48 h (no addition of Y-27632), which was repeated every other day throughout the time of culture (all without Y-27632). When the cultures reached confluence (usually between ~2-4 days post-seeding), chips were divided into two groups: control (flow rate 30 μ L/h top and bottom channel flow conditions) and stretch (30 μ L/h top and bottom channel flow conditions + 10% stretch at 0.25Hz) (Huh et al. 2010).

Imaging of cytospin preparations, organoids, Transwells and Chips

Cytospin preparations and Transwells: Fluorescent staining was performed on cytospin preparations, cells cultured on Transwells, and paraffin sections of the organoids according to the following protocol. In brief, after fixation cells were incubated with permeabilization and blocking buffer (1% w/v BSA, 0.3% v/v Triton-X100 (Sigma-Aldrich) in PBS) for 30 min at 4°C. Paraffin sections were pre-treated with DAKO pH 9 antigen retrieval solution according to manufacturer’s instruction (DakoCytomation, Denmark, Glostrup). The primary antibody (Table 2) was added in blocking solution to the cells for 1 h at RT. Next the samples were washed with PBS and incubated with fluorescent-labelled secondary antibody together with 4’,6-Diamidino-2-phenylindole (DAPI; Sigma-Aldrich) for 30 min at RT.

Organoids: After dissolving the droplets with recovery solution (Corning,

Corning, NY), the alveolar organoids were fixed in 4% formaldehyde (FA) in PBS for 30 min. Next the organoids were taken up in 2% (w/v) low melting agarose (ThermoFisher) and embedded in paraffin. Slices of 4 μ m were cut and the organoids were stained with various antibodies or H&E staining. All antibodies used can be found in Table 2.

Alveolus Lung-Chips: Alveolar cells in the chips were washed with PBS and fixed using 4% PFA solution, which was pipetted into both channels and incubated for 20 min at RT, washed with PBS and stored in PBS at 4°C until staining. Chips were subsequently removed from the carrier and cells were blocked and permeabilized using 0.5% (v/v) Triton-X 100 in PBS with 5% BSA for 1 h at RT. Chips were cut into 2 pieces using a razor blade and channels were filled with primary antibodies (Table 2) diluted in the Triton/BSA buffer and incubated for 1 h at RT. Samples were rinsed three times for 5 min with PBS. Next, channels were filled with secondary antibodies diluted in Triton/BSA buffer which was left incubating for 1 h at RT, followed by a triple 5 min wash with PBS. DAPI was used to stain cell nuclei. Channels were next filled with prolong gold anti-fade (Thermo Scientific) and stored in the dark at 4°C until imaging. Chips were imaged on coverslips 25x75mm (Bellco Glass, Vineland, NJ, U.S.A via Electron Microscopy Sciences, Hatfield, PA) with 0.13-0.17 mm thickness using a Leica DMi8 microscope equipped with an Andor Dragonfly 200 spinning disk confocal using a 10x objective (NA 0.30), 20x water objective (NA 0.50) or 40x water objective (NA 0.80).

Primary Antibody	Species	Company	Cat. No.	Dilution
HTII-280	Mouse	Terrace Biotech	TB-27AHT-280	1:200
HTI-56	Mouse	Terrace Biotech	TB-29AHT1-56	1:50
Surfactant protein C	Rabbit	EMD Millipore	Ab3786	1:100
E-cadherin	Mouse	BD Transduction Laboratories	610182	1:400
RAGE	Rabbit	R&D systems	AF1145-sp	1:50
Keratin 5	Rabbit	Abcam	ab52635	1:200
ZO-1	Mouse	ThermoFisher	339100	1:100
Secondary Antibody	Company	Cat. No.	Dilution	
Alexa Fluor 448 Donkey anti Mouse	ThermoFisher	A21202	1:200	
Alexa Fluor 568 Donkey anti Mouse	ThermoFisher	A10037	1:200	
Alexa Fluor 448 Goat anti Rabbit	ThermoFisher	A11008	1:200	
Alexa Fluor 568 Donkey anti Rabbit	ThermoFisher	A10047	1:200	

Table 2. Antibodies

Results

Generation of alveolar type-2 organoid cultures from homogenized lung tissue

We developed a straightforward procedure for isolation of AEC2 from human lung tissue, that was recently also reported by another group using healthy tissue (Katsura et al. 2020). We dissociated macroscopically normal lung tissue derived from lung cancer patients with or without a smoking history (current smokers, ex-smokers and non-smokers) and additionally, for the first time to our knowledge, also used emphysematous lung tissue from LVRS surgery and obtained a single cell suspension using protease digestion. We subsequently cultured this single cell suspension in BME2 droplets. AEC2 organoid formation was rarely observed unless the commercial alveolar medium was supplemented with the canonical WNT activator CHIR99021 (CHIR; a GSK3 inhibitor), resulting in formation of predominantly alveolar organoids in PO and pure cultures after the first passage (Fig. 1A&B). To confirm that the use of specialized media was sufficient to direct AEC2 organoid formation from the total lung homogenate suspension, we next cultured the total lung homogenate suspension in our complete alveolar organoid medium or in specialized airway organoid medium (Sachs et al. 2019). When cells from the homogenate were cultured in complete alveolar organoid medium, organoids generated were characterized by presence of the alveolar marker HTII-280 and absence of the airway basal cell marker keratin 5 (HTII-280⁺/KRT5⁻). Using the airway organoid medium, the development of predominantly bronchial organoids was observed (HTII-280⁻/KRT5⁺; Fig. 1C&D). Although HTII-280⁺-cell clumps were visible in these cultures, they remained small and did not progress into organoid development. However, despite developing a successful medium to support alveolar organoid formation, we noticed that some isolations failed. Characterization of the HTII-280⁺ population in the lung homogenate suspension using cytopspin preparations, showed a strong donor-dependent ratio of AEC2 to other cells. We therefore hypothesized that as a result, the AEC2 to other cell ratio per gel drop was insufficient in some donors for successful establishment of alveolar organoids. To overcome this issue, we decided to include an enrichment step for AEC2.

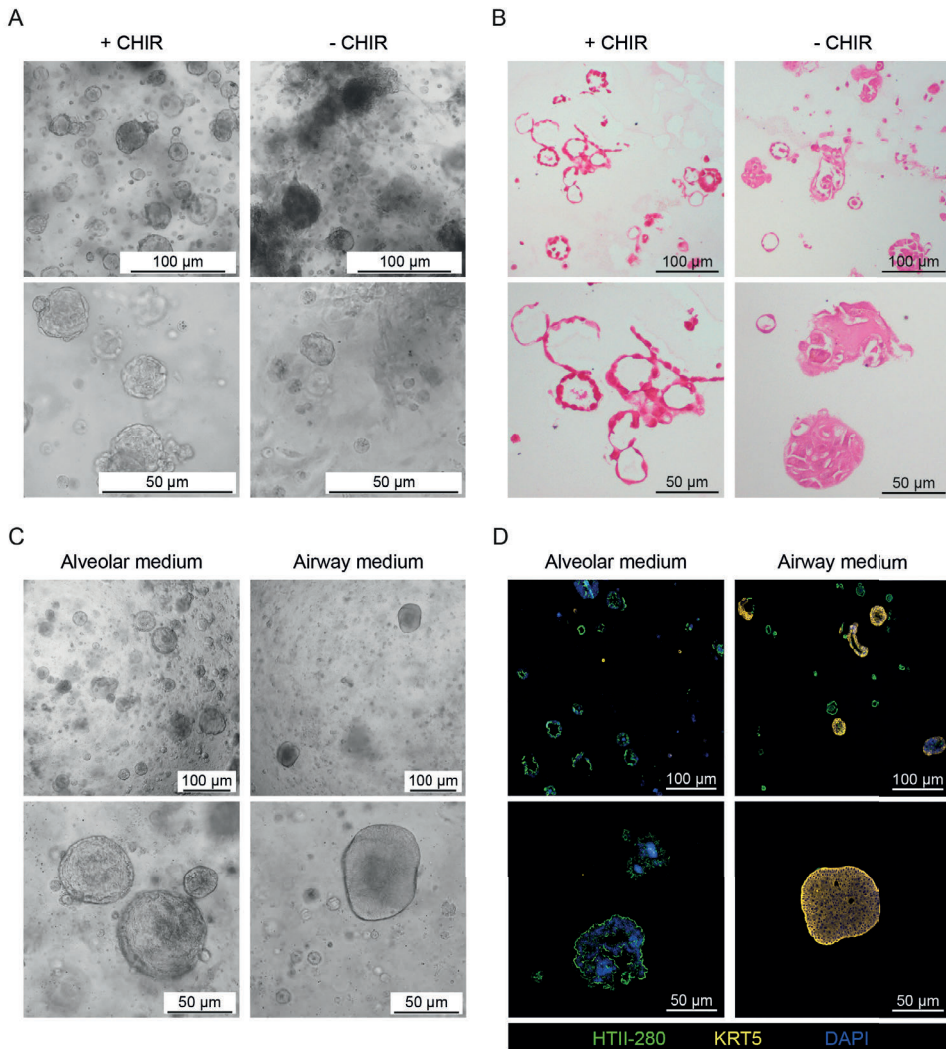


Figure 1. Generation of alveolar type-2 organoid cultures from homogenized lung tissue. Lung tissue was enzymatically digested to obtain a single cell suspension which was subsequently cultured in BME2 drops. A, Brightfield imaging of organoids cultured in alveolar medium supplemented with (+) or without (-) 4 μ M CHIR, a GSK3 inhibitor. B, Brightfield images of H&E staining of AEC2 cells cultured in alveolar medium supplemented with (+) or without (-) CHIR. Representative images of experiments performed with N=3 different donors (A, B). C, Brightfield images of organoids cultured from lung tissue homogenate in alveolar medium (including CHIR) or airway organoid medium. Representative image of experiments performed with N=3 different donors. D, Fluorescent imaging of organoids stained for HTII-280 (AEC2, green) and Keratin 5 (KRT5; airway basal cells, yellow), nuclei were stained with DAPI (blue).

Alveolar type-2 cell enrichment from peripheral lung tissue homogenate by HTII-280⁺ selection

Our initial studies revealed that cell cultures started from the whole lung homogenate caused issues with obtaining sufficient AEC2 for organoid

formation in some donors. Therefore, an enrichment step was included to first isolate AEC2 from the lung tissue homogenate. Isolation of AEC2 from peripheral tissue either by selection via adherence steps or EpCAM⁺ epithelial cell sorting results in an undesired mixture of cell types, including AEC2 but also airway epithelial cells and mesenchymal cells. A decade ago, Gonzalez and colleagues showed that the AEC2 marker HTII-280 could be

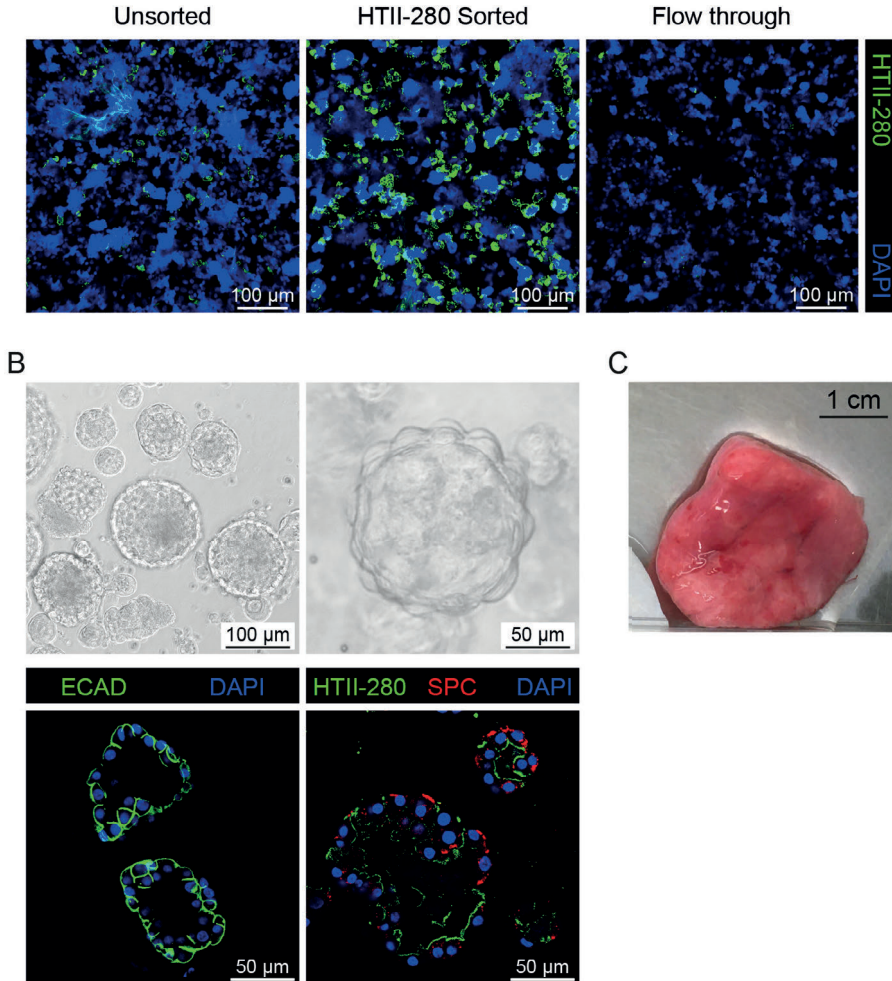


Figure 2. HTII-280⁺ selection of alveolar type-2 cells from homogenized lung tissue. Lung tissue was enzymatically digested to obtain a single cell suspension, after which HTII-280 selection via magnetic beads was performed. Sorted cells were subsequently cultured in BME2 drops. A, Representative immunofluorescent images of cytospin preparation of lung tissue homogenate (unsorted, sorted and the flow-through after sorting). AEC2 were stained with HTII-280 (green) and DAPI (blue) for nuclei staining. Representative image from N=3 independent experiments with different donors. B, Representative brightfield images of organoids derived from the HTII-280⁺ fraction cultured in alveolar medium. Representative image from N=4 independent experiments with different donors. Fluorescent images of organoids stained for HTII-280 (AEC2, green) and surfactant protein C (SP-C, red); nuclei were stained with DAPI (blue). Representative images of N=4 different donors. C, Example of amount of lung tissue that is minimally required to isolate sufficient cells for AEC2 organoid development.

used to increase the purity of the AEC2 population (Gonzalez et al. 2010). This method was based on fluorescence-activated cell sorting (FACS), which requires expensive equipment, skilled personnel and is time-consuming. Here we decided to integrate a magnetic bead-based isolation, that was recently also reported by Katsura et al. (Katsura et al. 2020). Lung tissue homogenate was incubated with an HTII-280 antibody, and next coupled to anti-mouse IgM-coated magnetic beads to allow magnetic bead-based AEC2 isolation. Although 100% pure AEC2 populations could not be achieved using this method, the enrichment was significant (Fig. 2A). Using this method, in combination with our complete alveolar organoid medium, we could obtain sufficient AEC2 to establish successful organoid cultures (Fig. 2B), while needing only relatively small pieces of tissue (Fig. 2C). We obtained a >85% (N=8/9 isolations) success rate using the finalized method for the formation of alveolar organoids up to P1. This method of isolation proved successful when using peripheral tissue obtained from macroscopically normal lung tissue from lung cancer surgery with or without a smoking history or COPD. In addition, AEC2 isolation from emphysematous lung tissue removed during LVRS for severe emphysema was successful in ~71% (10/14) of isolations, using different versions of the protocol, but successfully validated with the final protocol presented in the methods section for one donor.

Propagation and expansion of primary alveolar type-2 cells in feeder-free organoid cultures

After AEC2 enrichment by HTII-280⁺ selection, the cells were cultured in BME2 to allow organoid formation with the aim to propagate and expand the AEC2 for future experiments. We cultured the isolated AEC2 in a feeder-free

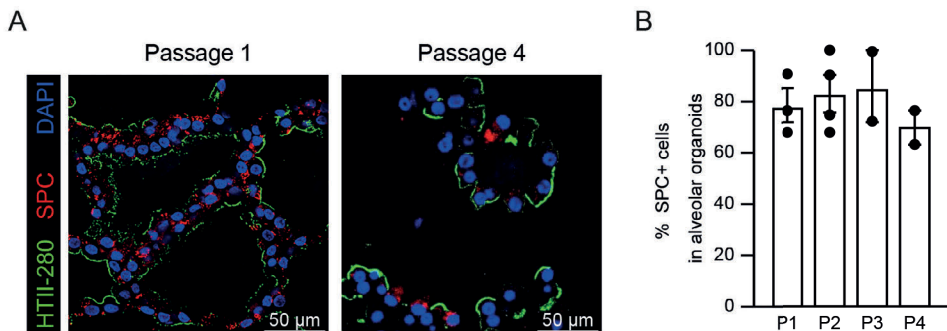


Figure 3. Propagation and expansion of primary alveolar type-2 cells AEC2 *in vitro*. A, Representative immunofluorescent images of a cross-section of embedded AEC2 organoids after passage 1 and after passage 4. Cells are stained for HTII-280 (green) and surfactant protein C (SP-C, red) and nuclei with DAPI (blue). B, Quantification of SP-C⁺ cells in organoids cultured at different passages (P#). N=2-4 different donors.

organoid system and were able to propagate the AEC2 organoids for weeks to months, depending on the donor, while maintaining AEC2 characteristics and increasing cell numbers (Fig. 3A). Generally, AEC2 were used for experiments before cessation of growth, but when propagated, P6 could be reached. It remains unclear which factor(s) play(s) a role in cessation of organoid growth. On average 80% of cultures that reached P1 were also able to reach passage P3. HTII-280 expression remained positive for all cells in the organoids over time of passaging (Fig. 3A) as well as surfactant protein C (SP-C) expression (Fig 3B), although SP-C decreased in organoids from some donors. Interestingly, propagation and expansion rates were similar between macroscopically normal lung tissue and LVRS-tissue derived AEC2 (observation), even though LVRS-resected lung tissue constitutes the most damaged part of the emphysematous lung.

Culturing alveolar type-2 cells on Transwell and Alveolus Lung-Chip cell culture platforms

To validate that patient-derived AEC2 propagated as organoids were suitable for experiments on traditional Transwells and an Organs-on-Chips platform, we dissociated the alveolar organoids and seeded them on Transwell or Lung-Chips. For Transwell we used a collagen I/fibronectin/BSA coating, since collagen IV coating did not result in successful attachment of the cells to the Transwell PET membrane. In contrast, for the Alveolus Lung-Chip, collagen IV coating resulted in a good attachment of the cells. AEC2 were kept in submerged culture for 7 days after which we fixed the cells and stained for AEC1 and AEC2 phenotypic markers and tight junctions. We found that AEC2 cultured for seven days, maintained expression of type-2 markers HTII-280⁺ and/or SP-C⁺, and ZO-1 staining throughout the monolayer (Fig. 4A), whereas AEC1 markers HTI-56 and RAGE could not be detected.

Since Organs-on-Chips technology allows a closer representation of the *in vivo* lung microenvironment compared to Transwells, we were interested in investigating how breathing-like motions such as cyclic stretch may preserve primary AEC2 phenotype in culture. To investigate this, we seeded the Alveolus Lung-Chip with AEC2 from 1 to max. 6 donors (donor mix) that were expanded via organoid culture and allowed the cells to reach confluency in 2-3 days. Next, we cultured the cells for an additional 5 days submerged in the presence or absence of dynamic stretch. We noticed a quick but small change in morphology of the cells cultured in the chips

that were exposed to dynamic stretch, which was more pronounced in some donor mixes than others (Fig. 4B). Next, we assessed HTII-280 and SP-C expression after 5 days of submerged culture in presence or absence of dynamic stretch. AEC2 are known to spontaneously differentiate toward an AEC1 phenotype in culture (Zhao, Yee, and O'Reilly 2013), but after 5 days we still found a substantial amount of HTII-280⁺ cells in both the control

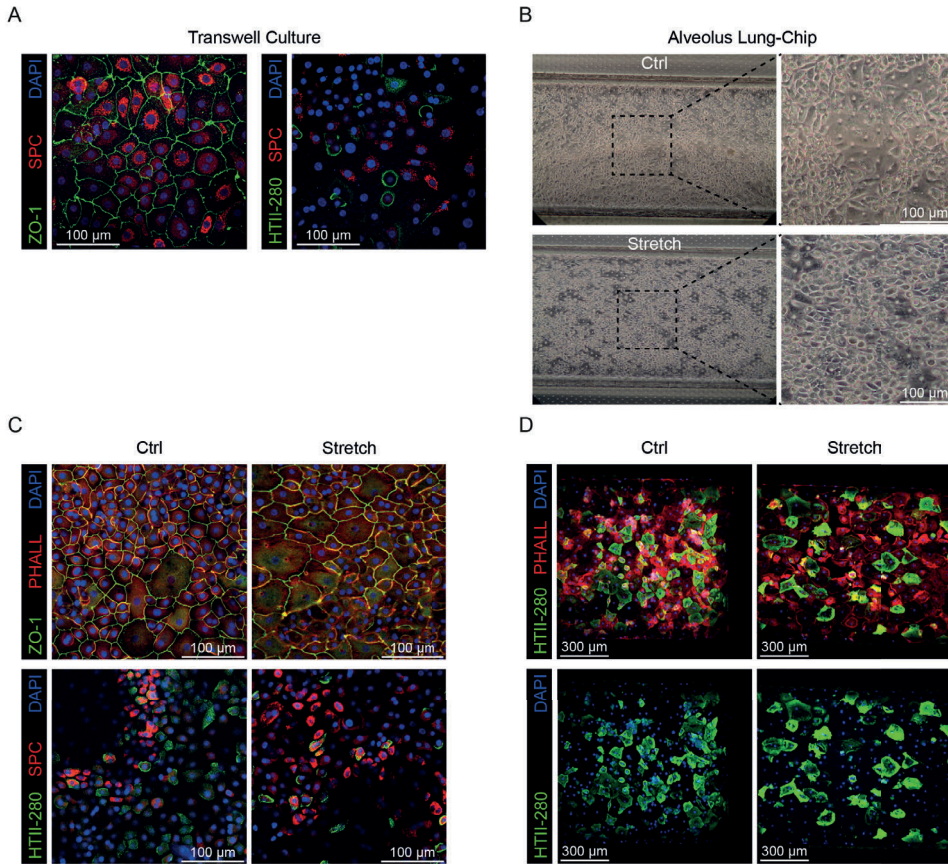


Figure 4. Alveolar type-2 cell culture after expansion as organoid on the Transwell and Alveolus Lung-Chip platform. Organoids from donors at different passages were dissociated, mixed and seeded on Transwells or the Alveolus Lung-Chip for seven days. A, Fluorescent images of Transwell cultures of AEC2 after seven days of culture. Cells were fixed and stained for HTII-280 (green), surfactant protein C (SP-C, red) or ZO-1 (green) and nuclei with DAPI (blue). Representative image from N=4 independent experiments with different donor(mixes). B, Representative images of Alveolus Lung-Chip: AEC2 organoids were dissociated and seeded on the Alveolus Lung-Chip platform and cultured for 5 days after reaching confluency (generally within 2-3 days). During these 5 days, some chips were exposed to 10% dynamic stretch at 0.25Hz (stretch). C, Cells in the chips were fixed and cut into two parts, ZO-1 (green), phalloidin (red) and a nuclei stain (DAPI, blue) were combined in one half of the chips, in the other half, AEC2 were stained with HTII-280 (green) and surfactant protein C (SP-C, red) and nuclei using DAPI (blue). N=4 independent experiments using different donor (mixes) per experiment, 1 chip each. D, Fluorescent images of Alveolus Lung-Chip cultures that were seeded with a lower cell density as the chips cultured in B, displaying different morphology with larger cell size. Cells were stained with HTII-280 (green) and surfactant protein C (SP-C, red) and nuclei using DAPI (blue).

and stretch-exposed chips and ZO-1 expression throughout (Fig. 4C). Since we were not successful in counting the cells in the dissociated organoid suspension, as we do not obtain a completely single cells suspension, we had variable seeding densities between experiments and we did observe that in some experiments the initial seeding density was lower than anticipated, but despite this the cells reached confluence and expressed HTII-280 (Fig. 4D). However, when these cells underwent dynamic stretch, some areas showed signs of cell detachment, suggesting that under these additional forces the cells may experience difficulties staying attached to the membrane when initial cell number is rather low. In addition, these cells displayed a different morphology as they were larger in size (Fig. 4D).

Discussion

Here we present a proof-of-principle application of AEC2 isolated from relatively small pieces of patient-derived emphysematous and non-emphysematous lung tissue, which after feeder-free expansion could be cultured on classical Transwell and the Alveolus Lung-Chip. AEC2 isolation was successful in relatively healthy unaffected lung tissue but also in tissue from long-term smokers, COPD patients and emphysematous lung tissue that was removed during lung volume reduction surgery. Strikingly, even this emphysematous tissue yielded high numbers of AEC2, demonstrating the versatility of this protocol for use with both healthy and (very) diseased lung tissue. Using a straightforward isolation and expansion method, we could culture these AEC2 for weeks up to months in organoids while maintaining AEC2 marker expression (Lamers et al. 2021). When expanding AEC2 using conventional 2D culture, the transient loss of AEC2 phenotype and the increase in AEC1 makers restricts studies from being performed over longer time periods and also limits the comparability between independent experiments. Using our newly developed protocol we observed that after 7 days of culture on the Alveolus Lung-Chip, HTII-280⁺ and/or SP-C₊ cells were still present, which provides future possibilities to perform functional assays on regenerative potential of AEC2.

The usefulness of HTII-280 as a marker for the isolation of AEC2 has been demonstrated previously (Glisinski et al. 2020; Gonzalez et al. 2010; Katsura et al. 2020). Isolation of AEC2 based on HTII-280 proved successful as the enrichment step was found to be essential due to the variable proportions of AEC2 in the total isolated cell suspension derived from different tissues.

Although we obtained a pure alveolar organoid culture upon passaging of the organoids, we did find additional non-epithelial cells in the isolated population at the initiation of organoid culture (PO). However, these cells were no longer present in our culture after the first passage. There was almost no contamination with airway epithelial cells in the alveolar organoid cultures after the first passage.

When we cultured the cells from the whole lung tissue homogenate (all epithelial cells still present) in airway organoid medium (Sachs et al. 2019), we obtained predominantly KRT5⁺ airway organoids and many small alveolar cell clumps that did not develop further. Conversely, when the lung homogenate was cultured in complete alveolar organoid medium, analysis of the culture revealed little to no KRT5⁺ airway epithelial cells but predominantly HTII-280⁺ AEC2 organoids. Although these observations provide strong support for the selection pressure issued by these specialized media, we cannot exclude that the non-AEC2 present after isolation and during the start of the culture may influence success of the alveolar cell cultures during the first or succeeding passages. Therefore, if required, for example when cells are directly used in experiments, the purity of the AEC2 population after isolation could be further optimized. To this end, we have so far also tested depletion of leukocytes via CD45 selection, which did not affect organoid formation. If sufficient AEC2 are present in relation to the other cells in the homogenate, this application however does allow for culture of small airway epithelial organoids and alveolar organoids from the same donor, with cells derived from adult tissue.

AEC2 are notoriously difficult to cryopreserve and this issue has unfortunately not been resolved yet but is focus of our current activities. Nevertheless, we were able to store pieces of unprocessed resected lung tissue at -80°C for longer periods of time (weeks) and still successfully isolated AEC2, although isolation of AEC2 from fresh tissue was preferred as this resulted in a significant better yield.

We observed that whereas alveolar cells grown in organoids retained HTII-280 expression, some of the organoid cultures (donor dependent) were found to decrease expression of SP-C upon prolonged culture. This raises the question of which additional markers should be used to define AEC2. The loss of SP-C was previously interpreted as a loss of AEC2 phenotype (Zhao, Yee, and O'Reilly 2013; Mao et al. 2015), however also AEC2 cultured on Transwell and chip demonstrated both HTII-280 and SP-C double or

single-positive cells. Transcriptomic analysis has revealed various subsets of alveolar cells, characterized by expression of subset-specific genes (Choi et al. 2020). These markers could potentially be interesting to use in the cultures used in this study. In addition, Choi and co-workers additionally showed that various alveolar cell subsets could be derived from AEC2 by exposure to (macrophage-derived) IL-1 β in mice. It would be interesting to assess whether this approach also affects human AEC2 differentiation in culture. Interestingly when isolating AEC2 from LVRS donors, we did not observe a difference in growth rate or organoid number, suggesting that these properties are not affected by in cells isolated from an emphysematous environment. One explanation could be is that the isolation procedure selects for a more robust AEC2 subset from this tissue, that may be present in varying amount in tissue from different donors. However, although tissue pieces from different donors are difficult to compare, we did not experience that yield was lower from LVRS tissue compared to the other tissues. Alternatively, differentiation from AEC2 to AEC1 may be impaired or affected in LVRS tissue, and therefore it will be interesting to further study this and other characteristics of these cells in culture.

When seeding the dissociated AEC2 organoids on Transwell or Alveolus Lung-Chip, we could still detect HTII-280 expression and/or SP-C after 7 days of culture. We tried to determine AEC1 numbers after these 7 days of culture, however expression of established markers for AEC1 (Kobayashi et al. 2020), HTI-56 and RAGE, could not be detected. It is unclear whether this relates to a technical issue or whether we were unable to achieve AEC1 differentiation by using our complete alveolar organoid medium. Investigations are ongoing to gain insight into this observation, but we speculate that the supplementation of CHIR contributes to the lack of observed AEC1 markers. The effect of canonical WNT activation on the propagation and AEC2 morphology has been described previously in organoid cultures (Nabhan et al. 2018).

The magnetic bead-based solution for enrichment of the AEC2 population in the lung homogenate suspension described here and previously (Katsura et al. 2020) greatly improves the workflow and time for AEC2 isolation, and also the use of minimally modified commercial medium limits the high costs often associated with feeder-free organoid culture. Being able to dissociate the expanded organoid cultures for seeding on Transwell and/or Lung-Chips allows a large range of experimental set-ups including those with gaseous exposures, or application of viruses on the luminal side of the alveolar cell

cultures once air-liquid interface cultures have also been validated with use of this procedure. Successful isolation from diseased tissue also extends the possible experimental approaches significantly and allows to study repair and regeneration using cells derived from a relevant microenvironment. A limitation of the method presented here as well as those of others, is that the rate of proliferation of the AEC2 is relatively low and the time it takes to obtain sufficient cells for experiments also depends on the initial yield of AEC2. In Alveolus Lung-Chip cultures, for example, the number of cells needed is still significant, which limited our experimental set-up and necessitates the use of donor mixes instead of single donors for use in experiments. Future endeavours will aim to promote expansion by modulation of signalling pathways, and use of AEC2-AEC1 differentiation media (Katsura et al. 2020) by determining those culture conditions that allow control over AEC2 to AEC1 differentiation, possibly by further modulation of WNT signalling (Zacharias et al. 2018).

The unique set-up of the Alveolus Lung-Chip allows for the implementation of cyclic stretch on the alveolar cell cultures (Hassell et al. 2017; Huh 2015). Especially with relevance to the lungs, the stiffness of current cell culture plastics does not allow application of breathing biomechanics and does not mimic the mechanical properties of this soft, dynamic tissue (Butcher, Alliston, and Weaver 2009). Application of patient-derived AEC2 in these models will aid in elucidating how biomechanical forces related to breathing play a role in alveolar homeostasis and disease. Recently, interesting links between biomechanics and cellular function have been revealed, as illustrated by Park and colleagues (Park et al. 2020) showing that stiffness of the substrate impacts bronchial epithelial cell metabolism. Furthermore, an increase in stiffness and reduced stretch can lead to cytoskeletal reorganization which can influence integrin-mediated latent TGF- β 1 activation, which in turn may contribute to disease progression in diseases such as COPD (Froese et al. 2016). However, this has not been studied in relation to alveolar epithelial cells. Organoid cultures could support studies on epithelial biology in relation to matrix stiffness, however since there is no air-liquid interface and no application of strain, a complementary approach with stretchable Lung-Chip models is preferred. To establish proof-of-principle that the primary AEC2 obtained via our isolation protocol could be cultured under cyclic stretch in the Alveolus Lung-Chip, we exposed them to similar levels of stretch as previously reported (Hassell et al. 2017) as this was well tolerated and mimics what is expected in an alveolus (Waters, Roan, and Navajas

2012; Fredberg et al. 1997). We observed that the alveolar cells exposed to stretch slightly aligned in the direction of the flow and perpendicular to the direction of the stretch already within 24 h after initiation of stretch. It is at present unclear whether this response mimics behaviour of the alveolar cells *in situ*, especially as this response varied highly between cultures/donor mixes. Although this first proof-of-principle showed the feasibility of stretch application to these primary alveolar cell cultures, derived from healthy and end stage emphysematous lung tissue, future research will focus on the impact of different stretch intensities in combination with air-liquid interface, preferably in co-culture with other cell types in the chip such as endothelial cells and/or fibroblasts. Such extensive experiments are beyond the current proof-of-principle as AEC2 cultures would need to be further upscaled. In addition, running combinations of different flow and stretch conditions on-Chip in the same experiment is still restricted due to the current level or resources needed for such a set-up using this technology.

In conclusion, we demonstrate the successful isolation of AEC2 from diseased human lung tissue which can subsequently be expanded using feeder-free organoid culture. The organoids retain expression of AEC2 markers over time and can be dissociated for further experiments. We showed the feasibility of culturing these patient-derived AEC2 in the Alveolus Lung-Chip under application of cyclic strain. This method is expected to aid future research on how forces related to breathing contribute to alveolar homeostasis and disease, which is needed in view of the important gaps in our knowledge of cellular biomechanics of the human alveolus in health and disease.

Acknowledgement

We would like to thank Emulate, especially Geraldine Hamilton and Lorna Ewart for their support in the development of the Alveolus Lung-Chip cultures. We would like to thank the LUMC Light and Electron Microscopy Facility for technical assistance during imaging of the Alveolus Lung-Chip. This study was supported by a grant of the Lung Foundation Netherlands (grant # 6.1.14.010), The Netherlands Organization for Health Research and Development (ZonMw; grant #114021508), Translationeel Adult Stamcelonderzoek – ZonMw (TAS-ZonMW; grant #40414009816007), EU Marie Curie Global Fellowship (#748569), Stichting Proefdiervrij.

Author contributions

Conception and design: SR, AS, PK, PH, AD; Patient selection and sample preparation: SR, AS, PK, JS, AD; Analysis and interpretation: SR, AS, PH, AD; Drafting the manuscript for important intellectual content: SR, AS, PK, JS, PH, AD. All authors have read the manuscript, provided input and agree with its submission.

References

- Agusti, A., and J. C. Hogg. 2019. 'Update on the Pathogenesis of Chronic Obstructive Pulmonary Disease', *N Engl J Med*, 381: 1248-56.
- Benam, K. H., R. Villenave, C. Lucchesi, A. Varone, C. Hubeau, H. H. Lee, S. E. Alves, M. Salmon, T. C. Ferrante, J. C. Weaver, A. Bahinski, G. A. Hamilton, and D. E. Ingber. 2016. 'Small airway-on-a-chip enables analysis of human lung inflammation and drug responses *in vitro*', *Nat Methods*, 13: 151-7.
- Butcher, D. T., T. Alliston, and V. M. Weaver. 2009. 'A tense situation: forcing tumour progression', *Nat Rev Cancer*, 9: 108-22.
- Celli, B. R., and J. A. Wedzicha. 2019. 'Update on Clinical Aspects of Chronic Obstructive Pulmonary Disease', *N Engl J Med*, 381: 1257-66.
- Choi, J., J. E. Park, G. Tsagkogeorga, M. Yanagita, B. K. Koo, N. Han, and J. H. Lee. 2020. 'Inflammatory Signals Induce AT2 Cell-Derived Damage-Associated Transient Progenitors that Mediate Alveolar Regeneration', *Cell Stem Cell*, 27: 366-82 e7.
- Evans, K. V., and J. H. Lee. 2020. 'Alveolar wars: The rise of *in vitro* models to understand human lung alveolar maintenance, regeneration, and disease', *Stem Cells Transl Med*, 9: 867-81.
- Fredberg, J. J., D. Inouye, B. Miller, M. Nathan, S. Jafari, S. H. Raboudi, J. P. Butler, and S. A. Shore. 1997. 'Airway smooth muscle, tidal stretches, and dynamically determined contractile states', *Am J Respir Crit Care Med*, 156: 1752-9.
- Froese, A. R., C. Shimbori, P. S. Bellaye, M. Inman, S. Obex, S. Fatima, G. Jenkins, J. Gaudie, K. Ask, and M. Kolb. 2016. 'Stretch-induced Activation of Transforming Growth Factor-beta1 in Pulmonary Fibrosis', *Am J Respir Crit Care Med*, 194: 84-96.
- Glisinski, K. M., A. J. Schlobohm, S. V. Paramore, A. Birukova, M. A. Moseley, M. W. Foster, and C. E. Barkauskas. 2020. 'Interleukin-13 disrupts type 2 pneumocyte stem cell activity', *JCI Insight*, 5.
- Gonzalez, R. F., L. Allen, L. Gonzales, P. L. Ballard, and L. G. Dobbs. 2010. 'HTII-280, a biomarker specific to the apical plasma membrane of human lung alveolar type II cells', *J Histochem Cytochem*, 58: 891-901.
- Hassell, B. A., G. Goyal, E. Lee, A. Sontheimer Phelps, O. Levy, C. S. Chen, and D. E. Ingber. 2017. 'Human Organ Chip Models Recapitulate Orthotopic Lung Cancer Growth, Therapeutic Responses, and Tumor Dormancy *In Vitro*', *Cell Rep*, 21: 508-16.
- Hiemstra, P. S., T. D. Tetley, and S. M. Janes. 2019. 'Airway and alveolar epithelial cells in culture', *Eur Respir J*, 54.
- Hogg, J. C., and W. Timens. 2009. 'The pathology of chronic obstructive pulmonary disease', *Annu Rev Pathol*, 4: 435-59.
- Huh, D. D. 2015. 'A human breathing lung-on-a-chip', *Ann Am Thorac Soc*, 12 Suppl 1: S42-4.
- Huh, D., B. D. Matthews, A. Mammoto, M. Montoya-Zavala, H. Y. Hsin, and D. E. Ingber. 2010. 'Reconstituting organ-level lung functions on a chip', *Science*, 328: 1662-8.
- Jacob, A., M. Morley, F. Hawkins, K. B. McCauley, J. C. Jean, H. Heins, C. L. Na, T. E. Weaver, M. Vedaie, K. Hurley, A. Hinds, S. J. Russo, S. Kook, W. Zacharias, M. Ochs, K. Traber, L. J. Quinton, A. Crane, B. R. Davis, F. V. White, J. Wambach, J. A. Whitsett, F. S. Cole, E. E. Morrissey, S. H. Guttentag, M. F. Beers, and D. N. Kotton. 2017. 'Differentiation of Human Pluripotent Stem Cells into Functional Lung Alveolar Epithelial Cells', *Cell Stem Cell*, 21: 472-88 e10.
- Katsura, H., V. Sontake, A. Tata, Y. Kobayashi, C. E. Edwards, B. E. Heaton, A. Konkimalla, T. Asakura, Y. Mikami, E. J. Fritch, P. J. Lee, N. S. Heaton, R. C. Boucher, S. H. Randell, R. S. Baric, and P. R. Tata. 2020. 'Human Lung Stem Cell-Based Alveolospheres Provide Insights into SARS-CoV-2-Mediated Interferon Responses and Pneumocyte Dysfunction', *Cell Stem Cell*.

- Khakban, A., D. D. Sin, J. M. FitzGerald, B. M. McManus, R. Ng, Z. Hollander, and M. Sadatsafavi. 2017. 'The Projected Epidemic of Chronic Obstructive Pulmonary Disease Hospitalizations over the Next 15 Years. A Population-based Perspective', *Am J Respir Crit Care Med*, 195: 287-91.
- Kobayashi, Y., A. Tata, A. Konkimalla, H. Katsura, R. F. Lee, J. Ou, N. E. Banovich, J. A. Kropski, and P. R. Tata. 2020. 'Persistence of a regeneration-associated, transitional alveolar epithelial cell state in pulmonary fibrosis', *Nat Cell Biol*, 22: 934-46.
- Lamers, M. M., J. van der Vaart, K. Knoop, S. Riesebosch, T. I. Breugem, A. Z. Mykytyn, J. Beumer, D. Schipper, K. Bezstarosti, C. D. Koopman, N. Groen, R. B. G. Ravelli, H. Q. Duimel, J. A. A. Demmers, Gmgm Verjans, M. P. G. Koopmans, M. J. Muraro, P. J. Peters, H. Clevers, and B. L. Haagmans. 2021. 'An organoid-derived bronchioalveolar model for SARS-CoV-2 infection of human alveolar type II-like cells', *EMBO J*, 40: e105912.
- Mao, P., S. Wu, J. Li, W. Fu, W. He, X. Liu, A. S. Slutsky, H. Zhang, and Y. Li. 2015. 'Human alveolar epithelial type II cells in primary culture', *Physiol Rep*, 3.
- Miravittles, M., C. Vogelmeier, N. Roche, D. Halpin, J. Cardoso, A. G. Chuchalin, H. Kankaanranta, T. Sandstrom, P. Sliwinski, J. Zatloukal, and F. Blasi. 2016. 'A review of national guidelines for management of COPD in Europe', *Eur Respir J*, 47: 625-37.
- Nabhan, A. N., D. G. Brownfield, P. B. Harbury, M. A. Krasnow, and T. J. Desai. 2018. 'Single-cell Wnt signaling niches maintain stemness of alveolar type 2 cells', *Science*, 359: 1118-23.
- Park, J. S., C. J. Burckhardt, R. Lazcano, L. M. Solis, T. Isogai, L. Li, C. S. Chen, B. Gao, J. D. Minna, R. Bachoo, R. J. DeBerardinis, and G. Danuser. 2020. 'Mechanical regulation of glycolysis via cytoskeleton architecture', *Nature*, 578: 621-26.
- Sachs, N., A. Pappasypoulos, D. D. Zomer-van Ommen, I. Heo, L. Bottinger, D. Klay, F. Weeber, G. Huelsz-Prince, N. Iakobachvili, G. D. Amatngalim, J. de Ligt, A. van Hoeck, N. Proost, M. C. Viveen, A. Lyubimova, L. Teeven, S. Derakhshan, J. Korving, H. Begthel, J. F. Dekkers, K. Kumawat, E. Ramos, M. F. van Oosterhout, G. J. Offerhaus, D. J. Wiener, E. P. Olimpio, K. K. Dijkstra, E. F. Smit, M. van der Linden, S. Jaksani, M. van de Ven, J. Jonkers, A. C. Rios, E. E. Voest, C. H. van Moorsel, C. K. van der Ent, E. Cuppen, A. van Oudenaarden, F. E. Coenjaerts, L. Meyaard, L. J. Bont, P. J. Peters, S. J. Tans, J. S. van Zon, S. F. Boj, R. G. Vries, J. M. Beekman, and H. Clevers. 2019. 'Long-term expanding human airway organoids for disease modeling', *EMBO J*, 38.
- Salahudeen, A. A., S. S. Choi, A. Rustagi, J. Zhu, V. van Unen, O. Sm de la, R. A. Flynn, M. Margalef-Catala, A. J. M. Santos, J. Ju, A. Batish, T. Usui, G. X. Y. Zheng, C. E. Edwards, L. E. Wagar, V. Luca, B. Anchang, M. Nagendran, K. Nguyen, D. J. Hart, J. M. Terry, P. Belgrader, S. B. Ziraldo, T. S. Mikkelsen, P. B. Harbury, J. S. Glenn, K. C. Garcia, M. M. Davis, R. S. Baric, C. Sabatti, M. R. Amieva, C. A. Blish, T. J. Desai, and C. J. Kuo. 2020. 'Progenitor identification and SARS-CoV-2 infection in human distal lung organoids', *Nature*.
- Uhl, E. W., and N. J. Warner. 2015. 'Mouse Models as Predictors of Human Responses: Evolutionary Medicine', *Curr Pathobiol Rep*, 3: 219-23.
- Waters, C. M., E. Roan, and D. Navajas. 2012. 'Mechanobiology in lung epithelial cells: measurements, perturbations, and responses', *Compr Physiol*, 2: 1-29.
- Witherden, I. R., and T. D. Tetley. 2001. 'Isolation and Culture of Human Alveolar Type II Pneumocytes', *Methods Mol Med*, 56: 137-46.
- World Health Organization. 2018. 'The top 10 causes of death'. <http://www.who.int/mediacentre/factsheets/fs310/en/>
- Zacharias, W. J., D. B. Frank, J. A. Zepp, M. P. Morley, F. A. Alkhaleel, J. Kong, S. Zhou, E. Cantu, and E. E. Morrisey. 2018. 'Regeneration of the lung alveolus by an evolutionarily conserved epithelial progenitor', *Nature*, 555: 251-55.
- Zamprogno, P., S. Wuthrich, S. Achenbach, G. Thoma, J. D. Stucki, N. Hobi, N. Schneider-Daum, C. M. Lehr, H. Huwer, T. Geiser, R. A. Schmid, and O. T. Guenat. 2021. 'Second-generation lung-on-a-chip with an array of stretchable alveoli made with a biological membrane', *Commun Biol*, 4: 168.
- Zhao, L., M. Yee, and M. A. O'Reilly. 2013. 'Transdifferentiation of alveolar epithelial type II to type I cells is controlled by opposing TGF-beta and BMP signaling', *Am J Physiol Lung Cell Mol Physiol*, 305: L409-18

CHAPTER 4

Disease modelling following organoid-based expansion of airway epithelial cells

Sander van Riet^{2,*}, Evelien Eenjes^{1,5,*}, Andre A. Kroon³, Annelies M. Slats², P. Padmini S. J. Khedoe², Anne Boerema- de Munck^{1,5}, Marjon Buscop-van Kempen^{1,5}, Dennis K. Ninaber², Irwin K.M. Reiss³, Hans Clevers⁴, Robbert J. Rottier^{1,5,**}, Pieter S. Hiemstra^{2,**,#}

¹Department of Pediatric Surgery, Erasmus MC-Sophia Children's Hospital, Rotterdam, The Netherlands

²Department of Pulmonology, Leiden University Medical Center, Leiden, The Netherlands

³Department of Neonatology, Erasmus MC-Sophia Children's Hospital, Rotterdam, The Netherlands

⁴Hubrecht Institute, Royal Netherlands Academy of Arts and Sciences, University of Medical Center, Utrecht, The Netherlands

⁵Department of Cell biology, Erasmus MC, Rotterdam, The Netherlands

* Both authors contributed equally to this manuscript and are co-first authors

** Shared senior co-authorship

American Journal of Physiology-Lung Cellular and Molecular Physiology; Accepted July 2021, In Press

Abstract

Air-liquid interface (ALI) cultures are frequently used in lung research but require substantial cell numbers that cannot readily be obtained from patients. We explored whether organoid expansion (3D) can be used to establish ALI cultures from clinical samples with low epithelial cell numbers. Airway epithelial cells were obtained from tracheal aspirates (TA) from preterm newborns, and from bronchoalveolar lavage (BAL) or bronchial tissue (BT) from adults. TA and BAL cells were 3D-expanded, whereas cells from BT were expanded in 3D and 2D. Following expansion, cells were cultured at ALI to induce differentiation. The impact of cell origin and 2D or 3D expansion was assessed with respect to (i) cellular composition; (ii) response to cigarette smoke exposure; (iii) effect of Notch inhibition or IL-13 stimulation on cellular differentiation. We established well-differentiated ALI cultures from all samples. Cellular compositions (basal, ciliated and goblet cells) were comparable. All 3D-expanded cultures showed a similar stress response following cigarette smoke exposure but differed from the 2D-expanded cultures. Higher peak levels of antioxidant genes *HMOX1* and *NQO1* and a more rapid return to baseline, and a lower unfolded protein response was observed after cigarette smoke exposure in 3D-derived cultures compared to 2D-derived cultures. Additionally, TA- and BAL-derived cultures were less sensitive to modulation by DAPT or IL-13 than BT-derived cultures. Organoid-based expansion of clinical samples with low cell numbers, such as TA from preterm newborns is a valid method and tool to establish ALI cultures.

Introduction

Recent advances in culture methods offer new and exciting possibilities to establish relevant human disease models. Many lung culture models include airway epithelial cells (AEC) because of their central role in various lung diseases. So far, most traditional methods using primary cells require substantial cell numbers to start such cultures and offer limited options for expansion either due to cellular senescence (Walters, Gomi et al. 2013) or premature differentiation of basal cells (Mou, Vinarsky et al. 2016). Therefore, there is a need for methods that allow establishment of cultures from patient samples containing small numbers of AEC. One major advance has been the culture of cells in matrix resulting in self-organizing 3D organoid cultures. Airway organoids can be grown from stem/progenitor cells of different parts of the lung and several methods for establishing human airway organoids have been described (Barkauskas, Chung et al. 2017, Nikolic, Sun et al. 2018). Airway organoids are used in various settings, including studies on viral infections (Hui, Ching et al. 2018, van der Sanden, Sachs et al. 2018, Zhou, Li et al. 2018), lung cancer (Kim, Mun et al. 2019) and drug responses (Sachs, Papaspyropoulos et al. 2019). A recent report demonstrated long-term expansion of patient specific airway organoids, without the need for feeder cells (Sachs, Papaspyropoulos et al. 2019). The ability of airway organoids to maintain patient characteristics is of particular interest for patient specific assays as demonstrated in cystic fibrosis research but might also be relevant for future research of more complex airway diseases, like asthma, COPD and bronchopulmonary dysplasia.

A major drawback is that airway organoids are oriented inwards, and the lumen is filled with fluid. Therefore, studying the effect of external airborne stimuli on airway epithelium such as air pollutants, as well as drugs administered through the airways, is not feasible or at the least not practical. In contrast, the well-established air-liquid interface (ALI) cultures have been widely used to study airway epithelial exposures (Hiemstra, Grootaers et al. 2018). We have previously shown effects of whole cigarette smoke exposure on differentiation and host defense (Amatngalim, Schrupf et al. 2018). Establishment of airway ALI cultures from primary cells, requires the availability of AEC that can be isolated from airway tissues that subsequently need to be expanded. Especially obtaining AEC from the lower respiratory tract is markedly hampered by the need for invasive procedures to obtain such samples. Furthermore, the amount of starting material obtained from

bronchoscopic procedures, is often limited. Because only limited cell numbers are required to establish an organoid culture (Sachs, Papaspyropoulos et al. 2019), we tested the feasibility to use airway organoids as a means to propagate and expand patient-derived cells which can subsequently be cultured and studied on ALI. Here we present a functional comparison of ALI cultures that were established from organoid-expanded AEC, with those derived from AEC that were expanded on conventional tissue culture plastic. Furthermore, a functional comparison was made between ALI cultures derived from different clinically available samples. We confirmed the establishment of AEC culture derived from bronchoalveolar lavage fluid, and show that tracheal aspirates of preterm newborns are a viable source for establishing ALI cultures.

Methods

Patient material

The use of all adult lung samples that were collected within the framework of patient care from adult patients during surgery or bronchoscopy, was in line with the “Human Tissue and Medical Research: Code of conduct for responsible use” (2011) (www.federa.org) and followed the advice of the LUMC Medical Ethical Committee. Tissue donation was based on a no-objection system for coded anonymous use of residual tissue, left-over from diagnostic or therapeutic procedures. “No-objection” negates the need for individual informed consent. For the tracheal aspirates, informed consent was obtained from parents and approval was given by the Medical Ethical Committee (METC nr. MEC-2017-302). All samples were completely anonymized.

Bronchial tissue

Macroscopically normal tumor-free bronchial tissue (BT) was obtained from patients undergoing resection surgery for lung cancer at the Leiden University Medical Center (LUMC; Leiden, The Netherlands). Human primary airway epithelial cells (AEC) were then cultured in 2D cultured as described previously (Amatngalim, Schrupf et al. 2018) or 3D as described below.

Tracheal aspirates

Tracheal aspirates were collected using a closed suction system from preterm infants (<28 weeks gestational age) in need of mechanical ventilation at the neonatal intensive care unit of Erasmus MC Sophia Children's Hospital. The tracheal aspirates collected were directly processed or stored at 4 °C within 1 h of the procedure.

Bronchoalveolar lavage

Bronchoalveolar lavage (BAL)-fluid was obtained from patients (>18 years) undergoing routine bronchoscopic procedures. The indication for the routine bronchoscopic procedure was either excluding atypical infection or suspicion of interstitial lung disease and therefore the procedure included a lavage. The bronchoscopy was performed according to the protocol of a bronchoalveolar lavage of the Department of Pulmonology of the LUMC: The bronchoscope was placed in a wedge position within the selected bronchopulmonary segment. Room temperature saline was instilled through the bronchoscope, with a total volume of between 100 and 200 ml and divided into three to five aliquots. Instilled saline is retrieved using a negative suction pressure. When the re-collection of fluid exceeded the amount required for the specific diagnostic procedures for the patient, the extra fluid could be used for 3D organoid expansion. The fluids collected were directly processed or stored at 4 °C within 1 h of the procedure.

Human primary epithelial cell culture from bronchial tissue

AEC were cultured as described previously (Amatngalim, Schrumpf et al. 2018, Schrumpf, Ninaber et al. 2020). Briefly, healthy bronchial tissue (BT) was incubated in 0.15% (w/v) Protease XIV (Sigma, St. Louis, MO, US) for 2 h at 37 °C. The luminal side of the BT was then scraped in PBS and 90% of the obtained AEC were centrifuged and resuspended in keratinocyte serum free medium (KSFM)-AEC expansion medium (Supplemental Table S1) for 2D expansion. The remaining 10% of the AEC was used for 3D expansion; additionally, in supplemental Figure S4C we also used 1% of the total AEC harvested from the BT (see next section). 2D culture plates were coated with 10 µg/mL human fibronectin (PromoCell, Bio-connect, Huissen, Netherlands), 30 µg/mL BSA (Thermo Fisher, Waltham, MA, US) and 10 µg/mL PureCol (Cellsystems GmbH, Troisdorf, Germany) for 2 h at 37 °C.

For ALI culture, cells were grown until confluence in KSFM-AEC expansion medium, trypsinized and 1×10^5 AEC were plated per coated 12-transwell insert (Corning, Corning, NY, US). AEC on inserts were cultured in Bronchial epithelial growth medium (BepiCM; ScienCell Research laboratories, Carlsbad, CA, US) diluted 1:1 with DMEM with 4500 mg/L D-Glucose (stem cell technologies, Vancouver, Canada) with BepiCM supplements and 100 U/mL penicillin and 100 μ g/mL streptomycin (ScienCell Research Laboratories). During submerged culture, cells were kept in medium containing 1 nM of the retinoic acid receptor agonist EC23 (bio-technie, Minneapolis, MN, US). When cells reached full confluence, the apical side was air exposed and medium was only supplied to the basal compartment supplemented with 50 nM EC23. The medium was changed three times a week. AEC were cultured in standard conditions at 37 °C in a humidified incubator with 5% CO₂. The cells were differentiated by culture at the ALI for 14 days. During differentiation, cultures were either control-treated, or treated with 10 ng/ml IL-13 (Peprotech, London, UK) or 5 μ M DAPT (bio-technie, Minneapolis, MN, US).

3D expansion of bronchial tissue, bronchoalveolar lavage and tracheal aspirate

Organoids were cultured as described before (Sachs, Papaspyropoulos et al. 2019). Cells from BT, bronchoalveolar lavage or tracheal aspirates were collected by centrifugation at 300g for 5 min at 4 °C. Cells were resuspended in BME2 (Cultrex, Gaithersburg, MD, US) and spotted in drops of 30 μ l in a 48-well plate and incubated at 37 °C to solidify. After 10 min, 300 μ l of organoid medium (Supplemental Table S1) was added. Medium was refreshed every 3-4 days. Every 2 weeks, organoids were split 1:3 to 1:6. When passaging the organoids, medium was aspirated and cold PBS was added to dissolve the BME. Organoids were collected and incubated for 2 min using soft trypsin (3% w/v Trypsin (Thermo Fisher), 1% w/v EDTA (Sigma, E1644), 10% w/v glucose in PBS; pH =7.45) at 37 °C. Trypsin activity was stopped by adding soy bean trypsin inhibitor (SBTI, Sigma, T-9128) (11% w/v in KSFM). A 1000 μ l tip with a 2 μ l tip on top was used to further disrupt the organoids. The disrupted organoids were centrifuged at 300g for 5 min, resuspended in 30 μ l BME droplets and re-plated. Organoids were grown under standard culture conditions (37°C, 5% CO₂).

For transfer to ALI culture, cold PBS was added to dissolve the BME and organoids were made single cell by first 7 min incubation in soft trypsin at

37 °C and disruption of the organoids by using a 1000 µl tip with a 2 µl tip on top. The disrupted organoids were centrifuged by 300g for 5 min and underwent a second trypsinization of 7 min to obtain a single cell suspension. SBTI was added to stop the trypsin action and 1×10^5 cells were plated per 12-well transwell insert. After re-seeding on transwell inserts, the cultures were treated as described above.

Acute whole cigarette smoke exposure

After 14 days of differentiation, the epithelial layer was exposed to freshly generated whole cigarette smoke using 3R4F reference cigarettes (University of Kentucky, Lexington, KY, USA) as previously described (Amatngalim, Schrupf et al. 2018). Cells were exposed in modified hypoxic chambers for 4–5 min to either cigarette smoke from one cigarette or to a similar airflow with room air, after which smoke was removed by ventilation with air for 10 min. Cells were harvested for analysis 3, 6 or 24 h after cigarette smoke exposure.

TEER measurements

Epithelial barrier integrity was determined by measuring the trans-epithelial electrical resistance (TEER) using the MilliCell-ERS (Millipore, Burlington, MA, US) according to manufacturer's instruction. TEER values calculated as: $TEER = (\text{measured value} - \text{background value}) \times \text{surface transwell insert in cm}^2$.

Immunofluorescence

Organoid sections. BME was dissolved by adding cold PBS. Organoids were centrifuged at 150g for 5 min and fixed overnight in 4% PFA at 4 °C (Eenjes, Mertens et al. 2018). Post-fixation, organoids were collected by letting them sink, intact, to the bottom of the tube. Centrifugation was avoided after fixation to keep the organoids intact. The organoids were embedded in 4% low-melting agarose (Thermo Fisher). Subsequently, the organoids were washed in PBS for 30 min and manually de-hydrated by 50 min incubation steps in 50%, 70%, 85%, 95% and 2 times 100% ethanol. Organoids were further processed by 3 times xylene for 20–30 min, washed 3 times for 20–30 min in 60 °C warm paraffin to remove all traces of xylene. The organoids were placed in a mold and embedded in paraffin. Paraffin blocks were sectioned at 5 µm and dried overnight at 37 °C.

Deparaffinization was performed by 2 times 3 min xylene washes, followed by rehydration to distilled water. Antigen retrieval was performed by boiling the slides in Tris-EDTA (10 mM Tris (Sigma, T6066), 1 mM EDTA (Sigma, E1644) buffer pH=9.0 in a microwave at 600W for 15 min. Slides were cooled down for 30 min and transferred to PBS. Non-specific bindings sites were blocked by incubating the sections for 1 h at room temperature (RT) in 3% (w/v) BSA (Roche, Basal, Switzerland 10735086001), 0.05% (v/v) Tween-20 (Sigma, P1379) in PBS. Primary antibodies (Supplemental Table S2) were diluted in blocking buffer and incubated overnight at 4°C. The next day, sections were washed 3 times for 5 min at RT in PBS with 0.05% Tween-20. Secondary antibodies (Supplemental Table S2) were added in blocking buffer and incubated for 2 h at RT. DAPI (4',6-Diamidino-2-Phenylindole) solution (BD Pharmingen, San Jose, CA, US, 564907, 1:4000) was added to the secondary antibody. After incubation, 3 times 5 min washes in PBS-0.05% Tween-20 and one wash in PBS was performed, sections were mounted using Miowol reagent (2.4% m/v Miowol, 4.75% m/v glycerol, 12% v/v Tris 0.2M pH=8.5 in dH₂O). All sections were imaged on a Leica SP5 confocal microscope.

Cytospin and membrane ALI culture staining. Cytospins were prepared from cells isolated from BT, BAL and TA using a Shandon Cytospin 3 (Marshall scientific, Hampton, NH, US), and fixed in 4% PFA at room temperature (RT) for 15 min. The membranes were fixed in 4% PFA at RT for 15 min and cut from the transwell using a scalpel. Inserts and cytopsin samples were washed 3 times for 5 min in 0.3% Triton-X100 (Sigma, T8787) in PBS and blocked for 1 h at RT in 5% normal donkey serum (Millipore, S30), 1% BSA, 0.3% Triton-X100 in PBS. Primary antibodies (Supplemental Table S2) were diluted in blocking buffer and incubated overnight at 4 °C. The next day, samples were 3 times rinsed with 0.03% Triton-X100 in PBS followed by 3 washes for 10 min at RT in PBS with 0.03% Triton-X100. Secondary antibodies (Supplemental Table S2) were added in blocking buffer and incubated for 2 h at RT. DAPI solution (BD Pharmingen, 564907, 1:2000) was added to the secondary antibodies. After incubation, samples were 3 times rinsed with 0.03% Triton-X100 in PBS followed by 3 washes for 10 min at RT. Samples were covered by a coverslip using Miowol reagent.

All inserts and cytopsin samples were imaged on a Leica SP5 confocal microscope.

Image analysis

ImageJ was used to analyze the fluorescence images. For each condition,

pictures of 5 non-overlapping fields-of-view were taken at 40x magnification using the SP5 Leica confocal microscope. The microscopic fields were randomly picked from within regions of evenly distributed DAPI positive staining throughout the insert. Z-stacks were made of each selected field to visualize both the basal and luminal cell layer. The images were further analyzed using maximum intensity view. In order to quantify the number of ciliated or basal cells, the number of FOXJ1⁺ and TP63⁺ nuclei were counted per 500 μm^2 field. Differentiation to ciliated and secretory cells (club and goblet cells) was assessed by determining the percentage of TUBIV⁺, SCGB1A1⁺, SCGB3A1⁺ and MUC5AC⁺ area per 500 μm^2 field. Per donor, 5 fields of 500 μm^2 were analyzed. The threshold was set based on the control condition and kept constant throughout the quantification of each staining.

RNA isolation, cDNA synthesis and qPCR analysis

RNA isolation was performed using Maxwell tissue RNA extraction kit (Promega, Madison, WI, US) according to the manufacturer's protocol. RNA concentrations were determined using the Nanodrop ND-1000 Spectrophotometer (Nanodrop technologies, Wilmington, DE, US) and cDNA was synthesized by reversed transcription of 1 μg of RNA, using oligo-dT primers (Qiagen, Venlo, Netherlands), dNTP (Promega) M-MLV Polymerase (Promega) in the presence of RNasin (Promega). Quantitative real-time PCR (qPCR) was conducted using IQ SYBR Green supermix (Bio-Rad, Hercules, CA, US) and a CFX-384 real-time PCR detection system (Bio-Rad). qPCR reactions were performed using the primers shown in Supplemental Table S3. Reference genes RPL13A and ATP5B were selected using the NormFinder method. qPCR reactions were performed using specific primers (Supplemental Table S3).

ELISA

CXCL8/IL-8 production by the AEC was determined in the basal medium by use of the CXCL8/IL-8 DuoSet kit (R&D, Minneapolis, MN, US) according to manufacturer's instructions.

Statistics

Statistical analysis was performed using Prism5 (GraphPad software, La Jolla, CA, US). The statistical tests used for each experiment are indicated in the figure legends. N indicates the number of individual donors.

Results

Effect of expansion method on differentiation of airway epithelial cells at the air-liquid interface

We investigated the influence of expansion methods on airway epithelial cells (AEC) differentiation and their responses to different stimuli. AEC isolated from bronchial tissue (BT) were expanded by conventional culture on culture plastic (2D) or as organoids (3D) using previously described media (Amatngalim, Schrupf et al. 2018, Sachs, Papaspyropoulos et al. 2019) (Supplemental Table S1). This comparison was not feasible for AEC collected from bronchoalveolar lavage (BAL) fluid, or from those obtained from tracheal aspirates (TA), because of the low numbers of viable cells in these samples. Following expansion, AEC from BT (2D and 3D), BAL and TA (3D) were grown at the ALI and differentiation, response to whole cigarette smoke, Notch inhibition and IL-13 stimulation were studied (Fig. 1).

We first investigated whether the expansion method would influence AEC differentiation. 2D (BT-2D) or 3D (BT-3D) expanded AEC from BT were

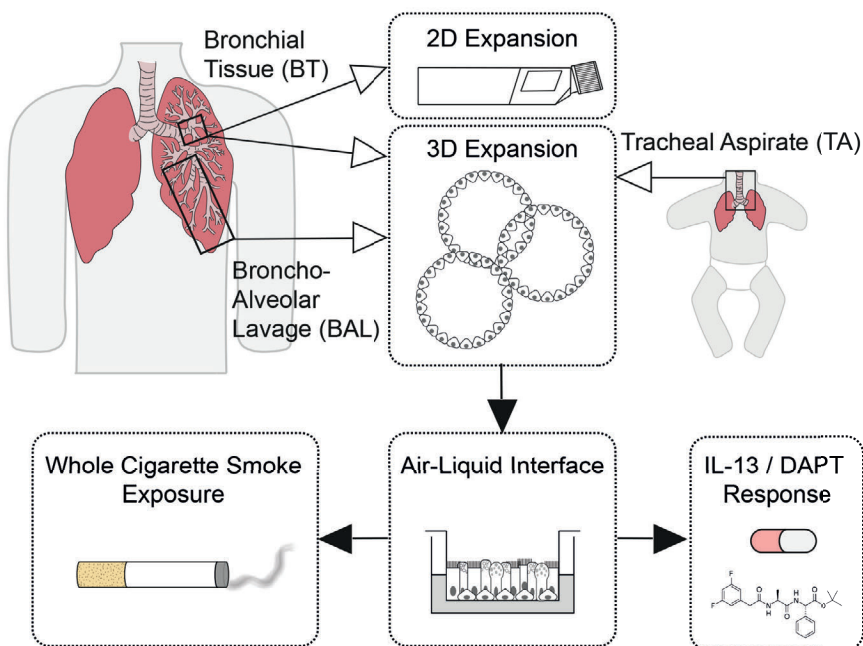


Figure 1. Schematic overview of expansion method and experimental design. Airway epithelial cells (AEC) were isolated from bronchial tissue (BT) and expanded in 2D submerged cultures and 3D organoids. AEC obtained from bronchoalveolar lavage (BAL) and tracheal aspirate (TA) were expanded in 3D. Following expansion, AEC were re-plated and grown at the air-liquid interface (ALI) for 14 days to induce differentiation. These cultures were exposed to whole cigarette smoke, or used to study the effect of IL-13 or DAPT (Notch inhibitor) on differentiation.

grown at ALI to induce differentiation (Fig. 2A). During differentiation, trans-epithelial electrical resistance (TEER) was measured (Fig. 2B). Both BT-2D and BT-3D showed a slight increase in barrier function during differentiation. At ALI day (D) 14, BT-3D showed a higher resistance compared to the BT-2D (Supplemental Fig. S1A).

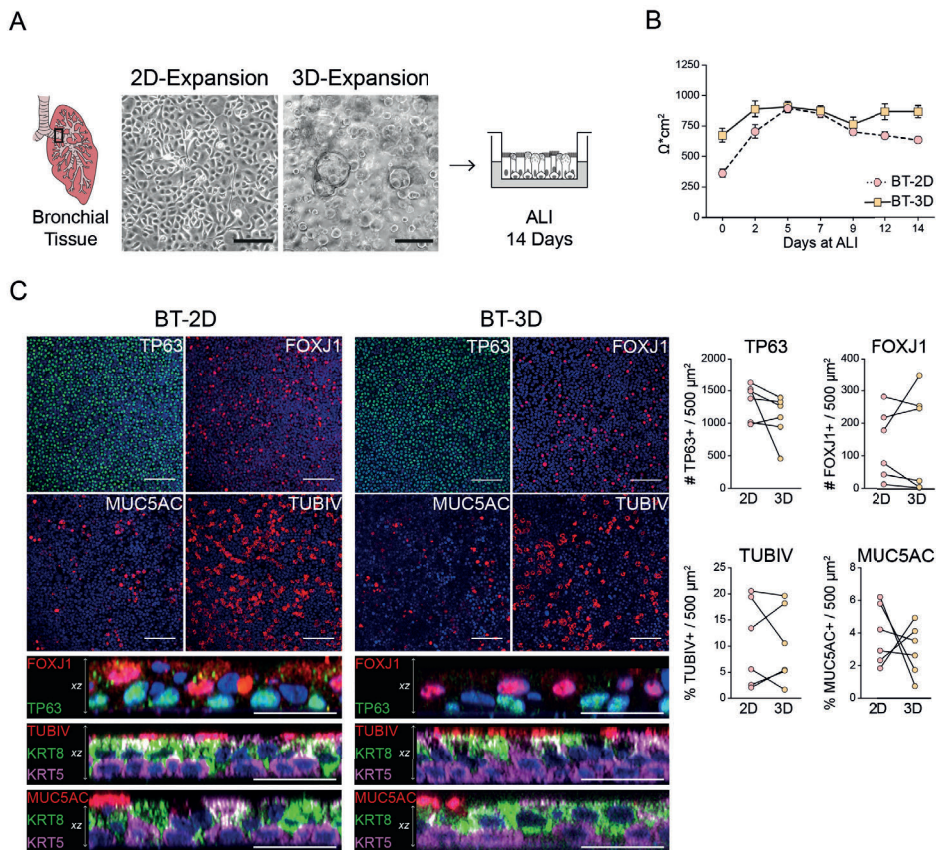


Figure 2. 2D and 3D expansion results in comparable well-differentiated ALI cultures. (A) Airway epithelial cells were isolated from bronchial tissue (BT) and expanded both 2D and 3D. Following expansion, cells were plated on transwell inserts, grown until confluence, and cultured at the air-liquid interface (ALI) for 14 days. Scale bar = 200 μm. (B) Trans-epithelial electrical resistance measured during ALI culture. n=6 donors, each n constitutes mean of 6 ALI cultures per donor. Data are shown as mean ± SEM. (C) Representative images of basal (TP63), ciliated (FOXJ1 and TUBIV) and goblet (MUC5AC) staining in ALI cultures at day 14. Scale bar = 100 μm. Side view of the cultures shows basal cells (TP63 and KRT5) in the basal layer, and ciliated (FOXJ1 and TUBIV), goblet (MUC5AC) and luminal (KRT8) cells at the apical side. Scale bar = 25 μm. The graphs show the quantification of each cell marker. Differences between expansion methods were tested by a paired t-test (n=6 donors), and showed no significant differences. Data are shown as mean ± SEM.

We quantified the number of basal, ciliated, club and goblet cells at ALI D14. We observed a similar cellular composition between BT-2D and BT-3D (Fig. 2C, Supplemental Fig. S1B). Furthermore, presence of basal cells (KRT5, TP63) at the basal side and luminal cells (KRT8) at the luminal side with

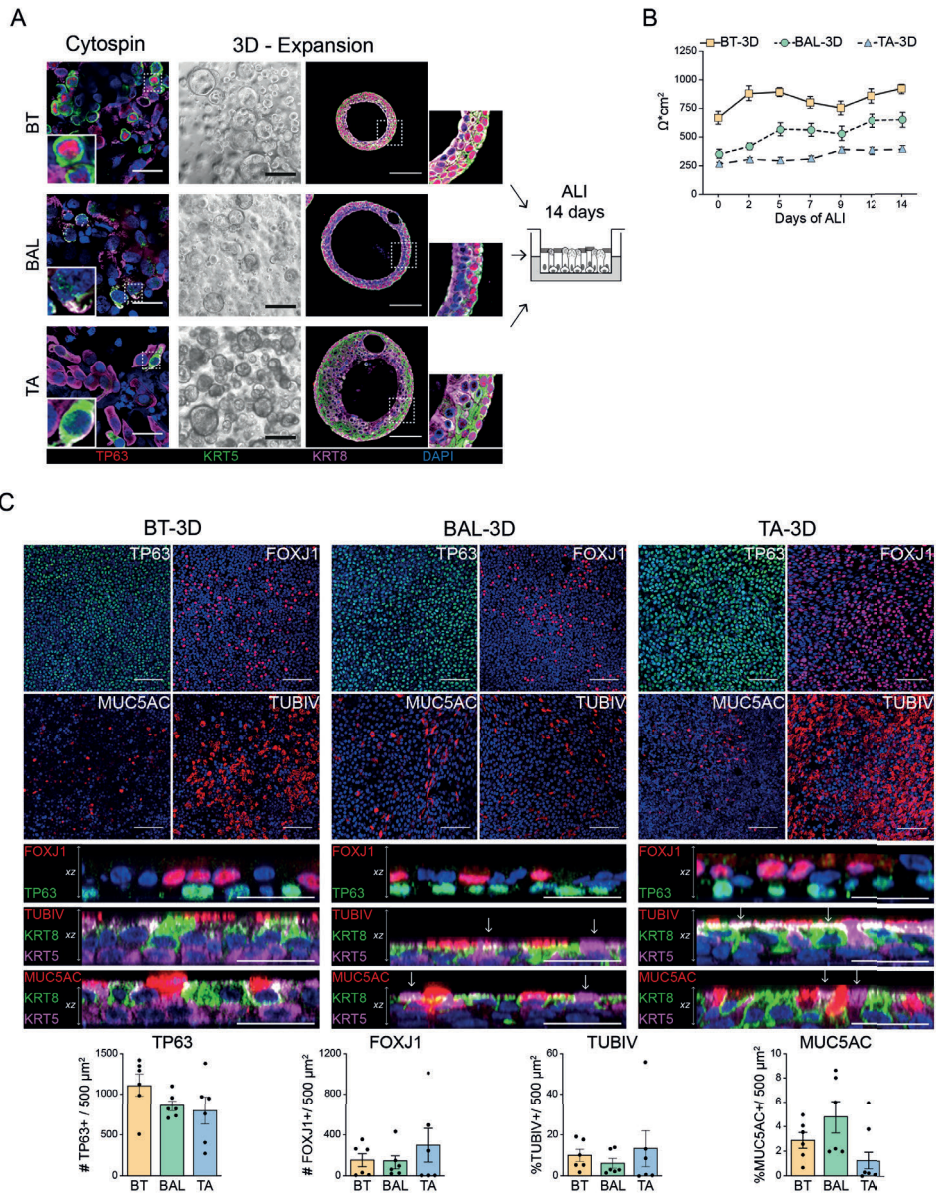


Figure 3. Differentiation of 3D expanded cells from bronchial tissue, bronchoalveolar lavage or tracheal aspirates. (A) Airway epithelial cells obtained from bronchial tissue (BT), bronchoalveolar lavage (BAL) or tracheal aspirate (TA) were expanded in 3D. Top: cytopsin of BT before expansion shows the presence of KRT5⁺TP63⁺ basal cells; cytopsin of TA and BAL shows KRT5⁺KRT8⁺ co-expressing cells in the absence of TP63. Cytopsin scale bar = 25 μm . Following expansion, cells were plated on transwell inserts, grown until confluence and cultured at ALI for 14 days. Middle panels: Bright field images of organoid cultures, scale bar = 200 μm . Lower panels: Immunofluorescence images show a staining of basal cell marker TP63 and KRT5 and luminal cell marker KRT8. All organoids show KRT5⁺TP63⁺ basal cells at the outer layer and KRT8⁺ luminal cells orientated inward. Scale bar = 100 μm . (B) Trans-epithelial electrical resistance was measured at different days of ALI. n=6 donors, each n constitutes mean of 3-6 ALI cultures per donor. Data are shown as mean \pm SEM. (C) Representative images of basal (TP63), ciliated (FOXJ1 and TUBIV) and goblet (MUC5AC) cells at ALI day 14. Scale bar = 100 μm . The graphs show the quantification of each cell

marker. Side views of the inserts show basal (TP63 and KRT5) and ciliated (FOXJ1 and TUBIV), goblet (MUC5AC) and luminal (KRT8) cells. Arrows indicate apical expression of KRT5⁺ or KRT5⁺KRT8⁺ cells (→). Scale bar = 25 μm. Differences between the number of cells in ALI cultures of BT, BAL and TA were tested by one-way ANOVA with a Tukey correction (n=6 donors). Data are shown as mean ± SEM.

either cilia (TUBIV) or mucus (MUC5AC) at the apical surface was similar in BT-2D and BT-3D ALI-differentiated cultures (Fig. 2C).

The club cell markers SCGB3A1 and SCGB1A1 showed large variation between donors, which made these results inconclusive (Supplemental Fig. S1C). Gene expression analysis revealed a comparable expression pattern to the immunofluorescence with no differences observed between BT-2D and BT-3D derived cultures. Expression of the ionocyte marker FOXI1 in the BT-2D-derived ALI cultures was low and not detected at the protein level (data not shown), whereas that of the tuft cell marker TRPM5, and the neuroendocrine cell marker CGRP was low in both BT-2D and BT-3D (Supplemental Fig. S1B).

We conclude that the expansion method, 2D or 3D, does not affect the ALI-induced differentiation of AEC.

3D expansion of AEC from bronchoalveolar lavage and tracheal aspirates generates well-differentiated ALI cultures

We next investigated whether 3D expansion could be used for patient samples that contain insufficient AEC numbers for direct 2D expansion. We compared ALI cultures derived from BT, BAL and TA that were 3D expanded (Fig. 1, 3A). We assessed the composition of our starting cell population and found substantial numbers of TP63⁺KRT5⁺ cells in the BT while the BAL and TA only contained some TP63⁻KRT5⁺KRT8⁺ and predominantly KRT8⁺ luminal cells (Fig. 3A). The BAL and TA samples contained debris, aggregates and dead cells, which made it difficult to assess the number of basal or luminal airway epithelial cells present. Regardless of the number of basal cells, AEC from all sources were able to form organoids and be expanded. Interestingly, although largely absent in the starting population, analysis showed that TP63⁺KRT5⁺ basal cells were present in the organoids from all sources (Fig. 3A), suggesting that the TP63⁻ cells present in BAL and TA are able to give rise to TP63⁺KRT5⁺ basal cells.

Following 3D expansion, organoids were dissociated and cultured at ALI for 14 days. TEER was monitored during differentiation and all 3D expanded sources showed a slight increase in barrier function during differentiation

(Fig. 3B). The ALI cultures obtained from BAL (BAL-3D) and TA (TA-3D) had a lower TEER at Do compared to BT-3D although only the difference with TA reached significance (Supplemental Fig. S2A). We observed that the cultures of all sources contained comparable numbers of ciliated, goblet and secretory cells (Fig. 3C, Supplemental Fig. S2B-2C). For all measured cell types, we observed some donor variation in the BAL-3D or TA-3D. mRNA expression of *TP63*, *FOXJ1*, *MUC5AC*, *SCGB1A1* and *SCGB3A1* also did not show a significant difference between the cultures. For the ionocyte marker *FOXI1*, the tuft cell marker *TRPM5* and neuroendocrine cell marker *CGRP*, no significant differences were found between BT-3D, BAL-3D and TA-3D, and expression levels of these markers were low.

The ALI cultures of BT-3D, BAL-3D and TA-3D all showed TP63⁺ cells to be present at the basal side and FOXJ1⁺ cells at the apical side (Fig. 3C). However, stratification of basal cells (KRT5) and luminal cells (KRT8) appeared disturbed in the BAL-3D and TA-3D with KRT5⁺KRT8⁺ double positive cells and KRT5⁺ cells at the apical side (arrows, Fig. 3C). Both cilia (TUBIV) and mucin (MUC5AC) were found on the apical side of the cultures.

Taken together, we demonstrate the feasibility of establishing an air exposed well-differentiated culture from sources containing limited numbers of AEC following 3D expansion.

Expansion method influences airway epithelial cell response to whole cigarette smoke exposure

We next investigated whether the 3D expanded cultures could be suitable for modelling airway diseases. ALI cultures were exposed to whole cigarette smoke (CS) and gene expression was measured after 3, 6 and 24 h and IL-8 production was measured after 24 h (Fig. 4A).

CS induces oxidative stress and the unfolded protein response (UPR) to endoplasmic reticulum (ER) stress in AEC (Fig. 4B). We validated and compared the response of the air exposed cultures to CS by analyzing different ER stress induced genes which previously shown to be responsive to CS (Marciniak 2017, Zarcone, van Schadewijk et al. 2017) (Fig. 4B). Expression of *CHOP* and *GADD34* were assessed since these are increased as a result of both the UPR and the integrated stress response (ISR) that both have been linked to oxidative stress (see legend Fig. 4B for details; (van 't Wout, Hiemstra et al. 2014, Marciniak 2017)); *sXBP1* mRNA was assessed to demonstrated activation of an ISR-independent UPR. In addition, we assessed expression of

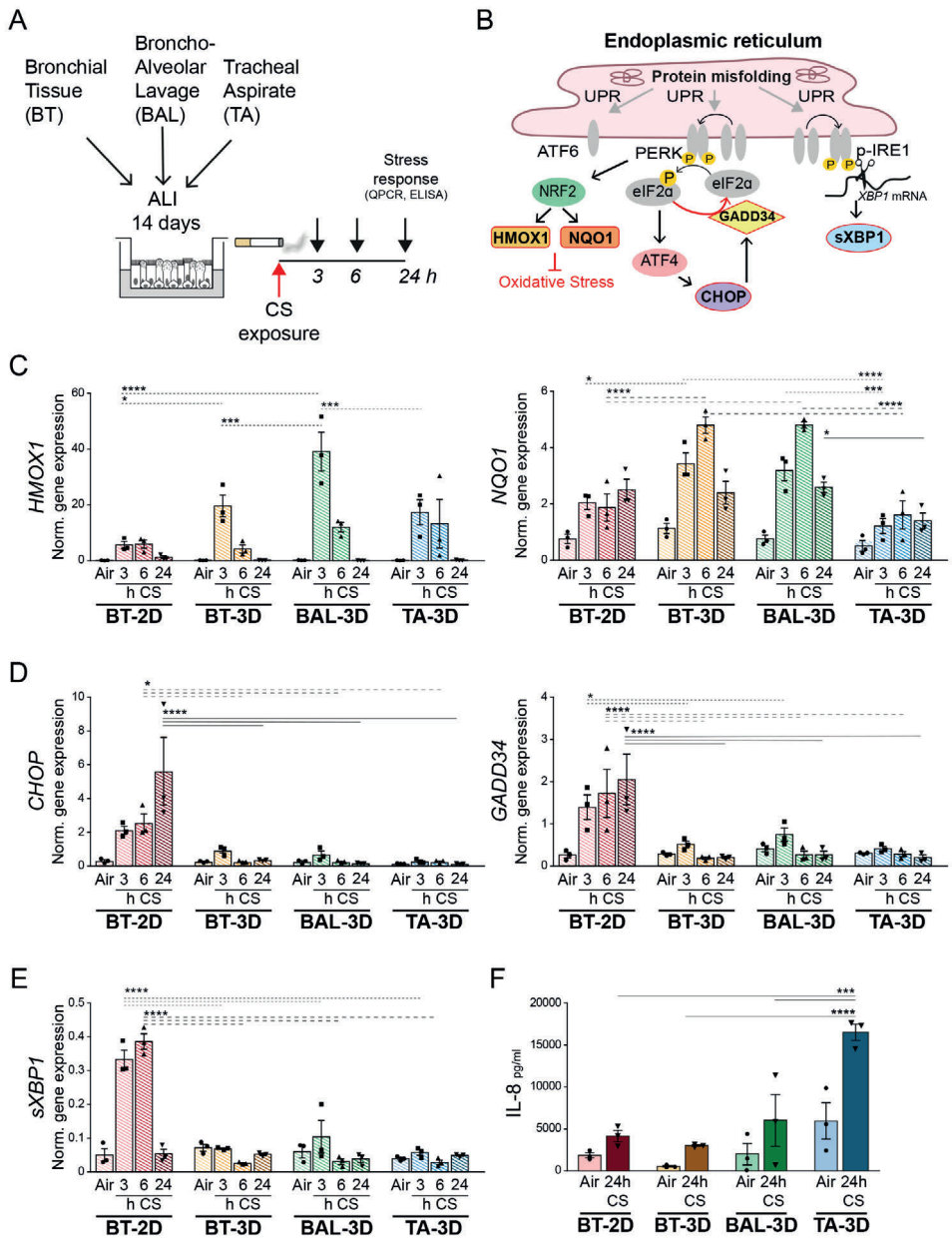


Figure 4. Responses to whole cigarette smoke exposure of differentiated ALI cultures from different sources. (A) Bronchial tissue (BT) expanded in 2D and 3D and cells from bronchoalveolar lavage (BAL) or tracheal aspirate (TA) were 3D expanded. After expansion the cells were re-seeded and differentiated for 14 days. After 14 days, ALI cultures were exposed to whole cigarette smoke. After 3, 6 and 24 hrs, response to smoke was analyzed by measuring IL-8 production and gene expression of several endoplasmic reticulum (ER) and oxidative stress markers. The control was exposed to air and cells were harvested 24 h after exposure. (B) Unfolded protein response (UPR) to endoplasmic reticulum (ER) stress (van 't Wout, Hiemstra et al. 2014, Marciniak 2017). Protein misfolding within the ER results in activation of the three sensors of the UPR: ATF6, PERK and IRE-1. PERK activation results in phosphorylation of eIF2α, which results in general translation attenuation with preferential translation of the transcription factor ATF4. In addition of PERK, also other kinases may cause phosphorylation of eIF2α as part of the integrated stress response

(ISR) to e.g. viral infection, amino acid starvation and oxidative stress (not shown in illustration). ATF4 regulates transcription of *CHOP* and *GADD34*, which acts as a negative feedback by dephosphorylation of eIF2 α . Activation of the UPR sensor IRE1 α results in splicing of *XBP1* mRNA into its active form, s*XBP1* mRNA. Activation of PERK also leads to the activation of NRF2, which is one of the factors that regulates to the expression of *HMOX1* and *NQO1*. *HMOX1* and *NQO1*, both contribute to protection against oxidative stress. Factors assessed in these experiments (*CHOP*, *GADD34*, s*XBP1*, *HMOX1* and *NQO1*) are encircled in red. (C) qPCR analysis of antioxidant genes *HMOX1* and *NQO1*. Differences in gene expression at 3, 6 and 24 h after air or smoke exposure between BT-2D, BT-3D, BAL and TA were tested by two-way ANOVA with a Tukey correction (n=3; **** p<0.0001, *** p<0.001, ** p<0.01, *p<0.05). Data are shown as mean \pm SEM (D-E) qPCR analysis of *CHOP* and *GADD34* (D) and s*XBP1* (E). Differences in gene expression after air or 3, 6 and 24 h after smoke exposure between BT-2D, BT-3D, BAL and TA were tested by two-way ANOVA with a Tukey correction (n=3; **** p<0.0001, *** p<0.001, ** p<0.01, *p<0.05). Data are shown as mean \pm SEM. (F) ELISA of IL-8 in basal medium 24 h after smoke exposure. Differences in gene expression after air or 24 h after smoke exposure between BT-2D, BT-3D, BAL and TA were tested by two-way ANOVA with a Tukey correction (n=3; **** p<0.0001, *** p<0.001). Data are shown as mean \pm SEM.

HMOX1 and *NQO1* that are both activated by oxidative stress and contribute to protection against oxidative stress (Fig. 4C). In BT-2D derived cultures, we observed increased expression of *HMOX1* 3 and 6 h after CS exposure, which returned to control levels after 24 h (Supplemental Fig. S3A). All 3D expanded cultures showed a similar increase of *HMOX1* 3 h after CS. In contrast to the BT-2D culture, this increase was reduced after 6 h and had returned to baseline after 24 h (Supplemental Fig. S3A). Furthermore, the BT-3D and BAL-3D cultures showed a higher peak of *HMOX1* expression 3 h after CS exposure compared to BT-2D (Fig. 4C). *NQO1* was increased in all cultures 3 and 6 h after CS exposure, but only the BT-3D and BAL-3D showed a reduction in *NQO1* expression after 24 h (Supplemental Fig. S3A). Similar to the *HMOX1* expression, the BT-3D and BAL-3D cultures showed a higher increase in *NQO1* compared to BT-2D culture (Fig. 4C). This suggests that 3D expanded cultures experience a steeper and more transient increase in *HMOX1* and *NQO1* expression levels after CS exposure. TA-3D showed a similar trend but was not-significant.

Next, we examined *CHOP*, *GADD34* and s*XBP1* mRNA as markers of the UPR to ER stress following CS exposure. In contrast to what was observed for the response to oxidative stress, the increase in *CHOP* and *GADD34* was higher in BT-2D compared to all 3D expanded cultures (Fig. 4D). Expression of both genes was still increased 24 h after CS exposure in BT-2D (Supplemental Fig. S3B). In contrast, the 3D expanded cultures showed already comparable levels to air exposure of *CHOP* and *GADD34* 6 h after CS exposure (Fig. S3B). s*XBP1* showed different kinetics in each culture, and only robust increases in the BT-2D cultures (Supplemental Fig. S3C, Fig. 4E). Therefore, not only the UPR to ER stress was less pronounced in 3D-expanded cultures compared to BT-2D, also the kinetics of this response differed between cultures.

As CS exposure results in an inflammatory response, we measured the IL-8 release of the different cultures. We found that for each culture an increased IL-8 production was observed following CS exposure (Supplemental Fig. S3D). The release of IL-8 after CS exposure was significantly higher in the BAL-3D and TA-3D compared to the BT-2D and BT-3D (Fig. 3F). However, BAL-3D and TA-3D already showed high IL-8 production during control conditions.

ALI cultures of BAL and TA are less responsive to Notch inhibition and IL-13 stimulation

We next determined the effect of IL-13 stimulation and Notch inhibition (DAPT) on AEC differentiation during ALI. IL-13 stimulation is used to induce goblet cell differentiation in *in vitro* models of asthma (Laoukili, Perret et al. 2001, Wills-Karp 2004, Danahay, Pessotti et al. 2015) (Fig. 5A). Notch inhibition is used to induce and study differentiation towards ciliated cells (Tsao, Vasconcelos et al. 2009, Amatngalim, Schruppf et al. 2018, Plasschaert, Zilionis et al. 2018). IL-13 stimulation showed a decrease in TEER in all cultures, except in the TA-3D which showed an overall lower TEER that was not further decreased by IL-13 (Fig. 5B). DAPT stimulation did not affect barrier function in cultures from BT, but both BAL-3D and TA-3D showed a trend towards decreased barrier function.

As expected, FOXJ1⁺ ciliated cells were increased in BT-2D and -3D stimulated with DAPT and decreased by IL-13 stimulation (Fig. 5C, Supplemental Fig. S4B). Similar results were obtained when analyzing tubulin IV (TUBIV)⁺ ciliated cells (Fig. S4A). Conversely, we observed a decrease in the number of goblet cells in the DAPT stimulated samples and an increase upon stimulation with IL-13 (Fig. 5D). Similar results were found by analyzing gene expression of *MUC5AC*, however this was more variable and not all differences reached significance (Supplemental Fig. S4B). Thus, expansion of AEC from BT in 2D or 3D does not result in differences in the response to DAPT or IL-13 with respect to differentiation into ciliated or goblet cells.

In contrast, the number of FOXJ1⁺ ciliated cells did not increase upon DAPT exposure in the BAL-3D and TA-3D (Fig. 5C). When we analyzed the number of ciliated cells by TUBIV⁺ staining, we found an increase in the BAL cultures, although this was not significant (Supplemental Fig. S4A). In most BAL-3D and TA-3D samples, we observed a decrease in MUC5AC⁺ goblet cells upon DAPT stimulation (Fig. 5D).

When stimulated with IL-13, we did not observe an increase of goblet cells in the BAL and TA cultures (Fig. 5D). The number of ciliated cells did decrease upon IL-13 stimulation in both BAL and TA cultures (Fig. 5C). Similar trends were found when analyzing gene expression levels (Supplemental Fig. S4B). Overall, the BAL and TA cultures proved to be less sensitive to modulation of differentiation by DAPT or IL-13.

We considered the possibility that the reduced response of BAL- and TA-derived cultures to DAPT and IL-13 is explained by the low number of cells present in the BAL and TA, thus requiring a larger number of cellular replications compared to BT to achieve similar numbers of cultured cells. To address this possibility, we seeded epithelial cells from the same BT as before (10% of cells obtained from BT) and at a lower density (1% of cells obtained from BT). The cells were expanded in 3D until sufficient cells were obtained after which the cells were re-seeded on transwells and differentiated at ALI in the presence of DAPT or IL-13. We observed that the control (10%) and the diluted concentration (1%) showed similar responses to DAPT and IL-13 stimulation during differentiation (Supplemental Fig. S4C). This suggests that the lower starting numbers alone cannot explain the lower response of BAL- and TA-derived ALI cultures to DAPT or IL-13.

Discussion

In this study, we present an organoid-based method (3D) to obtain sufficient numbers of AEC from patient samples that contain low numbers of AEC. We present a comparison of well-differentiated ALI cultures established following this 3D expansion, with ALI cultures obtained following conventional (2D) expansion. 3D expansion allowed us to establish ALI cultures from patient samples containing small numbers of AEC, such as BAL fluid or TA from intubated preterm newborns. The data presented demonstrates that comparable ALI cultures can be established from samples derived from 2D or 3D expanded AEC from different clinical samples. Importantly, the possibility of establishing ALI cultures of AEC obtained from TA presents new opportunities of obtaining healthy lung epithelial cell cultures as intubation of patients is standard procedure in non-lung related surgical procedures.

Preterm newborns are at a high risk of developing bronchopulmonary dysplasia (BPD), which is a result of lung damage induced by high oxygen exposure and inflammation induced by mechanical ventilation. Besides mechanical ventilation, newborns are exposed to various therapeutic agents

of which the contribution to the onset of BPD is largely unknown (Naem, Ahmed et al. 2019). Studies into the mechanisms underlying BPD are mostly animal based, partly because of difficulties in obtaining patient material from the preterm newborns (Nardiello, Mizikova et al. 2017). TA are the most

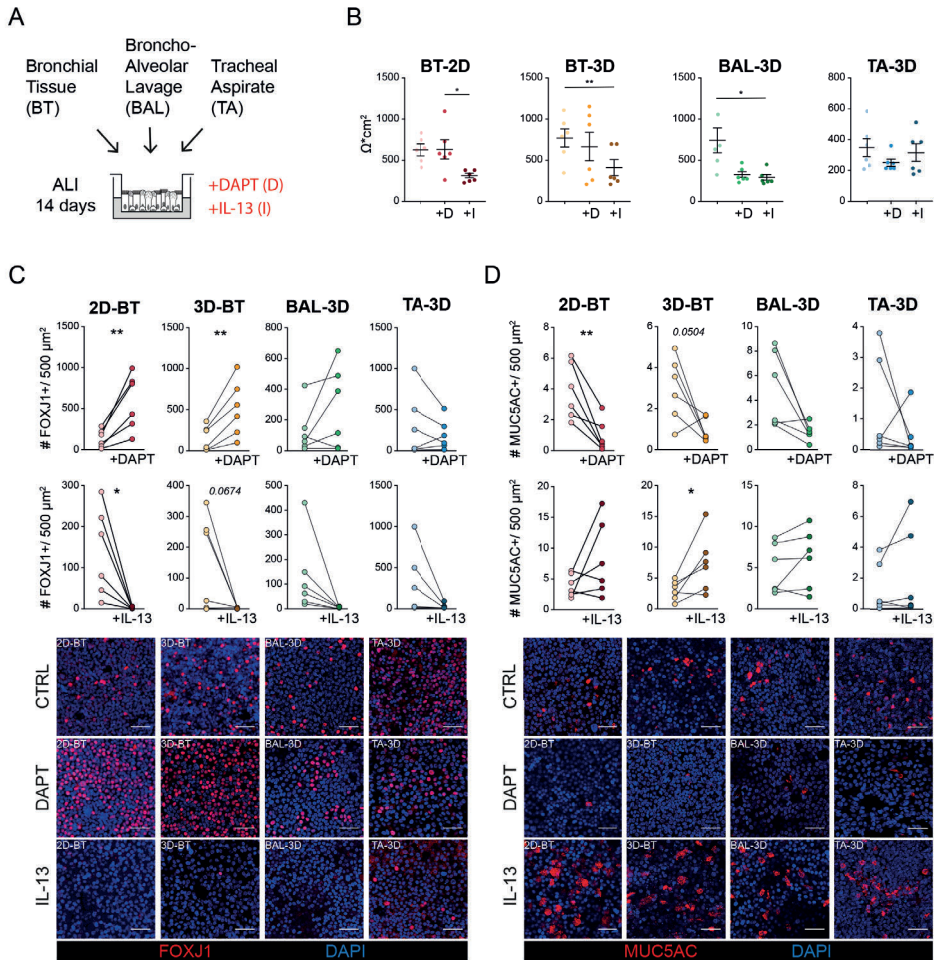


Figure 5. Effect of Notch inhibition (DAPT) and IL-13 stimulation on differentiation of ALI cultures. (A) Airway epithelial cells isolated from bronchial tissue (BT) were 2D or 3D expanded and cells from bronchoalveolar lavage (BAL) or tracheal aspirate (TA) were 3D expanded. Cells were differentiated at the air liquid interface (ALI) for 14 days in the absence or presence of DAPT (+D) or IL13 (+I). (B) Trans-epithelial Electrical Resistance measurements at ALI day 14. Differences between CTRL, DAPT or IL-13 were tested using a one-way ANOVA, repeated measures with a Tukey correction (n=6 donors, each n constitutes 3-6 ALI cultures per donor; * p<0.05). Data are shown as mean ± SEM. (C) Representative images of the number of ciliated cells (FOXJ1) after 14 days ALI without or with DAPT (+D) or IL13 (+I). The graphs show the quantification of the number of FOXJ1+ nuclei per condition. Differences in the number of ciliated cells in ALI cultures were tested by paired t-test (n=6 donors; ** p<0.01, * p<0.05). Data are shown as mean ± SEM. (D) Representative images of the number of goblet cells (MUC5AC) after 14 days ALI without or with DAPT (+D) or IL13 (+I). The graphs show the quantification of the percentage of MUC5AC+ area per condition. Differences in the number of goblet cells in ALI cultures were tested by paired t-test (n=6 donors; ** p<0.01, * p<0.05). Data are shown as mean ± SEM.

accessible lung samples available to study preterm newborns (Reicherzer, Haffner et al. 2018, van Mastrigt, Zweekhorst et al. 2018). Here, we describe a unique method to establish an *in vitro* patient-specific and disease-relevant model that can be used to study the epithelial contribution to the development of BPD. This supports previous published methods that obtain AEC from newborns, and we provide an accessible method to robustly expand AEC and get access to large numbers of AEC from premature newborns for the study of BPD (Mou, Vinarsky et al. 2016, Groves, Guo-Parke et al. 2018, Looi, Evans et al. 2019). The method described is also robust, as we had a 100% success rate in obtaining organoids from TA and BAL samples, possibly in part explained by the fact that we made sure that the time between obtaining the sample and putting the cells in culture was minimized. Furthermore, as preterm newborns are more susceptible to RSV infection (Resch, Kurath-Koller et al. 2016) and developing asthma (Been, Lugtenberg et al. 2014), an *in vitro* airway model using AEC obtained from preterm newborns has the potential to contribute to an increased understanding of disease mechanisms in BPD and its consequences later in life.

We observed a similar epithelial composition of ALI cultures from BT, BAL and TA with respect to the presence of basal, ciliated, secretory and goblet cells. ALI cultures derived from BAL and TA showed more variation in cellular composition, which might be due to intrinsic variability in the technique used to harvest these samples. Furthermore, BAL-derived ALI cultures showed a tendency towards more goblet cells. It is well-established that the cellular composition of the airway epithelium differs at the various anatomical sites along the respiratory tract (Yang, Zuo et al. 2017). We could not verify the location in the lung from where the AEC or the BAL originated, and therefore could not assess whether this could explain some of the observed differences between BAL and BT and between the donors.

In vitro disease modelling requires modulation of epithelial differentiation. All ALI cultures stimulated with IL-13 showed a decrease in ciliated cells, whereas DAPT decreased goblet cells. However, the expected increase in ciliated cells by DAPT and goblet cells by IL-13 was observed in BT-derived ALI cultures, whereas this was not found in BAL- and TA- derived cultures. Using cells derived from BT, we and others also showed that DAPT stimulation of ALI cultures robustly skews the epithelium to a ciliary phenotype (Tsao, Vasconcelos et al. 2009, Amatngalim, Schrupf et al. 2018, Plasschaert, Zilionis et al. 2018). However, others have shown that DAPT stimulation did

not result in an increase in cilia (Gomi, Arbelaez et al. 2015); interestingly, the cultures in that study were established from bronchial brushes which contain a high frequency of luminal cells and therefore may be similar to BAL and TA cell populations. In contrast, BT-derived AEC contained a substantial portion of basal cells, which are classically considered the airway epithelial progenitors from which the various luminal cells are derived (Rock, Onaitis et al. 2009). Collectively, our observations suggest that luminal cells, as a result of their previously described plasticity and possibly through a process of de-differentiation (Tata, Mou et al. 2013), can give rise to the TP63⁺KRT5⁺ basal cells observed in our organoid and ALI cultures. However, as the BAL and TA derived ALI cultures were found to be less responsive to modulation of differentiation, we speculate that the TP63⁺KRT5⁺ basal cells obtained in these organoid cultures do not necessarily regain all basal cell functionality. This difference in starting population might also help to explain the incomplete stratification, and the presence of KRT5⁺KRT8⁺ double positive cells in the ALI cultures derived from BAL and TA (Mori, Mahoney et al. 2015, Pardo-Saganta, Law et al. 2015, Watson, Rulands et al. 2015).

Exposure to CS of all cultures resulted in activation of both an oxidative stress, as well as the UPR to ER stress response, but the levels and kinetics varied. Both responses may contribute to protection against the effects of CS but chronic activation of the UPR to persistent ER stress may also contribute to injury (Marciniak 2017). We found an overall higher peak level of the oxidative stress response (*HMOX1* and *NQO1*) in the 3D-expanded cultures but also a more transient increase, whereas the BT-2D had a more limited induction of both *HMOX1* and *NQO1* which was maintained longer. In contrast, the UPR-related genes *CHOP*, *GADD34* and *sXBP1*, showed higher peak expression levels in BT-2D compared to all 3D expanded ALI cultures. The TA-3D culture was less responsive than the BT-3D and BAL-3D cultures, which might be related to the age of the donor. Thus, although the composition of the epithelial layer is comparable, these data show a clear difference in functional response of the cells to CS based on expansion method used.

A limitation of the present study is the relatively limited number of donors for BT, TA and BAL used for the individual experiments. This is the result of the fact that we aimed to compare cells derived from various sources, and study both effects of sample type and donor on cigarette smoke exposure and modulation of cellular differentiation by IL-13 and Notch inhibition.

Therefore, to further validate our results, in future studies the number of donors should be increased.

Our study shows that ALI cultures suitable for exposure to airborne substances can be established following expansion using organoid cultures that are derived from clinical samples containing few and mostly luminal AEC. Importantly, our study does show differences in cultures obtained following expansion in 3D organoids or conventional 2D culture and provides novel insight into the cellular plasticity of luminal epithelial cells. Finally, the demonstrated possibility to establish ALI cultures derived from TA of preterm newborns opens up exciting new avenues for studying the development and treatment of BPD and its consequences later in life.

Acknowledgements

The authors thank A.C. van der Linden (LUMC) for technical assistance.

Author contribution

EE and SvR designed and performed the majority of the experiments, processed the data and prepared the manuscript. AS, AK and IR provided clinical samples. PK, ABM, MBK and DN performed experiments. HC provided intellectual input for the manuscript. PH and RR designed and supervised the project and contributed to writing of the manuscript. All authors have read the manuscript and approve its submission.

Grants

This study was supported by a grant from The Netherlands Organization for Health Research and Development (ZonMw; grant # 114021508).

References

- Amatngalim, G. D., J. A. Schrupf, F. Dishchekenian, T. C. J. Mertens, D. K. Ninaber, A. C. van der Linden, C. Pilette, C. Taube, P. S. Hiemstra and A. M. van der Does (2018). "Aberrant epithelial differentiation by cigarette smoke dysregulates respiratory host defence." *Eur Respir J* 51(4).
- Barkauskas, C. E., M. I. Chung, B. Fioret, X. Gao, H. Katsura and B. L. Hogan (2017). "Lung organoids: current uses and future promise." *Development* 144(6): 986-997.
- Been, J. V., M. J. Lugtenberg, E. Smets, C. P. van Schayck, B. W. Kramer, M. Mommers and A. Sheikh (2014). "Preterm birth and childhood wheezing disorders: a systematic review and meta-analysis." *PLoS Med* 11(1): e1001596.
- Danahay, H., A. D. Pessotti, J. Coote, B. E. Montgomery, D. Xia, A. Wilson, H. Yang, Z. Wang, L. Bevan, C. Thomas, S. Petit, A. London, P. LeMotte, A. Doelemeyer, G. L. Velez-Reyes, P. Bernasconi, C. J. Fryer, M. Edwards, P. Capodiecici, A. Chen, M. Hild and A. B. Jaffe (2015). "Notch2 is required for inflammatory cytokine-driven goblet cell metaplasia in the lung." *Cell Rep* 10(2): 239-252.
- Eenjes, E., T. C. J. Mertens, M. J. Buscop-van Kempen, Y. van Wijck, C. Taube, R. J. Rottier and P. S. Hiemstra (2018). "A novel method for expansion and differentiation of mouse tracheal epithelial cells in culture." *Sci Rep* 8(1): 7349.
- Gomi, K., V. Arbelaez, R. G. Crystal and M. S. Walters (2015). "Activation of NOTCH1 or NOTCH3 signaling skews human airway basal cell differentiation toward a secretory pathway." *PLoS One* 10(2): e0116507.
- Groves, H. E., H. Guo-Parke, L. Broadbent, M. D. Shields and U. F. Power (2018). "Characterisation of morphological differences in well-differentiated nasal epithelial cell cultures from preterm and term infants at birth and one-year." *PLoS One* 13(12): e0201328.
- Hiemstra, P. S., G. Grootaers, A. M. van der Does, C. A. M. Krul and I. M. Kooter (2018). "Human lung epithelial cell cultures for analysis of inhaled toxicants: Lessons learned and future directions." *Toxicol In Vitro* 47: 137-146.
- Hui, K. P. Y., R. H. H. Ching, S. K. H. Chan, J. M. Nicholls, N. Sachs, H. Clevers, J. S. M. Peiris and M. C. W. Chan (2018). "Tropism, replication competence, and innate immune responses of influenza virus: an analysis of human airway organoids and ex-vivo bronchus cultures." *Lancet Respir Med* 6(11): 846-854.
- Kim, M., H. Mun, C. O. Sung, E. J. Cho, H. J. Jeon, S. M. Chun, D. J. Jung, T. H. Shin, G. S. Jeong, D. K. Kim, E. K. Choi, S. Y. Jeong, A. M. Taylor, S. Jain, M. Meyerson and S. J. Jang (2019). "Patient-derived lung cancer organoids as *in vitro* cancer models for therapeutic screening." *Nat Commun* 10(1): 3991.
- Laoukili, J., E. Perret, T. Willems, A. Minty, E. Parthoens, O. Houcine, A. Coste, M. Jorissen, F. Marano, D. Caput and F. Tournier (2001). "IL-13 alters mucociliary differentiation and ciliary beating of human respiratory epithelial cells." *J Clin Invest* 108(12): 1817-1824.
- Looi, K., D. J. Evans, L. W. Garratt, S. Ang, J. K. Hillas, A. Kicic and S. J. Simpson (2019). "Preterm birth: Born too soon for the developing airway epithelium?" *Paediatr Respir Rev* 31: 82-88.
- Marciniak, S. J. (2017). "Endoplasmic reticulum stress in lung disease." *Eur Respir Rev* 26(144).
- Mori, M., J. E. Mahoney, M. R. Stupnikov, J. R. Paez-Cortez, A. D. Szymaniak, X. Varelas, D. B. Herrick, J. Schwob, H. Zhang and W. V. Cardoso (2015). "Notch3-Jagged signaling controls the pool of undifferentiated airway progenitors." *Development* 142(2): 258-267.
- Mou, H., V. Vinarsky, P. R. Tata, K. Brazauskas, S. H. Choi, A. K. Croke, B. Zhang, G. M. Solomon, B. Turner, H. Bihler, J. Harrington, A. Lapey, C. Channick, C. Keyes, A. Freund, S. Artandi, M. Mense, S. Rowe, J. F. Engelhardt, Y. C. Hsu and J. Rajagopal (2016). "Dual SMAD Signaling Inhibition Enables Long-Term Expansion of Diverse Epithelial Basal Cells." *Cell Stem Cell* 19(2): 217-231.
- Naeem, A., I. Ahmed and P. Silveyra (2019). "Bronchopulmonary Dysplasia: An Update on Experimental Therapeutics." *Eur Med J (Chelmsf)* 4(1): 20-29.
- Nardiello, C., I. Mizikova and R. E. Morty (2017). "Looking ahead: where to next for animal models of bronchopulmonary dysplasia?" *Cell Tissue Res* 367(3): 457-468.
- Nikolic, M. Z., D. Sun and E. L. Rawlins (2018). "Human lung development: recent progress and new challenges." *Development* 145(16).
- Pardo-Saganta, A., B. M. Law, P. R. Tata, J. Villoria, B. Saez, H. Mou, R. Zhao and J. Rajagopal (2015). "Injury induces direct lineage segregation

- of functionally distinct airway basal stem/progenitor cell subpopulations." *Cell Stem Cell* 16(2): 184-197.
- Plasschaert, L. W., R. Zilionis, R. Choo-Wing, V. Savova, J. Knehr, G. Roma, A. M. Klein and A. B. Jaffe (2018). "A single-cell atlas of the airway epithelium reveals the CFTR-rich pulmonary ionocyte." *Nature* 560(7718): 377-381.
- Reicherzer, T., S. Haffner, T. Shahzad, J. Gronbach, J. Mysliwicz, C. Hubener, U. Hasbargen, J. Gertheiss, A. Schulze, S. Bellusci, R. E. Morty, A. Hilgendorff and H. Ehrhardt (2018). "Activation of the NF-kappaB pathway alters the phenotype of MSCs in the tracheal aspirates of preterm infants with severe BPD." *Am J Physiol Lung Cell Mol Physiol* 315(1): L87-L101.
- Resch, B., S. Kurath-Koller, M. Eibisberger and W. Zenz (2016). "Prematurity and the burden of influenza and respiratory syncytial virus disease." *World J Pediatr* 12(1): 8-18.
- Rock, J. R., M. W. Onaitis, E. L. Rawlins, Y. Lu, C. P. Clark, Y. Xue, S. H. Randell and B. L. Hogan (2009). "Basal cells as stem cells of the mouse trachea and human airway epithelium." *Proc Natl Acad Sci U S A* 106(31): 12771-12775.
- Sachs, N., A. Papaspyropoulos, D. D. Zomer-van Ommen, I. Heo, L. Bottinger, D. Klay, F. Weeber, G. Huelsz-Prince, N. Iakobachvili, G. D. Amatngalim, J. de Ligt, A. van Hoeck, N. Proost, M. C. Viveen, A. Lyubimova, L. Teeven, S. Derakhshan, J. Korving, H. Begthel, J. F. Dekkers, K. Kumawat, E. Ramos, M. F. van Oosterhout, G. J. Offerhaus, D. J. Wiener, E. P. Olimpio, K. K. Dijkstra, E. F. Smit, M. van der Linden, S. Jaksani, M. van de Ven, J. Jonkers, A. C. Rios, E. E. Voest, C. H. van Moorsel, C. K. van der Ent, E. Cuppen, A. van Oudenaarden, F. E. Coenjaerts, L. Meyaard, L. J. Bont, P. J. Peters, S. J. Tans, J. S. van Zon, S. F. Boj, R. G. Vries, J. M. Beekman and H. Clevers (2019). "Long-term expanding human airway organoids for disease modeling." *EMBO J* 38(4).
- Schrumpf, J. A., D. K. Ninaber, A. M. van der Does and P. S. Hiemstra (2020). "TGF-beta1 Impairs Vitamin D-Induced and Constitutive Airway Epithelial Host Defense Mechanisms." *J Innate Immun* 12(1): 74-89.
- Tata, P. R., H. Mou, A. Pardo-Saganta, R. Zhao, M. Prabhu, B. M. Law, V. Vinarsky, J. L. Cho, S. Breton, A. Sahay, B. D. Medoff and J. Rajagopal (2013). "Dedifferentiation of committed epithelial cells into stem cells in vivo." *Nature* 503(7475): 218-223.
- Tsao, P. N., M. Vasconcelos, K. I. Izvolsky, J. Qian, J. Lu and W. V. Cardoso (2009). "Notch signaling controls the balance of ciliated and secretory cell fates in developing airways." *Development* 136(13): 2297-2307.
- van 't Wout, E. F., P. S. Hiemstra and S. J. Marciniak (2014). "The integrated stress response in lung disease." *Am J Respir Cell Mol Biol* 50(6): 1005-1009.
- van der Sanden, S. M. G., N. Sachs, S. M. Koekkoek, G. Koen, D. Pajkrt, H. Clevers and K. C. Wolthers (2018). "Enterovirus 71 infection of human airway organoids reveals VP1-145 as a viral infectivity determinant." *Emerg Microbes Infect* 7(1): 84.
- van Mastrigt, E., S. Zweekhorst, B. Bol, J. Tibboel, J. van Rosmalen, J. N. Samsom, A. A. Kroon, J. C. de Jongste, I. K. M. Reiss, M. Post and M. W. Pijnenburg (2018). "Ceramides in tracheal aspirates of preterm infants: Marker for bronchopulmonary dysplasia." *PLoS One* 13(1): e0185969.
- Walters, M. S., K. Gomi, B. Ashbridge, M. A. Moore, V. Arbelaez, J. Heldrich, B. S. Ding, S. Rafii, M. R. Staudt and R. G. Crystal (2013). "Generation of a human airway epithelium derived basal cell line with multipotent differentiation capacity." *Respir Res* 14: 135.
- Watson, J. K., S. Rulands, A. C. Wilkinson, A. Wuidart, M. Ousset, A. Van Keymeulen, B. Gottgens, C. Blanpain, B. D. Simons and E. L. Rawlins (2015). "Clonal Dynamics Reveal Two Distinct Populations of Basal Cells in Slow-Turnover Airway Epithelium." *Cell Rep* 12(1): 90-101.
- Wills-Karp, M. (2004). "Interleukin-13 in asthma pathogenesis." *Curr Allergy Asthma Rep* 4(2): 123-131.
- Yang, J., W. L. Zuo, T. Fukui, I. Chao, K. Gomi, B. Lee, M. R. Staudt, R. J. Kaner, Y. Strulovici-Barel, J. Salit, R. G. Crystal and R. Shaykhev (2017). "Smoking-Dependent Distal-to-Proximal Repatterning of the Adult Human Small Airway Epithelium." *Am J Respir Crit Care Med* 196(3): 340-352.
- Zarcone, M. C., A. van Schadewijk, E. Duistermaat, P. S. Hiemstra and I. M. Kooter (2017). "Diesel exhaust alters the response of cultured primary bronchial epithelial cells from patients with chronic obstructive pulmonary disease (COPD) to non-typeable Haemophilus influenzae." *Respir*

Res 18(1): 27.

Zhou, J., C. Li, N. Sachs, M. C. Chiu, B. H. Wong, H. Chu, V. K. Poon, D. Wang, X. Zhao, L. Wen, W. Song, S. Yuan, K. K. Wong, J. F. Chan, K. K. To, H. Chen, H. Clevers and K. Y. Yuen (2018). “Differentiated human airway organoids to assess infectivity of emerging influenza virus.” Proc Natl Acad Sci U S A 115(26): 6822-6827

Supplementary tables

Supplementary Table 1. Medium

KSFM-AEC expansion medium

Reagent	Company	Cat. No.	Final Concentration
KSFM	Gibco	17005034	n/a
Penicillin / Streptomycin	Lonza	DE17-602e	100 U/ml 100 µg/ml
Bovine Pituitary Extract	Gibco	13028014	0.03 mg/ml
Human EGF	Peptotech	315-09	25 ng/ml
Isoproterenol	Sigma	I-6504	1 µM

Human Adult Organoid medium

Reagent	Company	Cat. No.	Final Concentration
Advanced DMEM:F12	Invitrogen	12634-034	n/a
R-Spondin	Peptotech	120-38	500 ng/ml
Noggin	Peptotech	120-10C	100 ng/ml
Fgf10	Peptotech	100-26	100 ng/ml
Fgf7	Peptotech	100-19	25 ng/ml
SB202190	Sigma	S7067	500 nM
A83-01	Toocris	2939	500 nM
Y-27632	Axon MedChem	1683	5 µM
B27 supplement	Gibco	17504-44	1x
N-Acetylcysteine	Sigma	A9165	1.25 mM
Nicotinamide	Sigma	N0636	5 mM
Glutamax 100x	Invitrogen	12634-034	1x
Hepes	Gibco	15630-56	10 mM
Penicillin / Streptomycin	Lonza	DE17-602e	100 U/ml 100 µg/ml
Primocin	Invivogen	Ant-pm-1	50 µg/ml

Supplementary Table 2. Antibodies

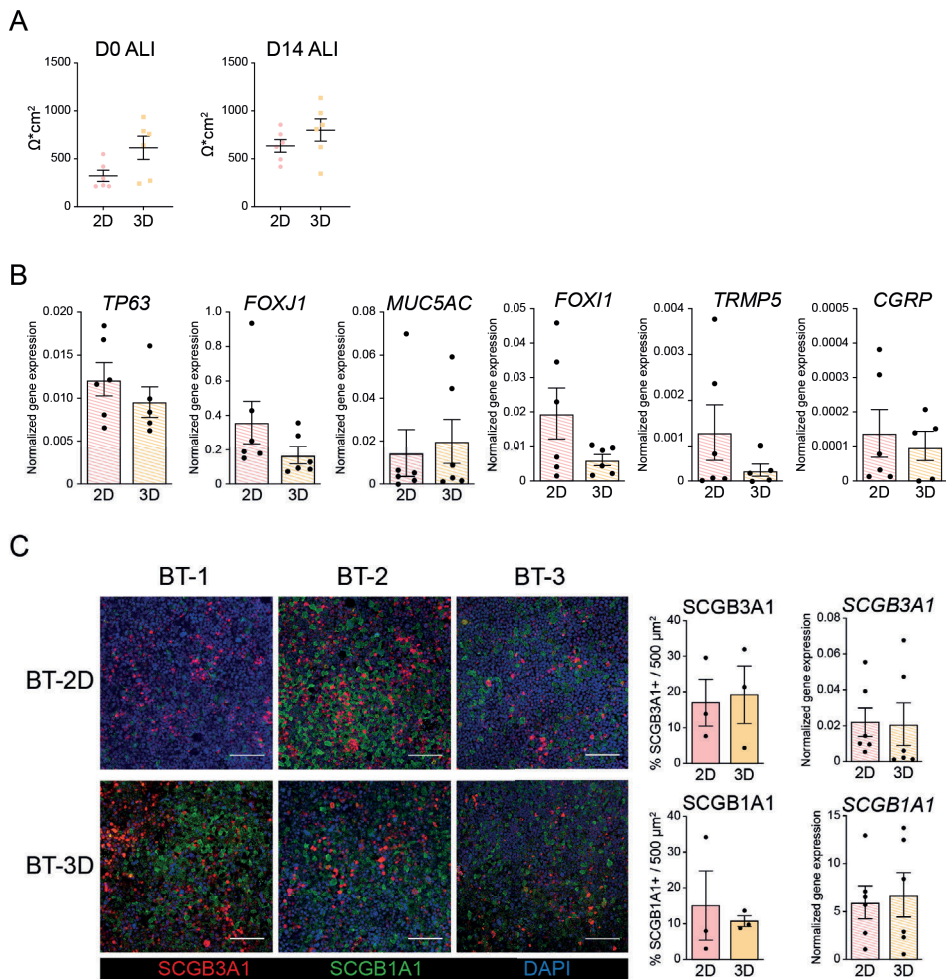
Primary antibodies				
Antibody	Species	Company	Cat. No.	Dilution
β -TUBULIN IV	Mouse	BioGenex	MU178-UC	1:100
FOXJ1	Mouse	eBioscience	14-9965	1:200
FOXJ1	Goat	R&D	AF3019	1:100
KRT5	Rabbit	Biolegend	Poly19055	1:500
KRT8	Rat	DSHB	TROMA-I	1:100
MUC5AC	Mouse	Abcam	AB3649	1:500
SCGB1A1 / CCSP	Rabbit	Abcam	AB40873	1:200
SCGB3A1 / HIN-1	Mouse	R&D systems	AF1790	1:200
TP63	Mouse	Abcam	AB735	1:100

Secondary antibodies			
Antibody	Company	Cat. No.	Dilution
Alexa Fluor $\text{\textcircled{R}}$ 488, 594 Donkey anti Goat IgG	Jackson ImmunoResearch	705-545-147, 705-585-147	1:500
Alexa Fluor $\text{\textcircled{R}}$ 488, 594, 647 Donkey anti Mouse IgG	Jackson ImmunoResearch	715-545-151, 715-585-151, 711-605-151	1:500
Alexa Fluor $\text{\textcircled{R}}$ 488, 594, 647 Donkey anti Rabbit IgG	Jackson ImmunoResearch	711-545-152, 711-585-151, 711-605-152	1:500
Alexa Fluor $\text{\textcircled{R}}$ 488, 594 Donkey anti Rat IgG	Jackson ImmunoResearch	712-545-150 712-585-153	1:500

Supplementary Table 3. qPCR primers

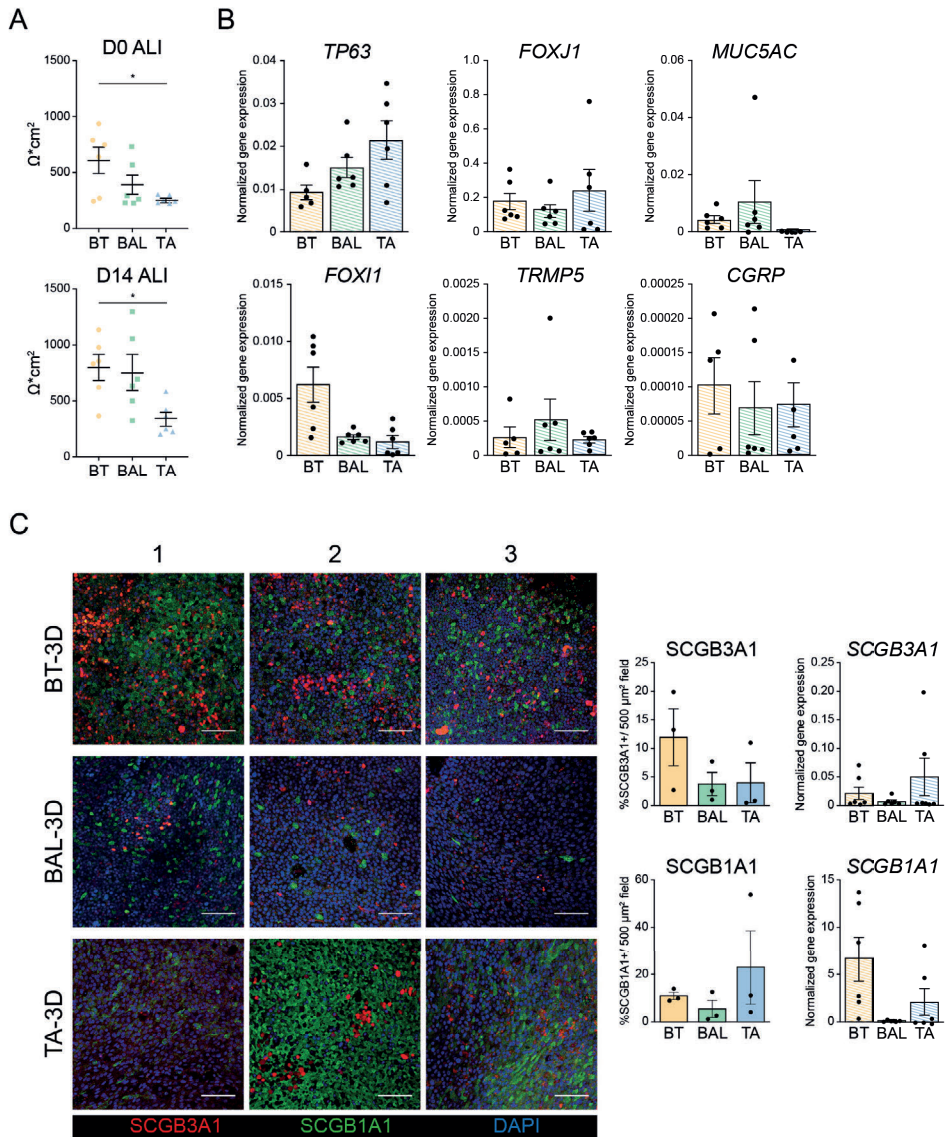
qPCR primers		
Name	Forward (5'→3')	Reverse (5'→3')
<i>ATP5B</i>	TCACCCAGGCTGGTTCAGA	AGTGGCCAGGGTAGGCTGAT
<i>CGRP</i>	CCACGCTCAGTGAGGACGAAG	AAGTACTCAGATTACCGCACCGC
<i>CHOP</i>	GCACCTCCCAGAGCCCTCACTCTCC	GTCTACTCCAAGCCTCCCCCTGCG
<i>FOXI1</i>	TGCTTCAAGAAGGTGCCCCG	GGCCAAGGAGGCTGTGCTAG
<i>FOXJ1</i>	GGAGGGGACGTAAATCCCTA	TTGGTCCCAGTAGTTCACGC
<i>GADD34</i>	ATGTATGGTGAGCGAGAGGC	GCAGTGTCTTATCAGAAGGC
<i>HMOX1</i>	AAGACTGCGTTCCTGCTCAAC	AAAGCCCTACAGCAACTGTCTG
<i>MUC5AC</i>	CCTTCGACGGACAGAGCTAC	TCTCGGTGACAACACGAAAG
<i>NQO1</i>	GAAGAGCACTGATCGTACTGGC	GGATACTGAAAGTTCGCAGGG
<i>RPL13A</i>	AAGGTGGTGGTTCGTACGCTGTG	CGGGAAGGGTTGGTGTTCATCC
<i>SCGB1A1</i>	ACATGAGGGAGGCAGGGGCTC	ACTCAAAGCATGGCAGCGGCA
<i>SCGB3A1</i>	TGCTGGGGGCCCTGACA	ACGTTTATTGAGAGGGGCCGG
<i>sXBP1</i>	TGCTGAGTCCGACAGAGGTG	GTCGGCAGGCTCTGGGGAAG
<i>TP63</i>	CCACCTGGACGTATTCCACTG	TCAATCAAATGACTAGGAGGGG
<i>TRPM5</i>	CCTGGGAGACAGTCCAGAAGG	CCCCGAGGTACTTGGCAATG

Supplementary figures

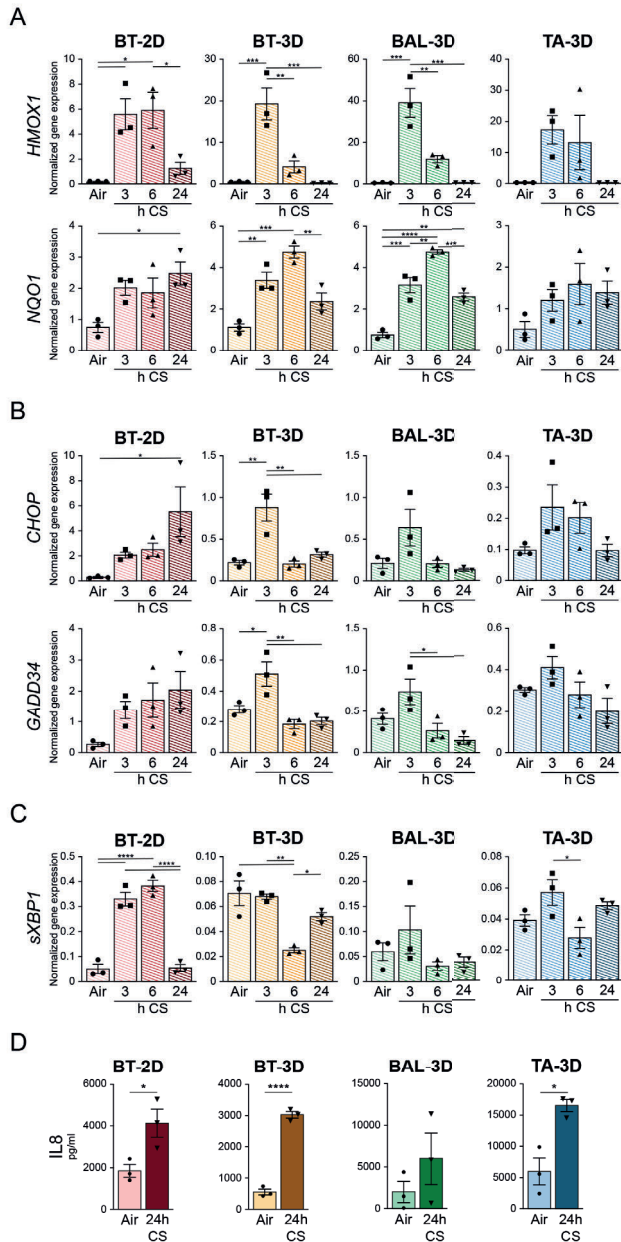


Supplemental Figure 1. 2D and 3D expansion results in comparable well-differentiated ALI cultures.

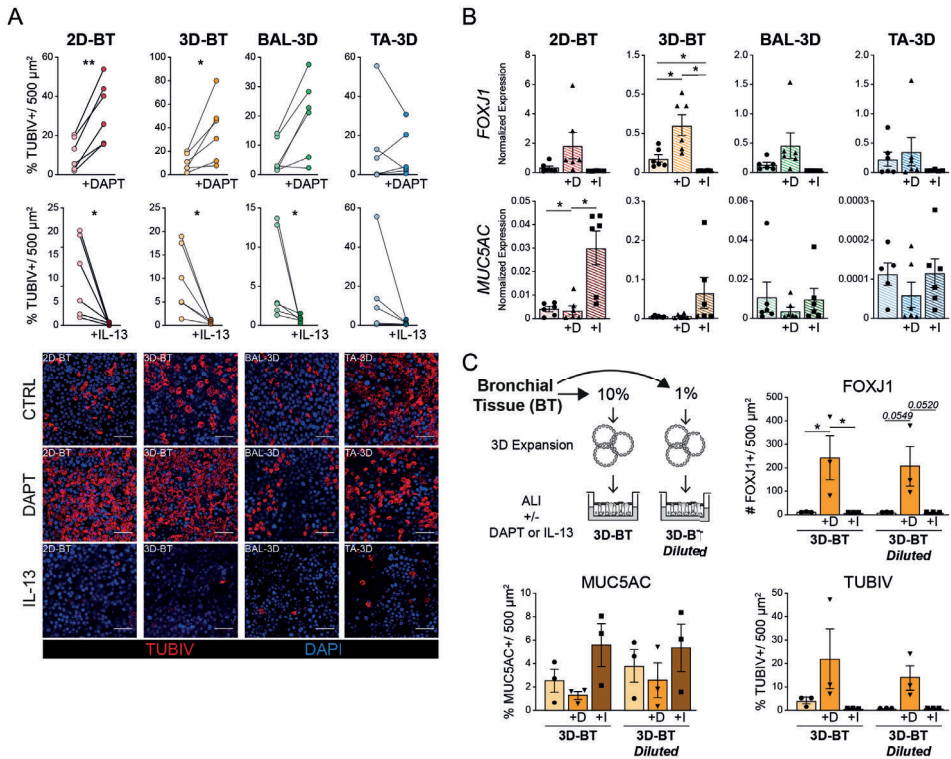
(A) Trans-epithelial electrical resistance was measured at ALI D0 and D14. Differences between 2D and 3D expansion on ALI D0 and D14 were tested using a paired t-test ($n=6$ donors, each n constitutes 6 ALI cultures per donor). Data are shown as mean \pm SEM. (B) qPCR analysis of basal cell marker *TP63*, ciliated cell marker *FOXJ1*, goblet cell marker *MUC5AC*, ionocyte marker *FOXI1*, tuft cell marker *TRMP5* and neuroendocrine cell marker *CGRP*. Differences in gene expression of each cell marker were tested using a paired t-test ($n=6$ donors). Data are shown as mean \pm SEM. (C) Representative images of SCGB3A1⁺ or SCGB1A1⁺ cells at ALI D14. BT=bronchial tissue and each number represents one donor. The graphs show the quantification of SCGB3A1 or SCGB1A1 (left graphs: immunofluorescence analysis; right graphs: gene expression analysis). Differences between expansion methods were tested by a paired t-test ($n=3-6$ donors). Data are shown as mean \pm SEM.



Supplemental Figure 2. Differentiation of 3D expanded cells from bronchial tissue, bronchoalveolar lavage or tracheal aspirates. (A) Trans-epithelial electrical resistance was measured at start of ALI D0 and D14. Differences between bronchial tissue (BT), bronchoalveolar lavage (BAL) and tracheal aspirate (TA) on ALI D0 and day 14 were tested using one way ANOVA with a Tukey correction (n=6 donors, each n constitutes 6 ALI cultures per donor); ** p<0.01). Data are shown as mean ± SEM. (B) qPCR analysis of basal cell marker *TP63*, ciliated cell marker *FOXJ1*, goblet cell marker *MUC5AC*, ionocyte marker *FOXI1*, tuft cell marker *TRMP5* and neuroendocrine cell marker *CGRP*. Differences in gene expression of each cell type marker between expansion methods were tested using one-way ANOVA with a Tukey correction (n=6 donors). Data are shown as mean ± SEM. (C) Representative images of the number of *SCGB3A1*⁺ or *SCGB1A1*⁺ cells at ALI D14 per donor. The graphs show the quantification of secretory cells and qPCR analysis of *SCGB3A1* and *SCGB1A1*. Each number represents one donor. Differences between the number of cells in ALI cultures of BT, BAL and TA were tested by one-way ANOVA with a Tukey correction (n=3-6 donors). Data are shown as mean ± SEM.



Supplemental Figure 3. Responses to whole cigarette smoke exposure of differentiated ALI cultures from different sources. (A) qPCR analysis of antioxidant genes *HMOX1* and *NQO1*. Differences in gene expression at 3, 6 and 24 h of BT-2D, BT-3D, BAL and TA were tested by one-way ANOVA with a Tukey correction (n=3; **** p<0.0001, *** p<0.001, ** p<0.01, *p<0.05). Data are shown as mean ± SEM. (B-C) qPCR analysis of *CHOP* and *GADD34* (B) and *sXBP1* (C). Differences in gene expression at 3, 6 and 24 h of BT-2D, BT-3D, BAL and TA were tested by one-way ANOVA with a Tukey correction (n=3; **** p<0.0001, *** p<0.001, ** p<0.01, *p<0.05)., Data are shown as mean ± SEM (D) ELISA of IL-8 in basal medium 24 h after smoke exposure. Differences in gene expression between air or 24 h after smoke exposure in BT-2D, BT-3D, BAL and TA were tested by unpaired t-test (n=3; **** p<0.0001, * p<0.05). Data are shown as mean ± SEM.



Supplemental Figure 4. Effect of Notch inhibition (DAPT) and IL-13 stimulation on differentiation of ALI cultures. (A) Representative images of the number of tubulin IV⁺ ciliated cells (TUBIV) at ALI D14 with or without DAPT or IL-13. The graphs show the quantification of each cell type. Differences in the number of ciliated cells was tested by paired t-test (n=6 donors; ** p<0.01, * p<0.05). Data are shown as mean \pm SEM. (B) qPCR analysis of gene expression of *FOXJ1* or *MUC5AC* at ALI D14 with or without DAPT (+D) or IL-13 (+I) stimulation. Difference in gene expression was tested by one-way ANOVA with a Tukey correction (n=6 donors; *p<0.05). Data are shown as mean \pm SEM. (C) AECs were isolated from BT and were 3D expanded using standard starting population (10 % of all AEC obtained) or a further diluted starting population (1% of all AEC obtained). After expansion, AEC were re-seeded on transwell inserts and treated with DAPT or IL-13 during differentiation at ALI. The graphs show the quantification of each cell type. Differences in the number of ciliated cells (FOXJ1⁺ and TUBIV⁺), or number of goblet cells (MUC5AC⁺) were evaluated by one-way ANOVA with a Tukey correction (n=3 donors; ** p<0.01, * p<0.05). Data are shown as mean \pm SEM.

CHAPTER 5

Modulation of airway epithelial innate immunity and wound repair by M(GM-CSF) and M(M-CSF) macrophages

Sander van Riet¹, Annemarie van Schadewijk¹, Steve De Vos², Nick Vandeghinste², Robbert J. Rottier³, Jan Stolk¹, Pieter S. Hiemstra¹, P. Padmini S. J. Khedoe¹

¹Dept. of Pulmonology, Leiden University Medical Center, Leiden, The Netherlands.

²Galapagos NV, Mechelen, Belgium

³Department of Pediatric Surgery, Erasmus MC-Sophia Children's Hospital, Rotterdam, The Netherlands

Journal of Innate Immunity 2020;12(5):410-421.

Abstract

Airway epithelial cells and macrophages participate in inflammatory responses to external noxious stimuli, which can cause epithelial injury. Upon injury, epithelial cells and macrophages act in concert to ensure rapid restoration of epithelial integrity. The nature of the interactions between these cell types during epithelial repair are incompletely understood. Here we use an *in vitro* human co-culture model of primary bronchial epithelial cells cultured at the air-liquid interface (ALI-PBEC) and polarized primary monocyte-derived macrophages. Using this co-culture, we studied the contribution of macrophages to epithelial innate immunity, wound healing capacity and epithelial exposure to whole cigarette smoke (WCS). Co-culture of ALI-PBEC with LPS-activated M(GM-CSF) macrophages increased expression of *DEFB4A*, *CXCL8* and *IL6* at 24 hours in the ALI-PBEC, whereas LPS-activated M(M-CSF) macrophages only increased epithelial *IL6* expression. Furthermore, wound repair was accelerated by co-culture with both activated M(GM-CSF) and M(M-CSF) macrophages, also following WCS exposure. Co-culture of ALI-PBEC and M(GM-CSF) macrophages resulted in increased *CAMP* expression in M(GM-CSF) macrophages, which was absent in M(M-CSF) macrophages. *CAMP* encodes LL-37, an antimicrobial peptide with immune modulating and repair enhancing activities. In conclusion, dynamic crosstalk between ALI-PBEC and macrophages enhances epithelial innate immunity and wound repair, even upon concomitant cigarette smoke exposure.

Introduction

Airway epithelial cells play a central role in the first line of defense against inhaled particles, gasses and pathogens. The epithelial lining acts as a physical barrier and epithelial cells produce protective mediators (e.g. cytokines, chemokines, antimicrobial peptides) to prevent intrusion of harmful substances and pathogens into the lungs. Epithelial cells also mediate mucociliary clearance to remove mucus-trapped-particles and pathogens from the airways (Hiemstra, McCray, and Bals 2015; Whitsett and Alenghat 2015). Injury to the epithelial layer, due to e.g. bacterial and/or viral infection or inhalation of toxicants (including cigarette smoke), may cause disruption of epithelial barrier integrity and impair epithelial repair (Hiemstra, McCray, and Bals 2015; Hiemstra et al. 2016). The epithelial repair process is tightly controlled to ensure rapid closure of the wound and restoration of lung tissue homeostasis. However, chronic insults to the epithelial layer contribute to dysfunction of airway epithelial cells and development and progression of lung diseases, such as chronic obstructive pulmonary disease (COPD), idiopathic pulmonary fibrosis (IPF) and asthma. Epithelial integrity, barrier function and host defense responses are impaired in various lung diseases (Amatngalim and Hiemstra 2018; Hiemstra, McCray, and Bals 2015), predisposing these patients to repeated infections and exacerbations. Inflammatory cells such as macrophages contribute to the epithelial wound repair process by releasing a range of mediators and by providing protection against infections following disruption of the epithelial barrier integrity (Gardner, Borthwick, and Fisher 2010; Alber et al. 2012).

Macrophages constitute a heterogeneous population of cells resulting from their high level of plasticity, and the various subsets contribute to the epithelial repair response and host defense (Gordon and Martinez-Pomares 2017; Snyder et al. 2016). The phenotype of macrophages is tightly controlled by their microenvironment, that provides signals for activation and differentiation. Insight into these mechanisms has resulted in a classification of macrophages based on their activation state and properties. Macrophages can thus be broadly subdivided in pro-inflammatory macrophages (known as classically activated macrophages, also known as M1 macrophages) and anti-inflammatory macrophages (known as alternatively activated macrophages, also known as M2 macrophages) (Arora et al. 2018; Murray 2017). Pro-inflammatory macrophages produce proinflammatory cytokines and their phenotype is driven by pro-inflammatory stimuli, including TNF- α , IFN- γ and lipopolysaccharide (LPS), whereas anti-inflammatory macrophages are

more diverse and can be divided into several subsets, which are involved in defence against parasitic infections (M2a), immunoregulation (M2b) and tissue remodeling and matrix deposition (M2c) (Byrne et al. 2015). In the lungs, macrophages are widely present in the airway lumen (airway macrophages), the alveolar lumen (alveolar macrophages), and in the lung parenchyma and airway wall (interstitial macrophages), whereas monocytes can be recruited upon inflammation (Hu and Christman 2019).

The function and phenotype of these cells depends on the local cytokine milieu (Byrne et al. 2015; Puttur, Gregory, and Lloyd 2019). Following injury to the lung epithelial lining, both resident macrophages and those derived from recruited monocytes contribute to the inflammatory and remodeling phase of epithelial repair, although the precise interaction with airway epithelial cells is insufficiently studied.

Despite the knowledge gained from various *in vivo* models on epithelial repair, the use of laboratory animals becomes more controversial and importantly the translation of results from such animal models to human disease is not always straightforward. However, whereas *in vitro* models with (primary) airway epithelial cells have provided much knowledge on the mechanism of epithelial wound repair (Amatngalim et al. 2016; Gardner, Borthwick, and Fisher 2010), these models do not accurately represent the complex cellular network of airway epithelial cells and inflammatory cells, including macrophages, that are essential during epithelial wound repair. Although various models are available to investigate the interaction between airway epithelial cells and immune and inflammatory cells, many of these studies have been performed using cell lines for either macrophages, airway epithelial cells or both, and are therefore not representative. Furthermore, many of these models lack lung specificity. In the present study, we therefore combined primary airway epithelial cells with primary monocyte-derived macrophages. To study the complex cellular crosstalk and interaction between airway epithelial cells and macrophages in more detail, we developed a co-culture model of human primary bronchial epithelial cells grown at the air-liquid interface (ALI-PBEC) and human peripheral blood CD14⁺ monocyte-derived macrophages, that were polarized to either a pro-inflammatory M(GM-CSF) or anti-inflammatory M(M-CSF) macrophage phenotype (Van't Wout et al. 2015). Using this model of primary cells, we studied the interaction between M(GM-CSF) or M(M-CSF) macrophages and ALI-PBEC and its effect on epithelial innate immunity and repair.

Materials and methods

Culture of primary bronchial epithelial cells (PBEC)

Primary bronchial epithelial cells (PBEC) were obtained from tumor-free lung tissue of patients undergoing lobectomy for lung cancer at the Leiden University Medical Center (Leiden, The Netherlands). The use of this lung tissue for research following surgery within the framework of patient care was in line with the “Human Tissue and Medical Research: Code of conduct for responsible use” (2011) (www.federa.org), that describes the no-objection system for coded anonymous further use of such tissue. All PBEC donors used for these experiments were considered not to have chronic airflow limitation (i.e. not having chronic obstructive pulmonary disease [COPD]), based on a predicted forced expiratory volume in 1 sec (FEV₁) >85% and all had an age of >55 at time of surgery. The cells were isolated, cultured and differentiated at the air-liquid interface (ALI) for 14 days (SFig. 1A), to develop a well-differentiated epithelial layer, in transwell-inserts in 12-well plates ALI as previously described (Amatngalim et al. 2018). During PBEC differentiation, the cells were cultured at ALI with Bronchial Epithelial Cell Medium-basal (BEpiCM-b ScienCell, Carlsbad, CA, USA) diluted 1:1 with DMEM from Stemcell Technologies (Vancouver, Canada) with bronchial epithelial cell growth supplements from ScienCell, further supplemented with the 50 nM EC-23 (synthetic retinoic acid analogue, Tocris, Bio-Techne Ltd. Abingdon, U.K.). Well-differentiated ALI-PBEC were used for further co-culture experiments. Approximately 1×10^6 ALI-PBEC were present on these inserts at the time of the experiment.

Isolation of monocytes and differentiation towards M(GM-CSF) and M(M-CSF) macrophage phenotype

CD14 positive monocytes were isolated from fresh buffycoats (Sanquin Blood Bank, Leiden, the Netherlands) obtained from healthy controls as described previously (Van't Wout et al. 2015). We seeded 0.5×10^6 monocytes per well of a 12-well plate with either 5 ng/ml GM-CSF (R&D Systems, Minneapolis, MN) or 50 ng/ml M-CSF (Myltenyi Biotec, Auburn, CA) to induce polarization to M(GM-CSF) or M(M-CSF) macrophages respectively. Following 7 days of culture in RPMI 1640 medium (Invitrogen, Breda Life Technologies, The Netherlands) containing 10% FCS (Invitrogen), 2 mM l-glutamine, 100 U/ml penicillin, and 100 µg/ml streptomycin (all from Bio Whittaker, Walkersville, MD, USA), M(GM-CSF) or M(M-CSF) macrophages were stimulated with

100 ng/ml lipopolysaccharide (LPS from *Pseudomonas aeruginosa*, Sigma-Aldrich, St. Louis, MO) during co-culture experiments (experimental outline shown in SFig. 1A). After 7 days, before start of co-culture with ALI-PBEC, similar numbers of M(GM-CSF) and M(CSF) were counted ($\sim 3.2 \times 10^6$ cells/well). M(GM-CSF) or M(M-CSF) macrophages were characterized by high expression of *CHI3L1* and IL-12/p40 release (M(GM-CSF)) or *CD163* expression and IL-10 release (M(M-CSF)), respectively (SFig. 2).

Co-culture of M(GM-CSF) or M(M-CSF) macrophages and ALI-PBEC

ALI-PBEC were cultured as described above. Twentyfour hours before co-culture, the medium of ALI-PBEC was switched to epithelial culture medium (Amatngalim et al. 2018) without growth factors, hydrocortisone and EC23 (starvation medium, 24h starvation). Co-culturing was performed by transfer of the transwell-inserts seeded with ALI-PBEC to another 12-wells plate that contained the polarized macrophages. All co-culture experiment were performed in starvation medium with or without LPS in the basal compartment, for activation of macrophages. ALI-PBEC were i) co-cultured with (LPS-activated) M(GM-CSF) or M(M-CSF) macrophages for 24 h (SFig. 1A), ii) mechanically wounded and then co-cultured with LPS-activated M(GM-CSF) or M(M-CSF) macrophages until wound closure, or iii) mechanically wounded, exposed to whole cigarette smoke (WCS) and subsequently co-cultured with LPS-activated M(GM-CSF) or M(M-CSF) macrophages until wound closure. Epithelial wounding was performed as described previously (Hiemstra et al. 2016). A list of compounds that were used for mechanistic experiments is shown in Table 1. These compounds were added during co-culture of ALI-PBEC and M(GM-CSF)/ M(M-CSF) macrophages.

Compound	Concentration	Supplier
LL-37	2.5 µg/ml	(37)
TGF-β1	5 ng/ml	R&D system
anti-LL-37 (Clone III D7 (09/02/00 ST))	1:100	(37)
GM6001	25 µM	Merck
SB-431542	5 µM	Sigma

Table 1. Compounds

Whole cigarette smoke exposure

Whole cigarette smoke (WCS) exposure was performed as described previously (Amatngalim et al. 2018). In brief, well-differentiated ALI-PBEC cultures were placed in a modified hypoxic chamber for WCS or air (control) exposure. In these chambers, the cultures were exposed to either 4-5 min of cigarette smoke from 1 3R4F research cigarette (University of Kentucky, Lexington, KY) or room air as control. Following 4-5 min of WCS exposure, the chambers were ventilated for 10 min to remove smoke from the chambers. The transwell inserts were subsequently removed from the plate, and transferred to the 12-well plates containing the macrophages for co-culture and placed back at 37°C.

Quantitative RT-PCR

RNA was isolated from ALI-PBEC (from transwell-insert) and macrophages (from 12-wells plate at bottom), separately, according to manufacturer's instruction using Maxwell RNA extraction kits (Promega, Madison, WI, USA). Quantitative RT-PCR was performed as described previously (Amatngalim et al. 2018) using primer pairs listed in Table 2. qPCR reactions were performed in triplicate, corrected for the geometric mean of expression of 2 reference genes (*ATP5B* and *RPL13A*), selected using the NormFinder algorithm software (Andersen, Jensen, and Orntoft 2004). Expression values were determined by the relative gene expression of a standard curve as determined by CFX manager software, and expressed as fold increase (Bio-Rad).

Gene	Forward primer (5' to 3')	Reverse primer (3' to 5')
<i>ATP5B</i>	TCACCCAGGCTGGTTCAGA	AGTGGCCAGGGTAGGCTGAT
<i>RPL13A</i>	AAGGTGGTGGTTCGTACGCTGTG	CGGGAAGGGTTGGTGTTCATCC
<i>CAMP</i>	TCATTGCCAGGTCCTCAG	TCCCATACACCGCTTCAC
<i>CXCL8</i>	CTGGACCCCAAGGAAAAC	TGGCAACCTACAACAGAC
<i>IL6</i>	CAGAGCTGTGCAGATGAGTACA	GATGAGTTGTCATGTCTGCA
<i>CD163</i>	TTTGTCAACTTGAGTCCCTTCAC	TCCCGCTACACTTGTTTTTCAC
<i>CHI3L1</i>	CTGTGGGGATAGTGAGGCAT	CTTGCCAAAATGGTGTCTTT
<i>HGF</i>	TCCAGAGGTACGCTACGAAGTCT	CCCATTGCAGGTCATGCAT
<i>MMP9</i>	ACCTCGAACTTTGACAGCGAC	GAGGAATGATCTAAGCCCAGC
<i>PDGFA</i>	CACCACCGCAGCGTCAA	CCTCACCTGGACTTCTTTTAATTTG
<i>TGFB1</i>	CTAATGGTGGAAACCCACAACG	TATCGCCAGGAATTGTTGCTG
<i>DEFB4A</i>	ATCAGCCATGAGGGTCTTG	GCAGCATTTTGTTCAGG
<i>IL-10</i>	GACTTTAAGGGTTACCTGGGTTG	TCACATGCGCCTTGATGTCTG

Table 2. Primers used for RT-PCR

ELISA

Levels of the interleukins (IL), IL-8 (R&D), IL-10 and IL-12/p70 (BD Bioscience), and human β -defensin 2 (hBD-2) (Antigenix America) were determined in supernatant, basal medium (IL-10, IL-12/p40, IL-8 and hBD-2) or in apical wash (IL-8, hBD-2) according to the manufacturer's instructions.

Apical wash

To assess levels of mediators secreted to the apical side by well-differentiated ALI-PBEC, apical washes were collected as described (Amatngalim et al. 2017). Briefly, apical washes were performed by applying 100 μ L PBS for 10 min. After 10 min the fluid was collected, and stored at -80°C pending analysis by ELISA as described above.

Statistical analyses

Statistical significance of differences was assessed using one-way ANOVA or repeated measures analysis, followed by post-hoc analysis using Fisher's LSD multiple comparison test using Graphpad Prism 7. Differences at $p < 0.05$ were regarded as statistically significant.

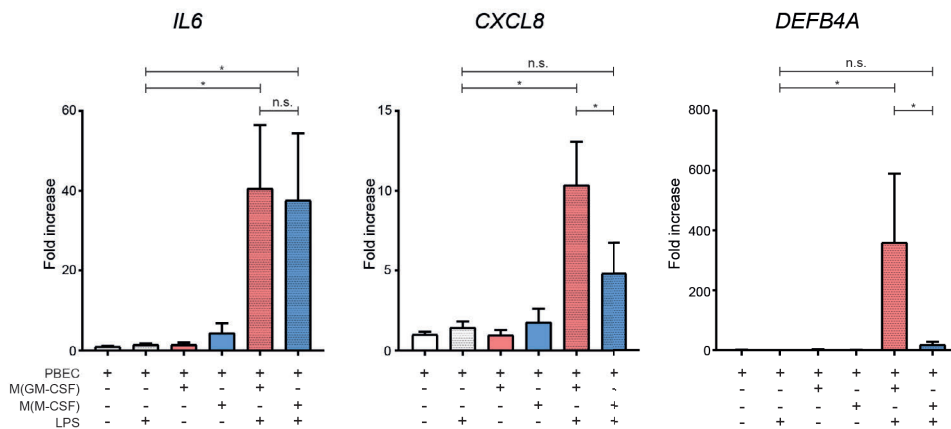
Results

LPS-activated M(GM-CSF) and M(M-CSF) macrophages alter epithelial innate immunity

As host defense is one of the key functions of airway epithelial cells, we first aimed to establish if there is an effect of macrophages on epithelial host defense in our co-culture model. To this end we used well-differentiated primary bronchial epithelial cells cultured at the air-liquid interface (ALI-PBEC) in the presence or absence of lipopolysaccharide (LPS)-stimulated M(GM-CSF) or M(M-CSF) macrophages (SFig. 1A). Following 24 hours of co-culture we measured the epithelial expression of host defense mediators (*IL6*, *CXCL8*, and *DEFB4A*). In absence of LPS, we found no effect of M(GM-CSF) or M(M-CSF) macrophages on the epithelial mRNA expression of *IL6*, *CXCL8* or *DEFB4A*. In presence of LPS, expression of *IL6* mRNA was increased in ALI-PBEC upon co-culture with both macrophage subtypes (Fig. 1A). Expression of *CXCL8* was increased in ALI-PBEC upon co-culture with LPS-activated M(GM-CSF) but not M(M-CSF) macrophages. Furthermore, epithelial expression of *DEFB4A*, the gene encoding hBD-2, was increased

upon co-culture with LPS-activated macrophages, and this effect was significantly higher in co-culture with M(GM-CSF) compared to M(GM-CSF) macrophages (Fig. 1A). Expression of other host defense proteins in ALI-PBEC (CAMP, RNASE7) was not altered (data not shown). We further investigated this effect on ALI-PBEC innate immune responses at the protein level (Fig. 1B). Confirming our findings on gene expression level in ALI-PBEC,

A.



B.

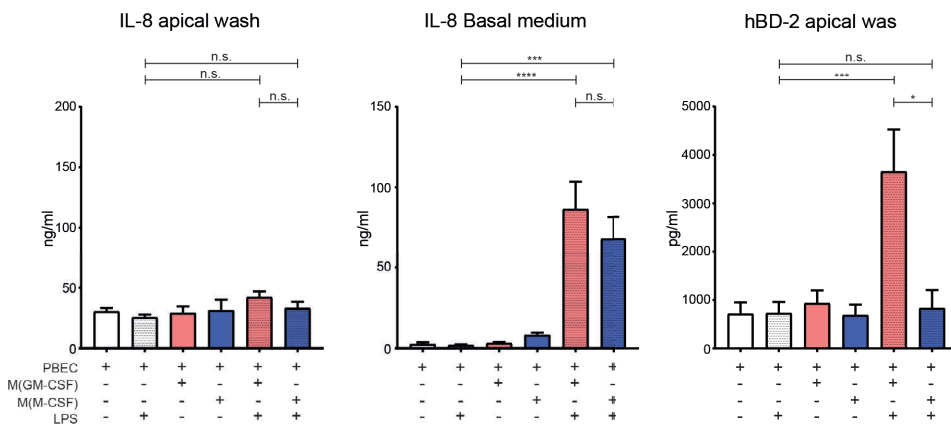


Figure 1. Activated M(GM-CSF) and M(M-CSF) macrophages modulate epithelial innate immunity. Well-differentiated ALI-PBEC were co-cultured with M(GM-CSF) or M(M-CSF) macrophages in the presence and absence of LPS and mRNA and protein levels of cytokines and antimicrobial peptides were measured after 24 hours in ALI-PBEC. (A) mRNA expression levels of *IL6*, *CXCL8* and *DEFB4A* were measured in ALI-PBEC upon co-culture with (activated) M(GM-CSF) (red bars) and M(M-CSF) (blue bars) macrophages (n= 7 independent ALI-PBEC donors). (B) IL-8 and hBD-2 protein levels were measured at 24 hours in basal medium and apical washes (n= 7 independent ALI-PBEC donors). Data are shown as mean ± SEM. * p < 0.05, ** p < 0.01, *** p < 0.001, **** p < 0.0001.

IL-8 was found to be increased in the basal medium of co-cultures with LPS-activated macrophages but not in the unstimulated controls. No increased IL-8 levels were observed in the apical washes. hBD-2 was not detected in the basal medium (data not shown) but was secreted on the apical side of the ALI-PBEC co-cultured with activated M(GM-CSF), but not M(M-CSF) macrophages. Since airway epithelial cells do not respond to LPS (Fig. 1A+B) (Jia et al. 2004), these findings show that ALI-PBEC initiate host defense responses in co-culture with LPS-activated M(GM-CSF) or M(M-CSF) macrophages.

Both activated M(GM-CSF) and M(M-CSF) macrophages enhance epithelial wound repair

After demonstrating that LPS-activated macrophages can modulate epithelial host defense responses, we next continued by investigating whether LPS-activated M(GM-CSF) or M(M-CSF) macrophages can alter epithelial wound repair. To this end, circular wounds were mechanically created in the epithelial layer (Hiemstra et al. 2016), and subsequently co-cultured with activated macrophages (SFig. 1B, Fig. 2A). LPS alone in the absence of macrophages did not affect epithelial wound closure. However, co-culture with both M(GM-CSF) and M(M-CSF) macrophages significantly increased epithelial wound closure compared to epithelial mono-cultures. Complete wound closure was reached at 30 and 50 hours post mechanical wounding in the presence of activated M(GM-CSF) or M(M-CSF) macrophages respectively, whereas mono-cultures reached only 75% at this time-point, indicating that epithelial wound closure was enhanced consistently in co-cultures with both LPS-activated M(GM-CSF) and M(M-CSF) macrophages.

Since we previously reported that exposure to whole cigarette smoke (WCS) decreases epithelial wound closure (Luppi et al. 2005; Hiemstra et al. 2016), we investigated whether LPS-activated macrophages also enhanced epithelial wound closure in WCS exposed ALI-PBEC cultures. To this end, ALI-PBEC were exposed to WCS following wounding and subsequently co-cultured with either M(GM-CSF) or M(M-CSF) macrophages (Fig. 2B). In line with our previous findings (Amatngalim et al. 2016), WCS exposure delayed wound closure especially at early time points ($t=8$ hours; $p=0.065$), irrespective of co- or mono-culture of ALI-PBEC. Co-culture with both M(GM-CSF) and M(M-CSF) macrophages also significantly increased epithelial wound closure in WCS-exposed cultures. These data suggest that LPS-activated

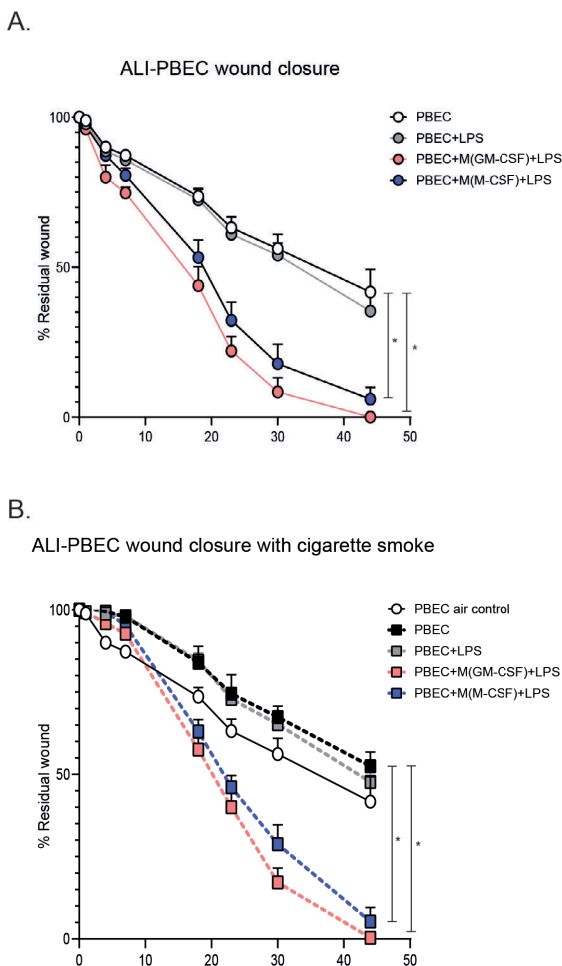


Figure 2. Activated M(GM-CSF) and M(M-CSF) macrophages enhance epithelial wound repair.

ALI-PBEC were mechanically injured and subsequently co-cultured with either activated M(GM-CSF) or M(M-CSF) macrophages. Wound closure was monitored in time using phase-contrast light microscopy. Wound closure is shown as percentage residual wound area. (A) Upon mechanical wounding, ALI-PBEC were cultured alone (black line) or co-cultured with activated M(GM-CSF) (red line) or M(M-CSF) (blue line) macrophages. (n=4 independent ALI-PBEC donors). (B) ALI-PBEC were exposed to whole cigarette smoke (WCS) and subsequently co-cultured with activated M(GM-CSF) (red line) or M(M-CSF) (blue line) macrophages (n=7 independent ALI-PBEC donors). Data are shown as mean \pm SEM. * $p < 0.05$

macrophages increase epithelial wound repair, also following exposure to cigarette smoke.

Macrophage-derived mediators enhance epithelial wound repair

To determine which macrophage-derived mediators contributed to the observed enhanced epithelial wound repair, we measured macrophage expression of various growth factors (*TGFB1*, *HGF*, *IL10* and *PDGFA*), the metalloproteinase *MMP9* and the antimicrobial peptide *CAMP*, all of which have been implicated in epithelial wound repair (Gardner, Borthwick, and Fisher 2010) (Fig. 3A+B). Activated M(M-CSF) macrophages showed higher expression of *IL10*, and to a lesser extent *HGF* compared to activated M(GM-CSF) macrophages. Macrophage expression of *TGFB1*, *MMP9* and *PDGFA* was not altered (Fig. 3A+B). Interestingly, LPS-activated M(GM-CSF)

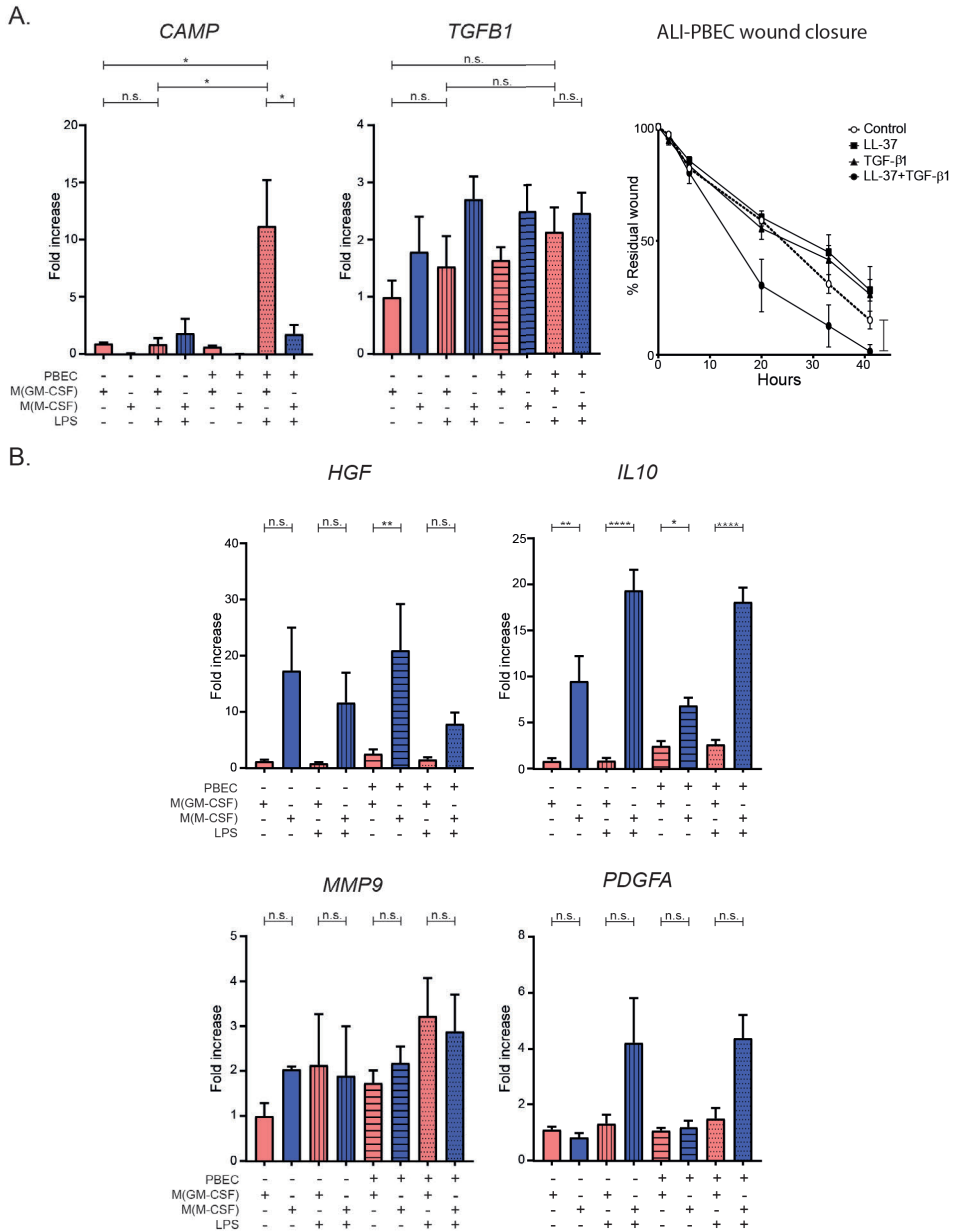


Figure 3. Macrophages-derived mediators enhance epithelial wound repair. mRNA expression levels of various genes in M(GM-CSF) and M(M-CSF) macrophages were measured upon co-culture with ALI-PBEC and epithelial wounding. (A) Expression levels of *CAMP* and *TGFB1* were measured in (LPS-activated) M(GM-CSF) (red bars) or M(M-CSF) (blue bars) macrophages in mono-cultures or upon co-culture with ALI-PBEC. (n=3 independent buffy donors). The role of these mediators in epithelial wound closure was assessed by addition of LL-37 and/or TGF-β1 in wounded ALI-PBEC (n=3 independent ALI-PBEC donors). (B) mRNA expression levels of *HGF*, *IL10*, *MMP9* and *PDGFA* in M(GM-CSF) (red bars) and M(M-CSF) (blue bars) macrophages was measured by q-PCR (n=3 independent buffy donors). Data are shown as mean ± SEM. * p < 0.05, ** p < 0.01

macrophages showed increased *CAMP* (encodes LL-37, an antimicrobial peptide with immune modulating and wound repair enhancing activities) expression only upon co-culture with ALI-PBEC (Fig. 3A). As *CAMP* expression in M(GM-CSF) macrophages was increased in presence of LPS and concomitant co-culture with ALI-PBEC, we investigated whether this increased *CAMP* expression may contribute to the observed enhanced wound closure in ALI-PBEC. We therefore added LL-37 and/or TGF- β 1 (which is known to contribute to epithelial repair) in wounded ALI-PBEC (Fig. 3A). Neither LL-37 nor TGF- β 1 alone affected wound closure, whereas their combination enhanced wound closure, with complete wound closure at 41 hours, as opposed to wound closure at t=30h in presence of activated M(GM-CSF) macrophages (Fig. 2A). The prolonged time till wound closure upon stimulation with LL-37/TGF- β 1 compared to M(GM-CSF) macrophage induced wound closure, suggests that additional factors in concert with LL-37 and TGF- β 1 contribute to the observed M(GM-CSF) macrophage-enhanced epithelial wound repair.

Therefore, we investigated whether inhibition of the TGF- β pathway (SB-431542), matrix metalloproteinases (GM6001) or LL-37 (neutralizing antibody) altered macrophage-induced enhanced epithelial wound repair (SFig. 3). Macrophage-induced epithelial wound closure was delayed by both SB-431542 and GM6001. However, since wound closure of ALI-PBEC monocultures was delayed as well in presence of these compounds, we concluded that the observed delayed wound repair was independent of the presence of macrophages (SFig. 3). The contribution of these pathways to macrophage-induced epithelial wound closure, therefore remained inconclusive. We studied the contribution of LL-37 to M(GM-CSF) enhanced epithelial wound repair using a selective LL-37 neutralizing antibody, however, this did not affect epithelial wound repair (SFig. 3). Collectively, these findings suggest that there is crosstalk between ALI-PBEC and macrophages and that this contributes to epithelial wound repair. We could demonstrate involvement of macrophage-derived factors in enhanced epithelial wound closure, including LL-37 (and TGF- β 1), but also found that cross-talk is not restricted to these factors alone. Additionally, M(M-CSF) macrophage-derived IL-10, HGF and MMP9 are likely candidates as driving factors of M(M-CSF) enhanced epithelial wound repair, which we did not further investigate in view of our observation that both types of macrophages enhanced wound repair.

Two-way crosstalk between ALI-PBEC and M(GM-CSF)macrophages

We established that activated M(GM-CSF) macrophages increase *CAMP* expression only in the presence of ALI-PBEC (Fig. 3A). We hypothesized that the increased *CAMP* in M(GM-CSF) macrophages resulted from crosstalk between the M(GM-CSF) macrophages and epithelial cells. We tested this hypothesis by assessing gene expression in macrophages in experiments using conditioned media from ALI-PBEC cultures and epithelial/macrophage co-cultures (Fig. 4A). Conditioned medium (CM) was collected from : i. ALI-PBEC only (ALI-PBEC-CM); ii. co-cultures of ALI-PBEC and macrophages (Co-culture-CM); and iii. conditioned medium that was obtained first from activated macrophages (24h), and then added to ALI-PBEC mono-cultures (24h) (Double-CM) (Fig. 4A). M(M-CSF) macrophages did not alter *CAMP* expression upon stimulation with ALI-PBEC-CM, co-culture-CM or Double-CM (Fig 4B, blue bars). In contrast, *CAMP* expression was increased in M(GM-CSF) macrophages upon addition of co-culture-CM or Double-CM (Fig 4B, red bars). ALI-PBEC-CM was not able to increase *CAMP* expression in M(GM-CSF) macrophages, suggesting that *CAMP* in M(GM-CSF) macrophages is induced only as a result of a two-way crosstalk between the M(GM-CSF) macrophages and ALI-PBEC.

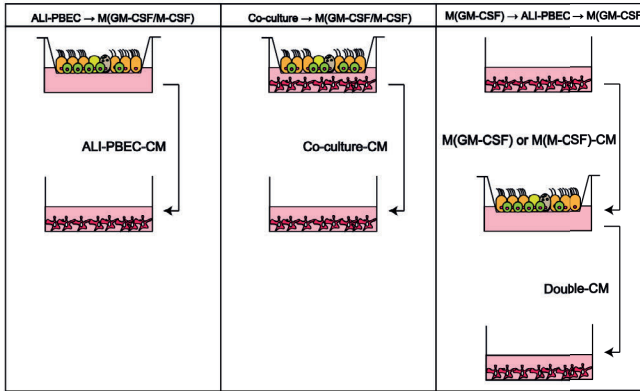
These data suggest that soluble mediators released by M(GM-CSF) macrophages, trigger the release of soluble mediators from ALI-PBEC that enhance *CAMP* expression in M(GM-CSF) macrophages.

Discussion

In this study, we investigated the crosstalk between primary bronchial epithelial cells cultured at the air-liquid interface (ALI-PBEC) and polarized macrophages. We found that co-culture of well-differentiated ALI-PBEC and activated macrophages displayed interactive crosstalk, and influenced epithelial innate immune responses and wound repair.

We show that epithelial IL-6 expression was increased upon co-culture with activated M(GM-CSF) and M(M-CSF) macrophages compared to epithelial monoculture. IL-6 is a multifunctional cytokine that has also been shown to promote intestinal epithelial proliferation (Kuhn et al. 2014). Co-culture with activated M(GM-CSF) macrophages furthermore increased epithelial expression of *DEFB4A* and *CXCL8*. We also confirmed this at protein level for *DEFB4A*, as hBD-2 levels in apical washes were increased upon co-culture with activated M(GM-CSF) macrophages. The effect on IL-8 secretion was

A.



B.

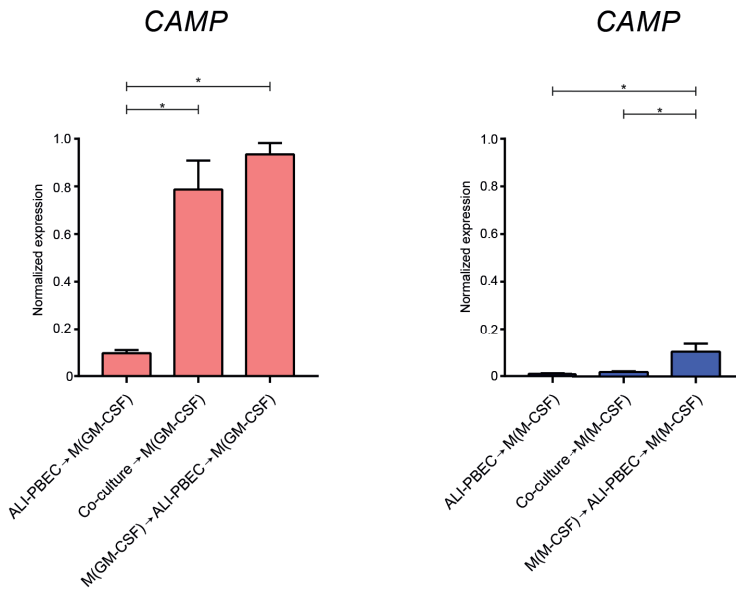


Figure 4. Effect of ALI-PBEC on *CAMP* expression in M(GM-CSF) macrophages. The mechanisms underlying increased *CAMP* expression in M(GM-CSF) macrophages in co-culture with ALI-PBEC were investigated by exposing macrophages to conditioned media (CM) collected from various culture conditions. (A) Overview of the culture condition from which the conditioned medium was collected (n=3 independent buffy donors). (B) *CAMP* expression at 24h was measured by q-PCR in M(GM-CSF) (red bars) or M(M-CSF) macrophages (blue bars) upon stimulation with the various conditioned media. Data are shown as mean \pm SEM. * $p < 0.05$, ** $p < 0.01$, *** $p < 0.001$

less clear, which may in part be explained by the fact that IL-8 is produced by epithelial cells as well as by activated macrophages and can be secreted in the basal compartment. hBD-2 however, is produced mainly by the epithelial cells and secreted apically. The induction of hBD-2 in epithelial cells is in line

with studies which show that pro-inflammatory cytokines induce hBD-2 (Kao et al. 2004; O’Neil et al. 1999) and that microbial products (e.g. LPS) activate macrophages to release inflammatory mediators. Activated pro-inflammatory macrophages also produce pro-inflammatory cytokines including IL-1 β , that subsequently enhance epithelial production of antimicrobial peptides and inflammatory cytokines (Bals and Hiemstra 2004). This cascade may act as an amplifying response to microbial products, as ALI-PBEC are less responsive to LPS compared to macrophages (Jia et al. 2004), which we also found in our study. These findings suggest that activated macrophages alter innate immune responses of well-differentiated ALI-PBEC through the release of soluble mediators.

In addition to an altered epithelial innate immune response, we show that co-culture with activated macrophages significantly enhanced epithelial wound repair. LPS addition to ALI-PBEC alone did not alter wound closure compared to unstimulated control. Our observations are in line with an *in vivo* response upon epithelial damage: following epithelial damage, pro-inflammatory macrophages are activated during the inflammatory phase, produce inflammatory cytokines and display antimicrobial activity (Yamada, Fujino, and Ichinose 2016). In the subsequent remodeling phase, anti-inflammatory macrophages will contribute to epithelial proliferation and migration followed by further restoration of the epithelial barrier and resolution of inflammation (Smigiel and Parks 2018).

There was no significant difference between M(GM-CSF) and M(M-CSF) polarized macrophages in their wound healing capacity. However, M(GM-CSF) polarized macrophages consistently induced faster epithelial wound closure compared to M(M-CSF) polarized macrophages, but this did not reach statistical significance at any of the time points investigated. At present, data on the wound healing capacity of pro- versus anti-inflammatory macrophages are conflicting (Wynn and Vannella 2016). Whereas one study also showed that M2 macrophage administration was not beneficial in murine cutaneous wound healing (Jetten et al. 2014), this is in contrast with other *in vitro* studies. These studies show that anti-inflammatory M(IL-10) macrophages increased wound repair of A549 epithelial cells, compared to pro-inflammatory M(IFN- γ) macrophages. This effect may be mediated through IL-10 (26) or hepatocyte growth factor (HGF) (Garnier et al. 2018), which is a prominent growth factor produced by alveolar macrophages (Garnier et al. 2018) and intestinal macrophages (D’Angelo et al. 2013). Also

in our study, HGF was also expressed in M(M-CSF) macrophages and lower in M(GM-CSF) macrophages. Interestingly, expression *IL10* was significantly higher in M(M-CSF) macrophages compared to M(GM-CSF) macrophages, again suggesting that there is cellular crosstalk between ALI-PBEC and activated macrophages, although we did not further examine this.

Interestingly, macrophages in bronchoalveolar lavage display higher levels of CD163⁺ anti-inflammatory macrophages compared to levels in induced sputum (Kunz et al. 2011), suggesting that macrophages in the airways display a pro-inflammatory phenotype, which may aid in the defense against the heterogeneity of inhaled substances/pathogens. In contrast, M2-type activity of macrophages in the alveolar compartment may protect against excessive inflammation and contributes to repair. This is supported by the proposed role of M2 macrophages in alveolar repair in a mouse pneumonectomy model (Lechner et al. 2017). In our model, we used ALI-PBEC as a model using epithelial cells isolated from the large conducting airways, where indeed M1 macrophages may induce rapid wound closure, to prevent intrusion of harmful pathogens or substances. Dependent on the localization and the micro-environment, the phenotype and function of macrophages may be adapted, and thereby influence repair processes (Puttur, Gregory, and Lloyd 2019). In COPD, macrophage polarization has been described to be dysregulated (Hiemstra 2013; Shaykhiev et al. 2009), which suggests that epithelial wound repair may be affected.

In a previous study we showed that cigarette smoke exposure delayed epithelial wound closure especially at early time points (Amatngalim et al. 2016). We confirmed this in the present study, irrespective of co- or monoculture of ALI-PBEC. Co-culture with both M(GM-CSF) and M(M-CSF) macrophages however, significantly increased epithelial wound closure in WCS-exposed. In our model, only airway epithelial cells were exposed to WCS, whereas macrophages were remained non-exposed. Other studies showed that cigarette smoke exposure also affects macrophage function (Strzelak et al. 2018), which we did not further investigate.

M(GM-CSF) macrophages may enhance wound repair in part by the selective increased expression of *CAMP* upon co-culture with ALI-PBEC. We have previously shown that LL-37 drives macrophage polarization towards a pro-inflammatory macrophage phenotype (van der Does et al. 2010). Part of the observed effect of M(GM-CSF) macrophages on epithelial innate immunity and wound repair may have been caused by an increased susceptibility of

epithelial cells to LPS resulting from exposure to macrophage-derived LL-37 (Shaykhiev et al. 2005). Apart from its prominent role in host defense, the antimicrobial peptide LL-37 has been shown to be involved in wound repair both *in vivo* and in *in vitro* skin models (Ramos et al. 2011; Carretero et al. 2008). LL-37 is able to activate airway epithelial cells through EGFR transactivation (Tjabringa et al. 2003), which may contribute to wound repair. In our model, exogenously added LL-37 enhanced wound repair only upon concomitant addition of TGF- β 1. A possible explanation for the synergistic effect of LL-37 or TGF- β 1 on wound repair could be an interaction between the putative induction of an epithelial migratory (by TGF- β 1) and proliferatory phenotype (by LL-37). We also determined the contribution of other mediators that may enhance wound repair, but since inhibition of the TGF- β 1 pathway or MMPs also markedly reduced epithelial wound closure in the ALI-PBEC mono-cultures, we could not determine the role of these pathways in M(GM-CSF) or M(M-CSF) macrophage-enhanced epithelial wound repair.

We did not observe alterations in macrophage polarization during co-culture (data not shown). These findings suggest that in our experimental set-up ALI-PBEC do not produce strong polarizing factors or the time in co-culture is insufficient to influence macrophage polarization. In this study we focused on only 2 subsets of macrophages (Van't Wout et al. 2015), however, for future studies our co-culture setup allows incorporation of various other macrophage subsets to study epithelial-macrophage interaction (Gindele et al. 2017; Boyette et al. 2017; Murray and Wynn 2011). Whereas other studies of airway epithelial cell co-cultures either focus solely on the host defense aspect of macrophages or use cell lines (Bodet, Chandad, and Grenier 2006; Blom et al. 2016; Bauer et al. 2015; Reuschl et al. 2017), we used both primary monocyte-derived macrophages and well-differentiated primary airway epithelial cells, which better reflects *in vivo* responses. Furthermore, other cell-types, such as structural cells may be incorporated as well, to better mimic the *in vivo* cellular niche. Previous studies have shown that macrophage-derived mediators have an effect on dermal fibroblasts (Ploeger et al. 2013), and this may also occur in the lung, assisting in modulation of epithelial cell function.

Although a limitation of our model is that the cells are cultured in separate compartments, and therefore cell-cell interactions are excluded (Leoni et al. 2015), we were able to reveal crosstalk between macrophages and epithelial

cells and show that they interact in part through secreted mediators. In recent years it has been found that cellular crosstalk may occur through extracellular vesicles, and this has also been described for the interaction between epithelial cells and macrophages (Lee et al. 2018). Another limitation is that we did not extend the co-culture beyond 72 hours, to avoid potential problems with different media requirements for primary bronchial epithelial cells and macrophages. Future studies are necessary to further optimize this model with prolonged co-culture time, without affecting ALI-PBEC integrity and/or M(GM-CSF) or M(M-CSF) macrophage polarization. Finally, we used CD14-monocyte-derived M(GM-CSF) and M(M-CSF) macrophages in this study, whereas these may not fully reflect the repertoire of airway, alveolar and interstitial macrophages in the lung (Byrne et al. 2015; Puttur, Gregory, and Lloyd 2019). The current culture set-up with 2-weeks differentiated ALI-PBEC limited the use of freshly isolated lung-derived macrophages, however, we did mimic the interaction between airway epithelial cells and recruited monocyte-derived macrophages. Furthermore, whereas macrophage phenotype *in vivo* displays plasticity, we simplified our model by using polarized macrophages, and thereby could investigate macrophage subtype specific responses on airway epithelial innate immunity and repair.

In summary, using primary cells, we show that ALI-PBEC and activated macrophage co-culture alters epithelial innate immune responses, enhances epithelial wound repair and induces interactive crosstalk between epithelial cells and macrophages, thereby better representing the *in vivo* situation compared to mono-cultures of airway epithelial cells.

Acknowledgements

We thank Marloes Hofstee and Bram van der Linden (Dept. of Pulmonology, Leiden University Medical Center, Leiden, The Netherlands) for the technical support during this study, and Dr. Anne van der Does (Dept of Pulmonology, Leiden University Medical Center, Leiden the Netherlands) for critical reviewing the manuscript.

Author contributions

SR designed, performed and analyzed the experiments, interpreted the data, prepared the figures and drafted the manuscript; AS provided technical support and helped with the data acquisition; SV and NV provided input during experimental design and manuscript preparation; JS, RR, PH and PK designed the study, and supervised experiments and manuscript writing. All authors have read and approved the final version of this manuscript.

Statement of Ethics

The use of lung tissue for research following surgery within the framework of patient care was in line with the “Human Tissue and Medical Research: Code of conduct for responsible use” (2011) (www.federa.org), that describes the no-objection system for coded anonymous further use of such tissue.

Disclosure statements

Dr. De Vos and Dr. Vandeghinste are employees of Galapagos NV. Prof. Hiemstra reports grants from Galapagos NV, grants from Lung Foundation Netherlands, during the conduct of the study; grants from Boehringer Ingelheim, outside the submitted work.

Funding

This study was supported by grants from the Lung Foundation Netherlands (grant 6.1.14.010 and grant 6.1.14.009) and Galapagos.

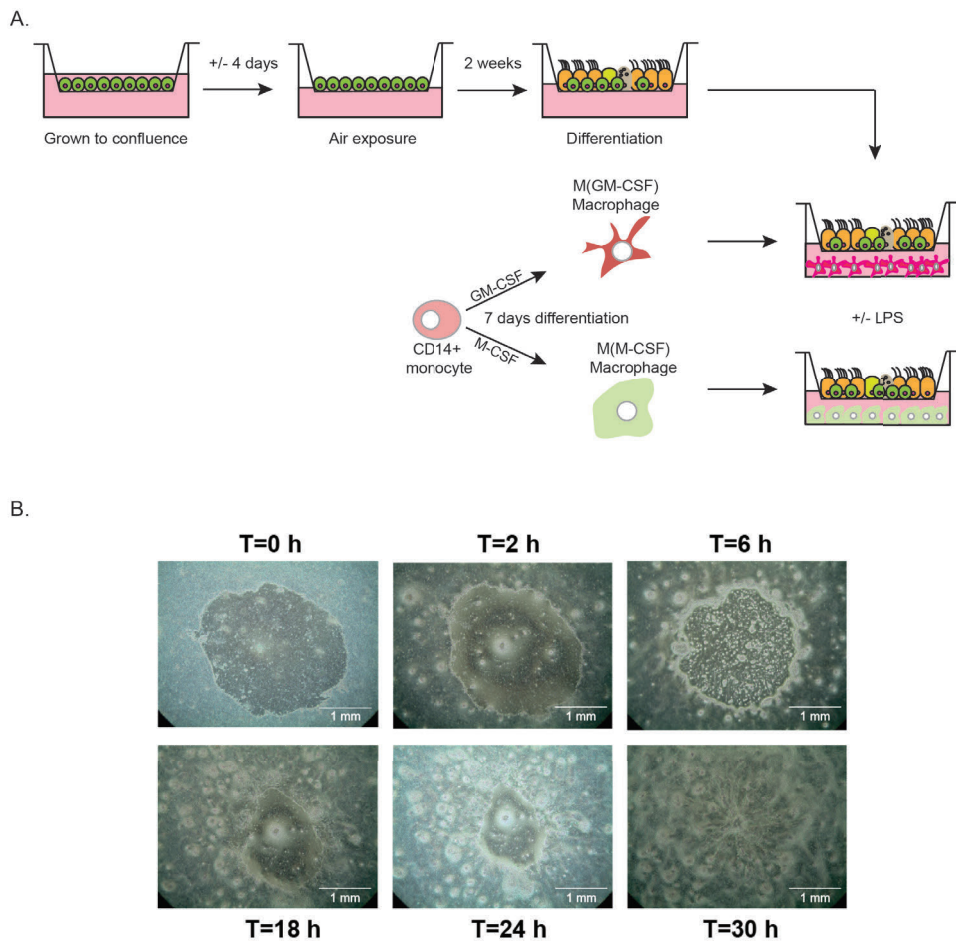
References

- Alber, A., S. E. Howie, W. A. Wallace, and N. Hirani. 2012. 'The role of macrophages in healing the wounded lung', *Int J Exp Pathol*, 93: 243-51.
- Amatngalim, G. D., W. Broekman, N. M. Daniel, L. E. van der Vlugt, A. van Schadewijk, C. Taube, and P. S. Hiemstra. 2016. 'Cigarette Smoke Modulates Repair and Innate Immunity following Injury to Airway Epithelial Cells', *PLoS One*, 11: e0166255.
- Amatngalim, G. D., and P. S. Hiemstra. 2018. 'Airway Epithelial Cell Function and Respiratory Host Defense in Chronic Obstructive Pulmonary Disease', *Chin Med J (Engl)*, 131: 1099-107.
- Amatngalim, G. D., J. A. Schrupf, F. Dishchekian, T. C. J. Mertens, D. K. Ninaber, A. C. van der Linden, C. Pilette, C. Taube, P. S. Hiemstra, and A. M. van der Does. 2018. 'Aberrant epithelial differentiation by cigarette smoke dysregulates respiratory host defence', *Eur Respir J*, 51.
- Amatngalim, G. D., J. A. Schrupf, A. Henic, E. Dronkers, R. M. Verhoosel, S. R. Ordonez, H. P. Haagsman, M. E. Fuentes, S. Sridhar, J. Aarbiou, R. A. J. Janssen, A. N. Lekkerkerker, and P. S. Hiemstra. 2017. 'Antibacterial Defense of Human Airway Epithelial Cells from Chronic Obstructive Pulmonary Disease Patients Induced by Acute Exposure to Nontypeable Haemophilus influenzae: Modulation by Cigarette Smoke', *J Innate Immun*, 9: 359-74.
- Andersen, C. L., J. L. Jensen, and T. F. Orntoft. 2004. 'Normalization of real-time quantitative reverse transcription-PCR data: a model-based variance estimation approach to identify genes suited for normalization, applied to bladder and colon cancer data sets', *Cancer Res*, 64: 5245-50.
- Arora, S., K. Dev, B. Agarwal, P. Das, and M. A. Syed. 2018. 'Macrophages: Their role, activation and polarization in pulmonary diseases', *Immunobiology*, 223: 383-96.
- Bals, R., and P. S. Hiemstra. 2004. 'Innate immunity in the lung: how epithelial cells fight against respiratory pathogens', *Eur Respir J*, 23: 327-33.
- Bauer, R. N., L. Muller, L. E. Brighton, K. E. Duncan, and I. Jaspers. 2015. 'Interaction with epithelial cells modifies airway macrophage response to ozone', *Am J Respir Cell Mol Biol*, 52: 285-94.
- Blom, R. A., S. T. Erni, K. Krempaska, O. Schaerer, R. M. van Dijk, M. Amacker, C. Moser, S. R. Hall, C. von Garnier, and F. Blank. 2016. 'A Triple Co-Culture Model of the Human Respiratory Tract to Study Immune-Modulatory Effects of Liposomes and Virosomes', *PLoS One*, 11: e0163539.
- Bodet, C., F. Chandad, and D. Grenier. 2006. 'Inflammatory responses of a macrophage/epithelial cell co-culture model to mono and mixed infections with *Porphyromonas gingivalis*, *Treponema denticola*, and *Tannerella forsythia*', *Microbes Infect*, 8: 27-35.
- Boyette, L. B., C. Macedo, K. Hadi, B. D. Elinoff, J. T. Walters, B. Ramaswami, G. Chalasani, J. M. Taboas, F. G. Lakkis, and D. M. Metes. 2017. 'Phenotype, function, and differentiation potential of human monocyte subsets', *PLoS One*, 12: e0176460.
- Byrne, A.J., S.A. Mathie, L.G. Gregory, and C.M. Lloyd. 2015. 'Pulmonary macrophages: key players in the innate defence of the airways', *Thorax*, 70: 1189-96.
- Carretero, M., M. J. Escamez, M. Garcia, B. Duarte, A. Holguin, L. Retamosa, J. L. Jorcano, M. D. Rio, and F. Larcher. 2008. '*In vitro* and *in vivo* wound healing-promoting activities of human cathelicidin LL-37', *J Invest Dermatol*, 128: 223-36.
- D'Angelo, F., E. Bernasconi, M. Schafer, M. Moyat, P. Michetti, M. H. Maillard, and D. Velin. 2013. 'Macrophages promote epithelial repair through hepatocyte growth factor secretion', *Clin Exp Immunol*, 174: 60-72.
- Gardner, A., L. A. Borthwick, and A. J. Fisher. 2010. 'Lung epithelial wound healing in health and disease', *Expert Rev Respir Med*, 4: 647-60.
- Garnier, M., A. Gibelin, A. A. Mailleux, V. Lecon, M. Hurtado-Nedelec, J. Laschet, G. Trebbia, M. Neuville, S. Tanaka, B. Crestani, M. Dehoux, and C. Quesnel. 2018. 'Macrophage Polarization Favors Epithelial Repair During Acute Respiratory Distress Syndrome', *Crit Care Med*, 46: e692-e701.
- Gindele, J. A., S. Mang, N. Pairet, I. Christ, F. Gantner, J. Schymeinsky, and D. J. Lamb. 2017. 'Opposing effects of *in vitro* differentiated macrophages sub-type on epithelial wound healing', *PLoS One*, 12: e0184386.
- Gordon, S., and L. Martinez Pomares. 2017. 'Physiological roles of macrophages', *Pflugers Arch*, 469: 365-74.
- Hiemstra, P. S. 2013. 'Altered macrophage function in chronic obstructive pulmonary disease', *Ann Am Thorac Soc*, 10 Suppl: S180-5.
- Hiemstra, P. S., G. D. Amatngalim, A. M. van der Does, and C. Taube. 2016. 'Antimicrobial

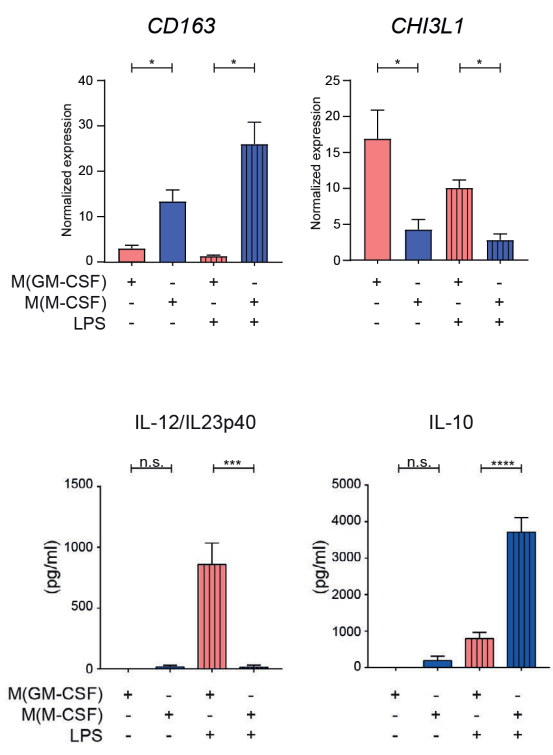
- Peptides and Innate Lung Defenses: Role in Infectious and Noninfectious Lung Diseases and Therapeutic Applications', *Chest*, 149: 545-51.
- Hiemstra, P. S., P. B. McCray, Jr., and R. Bals. 2015. 'The innate immune function of airway epithelial cells in inflammatory lung disease', *Eur Respir J*, 45: 1150-62.
- Hu, G., and J. W. Christman. 2019. 'Editorial: Alveolar Macrophages in Lung Inflammation and Resolution', *Front Immunol*, 10: 2275.
- Jetten, N., N. Roumans, M. J. Gijbels, A. Romano, M. J. Post, M. P. de Winther, R. R. van der Hulst, and S. Xanthoulea. 2014. 'Wound administration of M2-polarized macrophages does not improve murine cutaneous healing responses', *PLoS One*, 9: e102994.
- Jia, H. P., J. N. Kline, A. Penisten, M. A. Apicella, T. L. Gioannini, J. Weiss, and P. B. McCray, Jr. 2004. 'Endotoxin responsiveness of human airway epithelia is limited by low expression of MD-2', *Am J Physiol Lung Cell Mol Physiol*, 287: L428-37.
- Kao, C. Y., Y. Chen, P. Thai, S. Wachi, F. Huang, C. Kim, R. W. Harper, and R. Wu. 2004. 'IL-17 markedly up-regulates beta-defensin-2 expression in human airway epithelium via JAK and NF-kappaB signaling pathways', *J Immunol*, 173: 3482-91.
- Kuhn, K. A., N. A. Manieri, T. C. Liu, and T. S. Stappenbeck. 2014. 'IL-6 stimulates intestinal epithelial proliferation and repair after injury', *PLoS One*, 9: e114195.
- Kunz, L. I., T. S. Lapperre, J. B. Snoeck-Stroband, S. E. Budulac, W. Timens, S. van Wijngaarden, J. A. Schrupf, K. F. Rabe, D. S. Postma, P. J. Sterk, P. S. Hiemstra, and Group Groningen Leiden Universities Corticosteroids in Obstructive Lung Disease Study. 2011. 'Smoking status and anti-inflammatory macrophages in bronchoalveolar lavage and induced sputum in COPD', *Respir Res*, 12: 34.
- Lechner, A. J., I. H. Driver, J. Lee, C. M. Conroy, A. Nagle, R. M. Locksley, and J. R. Rock. 2017. 'Recruited Monocytes and Type 2 Immunity Promote Lung Regeneration following Pneumonectomy', *Cell Stem Cell*, 21: 120-34 e7.
- Lee, H., E. Abston, D. Zhang, A. Rai, and Y. Jin. 2018. 'Extracellular Vesicle: An Emerging Mediator of Intercellular Crosstalk in Lung Inflammation and Injury', *Front Immunol*, 9: 924.
- Leoni, G., P. A. Neumann, R. Sumagin, T. L. Denning, and A. Nusrat. 2015. 'Wound repair: role of immune-epithelial interactions', *Mucosal Immunol*, 8: 959-68.
- Luppi, F., J. Aarbiou, S. van Wetering, I. Rahman, W. I. de Boer, K. F. Rabe, and P. S. Hiemstra. 2005. 'Effects of cigarette smoke condensate on proliferation and wound closure of bronchial epithelial cells *in vitro*: role of glutathione', *Respir Res*, 6: 140.
- Murray, P. J. 2017. 'Macrophage Polarization', *Annu Rev Physiol*, 79: 541-66.
- Murray, P. J., and T. A. Wynn. 2011. 'Protective and pathogenic functions of macrophage subsets', *Nat Rev Immunol*, 11: 723-37.
- O'Neil, D. A., E. M. Porter, D. Elewaut, G. M. Anderson, L. Eckmann, T. Ganz, and M. F. Kagnoff. 1999. 'Expression and regulation of the human beta-defensins hBD-1 and hBD-2 in intestinal epithelium', *J Immunol*, 163: 6718-24.
- Ploeger, D. T., N. A. Hosper, M. Schipper, J. A. Koerts, S. de Rond, and R. A. Bank. 2013. 'Cell plasticity in wound healing: paracrine factors of M1/M2 polarized macrophages influence the phenotypical state of dermal fibroblasts', *Cell Commun Signal*, 11: 29.
- Puttur, F., L. G. Gregory, and C. M. Lloyd. 2019. 'Airway macrophages as the guardians of tissue repair in the lung', *Immunol Cell Biol*, 97: 246-57.
- Ramos, R., J. P. Silva, A. C. Rodrigues, R. Costa, L. Guardao, F. Schmitt, R. Soares, M. Vilanova, L. Domingues, and M. Gama. 2011. 'Wound healing activity of the human antimicrobial peptide LL37', *Peptides*, 32: 1469-76.
- Reuschl, A. K., M. R. Edwards, R. Parker, D. W. Connell, L. Hoang, A. Halliday, H. Jarvis, N. Siddiqui, C. Wright, S. Bremang, S. M. Newton, P. Beverley, R. J. Shattock, O. M. Kon, and A. Lalvani. 2017. 'Innate activation of human primary epithelial cells broadens the host response to *Mycobacterium tuberculosis* in the airways', *PLoS Pathog*, 13: e1006577.
- Shaykhiev, R., C. Beisswenger, K. Kandler, J. Senske, A. Puchner, T. Damm, J. Behr, and R. Bals. 2005. 'Human endogenous antibiotic LL-37 stimulates airway epithelial cell proliferation and wound closure', *Am J Physiol Lung Cell Mol Physiol*, 289: L842-8.
- Shaykhiev, R., A. Krause, J. Salit, Y. Strulovici-Barel, B. G. Harvey, T. P. O'Connor, and R. G. Crystal. 2009. 'Smoking-dependent reprogramming of alveolar macrophage polarization: implication for

- pathogenesis of chronic obstructive pulmonary disease', *J Immunol*, 183: 2867-83.
- Smigiel, K. S., and W. C. Parks. 2018. 'Macrophages, Wound Healing, and Fibrosis: Recent Insights', *Curr Rheumatol Rep*, 20: 17.
- Snyder, R. J., J. Lantis, R. S. Kirsner, V. Shah, M. Molyneaux, and M. J. Carter. 2016. 'Macrophages: A review of their role in wound healing and their therapeutic use', *Wound Repair Regen*, 24: 613-29.
- Strzelak, A., A. Ratajczak, A. Adamiec, and W. Feleszko. 2018. 'Tobacco Smoke Induces and Alters Immune Responses in the Lung Triggering Inflammation, Allergy, Asthma and Other Lung Diseases: A Mechanistic Review', *Int J Environ Res Public Health*, 15.
- Tjabringa, G. S., J. Aarbiou, D. K. Ninaber, J. W. Drijfhout, O. E. Sorensen, N. Borregaard, K. F. Rabe, and P. S. Hiemstra. 2003. 'The antimicrobial peptide LL-37 activates innate immunity at the airway epithelial surface by transactivation of the epidermal growth factor receptor', *J Immunol*, 171: 6690-6.
- Van't Wout, E. F., A. van Schadewijk, D. A. Lomas, J. Stolk, S. J. Marciniak, and P. S. Hiemstra. 2015. 'Function of monocytes and monocyte-derived macrophages in alpha1-antitrypsin deficiency', *Eur Respir J*, 45: 365-76.
- van der Does, A. M., H. Beekhuizen, B. Ravensbergen, T. Vos, T. H. Ottenhoff, J. T. van Dissel, J. W. Drijfhout, P. S. Hiemstra, and P. H. Nibbering. 2010. 'LL-37 directs macrophage differentiation toward macrophages with a proinflammatory signature', *J Immunol*, 185: 1442-9.
- Whitsett, J. A., and T. Alenghat. 2015. 'Respiratory epithelial cells orchestrate pulmonary innate immunity', *Nat Immunol*, 16: 27-35.
- Wynn, T. A., and K. M. Vannella. 2016. 'Macrophages in Tissue Repair, Regeneration, and Fibrosis', *Immunity*, 44: 450-62.
- Yamada, M., N. Fujino, and M. Ichinose. 2016. 'Inflammatory responses in the initiation of lung repair and regeneration: their role in stimulating lung resident stem cells', *Inflamm Regen*, 36: 1

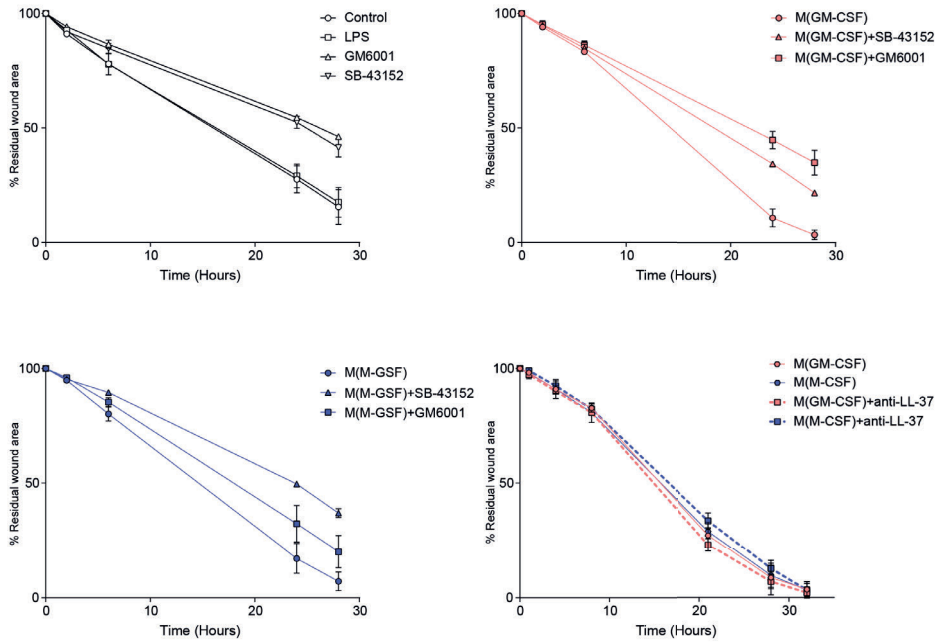
Supplementary figures



Supplementary Figure 1. Schematic overview of experimental setup. (A) Peripheral blood-derived CD14⁺ monocytes were cultured in presence of GM-CSF or M-CSF to induce a M(GM-CSF) or M(GM-CSF) macrophage phenotype, respectively. After 7 days in culture, macrophages were activated with 100 ng/mL LPS after which they were used in co-culture experiments. PBEC were cultured until confluent after which they were cultured at the air-liquid interface (ALI-PBEC) and differentiated for 2 weeks. Upon 2 weeks differentiation, ALI-PBEC and (LPS-activated) macrophages were co-cultured for 24h or until wound closure (B) Epithelial wounding was performed by mechanically scraping well-differentiated ALI-PBEC, using a template to ensure identical wound surface areas (Amatngalim et al. 2016). Wound closure was measured over time; representative light microscopic images were taken at various time points and are shown here.



Supplementary Figure 2. Macrophage polarization. (A) mRNA expression of *CD163* (M(M-CSF) macrophages – blue bars) and *CHI3L1* (M(GM-CSF) macrophages – red bars) in (LPS-activated) M(GM-CSF) and M(M-CSF) macrophages was measured by q-PCR (n=3 independent experiments). (B) Protein levels of IL-10 (M(M-CSF) macrophages – blue bars) and IL-12/IL-23p40 (M(GM-CSF) macrophages – red bars) were measured at 24h after LPS stimulation and upon co-culture (n=3 independent experiments). Data are shown as mean ± SEM. * p < 0.05, ** p < 0.01, *** p < 0.001, **** p < 0.0001.



Supplementary Figure 3. Inhibition of key repair pathways and molecules during epithelial wound repair. To determine the contribution of several pathways that play a role in epithelial wound repair to M(GM-CSF) (red line) or M(M-CSF) (blue line)-induced enhanced epithelial wound closure, various inhibitors were added in the epithelial mono (black lines)- and co-cultures upon epithelial wounding. Inhibitors of the TGF- β pathway (SB-434215), and MMP inhibitor (GM6001) and an anti-LL-37 antibody were added upon wounding and the residual wound area was measured over time (n=3 independent ALI-PBEC donors). Data are shown as mean \pm SEM.

CHAPTER 6

Flexible Poly(trimethylene carbonate) membranes for use in *in vitro* modelling of the airway epithelium

Sander van Riet¹, Thijs Pasman², Celine Roelse¹, Robbert J. Rottier^{3,4}, Dimitrios Stamatialis², André A. Poot², Pieter S. Hiemstra¹

¹Department of Pulmonology, Leiden University Medical Center, Leiden, The Netherlands

²Department of Biomaterials Science and Technology, Technical Medical (TechMed) Centre, Faculty of Science and Technology, University of Twente, Enschede, The Netherlands

³Department of Paediatric Surgery, Erasmus MC-Sophia Children's Hospital, Rotterdam, The Netherlands

⁴Department of Cell Biology, Erasmus MC, Rotterdam, The Netherlands

Work in progress

Abstract

In vitro lung models are increasingly used in respiratory research, but conditions in these models usually poorly reflect the mechanical properties of lung tissue. Contrasting traditional 2D cell cultures on plastic, lung tissue is much more flexible. A potential alternative to culture plastics are culture supports made of a biocompatible material that better mimic the mechanical properties of the studied tissue. The aim of the present study was to investigate growth and differentiation of primary bronchial epithelial cells (PBEC) on flexible membranes based on poly(trimethylene carbonate) (PTMC). We cultured the cells on PTMC membranes with different porosities and compared their growth to those grown on commercial poly(ethylene terephthalate) (PET) membranes in Transwells to allow culture at the physiological air-liquid interface (ALI). Whereas PBEC did grow on PTMC membranes, the cell cultures did not reach confluence, in contrast to those grown on polyethylene terephthalate (PET) membranes. Furthermore, whereas PBEC cultured at the ALI on PET membranes showed mucociliary differentiation, such differentiation was absent on PTMC membranes. Compared to PET cultures, PBEC cultured on PTMC membranes showed an increased expression of epithelial-mesenchymal transition (EMT) markers and of TGF β -R2 on PTMC membranes, which could explain the impaired differentiation. Treatment with the TGF- β signalling pathway inhibitor SB-431542 partly restored differentiation and growth, suggesting that culture on PTMC membranes had triggered TGF- β signalling. These findings demonstrate that further optimization is needed before use of PTMC membranes for culture of primary airway epithelial cells.

Introduction

Lung related diseases are listed 3 times in the WHO top 10 leading causes of death globally (World Health Organization 2018). The lungs are continuously exposed to potentially harmful, inhaled substances, including toxicants present in air pollution and respiratory pathogens. The airway epithelial cells lining the airways play a central role in the defence against these inhaled toxicants and pathogens by providing a physical barrier and providing a range of chemical and cellular defence mechanisms (Hiemstra, McCray, and Bals 2015). An inadequate epithelial defence may result in epithelial injury and remodelling, which are hallmarks of many pulmonary diseases (Fehrenbach, Wagner, and Wegmann 2017; Skold 2010). However, the mechanisms involved are incompletely understood which limits treatment options (Halbert et al. 2006). Epithelial cell culture models as well as animal models are widely used to study disease mechanisms, but many cell culture models use submerged culture conditions and are therefore not suitable for exposure to airborne substances. In contrast, air-liquid interface (ALI) epithelial culture models trigger differentiation of primary airway epithelial cells and allow exposure to airborne substances such as the noxious gases and particles that contribute to development of several lung diseases (Lacroix et al. 2018). Even though the current *in vitro* models do not recapitulate all features of epithelial function *in situ*, the use of advanced culture models and e.g. patient-derived cells could help to overcome some important limitations associated with the use of animal models. These include the poor cross-species translatability of observations from animal models to the human situation resulting from substantial differences in mechanisms and responses compared to human lung tissue (Schilders et al. 2016; Mullane and Williams 2014; Uhl and Warner 2015).

Continuous advances in the fields of biomaterials and bioengineering allows for the use of more biocompatible tissue culture supports in *in vitro* models. For most cell cultures, stiff culture plastics like polystyrene (PS), polycarbonate (PC) or polyethylene terephthalate (PET) are used (Amatngalim et al. 2016; Amatngalim et al. 2015; Amatngalim et al. 2018). PC and PET porous membranes are suitable for culture at the ALI, but these are not optimally suited to emulate the lung environment accurately, since lung tissue stretches, is not flat and is significantly more flexible (Cox and Erler 2011). The lungs are a flexible organ with an average stiffness of ± 350 Pa, whereas stiffness of PS and PET is in the GPa range, which resembles the

stiffness of bone (Butcher, Alliston, and Weaver 2009). The effect of material stiffness on cellular function has been described in various studies (Discher, Janmey, and Wang 2005; Cox and Erler 2011; Park et al. 2020). Currently, membranes made of poly(dimethylsiloxane) (PDMS) are frequently used in organ-on-chip systems because of their flexibility and transparency (Schuller-Ravoo et al. 2018; Huh et al. 2013). However, PDMS has a low biocompatibility requiring specific treatments to allow cell attachment, shows marked adsorption of various compounds, and the methods used to produce the membranes can be cumbersome (Moraes et al. 2009; Wala, Maji, and Das 2017).

An alternative to the currently widely used membranes is poly(trimethylene carbonate) (PTMC), a biocompatible polymer that can be used to produce a porous, flexible membrane for *in vitro* culture ALI culture (Pasman et al. 2020). The production of PTMC membranes is highly tuneable to e.g. facilitate formation of pores ranging between 3-8 μm to accommodate transmembrane medium transport and possibly migration of leukocytes. Whereas based on their mechanical properties, PTMC membranes could potentially better mimic lung tissue, the interaction between these membranes and primary airway epithelial cells has not been investigated. Overall, cell attachment and binding of extracellular matrix (ECM) have been insufficiently studied on these novel materials (Bershadsky, Balaban, and Geiger 2003). We recently reported a procedure for fabrication of flexible PTMC membranes with tuneable pore sizes between 5 and 8 μm and high water transport which may support culture at the ALI (Pasman et al. 2020). In an effort to elucidate whether these PTMC membranes could be used in an *in vitro* airway epithelial model, we analysed cellular function and differentiation of primary bronchial epithelial cells (PBEC) cultured on PTMC membranes, and compared these to standard PET Transwell inserts.

Methods

Fabrication of PTMC membranes

Poly(trimethylene carbonate) (PTMC) membranes were produced at the University of Twente. Over the course of the experiments, adjustments in the production of the membranes were made. Although all membranes have been manufactured using PTMC, the fabrication method changed slightly, ultimately resulting in the method described by Pasman et al. (Pasman et al. 2020). Furthermore, different batches of PTMC used to manufacture the membranes used in the present study may have contributed to the observed differences. As a result, 3 separate membrane batches are employed during this study, labeled PTMC1, 2 and 3; Details of the procedure used to prepare PTMC3 membranes is published by Pasman et al. Detailed information about the difference between the three batches PTMC membranes is presented in supplemental figure S1 and supplemental table S1. In the results section, we indicated which membranes were used for which experiments.

Water transport across the membranes

The permeance of the membranes was assessed using Water transport across the membranes (Pasman et al. 2020). Circular samples of membranes with a diameter of 26 mm were punched from larger membrane pieces and compared to commercial PET membranes with 0.4 μm pores (Corning Costar, Cambridge, MA) that were cut out from their inserts. The PTMC membranes were prewetted overnight in 100% ethanol, after which they were placed in an Amicon cell (Merck Millipore, Germany, Amicon cell 8003). The PET membranes were used without prewetting with ethanol since they performed better this way. A transmembrane pressure (TMP) was applied and afterwards the amount of permeated water through the membrane was estimated by the water flux.

Membrane morphology

The membrane morphology was assessed by Scanning Electron Microscopy (SEM) as described elsewhere (Pasman et al. 2020). Dry membrane samples were gold-sputtered under vacuum in a sputter coater (Cressington 108 Auto) equipped with a pure gold target (Aurion, The Netherlands, cat. 91017-AU) at 10 mA for 60 seconds. Subsequent imaging was performed on a JSM-6010LA from JEOL (Tokyo, Japan) at 5 kV.

Isolation and culture of primary bronchial epithelial cells

Macroscopically normal, tumour-free bronchial tissue was obtained from patients undergoing resection surgery for lung cancer at the Leiden University Medical Center (LUMC). The use of all lung samples for research that were collected within the framework of patient care from adult patients during surgery or bronchoscopy, was in line with the “Human Tissue and Medical Research: Code of conduct for responsible use” (2011) (www.federa.org). This code of conduct describes the no-objection system for coded anonymous further use of such samples. PBEC were isolated and expanded in culture as previously described (Amatngalim et al. 2018).

Culture of primary bronchial epithelial cells (PBEC)

1×10^5 PBEC at passage 2 were seeded per well of a 12-well PET membrane Transwell insert with pore size $0.4 \mu\text{m}$ (Corning Costar) or a PTMC membrane in a Transwell 12-well plates (Corning Costar). The PTMC membranes were inserted and attached to Transwell inserts using custom made rings (University of Twente). The standard coating used for PBEC on all membranes was $30 \mu\text{g/ml}$ PureCol (Advanced BioMatrix, San Diego, CA), $10 \mu\text{g/ml}$ BSA (Sigma-Aldrich, St. Louis, MO), and $10 \mu\text{g/ml}$ fibronectin (Sanbio, Uden, The Netherlands) in PBS. The membranes were coated for 1 hour at 37°C . PBEC were cultured in 1:1 bronchial epithelial growth medium (BEpiCM-b; ScienCell) and DMEM medium containing 4500 mg/l D-glucose (Stemcell Technologies) (B/D), supplemented with the retinoic acid analogue EC-23 (1 nM , Tocris), Hepes (1 mM , Lonza), BSA (1 mg/ml , Sigma-Aldrich), penicillin (100 U/ml) and streptomycin ($100 \mu\text{g/ml}$). Medium was refreshed three times a week until confluence was reached. Once confluent, apical medium was removed to culture the PBEC at the air-liquid interface (ALI). During ALI culture, the volume of the medium in the basal compartment was reduced from 1 ml to $600 \mu\text{l}$ per well to reduce leakage through the membrane (which was observed with PTMC membranes in pilot studies), and the EC-23 concentration was increased to 50 nM to promote differentiation.

Culture of Calu-3 cells

Calu-3 cells (ATCC, HTB-55) were cultured in uncoated T-75 flasks with Eagle’s minimum essential medium (EMEM; Lonza) supplemented with 10% fetal calf serum (FCS; Life Technologies, Carlsbad, CA) that was refreshed 3 times a week. Once the epithelial cell layer had grown nearly to

confluence, the cell layers were dissociated using trypsin (Life Technologies) and seeded on the PET or PTMC membranes. 1×10^5 cells were seeded per 12 well insert without additional coating. After reaching confluence (based on visual inspection of the transparent PET membranes; PTMC membranes are not transparent), the cells were cultured for 1 week at the ALI. During ALI culture, the volume of the medium in the basal compartment was reduced from 1 ml to 600 μ l per well to reduce leakage through the membrane.

Pretreatment of membranes with levodopa (L-DOPA)

L-DOPA (Sigma-Aldrich) was dissolved in Tris-buffer (pH 8.5) at 37°C while stirring to obtain a 2 mg/ml L-DOPA solution. The solution was sterilized by filtering through a 0.22 μ m filter (Sigma-Aldrich). The membranes were treated with L-DOPA overnight at 37°C, and subsequently washed with PBS. Following washing, either extracellular matrix components were added as additional coating, or the membranes were used immediately with only L-DOPA treatment.

Trans-epithelial electrical resistance measurement

Epithelial barrier integrity was determined by measuring the trans-epithelial electrical resistance (TEER) using the MilliCell-ERS (Millipore, Burlington, MA, US) according to the manufacturer's instructions.

Gene	Forward primer	Reverse primer
<i>TP63</i>	CCACCTGGACGTATTCCACTG	TCGAATCAAATGACTAGGAGGGG
<i>SCGB1A1</i>	ACATGAGGGAGGCAGGGGCTC	ACTCAAAGCATGGCAGCGGCA
<i>FOXJ1</i>	GGAGGGGACGTAAATCCCTA	TTGGTCCCAGTAGTTCCAGC
<i>MUC5AC</i>	ATTTTTTCCCCACTCCTGATG	AAGACAACCCACTCCCAACC
<i>SNAI2</i>	TCGGAAGCCTAACTACAGCGA	AGATGAGCATTGGCAGCGAG
<i>SNAI1</i>	TGTGACAAGGAATATGTGAGCC	TGAGCCCTCAGATTTGACCTG
<i>SERPINE1</i>	GTGGACTTTTCAGAGGTGGA	GCCGTTGAAGTAGAGGGCATT
<i>CCND1</i>	CTGGCCATGAACTACCTGGAC	GGTCACACTTGATCACTCTGG
<i>ATP5B</i>	TCACCCAGGCTGGTTCAGA	AGTGCCAGGGTAGGCTGAT
<i>ACTB</i>	TGCGTGACATTAAGGAGAAG	TGAAGGTAGTTTCGTGGATG

Table 1. RT-PCR primers

Immunofluorescence staining

ALI cultures were washed, fixed in 4% w/v paraformaldehyde and stained as described before (Eenjes et al. 2018). In brief, after fixation the cells were incubated with permeabilization and blocking buffer (1% w/v BSA, 0.3% v/v Triton-X100 in PBS) for 30 min at 4°C. The primary antibody was added in blocking solution to the cells for 1 h at room temperature (RT). Next, inserts

were washed in PBS and incubated with an Alexa Fluor 488 or 568-labeled secondary antibody together with DAPI for 30 min at RT. Images were obtained using a Leica SP8 confocal microscope. The list of antibodies can be found in table 2.

Target	Species	Dilution	Company
TP63	Rabbit	1:100	Abcam
TGFβ-R2	Rabbit	1:100	Santa Cruz
Ki-67	Mouse	1:100	Dako
ZO-1	Mouse	1:100	Invitrogen
Anti-Mouse alexa 488	Donkey	1:200	Life Technologies
Anti-Rabbit alexa 568	Donkey	1:200	Life Technologies

Table 2. Antibodies

Results

PTMC membrane parameters and Calu-3 cell culture

The PTMC membranes fabricated with various hexanol concentrations to modulate pore size demonstrated differences in surface topography between the side of evaporation (air side) and the side touching the silicon wafer during casting (substrate side) (See supplemental figure S1 and supplemental table S1). PTMC2 membranes were used to illustrate this observation in Fig. 1A. Due to the manufacturing process the air side of the membranes have a rougher surface area, which has been previously noted and is described in detail by Pasma et al.. Depending on the concentration of hexanol in the PTMC mixture, the number and size of pores in the membrane varied, which can be observed in the SEM images (Fig. 1A). The permeance of the membranes was estimated by applying a transmembrane pressure and measuring the permeated water compared to that of the commercial PET Transwell insert (Fig. 1B). The permeance of all PTMC (1-3) membranes was higher with increasing concentrations of hexanol. However, permeance of PTMC1 and 2 membranes prepared using the highest concentration of hexanol was still lower compared to the PET Transwell insert. The permeance of the PTMC3 membranes was vastly higher compared to PET membranes, regardless of hexanol concentration.

To explore the feasibility of establishing ALI cultures on permeable PTMC membranes, Calu-3 cells were grown to confluence on the various membranes, and next cultured for 7 days at the ALI. For these experiments PTMC1 was used (see methods section). We assessed cellular coverage and analyzed tight junction protein ZO-1 by immunofluorescence (Fig. 1C). The coverage of the Calu-3 cells as well as the staining of ZO-1 increased with

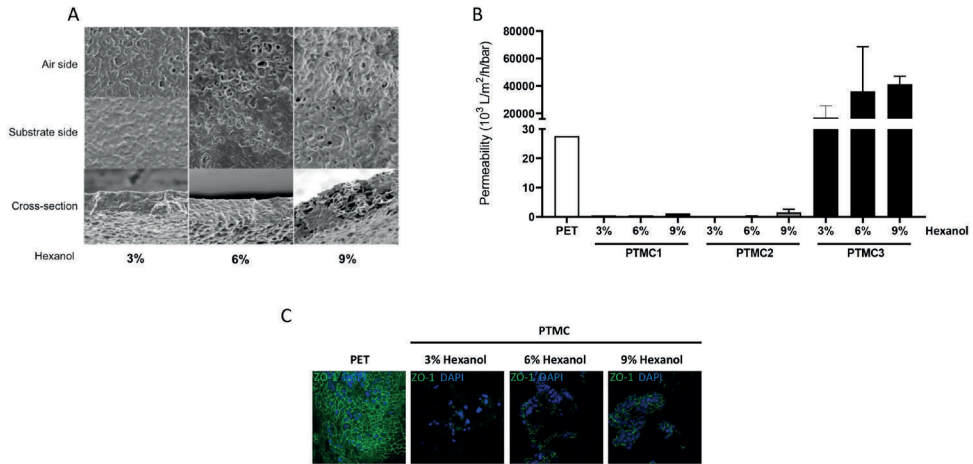


Figure 1. PTMC membrane characterization. (A) Electron microscopic images of the morphology of PTMC2 membranes. (B) Permeance of PTMC membranes (batch 1-3) produced with 0, 3, 6 or 9% hexanol compared to standard PET membrane Transwell inserts. Data are shown as mean \pm SD. (C) ZO-1 staining of Calu-3 cells cultured at the air-liquid interface for 7 days on PTMC1 membranes produced with 0, 3, 6 or 9% hexanol compared to those cultured on standard PET membrane Transwell inserts.

higher hexanol concentrations, as also described and discussed by Pasma et al. (submitted for publication). This is likely partly due to better permeance and access to nutrients on more porous membranes, which is essential to allow prolonged culture of cells at the ALI. Although the coverage of the cells increased with hexanol concentration, it did not reach the cell coverage of the PET membrane. This could be a result of batch-dependent differences in manufacturing, since the pores in the membrane were not evenly distributed, leaving various areas of the membrane non- or insufficiently porous.

Culture of primary bronchial epithelial cells on PTMC membranes

We next compared growth and differentiation of PBEC between PTMC and PET membranes. For these experiments PTMC1 was used, and a standard coating with Purecol (type I collagen), fibronectin and BSA was used for both PTMC and PET membranes. PBEC were grown submerged to confluence on the various membranes for 7 days and subsequently cultured at the ALI for 14 days. During ALI culture, the barrier function was assessed by monitoring trans-epithelial electrical resistance (Fig. 2A). The PET Transwell inserts showed an increase in barrier function as assessed by TEER measurements during 14 days of differentiation (Fig. 2A). However, cultures on PTMC1 fabricated with increasing concentrations of hexanol (3%, 6% and 9%) did not show an increase in barrier function. The PBEC could not be cultured at the ALI on the 0% hexanol membranes, as these membranes are not permeable.

Gene expression of epithelial differentiation markers was analyzed to assess differentiation (Fig. 2B). We could not analyze the 3% hexanol membrane, as there were insufficient cells following 14 days culture at ALI to collect sufficient RNA for RT-PCR analysis. *TP63* (basal cell), *SCGB1A1* (club cell), *FOXJ1* (ciliated cell) and *MUC5AC* (goblet cell) expression was measured. Cells cultured on the PTMC membranes showed a lower expression of *SCGB1A1* compared to the PET control, whereas *FOXJ1* expression was not detected on PTMC while expression on control membranes was present. Expression of *MUC5AC* could be only be detected to a limited extent in cells cultured on 9% hexanol PTMC1 membranes, whereas this was readily detectable in cells cultured on control PET membranes. Expression of the basal cell marker *TP63* was comparable or higher on PTMC when compared to control. These findings indicate an impaired differentiation of the cells on the PTMC1 membranes. Expression of *SCGB1A1* could suggest that some differentiation was initiated on the PTMC membranes, but the absence of *FOXJ1* and *MUC5AC* (with the exception of some expression on 9% hexanol membranes) indicates that (further) differentiation was impaired.

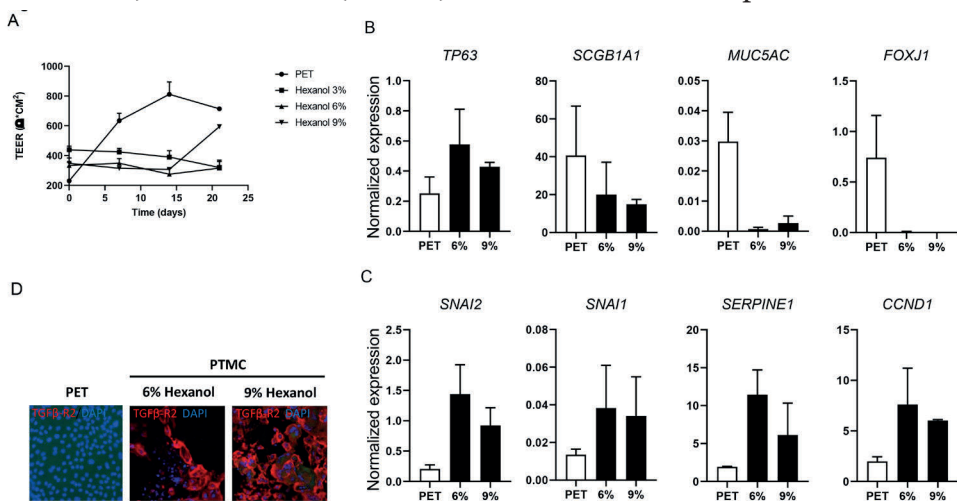


Figure 2. Differentiation of primary bronchial epithelial cells cultured on PTMC or PET membranes. (A) TEER measurement of PBEC during 21 days of culture at the ALI on PTMC1 membranes prepared using 3, 6 or 9 % hexanol, and compared to PET membranes. (B) Gene expression of differentiation markers following 14 days ALI culture on PET (open bars), or PTMC1 6% or 9% hexanol membranes (closed bars). (C) Gene expression of EMT-associated markers following 14 days ALI culture on PET, PTMC1 6% or 9% hexanol membranes. n = 2, data are shown as mean ± SEM.

Epithelial-mesenchymal transition in PBEC grown on PTMC membranes

In an effort to explain the impaired differentiation on PTMC1 membranes, we measured activation of various pathways and proteins that are important

for, or related to differentiation. For these experiments PTMC1 was used. We noted that the expression of markers associated with epithelial-mesenchymal transition (EMT), Slug (*SNAI2*), Snail (*SNAI1*) and PAI-1 (*SERPINE1*) was higher in the cells grown on the PTMC membranes (Fig. 2C). Furthermore, as we observed fewer cells on the PTMC cultures, we analysed Cyclin D1, a protein involved in the progression of the cell cycle checkpoints. We found expression of *CCND1* to be higher in the cells grown on the PTMC membranes than those grown on PET membranes. These findings could indicate that the cells grown on the PTMC membrane are undergoing EMT, whereas expression of *CCND1* could indicate the proliferative state of the cells. These observations are in line with the observed impaired mucociliary differentiation. EMT classically involves activation of the TGF- β pathway, and therefore we analysed TGF β -R2 expression and found this to be highly expressed in cells grown on PTMC membranes (Fig. 2D). These observations suggest activation of the TGF- β signalling pathway in the PTMC cultures.

Inhibition of TGF- β pathway using SB-431542

We next examined the role of the TGF- β pathway during differentiation by inhibiting TGF- β signalling using an inhibitor (SB-431542) of ALK5 and its homologues ALK4 and ALK7. PBEC were cultured on PTMC2 or PET membranes with or without SB-431542 during both submerged and ALI culture. For this and subsequent experiments the membranes produced with 9% hexanol were used as these were shown to be the most promising, as well as the non-porous control (0% hexanol). The cultures were analysed following 14 days culture at ALI. More RNA was isolated from the cultures grown on PTMC2 and treated with SB-431542 compared to the same cultures without the inhibitor, whereas no difference in RNA yield was observed on the PET membranes (data not shown). We next analysed expression of the various airway epithelial differentiation markers (Fig. 3A). The addition of SB-431542 resulted in lower expression of *TP63* and *MUC5AC* in the PET cultures, whereas expression of *SCGB1A1* and *FOXJ1* was not affected. In contrast, the addition of SB-431542 to the PTMC cultures could in part restore normal differentiation, as demonstrated by the observation that expression of *SCGB1A1*, *FOXJ1* and *MUC5AC* were all increased following inhibition of the TGF- β pathway. Furthermore, the expression of the EMT-associated genes *SNAI1*, *SNAI2* and *SERPINE1* was also highly reduced in the PTMC cultures treated with SB-431542 (Fig. 3B). These data suggest that activation of the TGF- β pathway plays a role in the disruption of the

differentiation of the cells on the PTMC membrane. However, as SB-431542 has an effect on multiple cellular responses and caused a reduction in *MUC5AC* expression in the PET control, it appears not ideal to keep the inhibitor present during both the proliferation and differentiation phase. It is unclear why the TGF- β pathway is activated in these cultures, as we found no increase in *TGFB1* expression in the PTMC cultures compared to control (data not shown; other TGF- β family members were not investigated). We hypothesised that the interaction of the cells with the ECM or directly with the PTMC membrane could possibly induce EMT, perhaps by enhancing responsiveness to epithelial cell-derived TGF- β . Fibronectin (FN), present in our coating, has been described to induce EMT (Park and Schwarzbauer 2014), although we have not observed a dominant effect of this in our standard PET cultures.

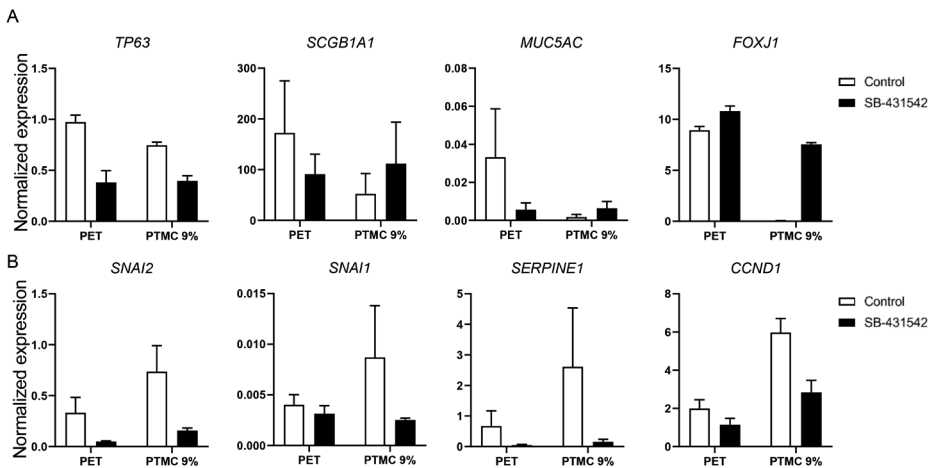


Figure 3. Effect of TGF- β signalling pathway inhibition on primary bronchial epithelial cells (PBEC) cultured on PTMC or PET membranes. (A) Gene expression of differentiation markers following 14 days ALI culture on PET or PTMC2 9% hexanol membranes with or without SB-431542 treatment. (B) Gene expression of EMT-associated markers following 14 days ALI culture on PET or PTMC2 9% hexanol membranes with or without SB-431542 treatment. $n = 2$ donors, data are shown as mean \pm SEM.

Effect of fibronectin on differentiation and EMT

To investigate whether FN had an effect on EMT-associated genes in our experiments, PBEC were cultured on PET or PTMC 9% membranes. These experiments were performed using PTMC1 membranes. The membranes were coated with collagen/BSA and with a FN concentration ranging from 1 to 20 $\mu\text{g/ml}$. Following 14 days at ALI, gene expression was measured to assess differentiation (Fig. 4A). Overall, the expression of differentiation markers in PBEC cultured on the different membranes was similar to previous experiments, and was not affected by the FN concentration. Again, *FOXJ1* was not detected

on cells grown on PTMC membranes, indicating impaired differentiation. Similarly, *SNAI2*, *SNAI1*, *SERPINE1* and *CCND1* were high compared to PET control and independent of FN concentration (Fig. 4B). The data presented suggest that the increase in EMT-associated genes in the PBEC grown on the PTMC membranes is independent of the FN concentration in the coating.

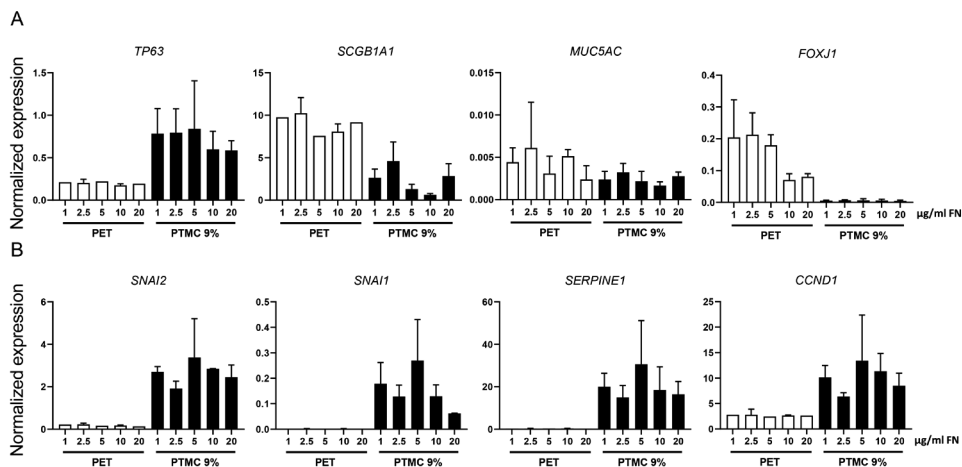


Figure 4. Effect of fibronectin in membrane coating on expression of EMT-associated genes in primary bronchial epithelial cells (PBEC) cultured on PTMC or PET membranes. (A) Differentiation-associated gene expression in PBEC cultures cultured for 14 days at ALI on PET or PTMC1 9% hexanol membranes with varying concentrations of fibronectin. (B) Gene expression in PBEC cultures of EMT-associated genes after 14 days at ALI culture on PET or PTMC1 9% hexanol membranes with varying concentrations of fibronectin. $n = 2$ donors, data are shown as mean \pm SEM.

L-DOPA as bioadhesive layer between membrane and ECM coating

We next investigated pre-treatment of the membrane surface with L-DOPA as a bioadhesive layer to improve the standard coating of the membrane. This was based on previous studies, proposing the use of L-DOPA as a non-toxic bioadhesive layer between ECM proteins and different substrates of varying stiffness (Lee et al. 2007). We reasoned that use of L-DOPA to improve coating by collagen and FN could limit direct interaction between the cells and the membrane, and thus prevent development of the previously observed EMT phenotype on PTMC membranes. PTMC3 membranes were treated with L-DOPA alone, or treated with L-DOPA and subsequently coated using the standard coating (Fig. 5A). First we analysed the growth of airway basal cells under submerged conditions. Following 5 days submerged culture the cells were fixed and analysed. On the PET Transwell inserts we observed a confluent layer of cells when using either L-DOPA alone, or treated with L-DOPA and subsequently coated using the standard coating. On the 0% hexanol we found limited cell coverage with L-DOPA alone but

much improved coverage when the additional standard coating was used. This effect was not observed when cells were grown on the 9% hexanol membrane, on which both conditions showed a similar and incomplete coverage of the membrane. Next, we analysed differentiation of the cells when grown at the ALI for 2 weeks on either PTMC membranes coated with L-DOPA alone or with L-DOPA and the standard coating (Fig. 5B). We analysed the presence of acetylated tubulin as a marker of ciliated cells and TGF β -R2. On the PET Transwell inserts we observed a confluent layer of cells in both conditions. We detected the presence of cilia in both conditions and the absence of TGF β -R2. On the PTMC 9% hexanol membrane almost no cells were detected on the L-DOPA alone and limited coverage was detected after additional standard coating. The cultures grown on these PTMC membranes showed no cilia and high expression of TGF β -R2. Based on these observations we conclude that L-DOPA pretreatment may increase adherence and growth of submerged cultured PBEC, but this does not overcome the problems encountered during culture and differentiation at the ALI.

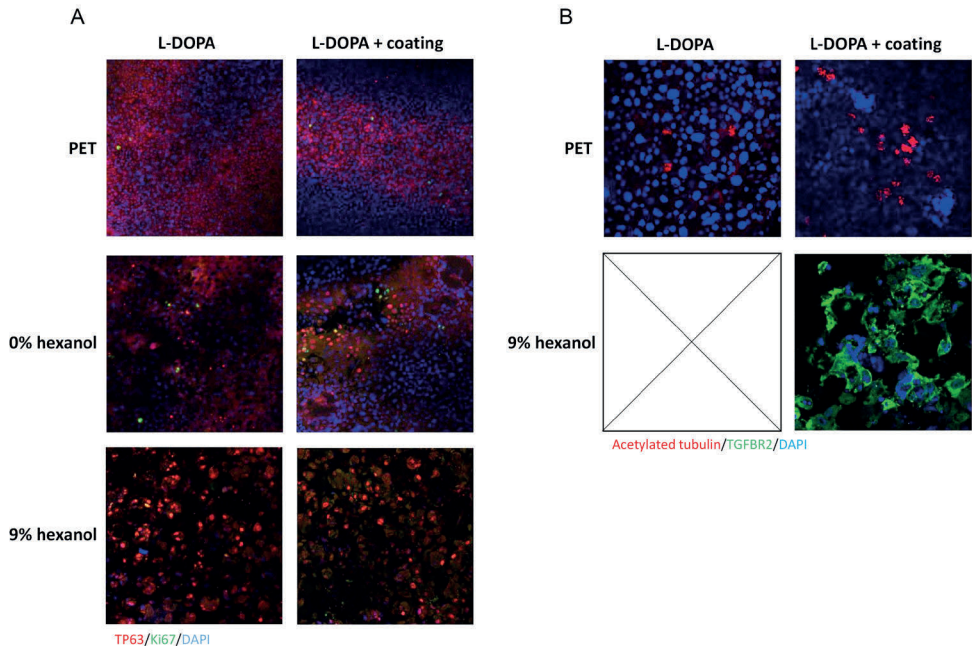


Figure 5. Effect of pretreatment of PTMC membranes using L-DOPA on PBEC culture. (A) Primary bronchial epithelial cells cultured submerged on PTMC3 membranes or PET Transwell inserts with L-DOPA alone or with additional standard coating. (B) Primary bronchial epithelial cells cultured air-exposed on PTMC3 membranes or PET Transwell inserts with L-DOPA alone or with additional standard coating.

Discussion

PTMC is a biocompatible polymer with properties that make membranes formed by PTMC an attractive alternative to widely used stiff standard PET membranes used in Transwell inserts or PDMS membranes (Pasman et al. 2020). We analysed the growth and differentiation of primary bronchial epithelial cells (PBEC) grown on flexible PTMC membranes compared to those cultured on commercial PET Transwell inserts, using three sets of consecutive PTMC membranes, numbered 1-3. First, we found that culture of Calu-3 cells on the PTMC1 membranes showed incomplete coverage after 7 days of ALI culture based on ZO-1 staining. This could be due to inhomogeneous distribution of the pores, resulting in some areas of the membrane being non-porous, or to the low permeance of the early PTMC1 membranes, thus not allowing cell growth at the ALI. We were also unable to establish a functional cell layer of well-differentiated pseudostratified PBEC on these PTMC1 membranes. When assessing epithelial differentiation, we observed expression of the club cell marker *SCGB1A1*, but only limited or no expression of *FOXJ1* and *MUC5AC*. This suggests that the differentiation of the PBEC on the PTMC membranes was impaired. We found that expression of genes associated with EMT was increased in the cells grown on the PTMC1-2 membranes, suggesting activation of EMT. Furthermore, we found that cells grown on PTMC1 membranes had high expression of TGF β -R2 on their surface membrane pointing to involvement of the TGF- β pathway (Rojas et al. 2009). Although we could not find an increase in TGFB1 expression in the cells grown on the PTMC membranes (data not shown), other ligands of TGF β -R2 or increased sensitivity to TGF- β levels may have led to increased TGF- β pathway signalling. We next tried to inhibit the TGF- β pathway using SB-431542. Addition of SB-431542 during submerged and ALI culture on PTMC2 membranes could in part restore differentiation, as shown by increased expression of differentiation markers and a reduction in the EMT-associated markers *SNAI1*, *SNAI2* and *SERPINE1*. These results suggest that the EMT pathway is activated during culture of PBEC on the PTMC membranes.

PTMC is a relatively new material that can be used to manufacture membranes for cell culture through different methods (Pasman et al. 2017; Papenburg et al. 2009). Our results indicate that the method of production and the subsequent *in vitro* cell culture need to be further optimized to facilitate long term primary airway epithelial cell ALI cultures. The membranes produced

using the method of (Pasman et al. 2020) are less transparent compared to PET Transwell insert making visual inspection of cells during culture difficult.

The induction of the EMT-associated genes is likely the result of the interaction between the cells, the membrane and the ECM. We have tried to elucidate the contribution of fibronectin present in our coating mixture, since it was described in some studies to induce EMT (Park and Schwarzbauer 2014). We found no clear effect of FN on the expression of EMT markers and it is therefore likely that a combination of factors is involved. We furthermore tried to first coat the membranes with L-DOPA as a bioadhesive layer between the membrane and the standard ECM coating. Although we did find slightly better growth of the PBEC while grown submerged, this effect was lost when grown at the ALI. Following ALI culture we observed that cells grown on L-DOPA and additional coating did not express acetylated tubulin and had high expression of TGF β -R2. Furthermore, L-DOPA is a precursor of dopamine and can be biologically active. The dopamine D1 receptor is expressed in the airway epithelium but we have not analysed whether the pathway is activated when grown on this coating (Matsuyama et al. 2018). Other factors described to have a direct effect on cellular function include the flexibility and topography of the membrane (Papenburg et al. 2009; Bershadsky, Balaban, and Geiger 2003; Park et al. 2020). However, it is unclear to which extent our observations are linked to the flexibility, roughness or (micro)curvature of the membrane and to which extent these parameters are sensed by the cells. Furthermore, the pores of the membrane are formed by a random process, in which homogeneous distribution of the pores cannot be guaranteed, thus leaving some area sparsely porous. This could explain why the PBEC could not form a confluent layer on PTMC membranes, with important consequences for culture at the ALI since at this culture stage cells are fully dependent on delivery of medium through the pores. This apparent inhomogeneity of the membranes combined with the inter-donor variation of the cells, created an additional barrier in the determination of the suitable culture conditions.

An important limitation to note is that slightly different methods of productions were used for the generation of different PTMC membranes. The method of manufacturing was changed over time and culminated in the one described in Pasman et al. (Pasman et al. 2020). Nevertheless, roughly similar problems were encountered using the different membrane sets used in the present study. Perhaps further improvements such as those reported

by Pasma et al. in a manuscript that has been submitted for publication may also improve PBEC culture, and future studies are needed to assess this.

Overall, the use of PTMC as a substitute substrate for cell culture offers interesting possibilities for expansion of our current toolbox of cell culture models. However, various culture and membrane-related parameters require further optimization before implementation of PTMC membranes for the study of airway epithelial cell biology.

Acknowledgements

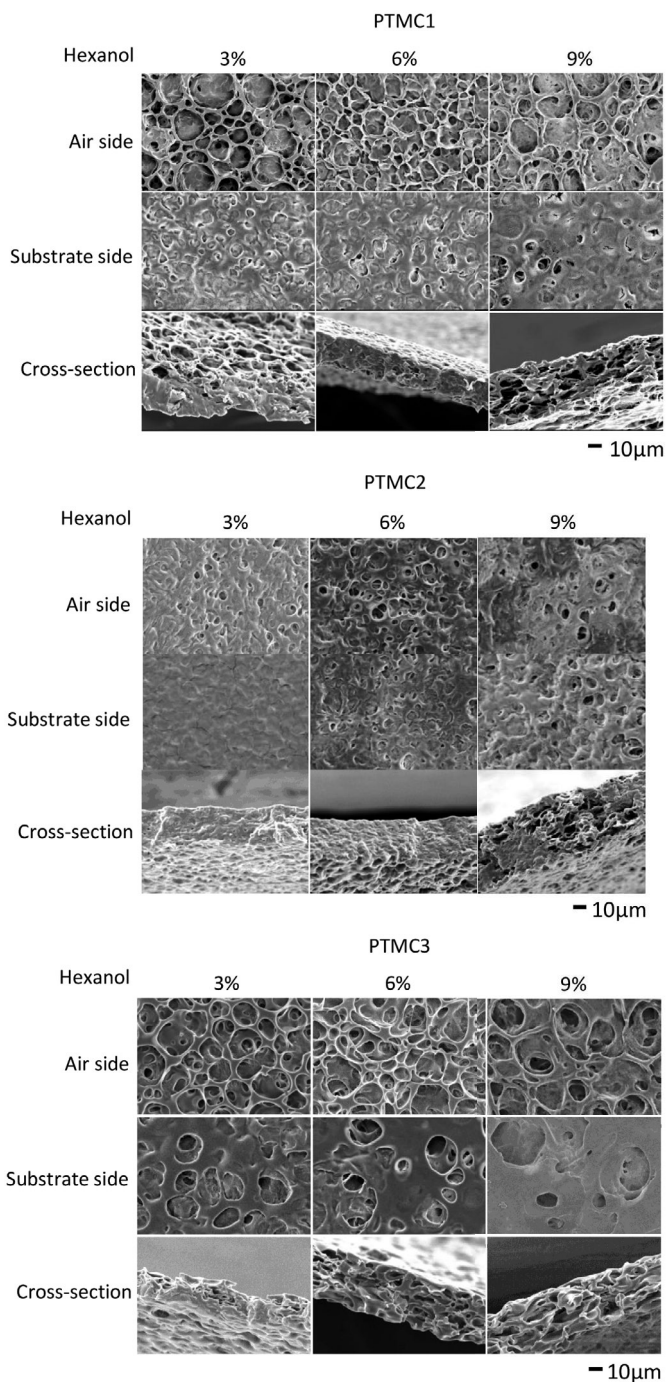
This study was supported by a grant of the Lung Foundation Netherlands (grant # 6.1.14.010). The authors thank D.K. Ninaber (LUMC) for technical assistance.

References

- Amatngalim, G. D., W. Broekman, N. M. Daniel, L. E. van der Vlugt, A. van Schadewijk, C. Taube, and P. S. Hiemstra. 2016. 'Cigarette Smoke Modulates Repair and Innate Immunity following Injury to Airway Epithelial Cells', *PLoS One*, 11: e0166255.
- Amatngalim, G. D., J. A. Schrupf, F. Dishchekenian, T. C. J. Mertens, D. K. Ninaber, A. C. van der Linden, C. Pilette, C. Taube, P. S. Hiemstra, and A. M. van der Does. 2018. 'Aberrant epithelial differentiation by cigarette smoke dysregulates respiratory host defence', *Eur Respir J*, 51.
- Amatngalim, G. D., Y. van Wijck, Y. de Mooij-Eijk, R. M. Verhoosel, J. Harder, A. N. Lekkerkerker, R. A. Janssen, and P. S. Hiemstra. 2015. 'Basal cells contribute to innate immunity of the airway epithelium through production of the antimicrobial protein RNase 7', *J Immunol*, 194: 3340-50.
- Bershadsky, A. D., N. Q. Balaban, and B. Geiger. 2003. 'Adhesion-dependent cell mechanosensitivity', *Annu Rev Cell Dev Biol*, 19: 677-95.
- Butcher, D. T., T. Alliston, and V. M. Weaver. 2009. 'A tense situation: forcing tumour progression', *Nat Rev Cancer*, 9: 108-22.
- Cox, T. R., and J. T. Erler. 2011. 'Remodeling and homeostasis of the extracellular matrix: implications for fibrotic diseases and cancer', *Dis Model Mech*, 4: 165-78.
- Discher, D. E., P. Janmey, and Y. L. Wang. 2005. 'Tissue cells feel and respond to the stiffness of their substrate', *Science*, 310: 1139-43.
- Eenjes, E., T. C. J. Mertens, M. J. Buscop-van Kempen, Y. van Wijck, C. Taube, R. J. Rottier, and P. S. Hiemstra. 2018. 'A novel method for expansion and differentiation of mouse tracheal epithelial cells in culture', *Sci Rep*, 8: 7349.
- Fehrenbach, H., C. Wagner, and M. Wegmann. 2017. 'Airway remodeling in asthma: what really matters', *Cell Tissue Res*, 367: 551-69.
- Halbert, R. J., J. L. Natoli, A. Gano, E. Badamgarav, A. S. Buist, and D. M. Mannino. 2006. 'Global burden of COPD: systematic review and meta-analysis', *Eur Respir J*, 28: 523-32.
- Hiemstra, P. S., P. B. McCray, Jr., and R. Bals. 2015. 'The innate immune function of airway epithelial cells in inflammatory lung disease', *Eur Respir J*, 45: 1150-62.
- Huh, D., H. J. Kim, J. P. Fraser, D. E. Shea, M. Khan, A. Bahinski, G. A. Hamilton, and D. E. Ingber. 2013. 'Microfabrication of human organs-on-chips', *Nat Protoc*, 8: 2135-57.
- Lacroix, G., W. Koch, D. Ritter, A. C. Gutleb, S. T. Larsen, T. Loret, F. Zanetti, S. Constant, S. Chortarea, B. Rothen-Rutishauser, P. S. Hiemstra, E. Frejafon, P. Hubert, L. Gribaldo, P. Kearns, J. M. Aublant, S. Diabate, C. Weiss, A. de Groot, and I. Kooter. 2018. 'Air-Liquid Interface *In Vitro* Models for Respiratory Toxicology Research: Consensus Workshop and Recommendations', *Appl In Vitro Toxicol*, 4: 91-106.
- Lee, H., S. M. Dellatore, W. M. Miller, and P. B. Messersmith. 2007. 'Mussel-inspired surface chemistry for multifunctional coatings', *Science*, 318: 426-30.
- Matsuyama, N., S. Shibata, A. Matoba, T. A. Kudo, J. Danielsson, A. Kohjitani, E. Masaki, C. W. Emala, and K. Mizuta. 2018. 'The dopamine D1 receptor is expressed and induces CREB phosphorylation and MUC5AC expression in human airway epithelium', *Respir Res*, 19: 53.
- Moraes, C., Y. K. Kagoma, B. M. Beca, R. L. Tonelli-Zasarsky, Y. Sun, and C. A. Simmons. 2009. 'Integrating polyurethane culture substrates into poly(dimethylsiloxane) microdevices', *Biomaterials*, 30: 5241-50.
- Mullane, K., and M. Williams. 2014. 'Animal models of asthma: reprise or reboot?', *Biochem Pharmacol*, 87: 131-9.
- Papenburg, B. J., S. Schuller-Ravoo, L. A. Bolhuis Versteeg, L. Hartsuiker, D. W. Grijpma, J. Feijen, M. Wessling, and D. Stamatialis. 2009. 'Designing porosity and topography of poly(1,3-trimethylene carbonate) scaffolds', *Acta Biomater*, 5: 3281-94.
- Park, J. S., C. J. Burekhardt, R. Lazcano, L. M. Solis, T. Isogai, L. Li, C. S. Chen, B. Gao, J. D. Minna, R. Bachoo, R. J. DeBerardinis, and G. Danuser. 2020. 'Mechanical regulation of glycolysis via cytoskeleton architecture', *Nature*, 578: 621-26.
- Park, J., and J. E. Schwarzbauer. 2014. 'Mammary epithelial cell interactions with fibronectin stimulate epithelial-mesenchymal transition', *Oncogene*, 33: 1649-57.
- Pasman, T., D. Baptista, S. van Riet, R. Truckenmuller, P. S. Hiemstra, R. J. Rottier, D. Stamatialis, and A. Poot. 2020. 'Development of Porous and Flexible PTMC Membranes for *In Vitro* Organ Models Fabricated by Evaporation-Induced Phase Separation', *Membranes*, 10: 300.
- Pasman, T., D. Grijpma, D. Stamatialis, and A. Poot. 2017. 'Fabricating porous, photo-crosslinked poly(trimethylene carbonate)

- membranes using temperature-induced phase separation', *Biomaterials Science and Technology*, 28: 1258-62.
- Rojas, A., M. Padidam, D. Cress, and W. M. Grady. 2009. 'TGF-beta receptor levels regulate the specificity of signaling pathway activation and biological effects of TGF-beta', *Biochim Biophys Acta*, 1793: 1165-73.
- Schilders, K. A., E. Eenjes, S. van Riet, A. A. Poot, D. Stamatialis, R. Truckenmuller, P. S. Hiemstra, and R. J. Rottier. 2016. 'Regeneration of the lung: Lung stem cells and the development of lung mimicking devices', *Respir Res*, 17: 44.
- Schuller-Ravoo, S., S. M. Teixeira, B. Papenburg, D. Stamatialis, J. Feijen, and D. W. Grijpma. 2018. 'Microstructured Photo-Crosslinked Poly(Trimethylene Carbonate) for Use in Soft Lithography Applications: A Biodegradable Alternative for Poly(Dimethylsiloxane)', *Chemphyschem*, 19: 2085-92.
- Skold, C. M. 2010. 'Remodeling in asthma and COPD--differences and similarities', *Clin Respir J*, 4 Suppl 1: 20-7.
- Uhl, E. W., and N. J. Warner. 2015. 'Mouse Models as Predictors of Human Responses: Evolutionary Medicine', *Curr Pathobiol Rep*, 3: 219-23.
- Wala, J., D. Maji, and S. Das. 2017. 'Influence of physico-mechanical properties of elastomeric material for different cell growth', *Biomed Mater*, 12: 065002.
- World Health Organization. 2018. 'The top 10 causes of death'. <http://www.who.int/mediacentre/factsheets/fs310/en>

Supplementary data



Supplemental Figure 1. Production variation in PTMC sets 1-3. Electron microscopic images of the morphology of PTMC 1-3 membranes produced with different concentrations of hexanol.

	PTMC1	PTMC2	PTMC3
Polymer solution	PTMC:~1000k g/mol	PTMC:~1300k g/mol	PTMC:~600k g/mol
Casting	-	-	-
Phase separation	70% humidity (ambient air)	50% humidity (ambient air)	60% humidity (humidifier)
UV- photocrosslinking	-	-	-
Washing/ extraction	5 days demineralized water → rinsing with 100% EtOH	1 day 100% EtOH → 1 day 50% EtOH → 4 days 50% EtOH → 1 day 100% EtOH → rinsing with 100% EtOH	1 day 100% EtOH → 1 day 50% EtOH → 4 days 50% EtOH → 1 day 100% EtOH → rinsing with 100% EtOH

Supplementary Table 1. Short overview of differences between PTMC membrane preparations.

CHAPTER 7

Summary and General discussion

Chronic and acute lung diseases affect many people worldwide and are a major cause of death (World Health Organization 2018). In order to study the mechanisms and signalling pathways that underlie these diseases, advanced patient specific models are required. In addition to studying lung health and disease, these models are also important and useful for their application in high-throughput screening of potential new therapeutics. There has been an increased demand for more comprehensive *in vitro* models with better translatability to the *in vivo* situation. This increased demand also relates to the ethical considerations related to the use of animal models, as well as the fact that translation of results from animal models to humans is often problematic (Uhl and Warner 2015). As a result of this demand from both the scientific community and society, there is an urgent need for better human *in vitro* lung models, and a reduction in the use of animals for (respiratory) research purposes. This is furthermore highlighted by the notion that replacement of animal models is now high on the national (Transitie proefdiervrije innovatie 2020) and European (political) agenda (European Commission 2020-08-31).

In the last decades, much progress has been made in the development of *in vitro* models of the lung. Many research groups have transitioned to the use of primary cells instead of tumour cell lines or immortalized cell lines. Furthermore, culture techniques like air-liquid interface (ALI) and organoids have become widely accepted in the field of lung research. The *in vitro* models have also increased in complexity as illustrated by developments in the organ-on-chip field, despite the fact that this is still somewhat in its infancy. The field keeps developing and we understand that all these models have their own advantages and disadvantages. In this thesis, several new models and improvements in existing models are described, with the aim to contribute to the *in vitro* toolbox required for studying lung biology in health and disease.

In this thesis we have focussed on methods for obtaining patient-specific lung cells through different means. We used human induced pluripotent stem cells (hiPSC) to develop a differentiation protocol to obtain alveolar-like cells as well as endothelial cells from the same donor. We used hiPSC-derived alveolar-like cells to study the growth at the ALI and analysed wound repair (Chapter 2). We also developed a method to expand and establish cultures of primary cells derived from sources with limited amounts of cells (Chapter 3 and 4). We demonstrate that the few cells present in tracheal aspirates of preterm new-borns or the cells present in bronchoalveolar lavage (BAL)

fluid can be used to develop ALI cultures (Chapter 4). Furthermore, we explored the effects of the different substrates that the cells are cultured on. Regular culture plastic is much stiffer than the natural matrix in the lung, so possible substitutes need to be evaluated. We have studied the effects on cell differentiation and function of airway and alveolar cells when cultured on poly(trimethylene carbonate (PTMC) and Polydimethylsiloxane (PDMS) respectively (Chapter 3 and 7). Finally, as the lungs are at the forefront of defence against inhaled pollutants and pathogens, they are supported in their function by surrounding immune cells. We have therefore developed a co-culture of airway epithelial cells and polarized macrophages. This model allowed us to study the interaction and cross-talk between airway epithelial cells and macrophages, and the role of this cross-talk in host defence and epithelial repair (Chapter 5).

In the next paragraphs I will highlight and discuss the main findings of this thesis. The findings will be placed into perspective of the current field as well as their future perspectives.

The use of human induced pluripotent stem cells in cellular models

The development of a model that can be used to analyse physiological relevant mechanisms or that can be used to test therapeutics is highly reliant on the cells and the sources used. In chapter 2 we used hiPSC-derived alveolar epithelial cells to model alveolar epithelial wound closure *in vitro* at the physiologically relevant air-liquid interface (ALI). We unexpectedly found that the canonical WNT activator CHIR99021 had a detrimental effect on the wound closure. We (as described in chapter 2) and other groups have found other instances where canonical WNT activation was beneficial for alveolar cell growth (Jacob et al. 2017). However, the unique setup in which the cells grown in 2D at the ALI might explain some of these differences. Additionally, while CHIR99021 is widely used as an effective canonical WNT activator it functions indirectly through the inhibition of GSK3 β , which is part of the β -catenin destruction complex. It is known that CHIR99021 via inhibition of GSK3 β can have additional effect on cellular signalling (An et al. 2010). Work is being done to compare the effects of CHIR99021 and recombinant WNT ligands on the induction of WNT. Unfortunately, this is still ongoing. Nevertheless, due to the relative instability of the recombinant WNT ligands CHIR99021 is predominantly used but the off target effects could explain some of the differences observed.

Furthermore, we found that EpCAM⁺ selection of the cells alone was not enough to obtain a pure cell population. Other groups have used surface expression of carboxyl peptidase M (CPM) for selection or have used NKX-2.1 or pro-surfactant protein C (SFTPC) reporter lines for selection during, at the end of the differentiation protocol or with every consecutive passage (Jacob et al. 2017; Gotoh et al. 2014). The introduction of these reporters is highly useful for *in vitro* cultures but will remain an issue if these cells will eventually be used for the use in humans. The variation in efficiency of differentiation protocols and the accompanying heterogeneity of the obtained population highlights the largest hurdles that need to be overcome in hiPSC related research, both for modelling the alveoli *in vitro* and the eventual application in humans (D'Antonio-Chronowska et al. 2019; Kilpinen et al. 2017). For example, the direct single cell analysis of SFTPC-sorted hiPSC-derived alveolar cells revealed the presence of many different subpopulation (Hurley et al. 2020). This illustrates that even the current most leading protocols are not yet capable of overcoming this issue but also shows that the SFTPC⁺ cell population might be very heterogeneous. Nevertheless, the application of single cell analysis following and during each step in the differentiation pathway will provide valuable insight in the different genes involved and cell subtypes traversed in generating the cell type of interest from the hiPSC state. If the homogeneity of the population is to be increased, we likely need to broaden the number of markers used in the validation of intermediate stages which are analysed and the methods used in the differentiation protocols.

The influence of epigenetic components in hiPSC-based models are currently understudied. For instance, it remains largely unclear what epigenetic changes occur when a cell changes from one type to another in a forced and relatively short timeframe, such as during hiPSC differentiation. Furthermore, it is unclear to which extent the residual epigenetic memory could influence cell behaviour after cellular reprogramming (Papp and Plath 2011; Takahashi and Yamanaka 2006; Brix, Zhou, and Luo 2015). *In vivo* organogenesis is a continuous and dynamic process that is driven by neighbouring tissue interaction. In contrast, most current methods of differentiation *in vitro* are directed and highly simplified compared the subtle changes that direct lung development *in utero*, and lack relevant interactions with the local (micro)environment. It was shown that the combined culture of anterior and posterior gut organoids without additional exogenous factors led to fusion of the organoids and further development of the organoid in the respective

anterior and posterior organs (Koike et al. 2019). This demonstrates that the differentiation and patterning of the structures is subtler and maybe more dependent on cell-cell interaction than expected previously. Furthermore, it was recently shown that differentiation and growth of hiPSC-derived alveolar cells benefited from intermittent withdrawal of triggers for WNT signalling (Hurley et al. 2020). The pulse wise activation of WNT signalling created a balance between proliferation and differentiation of the cells. This again is likely more representative of the *in vivo* situation where during development frequent fluctuations and gradients in concentrations of growth factors are expected (Christian 2012; Rosenbauer et al. 2020). A further aspect that is insufficiently integrated in many differentiation protocols is the influence of the extracellular matrix or signals that are downstream of the cell-matrix interaction. Some protocols already utilise 3D/organoid culture in Matrigel or substitutes thereof. This could for instance influence changes in geometry and polarization of the cells, which in turn affects differentiation and cell fate decisions (Kilian et al. 2010; Mosqueira et al. 2014; Warmflash et al. 2014), but is likely highly specific for different stages or organs (Goetzke et al. 2019). The modulation or supplementation of these Matrigel/hydrogel with extracellular matrix proteins can have beneficial effects on the growth and development as shown with pancreatic progenitors (Greggio et al. 2013). Furthermore, it is unclear how other mechanical queues could influence differentiation. For instance the interaction of the inner cell mass with the extraembryonic tissue and the uterus of the mother during or very shortly following gastrulation likely influences the polarization of the early embryo (Beddington and Robertson 1998).

Nevertheless, even with all these hurdles yet to be overcome, hiPSC are central in many research areas and more refined protocols are being developed continuously. The potential of generating an *in vitro* model in which all involved cells have the same genetic background would have major implications. We managed to generate CD31⁺CD144⁺ endothelial cells from the same hiPSC cell lines that we used to generate alveolar epithelial cells (AEC) 2-like. However, we did not manage to generate a stable co-culture due to the difficulties of fine-tuning a medium in which both cell types are comfortable.

Co-culture of different cell types in *in vitro* lung models

As emphasized previously, the lungs consist of many different cells, which

all have to work in unison to maintain a healthy functioning organ. This interaction between cell types is often not reflected in *in vitro* models, which can be partly attributed to culture or cell availability issues. It is important to realize that our knowledge on the way different cell types contribute and interact during certain responses and mechanisms is still limited. Nevertheless, we know that many biological processes are guided by an interplay between different cell types, indicating the need for more complexity in *in vitro* models. Different studies have described methods of studying cell-cell interaction, such as precision cut lung slices (Akram et al. 2019; Liu et al. 2019), or *ex vivo* explants (Powley et al. 2020; Jager et al. 2014). However, using these methods it is not always clear what cells and in what numbers they are present. In chapter 5 we have therefore focussed on the development of a defined co-culture model of airway epithelial cells with monocyte-derived macrophages polarized using GM-CSF or M-CSF (M(GM-CSF) or M(M-CSF)). This model was used to study the contribution of macrophages to epithelial repair following a mechanically applied wound. We found that the macrophages and especially the M(GM-CSF) macrophages had a positive effect on the wound closure of the epithelial cells. It is already known that macrophages play a role in tissue repair and homeostasis, but these cells are often lacking in epithelial repair models (Wynn and Vannella 2016; Minutti et al. 2017). The process of wound repair can be studied using only the airway epithelial cells (Amatngalim et al. 2016), but the addition of macrophages provides another dimension and layer of complexity. *In vivo* even more cell types are involved and thus this model can be expanded by adding additional cell types. Individual cell types have been combined in previous studies with epithelial cultures that focussed on a specific process or mechanism of interest. For instance, the addition of neutrophils to the culture has been used to study migration through the epithelial barrier as a response to an inflammatory stimulus (Yonker et al. 2017). The co-culture of peripheral blood monocytes (PBMC) with epithelial cells was used to study the contribution of secreted compounds on immune cell differentiation (Luukkainen et al. 2018). The combination with fibroblasts has been described as a model to mimic airway remodelling or to study epithelial-mesenchymal cross-talk and stimulate epithelial growth (Ishikawa, Ishimori, and Ito 2017; Skibinski, Elborn, and Ennis 2007). Also, individual co-cultures with mesenchymal stem cells have been set up (Schmelzer et al. 2020). Even triple co-cultures have been attempted although not solely using primary cells (De Rudder et al. 2020; Blom et al. 2016; Alfaro-Moreno et al. 2008).

The effects of the indirect cross-talk between macrophages and epithelium that we describe in chapter 5 are based on a culture setup where the cells are cultured in different compartments. All effects observed are thus due to secreted compounds and we have not analysed cultures in which cell-cell contact was possible. Studies in which cell-cell contact between macrophages and epithelial cells was possible show differential effects between macrophage subsets on wound healing (Gindele et al. 2017), but also some changes in macrophage behaviour or polarization based on the cell-cell interaction (Ji et al. 2018; Bauer et al. 2015). However, when cell-cell contact is studied it is difficult to separate the interactions of different signalling pathways active in the various cell types, although techniques such as single cell or bulk RNA sequencing may be helpful in this respect. We show that the compound-based cross-talk between M(GM-CSF) and the epithelium results in an upregulation of the CAMP gene, that encodes hCAP18/LL-37, an antimicrobial peptide central in defence against pathogens and implicated in wound repair. We also demonstrate an upregulation in DEFB4B in the epithelium and the apical secretion of its gene product the antimicrobial peptide hBD-2. The effect of the co-culture on expression of these antimicrobial peptides make this model interesting to use for infection studies. Overall, macrophages have long been known for their role in both repair as well as host defence *in vivo*, and it will be interesting to see how macrophage-epithelial cell co-cultures will contribute to our understanding of the functioning of both epithelial cells and macrophages in a variety of processes.

Organoid based expansion of limited cell populations

Both in chapter 3 and 4 organoid-based cultures were used to expand cells that do not proliferate well in 2D or samples that have low cell numbers. The use of organoids to grow airway epithelial cell cultures has been used in previous studies (Barkauskas et al. 2017; Benali et al. 1993; Tan et al. 2017). This culture method has increased in popularity since it was demonstrated in the Hubrecht institute that they could be cultured in a mesenchyme-free system (Sachs et al. 2019). Now, organoid cultures have become central in many fields of research. It was also shown that the organoids could be cultured over long periods of time (Sachs et al. 2019), experiencing less senescence compared to conventional 2D cultures, which eventually stop proliferating (Walters et al. 2013). Other groups have demonstrated that the use of dual SMAD inhibition together with Rho-kinase inhibition can be used to maintain the proliferative capacity of the airway basal cells (Mou et al.

2016). Although this method of expansion had a lower success rate when the starting population contained low numbers of cells (Lu et al. 2020). Our method of expansion using organoid cultures provides a promising and reliable method of obtaining sufficient cells. However, in contrast to studies that use organoid-based models (Dekkers et al. 2013), the lung is characterized by an air-exposed apical side. We have therefore focussed on expansion through organoids to ultimately establish air-exposed cultures. The possibility to expand cells from tracheal aspirates of preterm new-borns or bronchoalveolar lavage samples and subsequent establishment of *in vitro* cultures was previously not possible. The availability of these *in vitro* cultures of preterm new-borns to study, for instance, the development of Bronchopulmonary dysplasia (BPD) was an unmet need (Looi et al. 2019). It will now be possible to obtain samples from patients not or not yet suffering from lung diseases, building up biobanks before diseases arise. These can be diseases that manifest in childhood like asthma or BPD, but also later in life, like cancer or chronic obstructive pulmonary disease (COPD). This would enable side by side comparison of patient and control sample before onset of symptoms, thus allowing discovery of early biomarkers or risk factors. The clinical implications of this insight in cellular function before disease progression could be substantial.

We have demonstrated that epithelial cells present in human airway samples containing limited cell numbers of which most are luminal cells, can be expanded using organoids. Although the flexibility of the lung epithelium is suspected, de-differentiation of luminal to basal cells has so far only been demonstrated in animal models (Tata et al. 2013). This process has not been conclusively demonstrated in humans, although it is suspected. In our cultures, we cannot exclude the possibility that the few basal cells in our samples are responsible for the expansion. We demonstrate that the cultures generated from the samples containing primarily luminal cells do not respond to modulation of differentiation by IL-13 or Notch inhibition using DAPT as expected. An interesting possibility would be that the luminal cells in these cultures de-differentiate to a TP63⁺KRT5⁺ “basal” cell, but do not fully regain all functionality we classically ascribe to a basal cell. Another possibility could be that the very few basal cells initially in the culture have been exhausted to such an extent that their differentiation is impaired (Eenjes et al. 2018), but this remains unclear. We can also not exclude that other cells we did not consider to be able to form lung organoids do contribute to organoid formation, as was demonstrated in the intestine where not only

the stem cells are able to form gut organoids (Serra et al. 2019). Single cell analysis could potentially reveal underlying non-genetic differences in these basal cells that could explain the different responses.

The expansion of the alveolar cells in organoids cultures that we describe in chapter 3, again emphasises the observed phenomena that cells cultured in a 3D matrix are more capable of maintaining phenotype and proliferative capacity, although it remains unclear why or what mechanisms are involved. We demonstrate that alveolar cells grown in a 3D matrix maintain their proliferative capacity and expression of type 2 alveolar epithelial cell markers such as HTII-280 and SFTPC over multiple weeks. The difficulty of expanding alveolar cells has led to many studies using either cell lines or poorly characterized commercial cells that lack essential features of the epithelial cells that line the alveolar lumen (Hassell et al. 2017; Akimoto et al. 2016). This method could provide a more accessible way of obtaining alveolar epithelial cell cultures. We have so far been unsuccessful in freezing pure alveolar cell populations, as single cells or organoids, but if the cells can be maintained in matrix they can be transported and used accordingly.

Lung-on-chip

Lung-on-chip technology has emerged as a highly promising new area of study. It combines various different science disciplines and offers a range of possibilities for variation in parameters and adaption to the needs of the user. It can regulate the biomechanical forces that are sensed by tissue in health or disease, and will allow for the long-term study of cells, even allowing changing parameters during culture. Central parameters of the lung like shear stress (Galie et al. 2014), stretch (Huh 2015), concentration gradients (Wang et al. 2013), blood-epithelial barrier function (Booth and Kim 2012) or various other relevant physiological parameters can be integrated. It is only now when we are starting to expose various different cell types to these mechanical forces, that the impact of these forces on cellular function become more appreciated.

We cultured alveolar epithelial cells on PDMS S1 chips from Emulate to study the effect of the substrate and mechanical forces. We demonstrate that the alveolar cells seeded on chips are better capable of sustained HTII-280 expression compared to static ALI cultures on Transwell inserts with stiff PET membranes. When we expanded the alveolar cells as organoids, we observed that virtually all cells maintain HTII-280 expression at the

apical surface, which is in contrast to cells cultured on Transwell inserts. Our observations suggest that the alveolar cells on the chips maintained a balance between proliferation and differentiation. We observed that after 7 days there was a balance in cells expressing either AEC1 and AEC2 markers. Although various groups have analysed the growth of alveolar cells on chip, HTII-280 expression as a marker for AEC2 has not been used (Jain et al. 2018; Stucki et al. 2018). It remains unclear how long the cultures can be maintained and how long the culture will be stable as we stopped our experiments after 8 days on the chips. Furthermore, it is unclear through what mechanism the alveolar cells are able to maintain their phenotype on the chip. The control samples, in which there was a medium flow present, but that were not exposed to additional mechanical forces, also maintained HTII-280 expression. Whether this is due to the interaction with the different substrate or that the shear stress experienced by the medium has an effect is unclear.

When the cells were exposed to cyclic stretch, we observed changes in the orientation of the alveolar cells. The alveolar cells showed an elongated morphology and aligned perpendicular to the direction of the stretch. The effect observed is robust and is not present in airway cells exposed to stretch (unpublished observations) but it is unclear whether this is a process occurring *in vivo*. This observation is interesting, but also illustrates the gap in knowledge that needs to be overcome to utilize this technology to full effect.

Although the lung-on-chip technology is still in its infancy, it has the potential of making an impact and replacing many animal models (Reardon 2015). Although still expensive and not accessible to most laboratories, it has clear advantages over organoid cultures or static ALI cultures. The chips can be cultured submerged as well as at ALI whereas the organoids have their apical surface turned inwards. This makes it difficult to study physiological relevant exposures in organoid systems. The static Transwell culture systems do not allow for the application of physiologically relevant forces, however the apical surface of the culture is much better accessible. The choice of the model used will depend on the research question asked, but using one model will likely not be sufficient. More models should be used in parallel to corroborate and validate the results. However for this to happen, complex *in vitro* culture models need to become accessible and accepted.

Validation and acceptance of biological models

A difficult, but central question that arises with every model, is whether the added layers of complexity are a better representation of the *in vivo* situation than other models, and whether this increased complexity is required to address the specific research question. New or improved models frequently can and are only compared to the previous model or the *in vivo* situation in its entirety. Will the addition of more cell types, different substrates or mechanical forces provide a better prediction of therapeutic success? This will highly depend on the mechanism and interactions of the compounds being researched, known or unknown. The effect will most likely be difficult to predict beforehand. There are examples of relatively simple and high-throughput models that provide a high translational value like the successful CFTR gut organoid swelling assay (Dekkers et al. 2013). Once an effective compound has been identified that could restore CFTR-function using this assay, it can be readily tested in patients with the same mutations (de Winter-de Groot et al. 2020; Berkers et al. 2019). More complex diseases that chronically progress and over time involve more and different cell types are more difficult to simulate and subsequently validate. It was shown that the application of stretch influenced the migration of tumour epithelial cells and influenced the subsequent effectiveness of tyrosine kinase inhibitors (Hassell et al. 2017). The complexity of the model and the added interdonor variation means that this can likely only be validated by strenuous comparison between patients, animal models and *in vitro* models.

As the *in vitro* models become more complex and comprehensive, they will have the capacity to substitute, replace or complement in part animal experiments. However, most of these models are used in academic settings, and predominantly in the labs that developed them. This also leads to the lack of standardization in the field as different labs have different interests, making it difficult to achieve some consensus. The distribution of many culture techniques - with some notable exemptions - is slow. This holds true even more for their acceptance by international regulatory authorities and industries. Only when extensive validation studies show that an *in vitro* model could replace (part) of animal testing, will it be possible to be considered by the regulatory authorities. Comprehensive testing and validation is paramount and should not be rushed but the search for *in vitro* replacements should also be intensified. In addition to increasing societal pressures that call for a decrease in animal testing, the improvements in culture models also make these transitions more feasible.

Concluding remarks

Over the past decades, *in vitro* culture models have improved significantly and have become a vital tool in the field of lung biology. In this thesis we studied and developed different *in vitro* culture models and their roles in studying the lung. We have described different methods for obtaining cells, through differentiation of hiPSC (chapter 2), through isolation from lung tissue or using organoid-based expansion (chapter 3 and 4). We have studied the effects of the substrate the cells are cultured on (chapter 3 and 6), illustrating that the behaviour of the cells is strongly linked with its surroundings. We show impaired differentiation of airway epithelial cells on our PTMC membranes and a stable culture of alveolar cells on PDMS. This highlights the need for a strong cooperation between different academic fields to understand and integrate these findings in future *in vitro* models. We furthermore developed a co-culture setup of airway epithelial cells together with macrophages (chapter 5). We demonstrate that the addition of macrophages had a dominant effect on processes previously studied using only airway epithelial cells showing the importance of cross-talk between cell types.

Finally, the development of better more translatable *in vitro* models will need to be a cooperative effort of many fields. The combination of all topics described in this thesis could in the future lead to personalized *in vitro* models for therapeutically screening, as well as reduce the amount of required test animals. Although these advances are likely far in the future, the knowledge gained, the *in vitro* models studied and the methods developed could contribute to better protocols, screenings and clinically translatable results.

References

- Akimoto, M., J. I. Hayashi, S. Nakae, H. Saito, and K. Takenaga. 2016. 'Interleukin-33 enhances programmed oncosis of ST2L-positive low-metastatic cells in the tumour microenvironment of lung cancer', *Cell Death Dis*, 7: e2057.
- Akram, K. M., L. L. Yates, R. Mongey, S. Rothery, D. C. A. Gaboriau, J. Sanderson, M. Hind, M. Griffiths, and C. H. Dean. 2019. 'Live imaging of alveologenesis in precision-cut lung slices reveals dynamic epithelial cell behaviour', *Nat Commun*, 10: 1178.
- Alfaro-Moreno, E., T. S. Nawrot, B. M. Vanaudenaerde, M. F. Hoylaerts, J. A. Vanoirbeek, B. Nemery, and P. H. Hoet. 2008. 'Co-cultures of multiple cell types mimic pulmonary cell communication in response to urban PM10', *Eur Respir J*, 32: 1184-94.
- Amatngalim, G. D., W. Broekman, N. M. Daniel, L. E. van der Vlugt, A. van Schadewijk, C. Taube, and P. S. Hiemstra. 2016. 'Cigarette Smoke Modulates Repair and Innate Immunity following Injury to Airway Epithelial Cells', *PLoS One*, 11: e0166255.
- An, W. F., A. R. Germain, J. A. Bishop, P. P. Nag, S. Metkar, J. Ketterman, M. Walk, M. Weiwer, X. Liu, D. Patnaik, Y. L. Zhang, J. Gale, W. Zhao, T. Kaya, D. Barker, F. F. Wagner, E. B. Holson, S. Dandapani, J. Perez, B. Munoz, M. Palmer, J. Q. Pan, S. J. Haggarty, and S. L. Schreiber. 2010. 'Discovery of Potent and Highly Selective Inhibitors of GSK3b.' in, *Probe Reports from the NIH Molecular Libraries Program (Bethesda (MD))*.
- Barkauskas, C. E., M. I. Chung, B. Fioret, X. Gao, H. Katsura, and B. L. Hogan. 2017. 'Lung organoids: current uses and future promise', *Development*, 144: 986-97.
- Bauer, R. N., L. Muller, L. E. Brighton, K. E. Duncan, and I. Jaspers. 2015. 'Interaction with epithelial cells modifies airway macrophage response to ozone', *Am J Respir Cell Mol Biol*, 52: 285-94.
- Beddington, R. S., and E. J. Robertson. 1998. 'Anterior patterning in mouse', *Trends Genet*, 14: 277-84.
- Benali, R., J. M. Tournier, M. Chevillard, J. M. Zahm, J. M. Klosssek, J. Hinnrasky, D. Gaillard, F. X. Maquart, and E. Puchelle. 1993. 'Tubule formation by human surface respiratory epithelial cells cultured in a three-dimensional collagen lattice', *Am J Physiol*, 264: L183-92.
- Berkers, G., P. van Mourik, A. M. Vonk, E. Kruisselbrink, J. F. Dekkers, K. M. de Winter-de Groot, H. G. M. Arets, R. E. P. Marck-van der Wilt, J. S. Dijkema, M. M. Vanderschuren, R. H. J. Houwen, H. G. M. Heijerman, E. A. van de Graaf, S. G. Elias, C. J. Majoor, G. H. Koppelman, J. Roukema, M. Bakker, H. M. Janssens, R. van der Meer, R. G. J. Vries, H. C. Clevers, H. R. de Jonge, J. M. Beekman, and C. K. van der Ent. 2019. 'Rectal Organoids Enable Personalized Treatment of Cystic Fibrosis', *Cell Rep*, 26: 1701-08 e3.
- Blom, R. A., S. T. Erni, K. Krempaska, O. Schaerer, R. M. van Dijk, M. Amacker, C. Moser, S. R. Hall, C. von Garnier, and F. Blank. 2016. 'A Triple Co-Culture Model of the Human Respiratory Tract to Study Immune-Modulatory Effects of Liposomes and Virosomes', *PLoS One*, 11: e0163539.
- Booth, R., and H. Kim. 2012. 'Characterization of a microfluidic *in vitro* model of the blood-brain barrier (muBBB)', *Lab Chip*, 12: 1784-92.
- Brix, J., Y. Zhou, and Y. Luo. 2015. 'The Epigenetic Reprogramming Roadmap in Generation of iPSCs from Somatic Cells', *J Genet Genomics*, 42: 661-70.
- Christian, J. L. 2012. 'Morphogen gradients in development: from form to function', *Wiley Interdiscip Rev Dev Biol*, 1: 3-15.
- D'Antonio-Chronowska, A., M. K. R. Donovan, W. W. Young Greenwald, J. P. Nguyen, K. Fujita, S. Hashem, H. Matsui, F. Soncin, M. Parast, M. C. Ward, F. Coulet, E. N. Smith, E. Adler, M. D'Antonio, and K. A. Frazer. 2019. 'Association of Human iPSC Gene Signatures and X Chromosome Dosage with Two Distinct Cardiac Differentiation Trajectories', *Stem Cell Reports*, 13: 924-38.
- De Rudder, C., M. Calatayud Arroyo, S. Lebeer, and T. Van de Wiele. 2020. 'Dual and Triple Epithelial Coculture Model Systems with Donor-Derived Microbiota and THP-1 Macrophages To Mimic Host-Microbe Interactions in the Human Sinusoidal Cavities', *mSphere*, 5.
- de Winter-de Groot, K. M., G. Berkers, R. E. P. Marck-van der Wilt, R. van der Meer, A. Vonk, J. F. Dekkers, M. Geerdink, S. Michel, E. Kruisselbrink, R. Vries, H. Clevers, F. P. Vleggaar, S. G. Elias, H. G. M. Heijerman, C. K. van der Ent, and J. M. Beekman. 2020. 'Forskolin-induced swelling of intestinal organoids correlates with disease severity in adults with cystic fibrosis and homozygous F508del mutations', *J Cyst Fibros*, 19: 614-19.
- Dekkers, J. F., C. L. Wiegerinck, H. R. de Jonge,

- I. Bronsveld, H. M. Janssens, K. M. de Winter-de Groot, A. M. Brandsma, N. W. de Jong, M. J. Bijvelds, B. J. Scholte, E. E. Nieuwenhuis, S. van den Brink, H. Clevers, C. K. van der Ent, S. Middendorp, and J. M. Beekman. 2013. 'A functional CFTR assay using primary cystic fibrosis intestinal organoids', *Nat Med*, 19: 939-45.
- Eenjes, E., T. C. J. Mertens, M. J. Buscop-van Kempen, Y. van Wijck, C. Taube, R. J. Rottier, and P. S. Hiemstra. 2018. 'A novel method for expansion and differentiation of mouse tracheal epithelial cells in culture', *Sci Rep*, 8: 7349.
- European Commission. 2020-08-31. 'EURL ECVAM Review of non-animal models in biomedical research - Respiratory tract diseases'.
- Galie, P. A., D. H. Nguyen, C. K. Choi, D. M. Cohen, P. A. Janney, and C. S. Chen. 2014. 'Fluid shear stress threshold regulates angiogenic sprouting', *Proc Natl Acad Sci U S A*, 111: 7968-73.
- Gindele, J. A., S. Mang, N. Pairet, I. Christ, F. Gantner, J. Schymeinsky, and D. J. Lamb. 2017. 'Opposing effects of *in vitro* differentiated macrophages sub-type on epithelial wound healing', *PLoS One*, 12: e0184386.
- Goetzke, R., H. Keijder, J. Franzen, A. Ostrowska, S. Nuchtern, P. Mela, and W. Wagner. 2019. 'Differentiation of Induced Pluripotent Stem Cells towards Mesenchymal Stromal Cells is Hampered by Culture in 3D Hydrogels', *Sci Rep*, 9: 15578.
- Gotoh, S., I. Ito, T. Nagasaki, Y. Yamamoto, S. Konishi, Y. Korogi, H. Matsumoto, S. Muro, T. Hirai, M. Funato, S. Mae, T. Toyoda, A. Sato-Otsubo, S. Ogawa, K. Osafune, and M. Mishima. 2014. 'Generation of alveolar epithelial spheroids via isolated progenitor cells from human pluripotent stem cells', *Stem Cell Reports*, 3: 394-403.
- Greggio, C., F. De Franceschi, M. Figueiredo Larsen, S. Gobaa, A. Ranga, H. Semb, M. Lutolf, and A. Grapin-Botton. 2013. 'Artificial three-dimensional niches deconstruct pancreas development *in vitro*', *Development*, 140: 4452-62.
- Hassell, B. A., G. Goyal, E. Lee, A. Sontheimer Phelps, O. Levy, C. S. Chen, and D. E. Ingber. 2017. 'Human Organ Chip Models Recapitulate Orthotopic Lung Cancer Growth, Therapeutic Responses, and Tumor Dormancy *In Vitro*', *Cell Rep*, 21: 508-16.
- Huh, D. D. 2015. 'A human breathing lung-on-a-chip', *Ann Am Thorac Soc*, 12 Suppl 1: S42-4.
- Hurley, K., J. Ding, C. Villacorta-Martin, M. J. Herriges, A. Jacob, M. Vedaie, K. D. Alysandratos, Y. L. Sun, C. Lin, R. B. Werder, J. Huang, A. A. Wilson, A. Mithal, G. Mostoslavsky, I. Oglesby, I. S. Caballero, S. H. Guttentag, F. Ahangari, N. Kaminski, A. Rodriguez-Fraticelli, F. Camargo, Z. Bar-Joseph, and D. N. Kotton. 2020. 'Reconstructed Single-Cell Fate Trajectories Define Lineage Plasticity Windows during Differentiation of Human PSC-Derived Distal Lung Progenitors', *Cell Stem Cell*, 26: 593-608 e8.
- Ishikawa, S., K. Ishimori, and S. Ito. 2017. 'A 3D epithelial-mesenchymal co-culture model of human bronchial tissue recapitulates multiple features of airway tissue remodeling by TGF-beta1 treatment', *Respir Res*, 18: 195.
- Jacob, A., M. Morley, F. Hawkins, K. B. McCauley, J. C. Jean, H. Heins, C. L. Na, T. E. Weaver, M. Vedaie, K. Hurley, A. Hinds, S. J. Russo, S. Kook, W. Zacharias, M. Ochs, K. Traber, L. J. Quinton, A. Crane, B. R. Davis, F. V. White, J. Wambach, J. A. Whitsett, F. S. Cole, E. E. Morrissey, S. H. Guttentag, M. F. Beers, and D. N. Kotton. 2017. 'Differentiation of Human Pluripotent Stem Cells into Functional Lung Alveolar Epithelial Cells', *Cell Stem Cell*, 21: 472-88 e10.
- Jager, J., S. Marwitz, J. Tiefenau, J. Rasch, O. Shevchuk, C. Kugler, T. Goldmann, and M. Steinert. 2014. 'Human lung tissue explants reveal novel interactions during Legionella pneumophila infections', *Infect Immun*, 82: 275-85.
- Jain, A., R. Barrile, A. D. van der Meer, A. Mammoto, T. Mammoto, K. De Ceunynck, O. Aisiku, M. A. Otieno, C. S. Louden, G. A. Hamilton, R. Flaumenhaft, and D. E. Ingber. 2018. 'Primary Human Lung Alveolus-on-a-chip Model of Intravascular Thrombosis for Assessment of Therapeutics', *Clin Pharmacol Ther*, 103: 332-40.
- Ji, J., S. Upadhyay, X. Xiong, M. Malmlof, T. Sandstrom, P. Gerde, and L. Palmberg. 2018. 'Multi-cellular human bronchial models exposed to diesel exhaust particles: assessment of inflammation, oxidative stress and macrophage polarization', *Part Fibre Toxicol*, 15: 19.
- Kilian, K. A., B. Bugarija, B. T. Lahn, and M. Mrksich. 2010. 'Geometric cues for directing the differentiation of mesenchymal stem cells', *Proc*

- Natl Acad Sci U S A, 107: 4872-7.
- Kilpinen, H., A. Goncalves, A. Leha, V. Afzal, K. Alasoo, S. Ashford, S. Bala, D. Bensaddek, F. P. Casale, O. J. Cullley, P. Danecek, A. Faulconbridge, P. W. Harrison, A. Kathuria, D. McCarthy, S. A. McCarthy, R. Meleckyte, Y. Memari, N. Moens, F. Soares, A. Mann, I. Streeter, C. A. Agu, A. Alderton, R. Nelson, S. Harper, M. Patel, A. White, S. R. Patel, L. Clarke, R. Halai, C. M. Kirton, A. Kolb-Kokocinski, P. Beales, E. Birney, D. Danovi, A. I. Lamond, W. H. Ouwehand, L. Vallier, F. M. Watt, R. Durbin, O. Stegle, and D. J. Gaffney. 2017. 'Common genetic variation drives molecular heterogeneity in human iPSCs', *Nature*, 546: 370-75.
- Koike, H., K. Iwasawa, R. Ouchi, M. Maewaza, K. Giesbrecht, N. Saiki, A. Ferguson, M. Kimura, W. L. Thompson, J. M. Wells, A. M. Zorn, and T. Takebe. 2019. 'Modelling human hepato-biliary-pancreatic organogenesis from the foregut-midgut boundary', *Nature*, 574: 112-16.
- Liu, G., C. Betts, D. M. Cunoosamy, P. M. Aberg, J. J. Hornberg, K. B. Sivars, and T. S. Cohen. 2019. 'Use of precision cut lung slices as a translational model for the study of lung biology', *Respir Res*, 20: 162.
- Looi, K., D. J. Evans, L. W. Garratt, S. Ang, J. K. Hillas, A. Kicic, and S. J. Simpson. 2019. 'Preterm birth: Born too soon for the developing airway epithelium?', *Paediatr Respir Rev*, 31: 82-88.
- Lu, J., X. Zhu, J. E. Shui, L. Xiong, T. Gierahn, C. Zhang, M. Wood, S. Hally, J. C. Love, H. Li, B. C. Crawford, H. Mou, and P. H. Lerou. 2020. 'Rho/SMAD/mTOR triple inhibition enables long-term expansion of human neonatal tracheal aspirate-derived airway basal cell-like cells', *Pediatr Res*.
- Luukkainen, A., K. J. Puan, N. Yusof, B. Lee, K. S. Tan, J. Liu, Y. Yan, S. Toppila-Salmi, R. Renkonen, V. T. Chow, O. Rotzschke, and Y. Wang. 2018. 'A Co-culture Model of PBMC and Stem Cell Derived Human Nasal Epithelium Reveals Rapid Activation of NK and Innate T Cells Upon Influenza A Virus Infection of the Nasal Epithelium', *Front Immunol*, 9: 2514.
- Minutti, C. M., J. A. Knipper, J. E. Allen, and D. M. Zaiss. 2017. 'Tissue-specific contribution of macrophages to wound healing', *Semin Cell Dev Biol*, 61: 3-11.
- Mosqueira, D., S. Pagliari, K. Uto, M. Ebara, S. Romanazzo, C. Escobedo-Lucea, J. Nakanishi, A. Taniguchi, O. Franzese, P. Di Nardo, M. J. Goumans, E. Traversa, O. P. Pinto-do, T. Aoyagi, and G. Forte. 2014. 'Hippo pathway effectors control cardiac progenitor cell fate by acting as dynamic sensors of substrate mechanics and nanostructure', *ACS Nano*, 8: 2033-47.
- Mou, H., V. Vinarsky, P. R. Tata, K. Brazauskas, S. H. Choi, A. K. Croke, B. Zhang, G. M. Solomon, B. Turner, H. Bihler, J. Harrington, A. Lapey, C. Channick, C. Keyes, A. Freund, S. Artandi, M. Mense, S. Rowe, J. F. Engelhardt, Y. C. Hsu, and J. Rajagopal. 2016. 'Dual SMAD Signaling Inhibition Enables Long-Term Expansion of Diverse Epithelial Basal Cells', *Cell Stem Cell*, 19: 217-31.
- Papp, B., and K. Plath. 2011. 'Reprogramming to pluripotency: stepwise resetting of the epigenetic landscape', *Cell Res*, 21: 486-501.
- Powley, I. R., M. Patel, G. Miles, H. Pringle, L. Howells, A. Thomas, C. Kettleborough, J. Bryans, T. Hammonds, M. MacFarlane, and C. Pritchard. 2020. 'Patient-derived explants (PDEs) as a powerful preclinical platform for anti-cancer drug and biomarker discovery', *Br J Cancer*, 122: 735-44.
- Reardon, S. 2015. 'Organs-on-chips' go mainstream', *Nature*, 523: 266.
- Rosenbauer, J., C. Zhang, B. Mattes, I. Reinartz, K. Wedgwood, S. Schindler, C. Sinner, S. Scholpp, and A. Schug. 2020. 'Modeling of Wnt-mediated tissue patterning in vertebrate embryogenesis', *PLoS Comput Biol*, 16: e1007417.
- Sachs, N., A. Papaspyropoulos, D. D. Zomer-van Ommen, I. Heo, L. Bottinger, D. Klay, F. Weeber, G. Huelsz-Prince, N. Iakobachvili, G. D. Amatngalim, J. de Ligt, A. van Hoeck, N. Proost, M. C. Viveen, A. Lyubimova, L. Teeven, S. Derakhshan, J. Korving, H. Begthel, J. F. Dekkers, K. Kumawat, E. Ramos, M. F. van Oosterhout, G. J. Offerhaus, D. J. Wiener, E. P. Olimpio, K. K. Dijkstra, E. F. Smit, M. van der Linden, S. Jaksani, M. van de Ven, J. Jonkers, A. C. Rios, E. E. Voest, C. H. van Moorsel, C. K. van der Ent, E. Cuppen, A. van Oudenaarden, F. E. Coenjaerts, L. Meyaard, L. J. Bont, P. J. Peters, S. J. Tans, J. S. van Zon, S. F. Boj, R. G. Vries, J. M. Beekman, and H. Clevers. 2019. 'Long-term expanding human airway organoids for disease modeling', *EMBO J*, 38.
- Schmelzer, E., V. Miceli, C. M. Chinnici, A. Bertani, and J. C. Gerlach. 2020. 'Effects of Mesenchymal Stem Cell Coculture on Human Lung Small Airway Epithelial Cells', *Biomed Res Int*, 2020: 9847579.

- Serra, D., U. Mayr, A. Boni, I. Lukonin, M. Rempfler, L. Challet Meylan, M. B. Stadler, P. Strnad, P. Papasaikas, D. Vischi, A. Waldt, G. Roma, and P. Liberali. 2019. 'Self-organization and symmetry breaking in intestinal organoid development', *Nature*, 569: 66-72.
- Skibinski, G., J. S. Elborn, and M. Ennis. 2007. 'Bronchial epithelial cell growth regulation in fibroblast cocultures: the role of hepatocyte growth factor', *Am J Physiol Lung Cell Mol Physiol*, 293: L69-76.
- Stucki, J. D., N. Hobi, A. Galimov, A. O. Stucki, N. Schneider-Daum, C. M. Lehr, H. Huwer, M. Frick, M. Funke-Chambour, T. Geiser, and O. T. Guenat. 2018. 'Medium throughput breathing human primary cell alveolus-on-chip model', *Sci Rep*, 8: 14359.
- Takahashi, K., and S. Yamanaka. 2006. 'Induction of pluripotent stem cells from mouse embryonic and adult fibroblast cultures by defined factors', *Cell*, 126: 663-76.
- Tan, Q., K. M. Choi, D. Sicard, and D. J. Tschumperlin. 2017. 'Human airway organoid engineering as a step toward lung regeneration and disease modeling', *Biomaterials*, 113: 118-32.
- Tata, P. R., H. Mou, A. Pardo-Saganta, R. Zhao, M. Prabhu, B. M. Law, V. Vinarsky, J. L. Cho, S. Breton, A. Sahay, B. D. Medoff, and J. Rajagopal. 2013. 'Dedifferentiation of committed epithelial cells into stem cells *in vivo*', *Nature*, 503: 218-23.
- Transitie proefdiervrije innovatie. 2020. '<https://www.transitieproefdiervrijeinnovatie.nl/>'.
- Uhl, E. W., and N. J. Warner. 2015. 'Mouse Models as Predictors of Human Responses: Evolutionary Medicine', *Curr Pathobiol Rep*, 3: 219-23.
- Walters, M. S., K. Gomi, B. Ashbridge, M. A. Moore, V. Arbelaez, J. Heldrich, B. S. Ding, S. Rafii, M. R. Staudt, and R. G. Crystal. 2013. 'Generation of a human airway epithelium derived basal cell line with multipotent differentiation capacity', *Respir Res*, 14: 135.
- Wang, L., W. Liu, Y. Wang, J. C. Wang, Q. Tu, R. Liu, and J. Wang. 2013. 'Construction of oxygen and chemical concentration gradients in a single microfluidic device for studying tumor cell-drug interactions in a dynamic hypoxia microenvironment', *Lab Chip*, 13: 695-705.
- Warmflash, A., B. Sorre, F. Etoc, E. D. Siggia, and A. H. Brivanlou. 2014. 'A method to recapitulate early embryonic spatial patterning in human embryonic stem cells', *Nat Methods*, 11: 847-54.
- World Health Organization. 2018. 'The top 10 causes of death'. <http://www.who.int/mediacentre/factsheets/fs310/en/>
- Wynn, T. A., and K. M. Vannella. 2016. 'Macrophages in Tissue Repair, Regeneration, and Fibrosis', *Immunity*, 44: 450-62.
- Yonker, L. M., H. Mou, K. K. Chu, M. A. Pazos, H. Leung, D. Cui, J. Ryu, R. M. Hibbler, A. D. Eaton, T. N. Ford, J. R. Falck, T. B. Kinane, G. J. Tearney, J. Rajagopal, and B. P. Hurley. 2017. 'Development of a Primary Human Co-Culture Model of Inflamed Airway Mucosa', *Sci Rep*, 7: 8182

ADDENDUM

Nederlandse samenvatting

Curriculum Vitae

List of publications

Dankwoord / Acknowledgements

Nederlandse samenvatting

Miljoenen mensen ter wereld lijden en sterven jaarlijks aan long gerelateerde aandoeningen. Deze verschillende longziektes worden gekenmerkt door een breed en diverse scala aan ziektebeelden, en kunnen worden onderverdeeld in chronische en acute longziekten. Astma, chronische obstructieve longziekte (chronic obstructive pulmonary disease; COPD) en interstitiële longziektes zijn voorbeelden van chronische longziektes. Onder acute longziektes scharen we longontstekingen of infecties en longembolie. In veel van deze gevallen, maar met name voor de chronische longziektes, zijn er geen effectieve behandelmethodes beschikbaar. De ontwikkeling van nieuwe en betere behandelmethodes verloopt traag en wordt mede belemmerd door een gebrek aan betrouwbare *in vitro* modellen. Bij het bestuderen van onderliggende mechanismes van ziektes, en het identificeren van aanknopingspunten voor therapieën of het testen van potentiële geneesmiddelen, wordt veel gebruik gemaakt van cellijnen of diermodellen. Steeds vaker blijkt dat de data verkregen via deze methodes lastig vertaalbaar is naar de menselijke situatie. Bovendien is er steeds meer maatschappelijke druk om het aantal dieren dat wordt gebruikt in wetenschappelijk onderzoek terug te dringen. De afgelopen jaren is dan ook veel vooruitgang geboekt in de ontwikkeling en implementatie van nieuwe technieken. De inhoud van dit proefschrift is gericht op de verdere ontwikkeling en implementatie van nieuwe en geavanceerde kweektechnieken voor het bestuderen van de gezonde en zieke long.

In **hoofdstuk 2** wordt een model ontwikkeld waarvoor gebruik gemaakt wordt van alveolaire cellen verkregen uit geïnduceerde pluripotente stamcellen (iPS). Hiervoor werd eerst een protocol ontwikkeld waarmee de iPS stapsgewijs door de verschillende stadia van de embryonale ontwikkeling wordt geleid, richting een long fenotype. Door de signalen van differentiatie te variëren, en te controleren in concentratie en tijd, kon het celtype worden beïnvloed. Door zowel eiwit en genexpressie te meten op verschillende tijdstippen tijdens dit proces werd de mate van differentiatie bepaald. Na de differentiatie werden de cellen geselecteerd op basis van expressie van het epitheelwit EpCAM. De geselecteerde cellen werden vervolgens in kweek gebracht en aan de lucht blootgesteld (air-liquid interface; ALI). In de resulterende kweken werd een wond gemaakt door cellen weg te schrapen, zodat kon worden bestudeerd hoe deze wond herstelde onder invloed van verschillende stimulaties.

In **hoofdstuk 3** wordt een methode ontwikkeld om alveolaire epitheelcellen te isoleren uit humaan longweefsel via het oppervlakte eiwit HTII-280. De geïsoleerde cellen werden vervolgens gekweekt als 3-dimensionale (3D) organoïden in een gelachtige matrix. Met behulp van deze isolatie en kweektechniek konden we de alveolaire cellen langer in kweek houden in vergelijking met traditionele 2D kweken op kweekplastic. Doordat de cellen langer in kweek konden blijven, konden we ze expanderen en vergemakkelijkt dit het plannen van experimenten omdat de cellen nu niet direct gebruikt hoefden te worden na isolatie. Analyse van surfactant eiwitten en HTII-280 expressie toonde aan dat de cellen stabiel waren gedurende de kweek. De cellen werden vervolgens gebruikt in een Long-Chip systeem waarmee de effecten van cyclische stretch op de cellen bestudeerd kan worden. De alveolaire cellen groeiden in de Long-Chip en reageerden op cyclische stretch door zich anders te oriënteren. Hiermee laten we zien dat de Long-Chip een interessant nieuw model is om de alveolaire epitheelcellen te bestuderen.

In **hoofdstuk 4** wordt de mogelijkheid onderzocht om vanuit klinische monsters met lage aantallen longepitheelcellen, organoïden te maken. Deze organoïden werden vervolgens gebruikt om de epitheelcellen te expanderen zodat er voldoende cellen konden worden verkregen om aan lucht blootgestelde (air-liquid interface; ALI) kweken op te starten. Deze ALI kweekmethode is van belang omdat epitheelcellen in de long ook aan lucht zijn blootgesteld, en om het effect van blootstelling aan geïnhaleerde stoffen (zoals sigarettenrook) te kunnen bestuderen. Eerst werd onderzocht of de cellen verkregen via deze nieuwe expansiemethode verschilden van de cellen die via de standaard manier uit bronchiaal weefsel (BW) zijn verkregen. Vervolgens werd gekeken hoe de cellen verkregen uit tracheaal aspiraten (TA) en bronchio-alveolaire lavages (BAL) zich verhouden tot cellen die waren verkregen uit BW als ze als ALI werden verder gekweekt. De differentiatie van de cellen uit de verschillende bronnen in ALI kweken was vergelijkbaar: de kweken bevatten vergelijkbare aantallen basale-, slijmbeker (goblet)- en gecilieerde cellen. De verschillende kweken reageerden wel anders op blootstelling aan sigarettenrook en blootstelling aan het inflammatoire signaalmolecuul IL-13 of de Notch remmer DAPT. De kweken verkregen uit TA of BAL reageerde minder sterk op IL-13 stimulatie of Notch inhibitie. Mogelijk komt dit omdat het aantal basaalcellen in de startpopulatie van de TA en BAL aanzienlijk lager is dan in de BW. De TA en BAL bestaan voornamelijk uit luminale cellen die mogelijk eerst de-differentiëren om basaalcellen te worden. Mogelijk zorgt dit voor de vermindering in de respons

op IL-13 en DAPT die voornamelijk via de basaal cellen loopt.

In **hoofdstuk 5** werd een model ontwikkeld dat het mogelijk maakt om de interactie tussen macrofagen en long epitheelcellen te bestuderen. Monocyten werden geïsoleerd uit bloed en gepolariseerd naar 'pro-inflammatoire' M1 of 'pro-reparatie' M2 macrofagen. Na polarisatie werden de macrofagen samengevoegd met de long epitheelcellen die groeiden en differentieerden op ALI. De macrofagen groeiden in een eigen compartiment waardoor geen cel-cel contact mogelijk was maar alleen interactie via uitgescheiden signaalmoleculen. We laten zien dat beide typen macrofagen het wondherstel van de long epitheelcellen kunnen versnellen. Opmerkelijk is dat in aanwezigheid van M1 macrofagen altijd een net iets snellere wondsluiting werd gezien. Daarnaast laten we zien dat interactie tussen M1 en long epitheelcellen nodig is voor de actieve transcriptie van het CAMP gen in de M1 macrofagen. *CAMP* codeert voor het peptide LL-37 dat een anti-microbiële functie heeft maar ook reparatie kan stimuleren.

In **hoofdstuk 6** verkennen we de mogelijkheid om Poly(trimethylene carbonate) (PTMC) te gebruiken als substraat voor het kweken van long epitheelcellen. Dit is vooral interessant omdat veel kweekmateriaal is gemaakt van hard plastic, het tegenovergestelde van de long. We laten zien dat de long epitheelcellen geen solide cellaag maken op deze membranen. Bovendien is de differentiatie van de cellen verstoord. Het lijkt dat de cellen die worden gekweekt op deze membranen epitheel-tot-mesenchymale transitie (EMT) ondergaan. We laten zien dat de differentiatie gedeeltelijk kan worden hersteld door de effecten van TGFβ te inhiberen. Verdere optimalisatie van kweek- en productietechnieken zullen nodig zijn om PTMC te gebruiken in long kweekmodellen.

In **hoofdstuk 7** worden de hoofdbevindingen van dit proefschrift in perspectief gezet, en beschreven hoe deze bijdragen aan de vooruitgang van het veld.

A

Curriculum vitae

Sander van Riet is geboren op 10 augustus 1989 te Goes. Hij behaalde het VWO diploma aan het Goese lyceum te Goes. In 2008 begon hij aan de studie Biomedische wetenschappen aan de Universiteit Leiden. Hij behaalde zijn bachelor in 2012 na een onderzoeksstage op de afdeling infectieziekten van het Leids Universitair Medisch Centrum (LUMC) in de groep van Dr. E. Van de Vosse. Hij vervolgde zijn studie aan de Universiteit Leiden met de Master Biomedische wetenschappen met de focus op research. Hij behaalde zijn master diploma na het succesvol afronden van 2 master onderzoeksstages, een op de afdeling virologie in de groep van Dr. M. Kikkert en een afstudeerstage op de afdeling longziekten onder begeleiding van Prof. dr. P.S. Hiemstra, beide op het LUMC. In 2015 begon hij aan zijn promotie onderzoek op de afdeling longziekten van het LUMC met als onderwerp het modeleren van long biologie *in vitro* met Prof. Dr. P.S. Hiemstra als promotor en Dr. R.J. Rottier van het Erasmus MC in Rotterdam als copromotor. In januari 2021 is hij begonnen aan een nieuw onderzoek over niet-alcoholische lever fibrose in de groep van Prof. dr. M. Ingelman-Sundberg aan het Karolinska instituut in Stockholm, Zweden.

List of publications

Breathing on Chip: Biomechanical forces change airway epithelial cell biology in a human Airway Lung-Chip

Nawroth JC, Roth D, van Schadewijk A, Ravi A, Maulana TI, Senger CN, **van Riet S**, Ninaber DK, Ryan AL, Hiemstra PS, van der Does AM

<https://www.biorxiv.org/content/10.1101/2021.05.07.443164v2>

Alveolus Lung-Chip Cultures of Patient-Derived Primary Alveolar Type-2 Cells

van Riet S, van Schadewijk A, Khedoe PPSJ, Stolk J, Hiemstra PS, van der Does AM.

In revision at the American Journal of Physiology-Lung Cellular and Molecular Physiology

Development of porous and flexible PTMC membranes for *in vitro* organ models fabricated by evaporation-induced phase separation

Pasman T, Baptista D, **van Riet S**, Truckenmüller R, Hiemstra PS, Rottier R, Stamatialis D, Poot A.

Membranes (Basel). 2020 Nov 5;10(11):330

Disease modelling following organoid-based expansion of airway epithelial cells

van Riet S*, Eenjes E*, Kroon AA, Slats AM, Khedoe PPSJ, Boerem-de Munck A, Buscop-van Kempen M, Ninaber DK, Reiss IKM, Cleves H, Rottier RJ, Hiemstra PS.

American Journal of Physiology-Lung Cellular and Molecular Physiology 2021 July

3D alveolar *in vitro* model based on epithelialized biomimetically curved culture membranes

Baptista D, Teixeira L, Birgani Z, **van Riet S**, Pasman T, Poot A, Stamatialis D, Rottier R, Hiemstra PS, Habibović P, Blitterswijk C, Giselbrecht S, Truckenmüller R.

Biomaterials. 2021 Jan;266:120436.

In vitro modelling of alveolar repair using alveolar epithelial cells derived from human induced pluripotent stem cells

van Riet S, Ninaber DK, Mikkers H, Tetley T, Jost C, Mulder A, Pasman T, Baptista D, Poot A, Truckenmüller R, Mummery C, Freund C, Rottier RJ, Hiemstra PS.

Sci Rep. 2020 Mar 26;10(1):5499

Modulation of airway epithelial innate immunity and wound repair by M(GM-CSF) and M(M-CSF) macrophages

van Riet S, van Schadewijk AM, De Vos S, Vandeghinste N, Rottier RJ, Stolk J, Hiemstra PS, Khedoe PPSJ.

J Innate Immun. 2020 Apr 14;14:1-12.

Stem cell-based Lung-on-Chips: The best of both worlds?

Nawroth JC, Barrile R, Conegliano D, **van Riet S**, Hiemstra PS, Villenave R.

Adv Drug Deliv Rev. 2018 Jul 25. Review

Regeneration of the lung: Lung stem cells and the development of lung mimicking devices.

Schilders KA, Eenjes E, **van Riet S**, Poot AA, Stamatialis D, Truckenmüller R, Hiemstra PS, Rottier RJ.

Respir Res. 2016 Apr 23;17:44. Review.

The positive prognostic effect of stromal CD8+ tumor-infiltrating T cells is restrained by the expression of HLA-E in non-small cell lung carcinoma.

Talebian Yazdi M, **van Riet S**, van Schadewijk A, Fiocco M, van Hall T, Taube C, Hiemstra PS, van der Burg SH.

Oncotarget. 2016 Jan 19;7(3):3477-88.

Differential expression and function of human IL-12R β 2 polymorphic variants.

de Paus RA, Geilenkirchen MA, **van Riet S**, van Dissel JT, van de Vosse E.

Mol Immunol. 2013. 56(4): p. 380-9

Dankwoord / Acknowledgements

Graag wil ik iedereen bedanken die heeft bijgedragen aan het tot stand komen van dit proefschrift, zonder de inzet van al mijn collegas en vrienden was dit nooit gelukt.

Beste Pieter, graag zou ik je bedanken voor je nagenoeg eindeloze inzet en energie. Ik heb altijd veel bewondering gehad voor je kennis, enthousiasme en optimisme, waar ik altijd op kon rekenen, ook als het even niet voor de wind ging. Ik heb genoten van onze discussies en door je (geduldige) feedback heb ik veel geleerd en ben ik een betere en zelfstandige wetenschapper geworden. Beste (bijna professor) Robbert, bedankt voor je input en feedback gedurende mijn hele promotie. Je pragmatische en nuchtere blik is vaak heel verfrissend en heeft tot mooie resultaten geleid.

Ik wil ook graag de leden van mijn promotie commissie bedanken, Hermelijn Smits, Reinoud Gosens, Andries van der Meer, Rudi Hendriks en Marie-José Goumans voor het lezen van mijn thesis en deelnemen aan mijn promotie.

Graag wil ik ons Longfonds consortium bedanken voor de samenwerking in de afgelopen jaren.

Ook wil ik Harald Mikkers en Christian Freund van de iPSC core facility bedanken voor het faciliteren van de iPSC lijnen en het meedenken met mijn project.

Beste, lieve en behulpzame collega's van het longlab. Ik had me geen betere groep kunnen wensen. De gezellige tijd binnen en buiten het lab hebben mijn jaren onvergetelijk gemaakt. Dennis, wij leerden elkaar kennen op de virologie en kwamen elkaar weer tegen op de longafdeling. Bedankt voor je betrokkenheid bij mijn projecten en meetings. Bram, jij stond altijd voor iedereen klaar, op werk en daarbuiten. Padmini, ik ben blij dat we kamergenoten waren, ik heb genoten van onze discussies en om met je samen te werken. Ying, it was great to get to know you and I wish you all the best in your further research and projects. Merian en Iris success met het afronden van jullie PhD project. Abilash, we only worked together for a short while and under strange COVID circumstances but I wish you luck with your projects. Beste Jasmijn, nogmaals gefeliciteerd met het afronden van jouw PhD traject en succes met het volgende project. Beste Letty, bedankt voor de gezelligheid en input. Ik zal nooit meer het zelfde naar pollen kijken, ik hoor vast snel weer van je op het nieuws.

Beste Jan en Annelies, bedankt voor de discussies, de samenwerking en het verzorgen van het waardevolle klinische materiaal. Zonder de sterke samenwerking met de kliniek en het lab waren verschillende projecten niet mogelijk geweest.

Beste Annemarie, toen ik voor mijn stage het lab longziekten binnenkwam heb jij me wegwijs gemaakt. Van het eerste tot het laatste project hebben we altijd goed samen kunnen werken en je no-nonsense visie kan vaak heel verhelderend zijn. Van het begin tot het eind hebben we samen gewerkt en ben dan ook dankbaar dat je naast me wil staan als paranimf.

Dear Gerrit, the G man, Big G, it was amazing to have you in the lab. I have enjoyed the craziness to no end, and I hope to see you again soon.

Lieve Anne, bedankt voor alles. Ik ben blij dat ze je eindelijk een titel hebben gegeven die er een beetje op begint te lijken, je hebt het verdiend.

Beste Alexander, Mattie, WT en Lucho bedankt voor de laaste jaren aan ontspannende avonden en weekenden in de kroeg, op de computer, het festival terrein, of over het bord. De momenten van ontspanning en afleiding zijn van onschatbare waarde geweest. Alexander ook bedankt dat je mijn paranimf wilt zijn. Mocht het snel weer mogelijk zijn zou ik jullie allemaal graag willen verwelkomen in Stockholm.

Lieve Evelien bedankt voor je hulp en steun het afgelopen jaar, ik kijk uit naar de rest van onze tijd in Stockholm.

Lieve Pa en Ma bedankt voor alle steun en vertrouwen de afgelopen jaren. Zowel tijdens de studie als de promotie, het is er dan uiteindelijk toch nog van gekomen ;).

